

Synthesis of New Heterocyclic TCNQ Analogues



A thesis presented for the degree of Doctor of Philosophy

by

James J. Delaney B.Sc.

at

DUBLIN CITY UNIVERSITY
School of Chemical Sciences

FEBRUARY 1997

To my parents and my wife

Declaration

I, the undersigned, hereby declare that this thesis, which I now submit for assessment on the programme of study leading to the award of Ph.D. represents the sole work of the author and has not been taken from the work of others save and to the extent that such work has been cited and acknowledged within the text of work.



James J. Delaney

Acknowledgements

I would like to thank my supervisor Prof Albert Pratt for his encouragement and guidance during the course of this work

I would like to thank Fobairt, Laois Co Council and the School of Chemical Sciences for financial assistance

I am very grateful to both the academic and technical staff of the School of Chemical Sciences, particularly Dr Robert Forster and Joe O'Kelly for their help, advice and use of their equipment for the Cyclic Voltammetry experiments, Dr Conor Long for the X-ray crystallographic data and Mick Burke and Damien McGurk for their assistance in the recording of NMR spectra

I would also like to thank my fellow postgraduates for their friendship, particularly members of the Albert Pratt research group, Ben, Collette, Cormac, Enrico, Fang, Jing, Joe, Mark, Mauro, Ollie, Orla, Paul, Rory and Shane and all postgraduates, past and present that worked in AG 07

I would like to thank my parents and family for their assistance, financial and otherwise, without whom this work would have otherwise been impossible

Finally I would like to thank my wife, Regina for putting up with me, for her help in typing this thesis and for her continuous encouragement and patience

Abstract

There has been considerable interest in the synthesis of derivatives of 7,7,8,8-tetracyano-*p*-quinodimethane (TCNQ) that have potential as electron acceptors in the formation of charge-transfer complexes and radical ion salts. Interest in these materials arises from their electrically conducting properties and the fact that at low temperatures many such salts exhibit superconductivity. New electron acceptors are sought in an attempt to raise the temperature at which onset of superconductivity is observed.

Our approach has been to investigate the synthesis of heterocyclic analogues of TCNQ, in which isoelectronic replacement of a double bond π -electron pair has been achieved by a heteroatom carrying a lone pair of electrons capable of π -type conjugation.

Condensation of maleic anhydride with malononitrile, followed by treatment of the resultant salt with thionyl chloride yielded a dicyanomethylene lactone whose synthesis and chemistry was investigated as a potential precursor to the desired TCNQ analogues. The lactone reacts with alcohols and amines under mild conditions to give the corresponding hydroxy esters and amides respectively. Cyclisation of the hydroxy esters was attempted by converting them to amide esters at elevated temperatures. However, thermal decomposition of the amide esters resulted and product isolation was impossible.

New heterocyclic TCNQ systems based on pyrazine were also synthesised. For example, 5,6-diphenyl-2,3-dicyanopyrazine was reacted with ammonia gas and condensation of the resultant diimino derivative with malononitrile gave the bis(dicyanomethylene) ammonium salt. This ammonium salt was used as a precursor for a range of derivatives. Acidification gave the protonated (N-H) compound and reaction with tetraalkylammonium halides gave the corresponding bis(dicyanomethylene) tetraalkylammonium salts. Pyrolysis of these tetraalkylammonium salts, with the elimination of the appropriate trialkylamine, resulted in the preparation of N-alkyl derivatives in reasonable yields. The charge-transfer complexing ability of these electron acceptors (N-H compound and N-alkyl derivatives) with appropriate electron donors [tetrathiafulvalene (TTF) and *N,N,N',N'*-tetramethyl-*p*-phenylenediamine (TMPD)] was investigated. Cyclic voltammetry measurements of the N-H and N-alkyl derivatives showed that they are electrochemically reversible exhibiting one and two electron reductions respectively.

Abbreviations

TCNQ	7,7,8,8-Tetracyano- <i>p</i> -quinodimethane
TTF	Tetrathiafulvalene
C-T	Charge-transfer
TMTSF	Tetramethyltetraselenafulvalene
BEDT-TTF	Bis(ethylenedithio)tetrathiafulvalene
HOMO	Highest Occupied Molecular Orbital
LUMO	Lowest Unoccupied Molecular Orbital
D	Donor
A	Acceptor
UV	Ultraviolet
I	Ionisation
EA	Electron Affinity
U	Coulomb Repulsion
TCNQF ₄	Tetrafluorotetracyano- <i>p</i> -quinodimethane
HMTSF	Hexamethylenetetraselenafulvalene
TTeF	Tetratellurafulvalene
TSF	Tetraselenafulvalene
CDW	Charge Density Wave
T _{MI}	Lattice Distortion Temperature
SDW	Spin Density Wave
T _c	Superconducting Transition Temperature
TMTTF	Tetramethyltetrathiafulvalene
HMTTF	Hexamethylenetetrathiafulvalene
LDA	Lithium Diisopropylamide
SEM	Trimethylsilylethoxymethyl
EDT-TTF	Ethylenedithiotetrathiafulvalene
S-S	Sulphur-Sulphur
DMET	Dimethyl(ethylenedithio)diselenodithiafulvalene
MDT-TTF	Methylenedithiotetrathiafulvalene
BEDO-TTF	Bis(ethylenedioxo)tetrathiafulvalene
EDBDT	Ethanediyldiene-2-2'-bis(1,3-dithiole)
HMPA	Hexamethylphosphoramide
BDBDT	1,4-Butenediyldiene-2,2'-bis(1,3-dithiole)

$E^1_{1/2}$	First half-wave reduction potential
$E^2_{1/2}$	Second half-wave reduction potential
DMTCNQ	2,5-Dimethyl-tetracyano- <i>p</i> -quinodimethane
V_c	Crystallographic unit cell volume
HMTTeF	Hexamethylenetetratellurafulvalene
DBTTeF	Dibenzotetratellurafulvalene
TMTTeF	Tetramethyltetratellurafulvalene
TCNE	Tetracyanoethylene
DMIT	1,3-Dithiole-2-thiole-4,5-dithiolate
TTT	Tetrathiatetracene
TNAP	11,11,12,12,-Tetracyano-2,6-naphthoquinodimethane
TCNDQ	Tetracyanodiphenoquinodimethane
TCNTP	13,13,14,14-Tetracyano-4,5,9,10-tetrahydropyrenoquinodimethane
DDQ	2,3-Dichloro-5,6-dicyano-1,4-benzoquinone
TCNP	13,13,14,14-Tetracyanopyreno-2,7-quinodimethane
TCNNQ	11,11,12,12-Tetracyano-1,4-naphthoquinodimethane
1,4-TCAQ	11,11,12,12-Tetracyano-1,4-anthraquinodimethane
9,10-TCAQ	11,11,12,12-Tetracyano-9,10-anthraquinodimethane
TCPQ	15,15,16,16-Tetracyano-6,13-pentacenequinodimethane
OCNAQ	11,11,12,12,13,13,14,14-Octacyano-1,4 5,8-anthradiquinotetramethane
TCNEO	Tetracyanoethylene oxide
TDA-TCNQ	1,2,5-Thiadiazolotetracyano- <i>p</i> -quinodimethane
BTDA-TCNQ	Bis[1,2,5]thiadiazolotetracyanoquinodimethane
DCNQI	<i>N,N'</i> -Dicyanoquinonediimine
BTC	Bis(trimethylsilyl)carbodiimide
TCNQI	<i>N,7,7</i> -Tricyanoquinomethanimine
DCNNI	<i>N,N'</i> -Dicyano-1,4-naphthoquinodiimine
DCNTT	2,5-Bis(cyanoimino)-2,5-dihydrothieno[3,2- <i>b</i>]thiophene
SCE	Saturated Calomel Electrode
TMPD	<i>N,N,N',N'</i> -Tetramethyl- <i>p</i> -phenylenediamine

Table of Contents

Title Page	I
Dedication	II
Declaration	III
Acknowledgements	IV
Abstract	V
Abbreviations	VI

Chapter 1 INTRODUCTION

1 A 1	Introduction, 2
1 A 2	Development of Organic Electrical Conductors, 3
1 A 3	Electronic Conductivity Mechanisms in Molecular Solids, 4
1 A 4	Charge-Transfer (C-T) Complexes, 6
1 A 4 1	Stacking in C-T Complexes, 9
1 A 4 2	Stoichiometry of C-T Complexes, 11
1 A 5	Lattice Distortions in Quasi-One-Dimensional Conductors, 12
1 A 6	Superconductivity, 14
1 A 6 1	BCS Theory of Superconductivity, 14
1 A 6 2	Mechanism for Formation of Cooper pairs, 15
1 A 7	The Design of Organic Metals, 16

1 B Electron Donors

1 B 1	Introduction, 18
1 B 2	Substituted TTF Derivatives, 19
1 B 2 1	Bis(ethylenedithio)tetrathiafulvalene (BEDT-TTF), 24
1 B 3	π -Extended TTF Derivatives, 28
1 B 4	Selenium and Tellurium Organic Metals, 33
1 B 4 1	Selenium Derivatives, 33
1 B 4 2	Tellurium Derivatives, 37

1 C Electron Acceptors

1 C 1	Introduction, 41
1 C 2	Synthesis and Properties of TCNQ, 42
1 C 3	Substituted TCNQ Derivatives, 44
1 C 3 1	C-T Complexes of Substituted TCNQ Derivatives, 46

1 C 4	Alternative Routes to TCNQ Derivatives, 47
1 C 5	π -Extended TCNQ Derivatives, 51
1 C 5 1	Electrochemical Properties of π -Extended TCNQ Derivatives, 55
1 C 6	Heterocyclic-TCNQs, 58
1 C 6 1	Electrochemical Properties of Heterocyclic-TCNQs, 61
1 C 6 2	C-T Complexes of Heterocyclic-TCNQs, 61
1 C 7	<i>N,N'</i> -Dicyanoquinonediimines, 66
1 C 7 1	C-T Complexes of DCNQI Acceptors, 69
1 C 7 2	DCNQI Radical Anion Salts, 71
1 C 8	Metal(DMIT) ₂ Acceptors, 73
1 C 9	Buckminsterfullerene Electron Acceptors, 76

RESULTS AND DISCUSSION

Chapter 2	Synthesis of Dicyanomethylene Electron Acceptors
2 1	Introduction, 79
2 2	Synthesis of Sodium (Z)-4-Dicyanomethylene-4-hydroxy-2-butenolate, Tetraethylammonium (Z)-4-Dicyanomethylene-4-hydroxy-2-butenolate and (Z)-4-Dicyanomethylene-4-hydroxy-2-butenic acid, 82
2 3	Synthesis and Chemistry of 4-Dicyanomethylene-2-butenolide, 85
2 3 1	Synthesis of Ethyl (Z)-4-Dicyanomethylene-4-hydroxy-2-butenolate and Methyl (Z)-4-Dicyanomethylene-4-hydroxy-2-butenolate, 87
2 3 2	Attempted Synthesis of 1,4-Bis(dicyanomethylene)-1,4-dihydroxy-2-butene, 88
2 3 3	Synthesis of (Z)- <i>N</i> -Butyl-4-dicyanomethylene-4-hydroxy-2-butenamide and (Z)- <i>N</i> -Phenyl-4-dicyanomethylene-4-hydroxy-2-butenamide, 89
2 3 4	Attempted Cyclisation of (Z)- <i>N</i> -Butyl-4-dicyanomethylene-4-hydroxy-2-butenamide and (Z)- <i>N</i> -Phenyl-4-dicyanomethylene-4-hydroxy-2-butenamide, 92

2 4	Synthesis and Reactions of Ethyl (Z)-4-Dicyanomethylene-4-chloro-2-butenolate, 95
2 4 1	Synthesis of Ethyl (Z)-4-Dicyanomethylene-4-dibutylamino-2-butenolate, Ethyl (Z)-4-Dicyanomethylene-4- <i>p</i> -anisidino-2-butenolate and Ethyl (Z)-4-Dicyanomethylene-4-anilino-2-butenolate, 96
2 4 2	Attempted Cyclisation of Ethyl (Z)-4-Dicyanomethylene-4- <i>p</i> -anisidino-2-butenolate and Ethyl (Z)-4-Dicyanomethylene-2,4-dianilinobutanoate, 104
2 5	Discussion, 105
2 6	Future Work, 107
Chapter 3	Synthesis of Heterocyclic TCNQ Analogues
3 1	Introduction, 111
3 2	Reaction of Dimino-6 <i>H</i> -5,7-dihydropyrrolo[3,4- <i>b</i>]pyrazine with Malononitrile, 113
3 3	Synthesis of <i>N</i> -Substituted Pyrazine Derivatives, 116
3 3 1	Synthesis of Tetraalkylammonium Salts, 117
3 3 2	<i>N</i> -Alkylation using the Tetraalkylammonium Salts, 119
3 3 3	Electronic Absorption Spectra of <i>N</i> -Substituted Heterocyclic TCNQ Analogues, 123
3 4	Future Work, 126
Chapter 4	Charge-Transfer Studies
4 1	Introduction, 129
4 2	Charge-Transfer Studies with 2,3-Diphenyl-5,7-bis(dicyanomethylene)-6 <i>H</i> -5,7-dihydropyrrolo[3,4- <i>b</i>]pyrazine, 130
4 2 1	Attempted C-T Complex formation between 2,3-Diphenyl-5,7-bis(dicyanomethylene)-6 <i>H</i> -5,7-dihydropyrrolo[3,4- <i>b</i>]pyrazine and TMPD, 130
4 2 2	C-T Complex formation between 2,3-Diphenyl-5,7-bis(dicyanomethylene)-6 <i>H</i> -5,7-dihydropyrrolo[3,4- <i>b</i>]pyrazine and TTF, 131
4 3	Charge Transfer Studies with 2,3-Diphenyl-5,7-bis(dicyanomethylene)-6-ethyl-5,7-dihydropyrrolo[3,4- <i>b</i>]pyrazine, 136
4 3 1	C-T Complex formation between 2,3-Diphenyl-5,7-bis(dicyanomethylene)-6-ethyl-5,7-dihydropyrrolo[3,4- <i>b</i>]pyrazine and TMPD, 136

- 4 3 2 Attempted C-T Complex formation between 2,3-Diphenyl-5,7-bis(dicyanomethylene)-6-ethyl-5,7-dihydropyrrolo[3,4-b]-pyrazine and TTF, 141

Chapter 5 Cyclic Voltammetry Studies

- 5 1 Introduction, 144
5 2 Cyclic Voltammetry, 144
5 3 Electrochemical studies of Bis(dicyanomethylene)-5,7-dihydropyrrolo[3,4-b]pyrazines, 148
5 3 1 Discussion, 153

Chapter 6 EXPERIMENTAL

Introductory Remarks, 155

Synthesis of Sodium (*Z*)-4-Dicyanomethylene-4-hydroxy-2-butenolate, 157

Synthesis of Tetraethylammonium (*Z*)-4-Dicyanomethylene-4-hydroxy-2-butenolate, 157

Synthesis of (*Z*)-4-Dicyanomethylene-4-hydroxy-2-butenic acid, 158

Synthesis of 4-Dicyanomethylene-2-butenolide, 158

Synthesis of Ethyl (*Z*)-4-Dicyanomethylene-4-hydroxy-2-butenolate, 159

Synthesis of Methyl (*Z*)-4-Dicyanomethylene-4-hydroxy-2-butenolate, 160

Attempted Synthesis of 1,4-Bis(dicyanomethylene)-1,4-dihydroxy-2-butene, 160

Synthesis of (*Z*)-*N*-Butyl-4-dicyanomethylene-4-hydroxy-2-butenamide, 161

Synthesis of (*Z*)-*N*-Phenyl-4-dicyanomethylene-4-hydroxy-2-butenamide, 162

Attempted Cyclisation of (*Z*)-*N*-Butyl-4-dicyanomethylene-4-hydroxy-2-butenamide and (*Z*)-*N*-Phenyl-4-dicyanomethylene-4-hydroxy-2-butenamide, 162

Synthesis of Ethyl (*Z*)-4-Dicyanomethylene-4-chloro-2-butenolate, 163

Synthesis of Ethyl (*Z*)-4-Dicyanomethylene-4-dibutylamino-2-butenolate, 163

Synthesis of Ethyl (*Z*)-4-Dicyanomethylene-4-*p*-anisidino-2-butenolate, 164

Synthesis of Ethyl (*Z*)-4-Dicyanomethylene-4-anilino-2-butenolate, 165

Addition of Malononitrile to 7-Oxabicyclo[2.2.1]hept-5-ene-2,3-dicarboxylic anhydride, 167

Attempted Cyclisation of Ethyl (*Z*)-4-Dicyanomethylene-4-*p*-anisidino-2-butenolate and Ethyl (*Z*)-4-Dicyanomethylene-2,4-dianilinobutanoate, 167

Synthesis of 5,6-Diphenyl-2,3-dicyanopyrazine, 168

Synthesis of 2,3-Diphenyl-5,7-dimino-6*H*-5,7-dihydropyrrolo[3,4-*b*]-pyrazine, 168

Synthesis of 2,3-Diphenyl-5-imino-7-phenylimino-6*H*-5,7-dihydropyrrolo[3,4-*b*]pyrazine, 169

Synthesis of the Ammonium salt of 2,3-Diphenyl-5,7-bis(dicyanomethylene)-6*H*-5,7-dihydropyrrolo[3,4-*b*]pyrazine, 169

Synthesis of 2,3-Diphenyl-5,7-bis(dicyanomethylene)-6*H*-5,7-dihydropyrrolo[3,4-*b*]pyrazine, 170

Synthesis of Tetraalkylammonium salts of 2,3-Diphenyl-5,7-bis(dicyanomethylene)-6*H*-5,7-dihydropyrrolo[3,4-*b*]pyrazine, 170

Synthesis of Tetramethylammonium salt of 2,3-Diphenyl-5,7-bis(dicyanomethylene)-6*H*-5,7-dihydropyrrolo[3,4-*b*]pyrazine, 171

Synthesis of Tetraethylammonium salt of 2,3-Diphenyl-5,7-bis(dicyanomethylene)-6*H*-5,7-dihydropyrrolo[3,4-*b*]pyrazine, 171

Synthesis of *N*-Benzylpyridinium salt of 2,3-Diphenyl-5,7-bis(dicyanomethylene)-6*H*-5,7-dihydropyrrolo[3,4-*b*]pyrazine, 172

Attempted Synthesis of 2,3-Diphenyl-5,7-bis(dicyanomethylene)-6-ethyl-5,7-dihydropyrrolo[3,4-*b*]pyrazine, 172

Synthesis of 2,3-Diphenyl-5,7-bis(dicyanomethylene)-6-alkyl-5,7-dihydropyrrolo[3,4-*b*]pyrazine derivatives, 173

Synthesis of 2,3-Diphenyl-5,7-bis(dicyanomethylene)-6-methyl-5,7-dihydropyrrolo[3,4-*b*]pyrazine, 173

Synthesis of 2,3-Diphenyl-5,7-bis(dicyanomethylene)-6-ethyl-5,7-dihydropyrrolo[3,4-*b*]pyrazine, 174

Synthesis of 2,3-Diphenyl-5,7-bis(dicyanomethylene)-6-benzyl-5,7-dihydropyrrolo[3,4-*b*]pyrazine, 174

Crystal Structure Determination

Structure Analysis and Refinement, 175

Crystal Data for Ethyl (*Z*)-4-Dicyanomethylene-2,4-dianilinobutanoate, 175

Crystal Data for *N,N,N',N'*-Tetramethyl-*p*-phenylenediaminium salt of 2,3-Diphenyl-5,7-bis(dicyanomethylene)-6*H*-5,7-dihydropyrrolo[3,4-*b*]pyrazine, 175

Synthesis of Charge-Transfer Complexes

Attempted C-T Complex formation between 2,3-Diphenyl-5,7-bis(dicyanomethylene)-6*H*-5,7-dihydropyrrolo[3,4-*b*]pyrazine and TMPD, 176

Synthesis of 2,3-Diphenyl-5,7-bis(dicyanomethylene)-6*H*-5,7-dihydropyrrolo[3,4-*b*]pyrazine-TTF C-T Complex, 176

Synthesis of 2,3-Diphenyl-5,7-bis(dicyanomethylene)-6-ethyl-5,7-dihydropyrrolo[3,4-*b*]pyrazine-TMPD C-T Complex, 177

Attempted C-T Complex formation between 2,3-Diphenyl-5,7-bis(dicyanomethylene)-6-ethyl-5,7-dihydropyrrolo[3,4-*b*]pyrazine and TTF, 177

Cyclic Voltammetry, 177

Chapter 7 References, 178

Chapter 1

INTRODUCTION

1 A 1 Introduction

Conducting organic materials have been extensively researched, since it was suggested, at the beginning of this century,¹ that organic solids could exhibit electrical conductivities comparable to metals. The fact that most organic solids were electrical insulators with room temperature conductivities in the range 10^{-9} - 10^{-14} Scm^{-1} (figure 1.1) seemed contradictory to this suggestion. However, this scenario has changed dramatically in the last 20-30 years and now "organic metals" (charge-transfer complexes and polymeric hydrocarbons) which exhibit electrical,² non-linear optical³ and magnetic⁴ properties in the solid state, along with partially-filled spatially delocalised electronic energy levels (bands) analogous to metals have become a reality! These organic metals, although metallic in nature, have low conductivities (10 - 10^4 Scm^{-1}) compared to copper metal ($\sim 10^6$ Scm^{-1}), but the conductivity does increase with decreasing temperature.

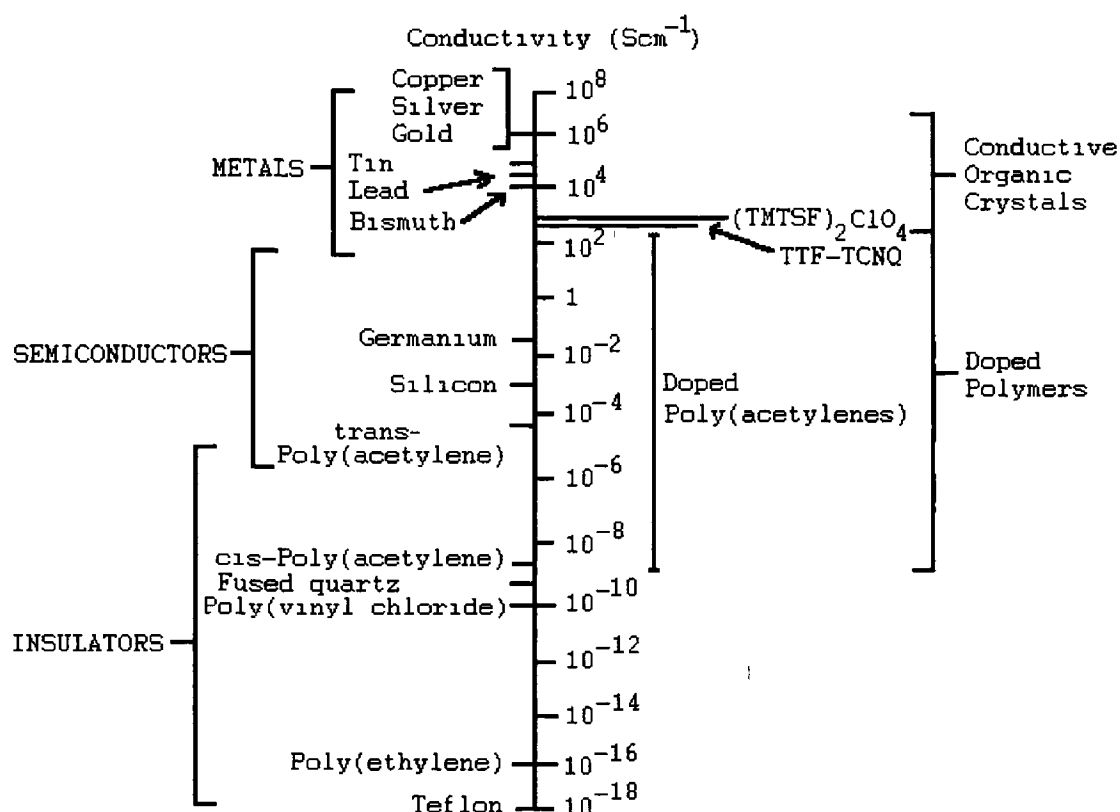


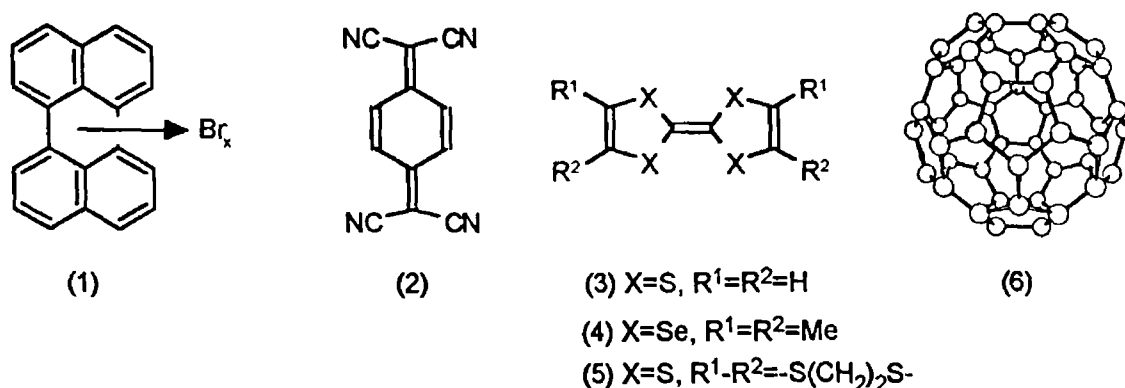
Figure 1.1 Conductivity of materials

There has been intense interest in these organic metals from solid-state physicists, material scientists and chemists alike, with respect to their properties (electronic and otherwise). This interest was further stimulated by

the prediction that superconductivity (the passage of an electric current without resistance) might occur in these organic solids at room temperature⁵ In contrast to copper, some of these organic metals become superconducting at very low temperatures but superconductivity at room temperature has not yet been achieved The development of conducting and superconducting materials and their study via physical and theoretical investigations is required in order to understand and provide information about their electronic properties This understanding is necessary as these materials have potential technological applications in the design of molecular electronic devices *e.g.* sensors, batteries, switching devices and chemoselective electrodes

1.A 2 Development of Organic Electrical Conductors

The first conducting organic material to be reported was an unstable perylene-bromine complex [perylene Br_x , 1, room temperature conductivity (σ_{RT}) $\sim 1 \text{ Scm}^{-1}$] in 1954⁶ However, it wasn't until the discovery of 7,7,8,8-tetracyano-*p*-quinodimethane (TCNQ, 2)⁷ and tetrathiafulvalene (TTF, 3)⁸ and their amalgamation to form the first π -molecular charge-transfer (C-T) complex,⁹ TTF-TCNQ, in 1973 that the area of organic conductors was extensively researched This C-T complex was of interest to chemists and physicists when it was discovered that at 59K ($\sigma_{\text{RT}}=500 \text{ Scm}^{-1}$, $\sigma_{\text{max}}\sim 10^4 \text{ Scm}^{-1}$) it underwent a metal-to-insulator transition (Peierls distortion) The suppression of this transition so as to retain metallic character down to the lowest observable temperature and achieve higher conductivities has been a major challenge to researchers



Therefore a large number of C-T complexes analogous to TTF-TCNQ were investigated with the impetus of achieving this goal and providing the concepts necessary for the development of organic superconductors As a result, it wasn't long before superconductivity was achieved in

tetramethyltetraselenafulvalene (TMTSF, 4)¹⁰ and bis(ethylenedithio)-tetrathiafulvalene (BEDT-TTF, 5)¹¹ salts. This was another major advance in the development of organic materials as these two-dimensional salts had intra- and inter-stack interactions which were capable of suppressing Peierls distortion. The highest temperature for superconductivity in this class of compound was 12.5 K at 0.3 kbar for a salt based on BEDT-TTF, (BEDT-TTF)₂Cu[N(CN)₂]Cl.¹²

The design of new molecular superconductors received a welcome boost with the discovery that the organic electron acceptor buckminsterfullerene, C₆₀ (6), forms a range of superconducting salts with metal cations. Currently the highest temperature at which organic superconductors are stable is 40 K, comprising of a caesium doped buckminsterfullerene, Cs₃C₆₀.¹³ It is through further investigations by organic chemists and physicists on the solid-state properties and synthesis of new electron donors and acceptors that insights into the concepts required for metallic conductivity are elucidated.

1 A 3 Electronic Conductivity Mechanisms in Molecular Solids

Band theory provides an understanding as to why organic materials behave like metals. The formation of energy bands in a solid results from the overlap of orbitals of adjacent atoms. In an isolated atom each orbital can hold no more than two electrons. When two atoms are brought close together their orbitals overlap and the energy level is split into two, producing new molecular orbitals, some of which have higher energy (antibonding) and some of which have lower energy (bonding). This results in the formation of two bands, the valence band (highest filled band, HOMO) and the conduction band (lowest unfilled band, LUMO) having an energy separation of 2β (figure 1.2). The extent of the overlap determines the magnitude of splitting. Adding a third atom splits the levels into three and so on.

When a large number of atoms (as in elemental metals) or molecules (as in organic metals) interact within a crystalline solid or polymer chain their atomic orbitals interact to produce new molecular orbitals which form a continuous band (figures 1.2 and 1.3). This continuous band is bounded within a bandwidth, $2W$, and is composed of n orbitals capable of accommodating $2n$ electrons. The bandwidth is proportional to the transfer integral, t (corresponds to the resonance integral β in Hückel theory) by $2W=4t$. Band filling is analogous to the Aufbau principle for atoms: *i.e.* electrons are placed in the lowest energy states and then succeeding higher energy states are filled. Tight-binding theory, which is analogous to simple Hückel molecular orbital

theory, is used to describe the bands. This approach assumes that the energetic cost in putting two electrons on the same molecule is relatively small. From this theory the extent of interaction between adjacent molecules in the stack is calculated from the transfer integral, t .

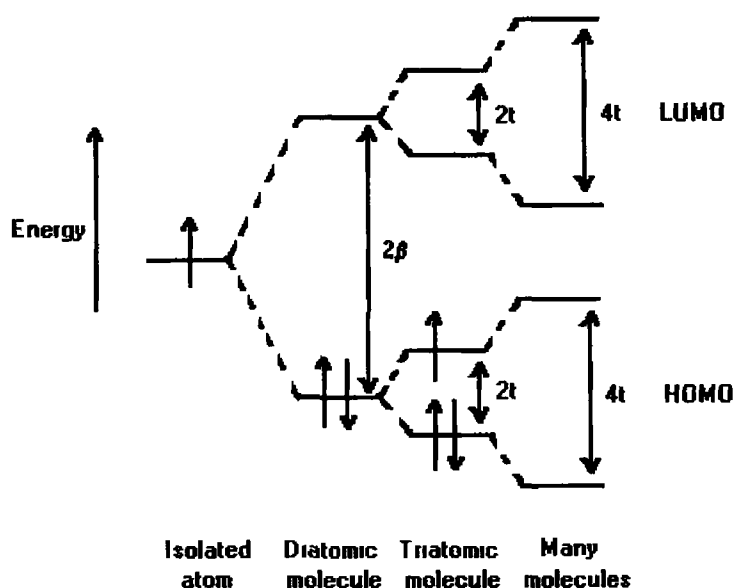


Figure 1 2 Mixing of Electronic States to form Energy Bands

But the interaction of molecular orbitals is not enough to produce metallic or semiconducting properties in a material. The physical properties of a material are also influenced by the electrons that are present in the energy states very near to the highest occupied state (the Fermi level) and it is these electrons that are involved in conduction (to promote an electron to empty states far above the Fermi level requires too much energy).

Materials that have a large energy gap ($\sim 3-6$ eV) between a completely filled valence band and a completely empty conduction band are called insulators. The electrons cannot move about in a filled band (because of Pauli Exclusion Principle), thus insulators are poor conductors of electricity. Semiconductors have the same band structure as insulators but differ in the fact that they have a smaller energy gap ($\sim 0.1-1$ eV) between the conduction and valence bands. However, in semiconductors, there are fewer electrons to act as charge carriers and the number of available carriers is dependent on temperature. Therefore at high temperature more electrons can be promoted into the conduction band i.e. an increase in temperature gives a corresponding increase in conductivity. Likewise lowering the temperature decreases the

conductivity because there is less energy available to excite charge carriers across the band gap. Metals, on the other hand, have a partially filled valence band or if the valence band is filled, the next unfilled band overlaps the filled valence band. Both cases have unfilled states which is a necessary prerequisite for metallic conduction and so the electrons can move easily into higher energy states within the band (figure 1.3).

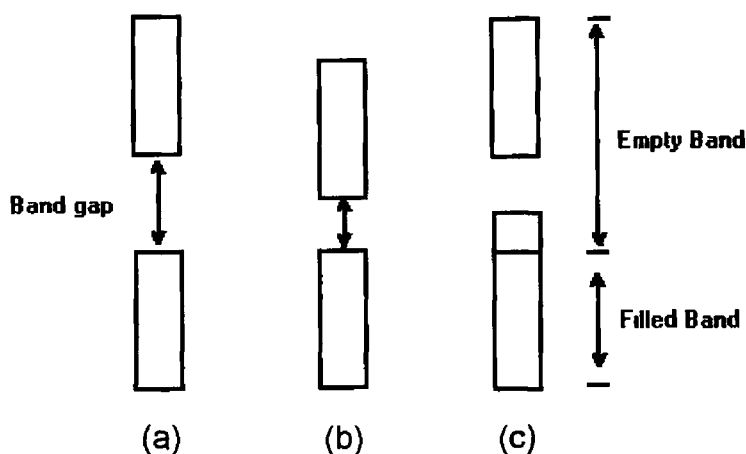
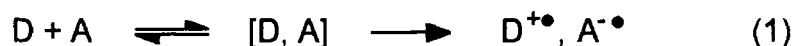


Figure 1.3 Band Structure of (a) an insulator, (b) a semiconductor and (c) a conductor

1 A 4 Charge-Transfer (C-T) Complexes

Charge-transfer (C-T) or electron-donor-acceptor (EDA) complexes are formed when planar (or nearly planar) neutral electron donor and acceptor components combine, via partial electron transfer from donor (D) to acceptor (A), to give a complex (equation 1) whose structure is analogous to that of ionic solids. The donor and acceptor molecules are stacked with a very small distance between the planes (~3-4 Å) having relatively low enthalpies of association (10-30 kJ mol⁻¹, 3-8 kcal mol⁻¹). However in contrast to this, conventional molecular crystals of neutral organic molecules are held together by van der Waals forces. The donor molecule will have low ionisation potential and the acceptor molecule will have high electron affinity each having closed-shell electronic structures



The structure of molecular C-T complexes was investigated by Mulliken who suggested¹⁴ that in the ground state (N) a C-T complex between donor (D)

and acceptor (A) consisted of a "no-bond" (A, D) and a "dative bond" (A⁻D⁺) structure which had the wavefunction

$$\Psi_N = a\Psi(A, D) + b\Psi(A^-D^+) \quad (2)$$

where a and b are coefficients

In addition to the ground state wavefunction (equation 2), there also exists an excited state function of the form

$$\Psi_E = a^*\Psi(A^-D^+) - b^*\Psi(A, D) \quad (3)$$

where $a^* \approx a$, $b^* \approx b$

These C-T complexes exhibit characteristic C-T bands in the ultraviolet (UV) or visible spectra which are distinct from those of the component molecules. Mulliken attributed the new bands to electronic excitations from the HOMO of the donor to the LUMO of the acceptor molecule (figure 1.4). The overlap of donor HOMO and acceptor LUMO are such that maximum intensity in the C-T transition is allowed.

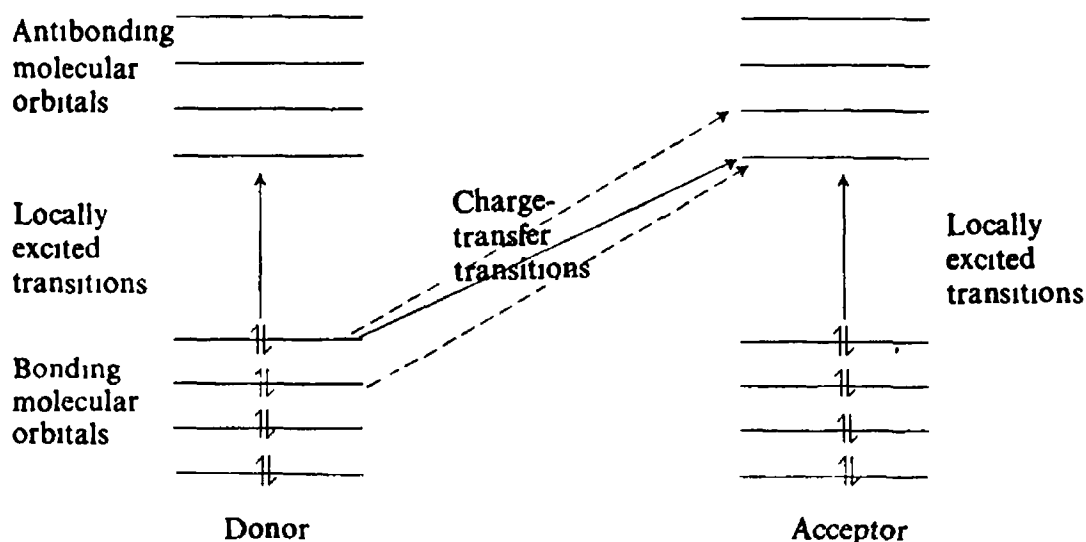
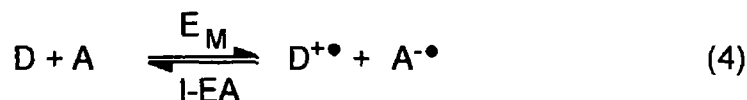


Figure 1.4 Electronic excitations in Charge-Transfer Complexes

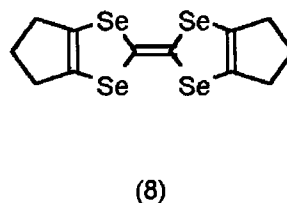
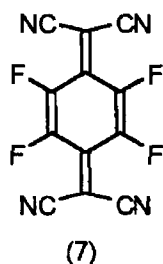
The degree of C-T from the donor to acceptor can be either partial or complete and is determined by the ionic binding in the materials. For example, if the electrons in a crystal of D-A are in equilibrium (equation 4) the

electrostatic Madelung binding energy (E_M) and the molecular energy of C-T ($I-EA$, where I is the ionisation potential of the donor and EA is the electron affinity of the acceptor) determine the direction of equilibrium



Complete C-T ($C-T=1$) gives rise to the formation of a pair of ion-radicals ($D^{+\bullet}$, $A^{-\bullet}$). The acceptor radical anion has one extra electron per molecule and moving an electron along the chain results in two electrons being on the same molecule. The Coulombic repulsion (U) between the two negative charges involves an increase in energy ($U \gg 4t$) and so a single electron remains on each molecule, thus the radical ion is a poor conductor called a Mott-Hubbard insulator. If incomplete C-T ($C-T < 1$) takes place there will be empty sites to which the electrons can move. A partially occupied metallic band then occurs and the conduction process is more energetically favourable.

The importance of incomplete electron transfer in the development of conductivity was shown in the C-T complexes of TCNQ (2) and tetrafluorotetracyano-*p*-quinodimethane (TCNQF₄, 7) with hexamethylenetetraselenafulvalene (HMTSF, 8). Although both C-T complexes are isomorphous, the HMTSF-TCNQ salt is one of the most highly conducting organic salts known ($\sigma_{rt}=1500 \text{ Scm}^{-1}$) whereas the TCNQF₄ salt has a room temperature conductivity of almost nine orders of magnitude lower ($\sigma_{rt}=10^{-6} \text{ Scm}^{-1}$)¹⁵. This is because TCNQF₄ has a higher electron affinity than TCNQ, and on mixing with HMTSF complete electron transfer to TCNQF₄ occurs, the resulting ion-radical salt being non-conducting.



C-T salts can be of two types, (i) single-chain conductors the anion being a closed shell species e.g. $(TMTSF)_2^+ X^-$ or (ii) two-chain conductors both components are open shell molecules e.g. $TTF^+ \cdot TCNQ^{\bullet -}$.

1 A 4 1 Stacking in C-T Complexes

C-T complexes can form mixed stacks or segregated stacks (figure 1 5) with the conductivity being determined by the stacking arrangement in the crystal lattice. The mixed stacking arrangement has electrons which are localised on the acceptor leading to low conductivity (semiconductors or insulators). This contrasts with segregated stacks in C-T complexes which have donors and acceptors with close face-to-face contacts and maximum π -overlap between adjacent molecules in the stacking direction (figure 1 6). This allows charge to move easily along the separate donor and acceptor stacks.

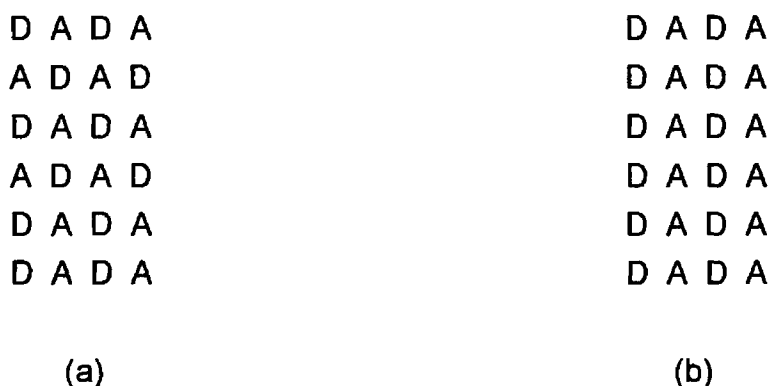


Figure 1 5 Stacking arrangements in C-T complexes, (a) mixed stacks and (b) segregated stacks

As previously mentioned a conduction band is formed from the overlap of π -orbitals on neighbouring molecules along the stack and the extent of interaction between adjacent molecules can be calculated using the transfer integral, t . The partial filling of this band with electrons by C-T from donor to acceptor molecules leads to the observed levels of metallic conductivity. High electrical conductivity in C-T salts is associated with segregated stacks of donor and acceptor molecules which have extensive π -electron delocalisation in the stacking direction (figure 1 6).

In the 1:1 TTF-TCNQ C-T complex, the TTF and TCNQ molecules have segregated stacks and incomplete C-T (0.59 of an electron).¹⁶ Electron transfer causes the electrons to move along both stacks and the material is conductive. The material is conducting in one direction only, thus the electrical properties of the salt are highly anisotropic (associated with a unique direction where orbital overlap is greatest, i.e. the stacking direction). The reason for this is that all the constituent molecules of the crystal are stacked in parallel planes, so like many organic metals, TTF-TCNQ is termed a quasi-one-dimensional conductor.

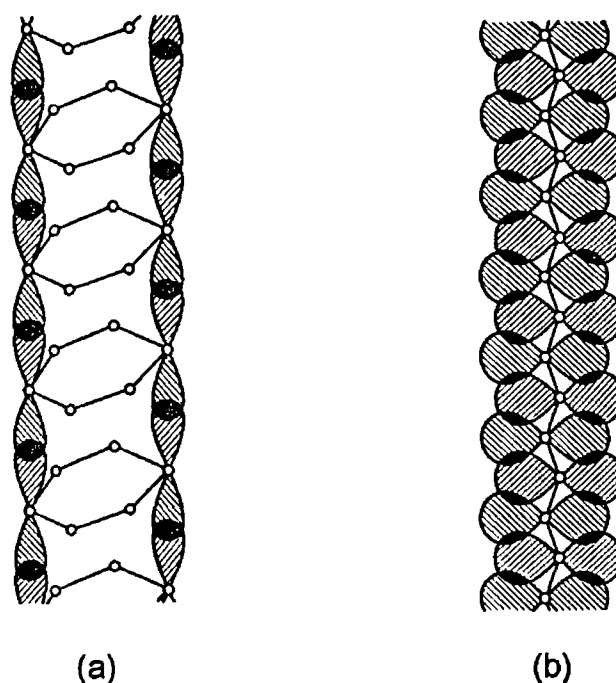


Figure 1 6 Stacked Orbital Arrangement, (a) a stack of flat molecules with delocalised electrons above and below the plane, giving a stack of overlapping orbitals running along the stack and (b) a linear polymer giving overlapping orbitals running the length of the polymer

The crystal structure of organic materials is important in determining the unusual physical properties. In most organic conductors the organic moieties adopt a planar or nearly planar arrangement. The mode of stacking (ring-over-bond, zigzag, herringbone, direct overlap, figure 1 7) and their electronic communication in the solid may or may not favour electron delocalisation and high electrical conductivity.

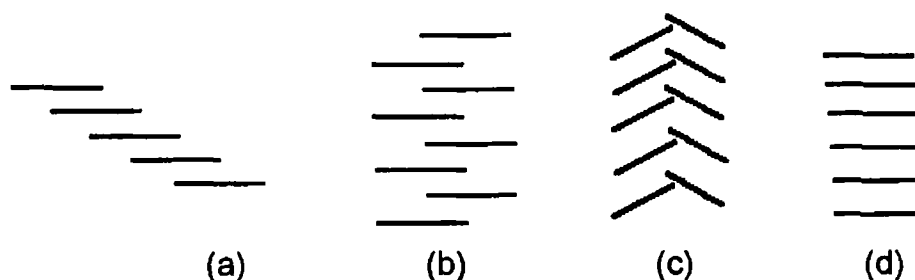
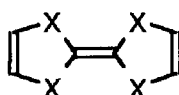


Figure 1 7 Mode of Stacking in C-T complexes, (a) ring-over-bond, (b) zigzag, (c) herringbone and (d) direct overlap

TTF-TCNQ possesses the important structural feature of strong intrastack delocalisation leading to only weak interactions between the segregated stacks and this produces a highly anisotropic conductivity ($\sigma_{\text{rt}}=500 \text{ Scm}^{-1}$ and $\sigma_{\text{max}}\sim 10^4 \text{ Scm}^{-1}$ at 59K). In these segregated stacks there is ring-over-bond overlap (slipped stack, the exocyclic carbon-carbon double bond lies over the ring of the molecule adjacent to it in the stack) (figure 1.7a).¹⁷ The electrical conductivity also increases when the heteroatom is changed from sulphur to selenium to tellurium in the series TXF-TCNQ [X=S (500 Scm^{-1}), Se (800 Scm^{-1}), Te (1800 Scm^{-1})]. This can be accounted for by the expected increase in the donor overlap. The tetratellurafulvalene (TTeF, 9)-TCNQ C-T complex does not undergo a transition to a superconducting state as the temperature is lowered at ambient pressure and neither does it undergo a metal-to-insulator transition similar to TTF (3)-TCNQ ($T_{\text{max}}=59\text{K}$) or tetraselenafulvalene (TSF, 10)-TCNQ ($T_{\text{max}}=40\text{K}$). This behaviour is partly due to the increased interchain interaction and more two-dimensional character.



(9) X=Te

(10) X=Se

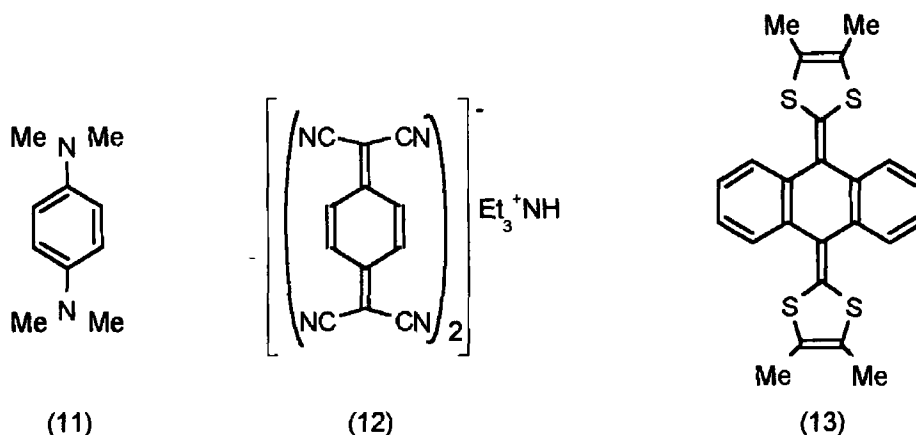
All of these materials behave as quasi-one-dimensional conductors without increased two- and three-dimensional electronic interactions between the segregated stacks and so undergo insulating transitions at low temperatures. This transition involves a one-dimensional instability, a crystal lattice distortion and a rapid decrease in electrical conductivity. In both organic and inorganic metals, the temperature dependence of conductivity is dominated by the interaction (scattering) of electrons with vibrations of the atomic lattice (phonons). Thus when the temperature is lowered there are fewer lattice vibrations, which increases the intermolecular orbital overlap and so the conductivity increases.

1 A 4 2 Stoichiometry of C-T Complexes

The design of efficient conductors consisting of donor (D) and acceptor (A) moieties requires control over the D/A stoichiometry. The majority of C-T complexes contain a 1:1 stoichiometry of the donor-acceptor pair. However, higher order complexes are achievable, e.g. $(D)_nA$, $(A)_nD$, but their existence

becomes less likely as the order increases i.e. $n > 2$. Wheland and Gillson showed¹⁸ that complex formation by metathesis occasionally affords control over stoichiometry. This relies on the donor and acceptor combining in a ratio that reflects their charges. They also altered the stoichiometry by reacting preformed complex with additional donor or acceptor.

The electron acceptor TCNQ has formed C-T complexes with multiple stoichiometries (D/A) i.e. 1/1 with *N,N,N',N'*-tetramethyl-*p*-phenylenediamine (11),¹⁹ 1/2 with complex salts e.g. triethylammonium-(TCNQ)₂ (12)²⁰ and a 1/4 complex with the anthracenediylidene donor (13).²¹



1 A 5 Lattice Distortions in Quasi-One-Dimensional Conductors

Quasi-one-dimensional conductors are unstable against distortions as the temperature is lowered and this leads to phase transitions. These transitions are caused by

(i) Peierls Distortion or Charge Density Wave (CDW)

Quasi-one-dimensional conductors (figure 1 8a) are sensitive to the interactions of electrons with vibrations of the atomic lattice (phonons). At low temperatures these conductors are unstable with respect to lattice distortions (Peierls distortion, figure 1 8b-d),²² and the degree of instability is dependent on the number of radical ionic and neutral molecules in the stack. The lattice distortion is accompanied by the opening of a gap in the conduction band because in a half-filled band there are no neutral molecules in the stack and thus spin pairing occurs (each molecule has unpaired spin and there is an electronic driving force for spin pairing) creating this gap and so losing metallic conduction (figure 1 8b) i.e. the conducting electrons are now localised with a filled electron band at lower energy and an empty band at higher energy.

The alternating regions within the lattice of higher and lower charge density results in the generation of a charge density wave (CDW). The energy gap (Peierls gap) that opens at the Fermi level results in a metal-to-semiconductor (or insulator) transition analogous to Jahn-Teller distortion. As a result of this split between the valence and conduction bands, conduction can occur only if electrons are promoted across the energy gap by an external source of thermal or electromagnetic energy. The introduction of neutral molecules into the stack results in a less than half-filled band and so the energy in going to a distorted structure is less favourable because the CDW is not commensurate with the lattice. The metallic state is now allowed between room temperature and the lattice distortion temperature, (T_M). The onset of a CDW can cause a material to change from a conductor to a semiconductor. If an organic conductor is not susceptible to distortions introduced by the CDW the material becomes a superconductor instead of an insulator at low temperatures.

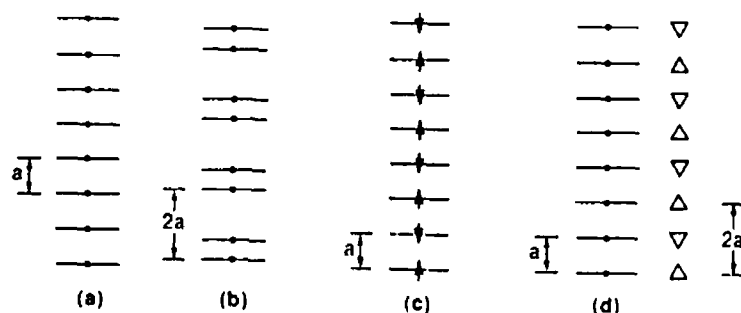


Figure 1.8 Configuration of a one-dimensional stack of molecules with one electron in the HOMO, (a) metal with uniform spacing of lattice constant a , (b) insulator with dimerization caused by Peierls distortion, (c) SDW insulator with spin (\uparrow) periodicity caused by Coulomb interactions and (d) insulator with periodicity caused by ordering of nonsymmetric anions (Δ)

(ii) Spin Density Waves (SDW)

Metal-to-insulator transitions in low dimensional conductors can also be driven by either spin density waves (SDW) or anion ordering. Spin density waves were first identified by Bechgaard in his study of the tetramethyltetraselenafulvalene (4) salt, $(TMTSF)_2PF_6$.¹⁰ The formation of the SDW state was due to the Coulombic repulsion between electrons on the

molecular stack being greater than their interaction with the lattice. In the SDW state the electrons spin up and spin down alternately (antiferromagnetically) and this introduces a gap in the electronic band which restricts movement of the electrons (insulating magnetic state, figure 1.8c). Bechgaard also found that the metal-to-insulator transition in the $(\text{TMTSF})_2\text{X}$ (where $\text{X}=\text{AsF}_6^-$, PF_6^-) salts could be suppressed by applying an electric field or pressure. When X was the hexafluoro-arsenate or -phosphate anion there was no lattice distortion associated with the loss of conductivity and in some cases a superconducting ground state occurs. An insulating state also occurs when an ordered array of anions with periodicity '2a' causes doubling of the original lattice (figure 1.8d).

Anion ordering which occurs at low temperature also causes metal-to-insulator transitions e.g. in $(\text{TMTSF})_2\text{ReO}_4$ the metal-to-insulator transition which occurs at ~180K is caused by anion ordering. The symmetry of the anion influences the insulating state and tetrahedral anions in contrast to the octahedral anions introduce anion ordering except when X is the perchlorate anion. This salt remains metallic down to ~1.2K.²³

1 A 6 Superconductivity

Superconductivity is the ability to conduct an electric current without resistance. The resistance of a superconductor is zero and a current set up in a superconductor is not dissipated as heat, like ordinary conductors, but continues to flow forever. Superconductivity was first discovered by Onnes in 1911 when he observed that the resistance of mercury wire fell to zero at 4.2K. In 1933 Meissner and Ochsenfeld observed that superconductivity could be characterised by a magnetic effect (Meissner effect) i.e. a superconductor placed in a magnetic field generates its own internal field that expels the external one (diamagnetism). The lines of force of the external magnetic field bend around the surface of the superconductor instead of passing through it. The impermeability of superconductors to a magnetic field is also useful when dealing with the applicability of superconducting materials. For example, a magnet can float on its magnetic field if placed above a superconductor and so the field acts as a cushion for the magnet. Therefore in the future it may be possible to travel on trains that can fly at 300 miles per hour, levitated above the tracks on a frictionless cloud of magnetic force.

1 A 6 1 BCS Theory of Superconductivity

Bardeen, Cooper and Schrieffer put forward a theory for superconductivity (BCS Theory) in 1957 which suggested that superconductivity arises when

electrons in a conductor form loosely bound pairs (Cooper pairs)²⁴ The electrons in a Cooper pair move at the same speed but in opposite directions. Much more energy is required to hinder the motion of Cooper pairs than ordinary electrons and at low temperature this energy is unavailable so the Cooper pairs are not scattered and electrical resistance disappears.

1 A 6 2 Mechanism for Formation of Cooper pairs

Atoms in a solid are arranged such that the orbitals of the outer electrons overlap and thus the electrons can move within these orbitals. The atoms that remain fixed in the lattice are positively charged (one electron has been removed) which enables the valence electrons to pair up. As an electron moves through the lattice the electrostatic attraction between the electron and the positive ion generates a distortion in the lattice. The negatively charged electron, as it passes, pulls the positive ions towards each other and interactions among the ions lead to restorative forces that cause the lattice to vibrate. After the passage of the electron the positive ions remain close together for a long time which creates a region of positive charge and thus another electron is attracted indirectly to the first electron and a Cooper pair is formed (figure 1 9a). As the ions move apart under the influence of restorative forces a region of positive charge is created in which the density is less than the surrounding parts of the lattice. The two electrons tend to avoid this region (figure 1 9b). This effect emerges below a critical temperature, T_C (the temperature at which the transition to superconductivity occurs) and causes the electrons that make up each Cooper pair to act as if they were connected to a spring. The electrons which form the pair vibrate back and forth in response to variations in charge density.

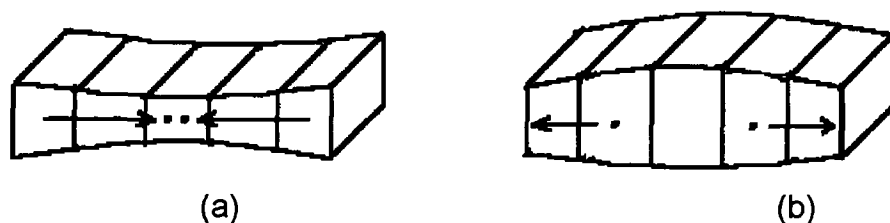


Figure 1 9 Formation of Cooper pairs, (a) an electron moving through a metal attracts the positively charged ions of the lattice, causing distortion of the lattice and (b) the positive ions move apart thus creating a region of positive charge, which the electrons making up the Cooper pair, avoid

Superconduction is the result of the highly coordinated motion of the Cooper pairs whereas in ordinary metals electrical conduction is caused by the net motion of the individual valence electrons. When no current is flowing through the material the momentum of each Cooper pair is zero, the electrons move in opposite directions with respect to the lattice. When there is current in the material the electrons in each pair move such that the centers of mass of all the Cooper pairs have the same constant momentum. Condensation of the electrons into Cooper pairs depends on lattice distortions and T_C is related to the stiffness of the lattice.

In 1964 Little proposed a mechanism for the formation of Cooper pairs which does not depend on lattice distortions.⁵ He suggested that a superconductor could be prepared from a chain of organic molecules containing loosely bound valence electrons. This molecule would be polarised easily and so one part would be positively charged and the other would be negatively charged and thus electrons could pass along the chain from one site to another.

1.A 7 The Design of Organic Metals

Since the preparation of the C-T complex, TTF-TCNQ in 1973,⁹ intense investigations on systems analogous to the donor TTF and the acceptor TCNQ have occurred with the intention of meeting the requirements for inter- and intra-molecular conductivity or superconductivity. From the information available the design of new conducting materials requires control of the properties of the individual molecules to stabilise the metallic state. These molecules must satisfy the following requirements:

- (i) planar molecules with similar size are required having delocalised π -molecular orbitals so that effective overlap of the donor HOMO and the acceptor LUMO can occur,
- (ii) stable open-shell (free radical) species are needed to form a partially filled band since it is unlikely that good organic metals are formed from the HOMO and LUMO of closed shell organic molecules, the best organic metals result from open shell anion and cation species,
- (iii) there should be no periodic distortion which opens a gap at the Fermi level,

- (iv) mixed valence is necessary and the on-site Coulomb repulsion (U) should be small compared to the bandwidth ($4t$), the condition for the metallic state being $U_{\text{eff}}/4t \sim 1$,
- (v) segregated stacks of radical species are required,
- (vi) strong interchain coupling to suppress phase transitions is necessary

A considerable amount of research has been directed towards the synthesis of new donors and acceptors with emphasis on the importance of these factors. The ability to induce molecules to pack within a crystal lattice in a prescribed manner (e.g. in sheets, stacks or dimer pairs) is still very limited so that the rational design of organic metals is restricted to controlling the key properties of the individual component molecules i.e. planarity, ionisation potential/electron affinity and extent of conjugation.

C-T systems with increased dimensionality of the structural properties has also been prevalent since BEDT-TTF and TMTSF were found to be two-dimensional. This was achieved by close interstack chalcogen-chalcogen interactions which stabilise the metallic state by suppressing Peierls instability. The design and synthesis of new systems which could further improve the low-temperature electrical and magnetic properties in addition to stabilising the metallic state and superconductivity have been major goals for chemists in recent years.

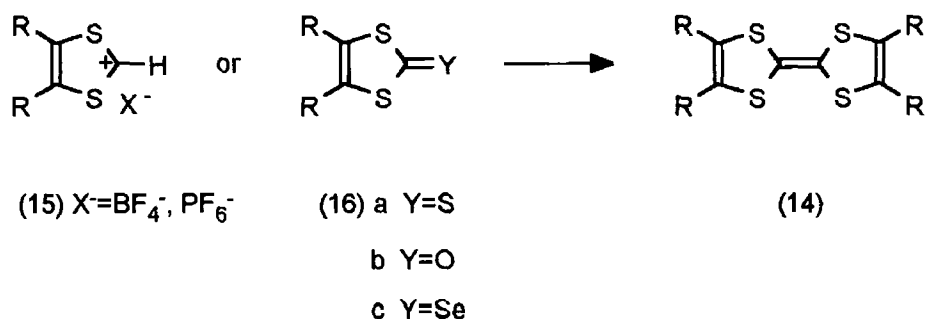
1 B Electron Donors

1 B 1 Introduction

Since the discovery in the early 1970s, that TTF forms a stable radical cation⁸ and a highly conducting C-T complex with TCNQ,⁹ investigations into TTF chemistry have intensified with the aim of discovering new and better donors. Many TTF analogues were prepared, with BEDT-TTF (5) being the most extensively studied (section 1 B 2 1). Derivatives of TTF are important for the development of new highly conducting organic metals and superconductors. The synthesis of TTF derivatives has followed three main routes

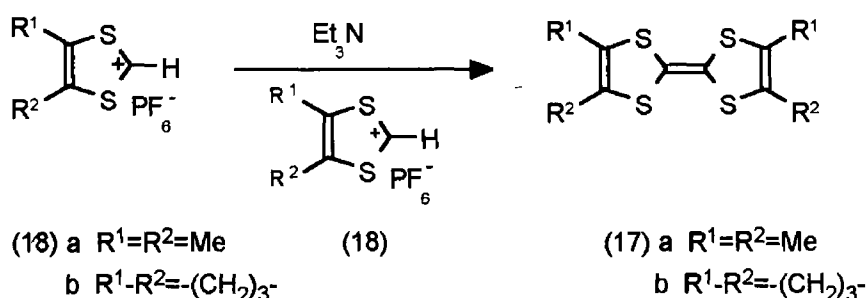
- (i) substituents on the 2,3 and 6,7 positions. This mainly involves peripherally substituted heteroatoms which enhance the dimensionality due to their larger size and greater polarizability compared to sulphur. This suppresses the instabilities observed in one-dimensional metals.
- (ii) π -extension between the two dithiole units. This reduces the on-site Coulomb repulsion in the doubly ionised state of the donor and is important for attaining high conductivity.
- (iii) heteroatom exchange. Replacement of the sulphur atoms in TTF by selenium or tellurium atoms enhances the interstack interactions which results in increased dimensionality.

The commonly used routes to TTF derivatives (14) are (i) coupling of 1,3-dithiolium salts (15) or (ii) coupling of 1,3-dithiole-2-thiones (16a) or -2-ones (16b) or -2-selenones (16c) (scheme 1 1).



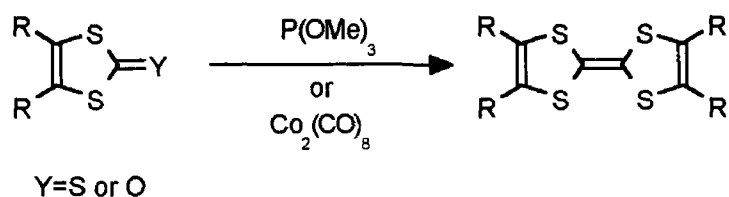
Scheme 1 1

The first TTF derivatives to be studied were tetramethyltetrathiafulvalene (TMTTF, 17a)²⁵ and hexamethylenetetrathiafulvalene (HMTTF, 17b)²⁶ These derivatives may be prepared by deprotonation of cation (18) to yield a stabilised carbene, which then reacts with another 1,3-dithiolium cation (scheme 1 2)



Scheme 1 2

TTFs were also synthesised by the desulphurization or deoxygenation of 1,3-dithiole-2-thiones or -2-ones using trivalent phosphorus compounds^{27a} (scheme 1 3) This reaction is widely used when electron-withdrawing groups are present on the dithiole ring, however it gives poor yields and alternatively dicobalt octacarbonyl can be used instead of the phosphorus reagent^{27b} since a wider range of substituents can be tolerated



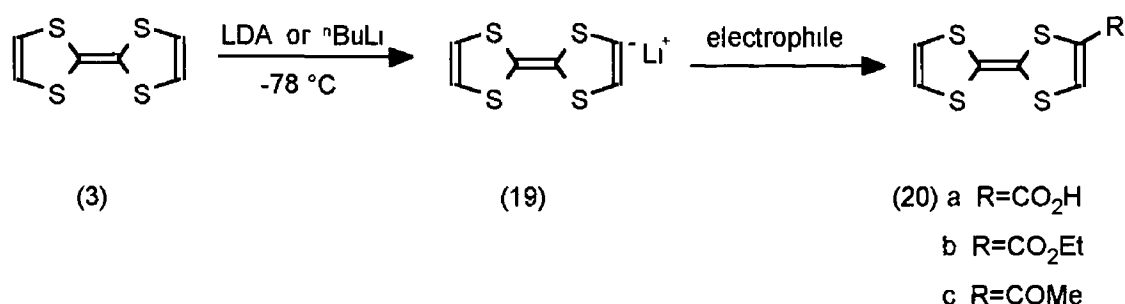
Scheme 1 3

1 B 2 Substituted TTF Derivatives

The most widespread modification to the TTF skeleton has concentrated on the replacement of the sulphur atoms by selenium (e g TMTSF) and the fusion of heterocyclic rings (e g BEDT-TTF) In contrast, little attention has been focussed on the attachment of functionalised substituents to the TTF framework²⁸ These functionalised TTFs have potential as building blocks for new electron donors However, direct substitution on TTF is difficult by most of the known methods because of its low ionisation potential but can be effected by using non-oxidising agents such as butyllithium This direct substitution has advantages in that it has increased versatility and leads to the preparation of

functionalised TTFs which offer unique potential for the development of new organic materials with unconventional solid-state properties

TTF derivatives with one functionalised side-chain were prepared from monolithiated TTF (TTF-Li^+ , 19), which was generated²⁹ by metallation of TTF (3) using butyllithium or lithium diisopropylamide (LDA) in ether at -78°C . TTF-Li^+ (19) can be trapped *in situ* with electrophiles. For example, reaction of (19) with carbon dioxide, ethyl chloroformate or acetyl chloride affords the monosubstituted carboxylic acid (20a), ester (20b) or acyl (20c) derivatives in reasonable yield (30-70%)³⁰ (scheme 1.4)

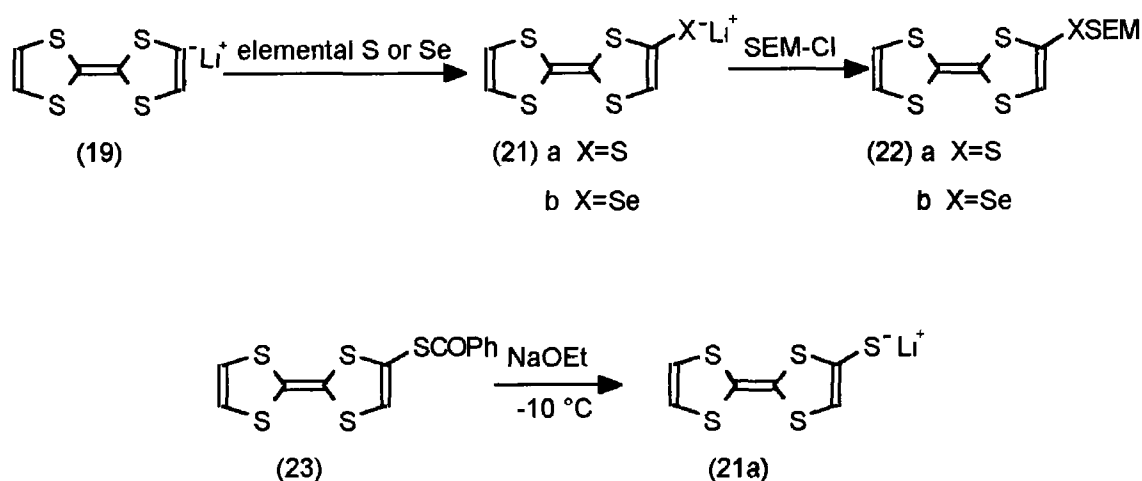


Scheme 1.4

This procedure affords a simple and efficient route to unsymmetrical TTFs but it does have its disadvantages in that strict temperature control is necessary since, above -78°C , TTF-Li^+ (19) disproportionates to yield di- and multi-substituted products. The presence of substituents on TTF exerts a directional effect permitting control over the metallation position. For example, the attachment of electron-withdrawing substituents on TTF activates the adjacent position to metallation (increases the acidity of the adjacent proton) and gives the 4,5-disubstituted products whereas electron-donating substituents (decrease the acidity of the adjacent proton) direct a second substitution into the 4' or 5' position. This was sometimes complicated by temperature dependency³⁰. In addition to this, the electron-donating substituents have been shown to decrease the oxidation potential whereas electron-withdrawing substituents have the opposite effect.

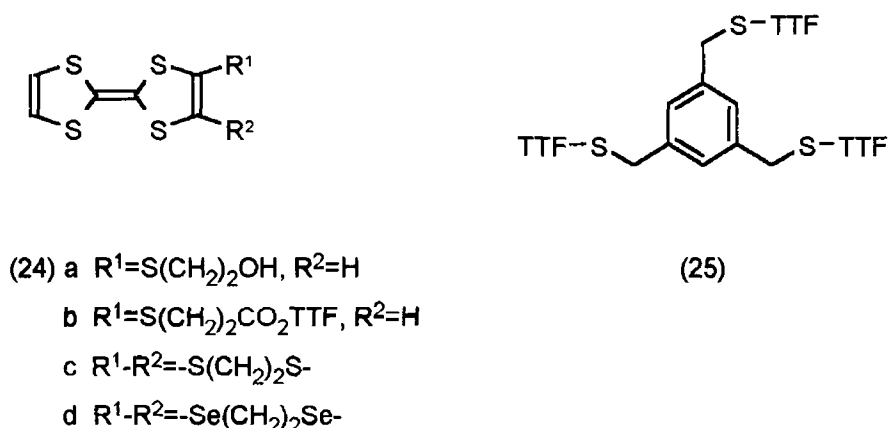
Mono- and di-chalcogen TTF derivatives have been prepared³¹ by the reaction of monolithiated TTF (19) with elemental sulphur and selenium at -78°C to give the corresponding thiolate (21a) and selenolate (21b) anion respectively. These were more reactive towards electrophiles than lithiated TTFs (scheme 1.5). This new route to TTF donors is preferable to phosphite-mediated coupling of the two half-units. Reaction of (21b) with

trimethylsilylethoxymethyl (SEM) chloride afforded the SEM protected compound (22b) which could be regenerated upon treatment with fluoride ion (in the form of tetrabutylammonium fluoride) (scheme 1 5) Thus (22b) is a shelf-stable equivalent of the selenolate anion (21b) Analogous reactions of the thiolate anion (21a), followed by treatment of (22a) with fluoride ion gave no evidence that (21a) was generated ^{31b} However the benzoyl thioester (23) is a shelf-stable equivalent of the TTF-thiolate anion (21a) and the anion can be efficiently regenerated, as the sodium salt, by treating (22a) with sodium ethoxide in ethanol at -10 °C ³²



Scheme 1 5

Reaction of TTF-thiolate anion (21a) with 2-bromoethanol gave 4-(2-hydroxyethylthio)TTF (24a) which is a versatile building block for the synthesis of a range of new mono-functionalised TTF derivatives containing ether, ester, acrylate and vinylthio groups ^{31a} Derivative (24a) has been used in the synthesis of bis- and tris-TTF derivatives (24b) and (25) ³²



Other reactions of monolithiated TTF included the one-pot synthesis of unsymmetrical donors ethylenedithio-TTF (EDT-TTF, 24c) and ethylenediseleno-TTF (EDS-TTF, 24d) in low yield (10-20%)^{31b} However, varying the molar ratio of the reactants TTF, LDA, sulphur and dibromoethane gave a mixture of unchanged TTF and BEDT-TTF. The X-ray crystal structure of EDS-TTF (24d)^{31b} has a non-planar, boat-like TTF framework (similar to BEDT-TTF). The bond distances in the TTF part of EDS-TTF are similar to the equivalent distances in BEDT-TTF (5). The packing of the EDS-TTF dimers (figure 1 10) is similar to that of the κ -type structures of (BEDT-TTF)₂X salts except that in the latter the molecules are aligned along the long axis perpendicular to the layer (parallel to each other) while in the former they lie within the layer and perpendicular to each other.

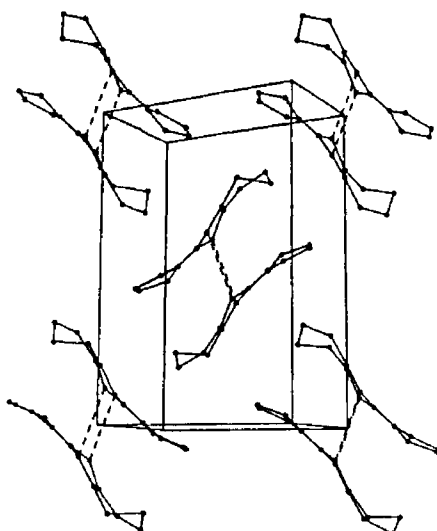
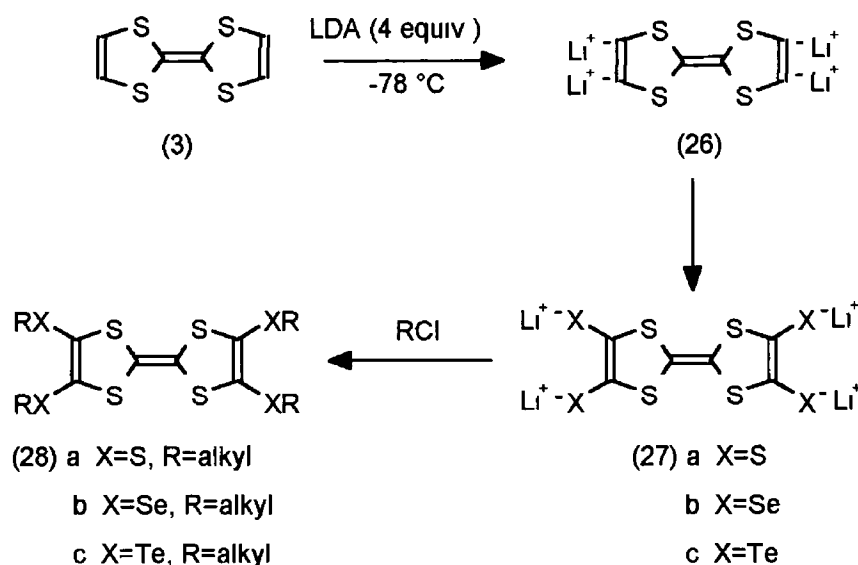


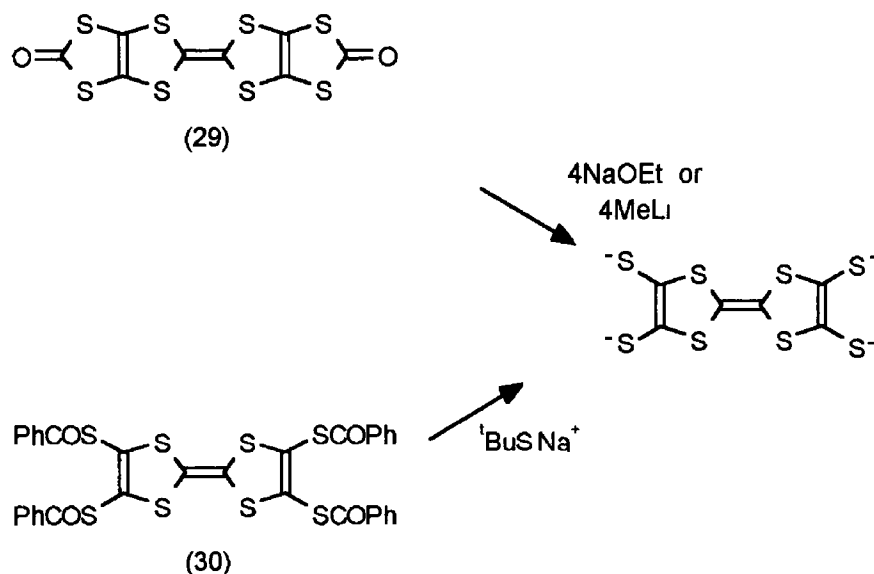
Figure 1 10 Crystal packing of EDS-TTF (24c) within a layer of dimers

Symmetrical tetrakis(alkylthio)TTF derivatives have been prepared³³ by the coupling reaction between two identical species *i.e.* 1,3-dithiole-2-thiones (16a), 1,3-dithiol-2-ones (16b) or 1,3-dithiole-2-selenones (16c) with trivalent phosphorus compounds but this gave poor yields of tetrachalcogenated TTF derivatives. This problem was overcome by the preparation of the tetralithiated anion of TTF (TTF⁴⁻ 4Li⁺, 26) by deprotonating TTF (3) with four equivalents of LDA at -78 °C and reaction of the anion with elemental sulphur, selenium or tellurium to yield the tetrathiolate (27a), tetraselenolate (27b) and tetratelluroolate (27c) anions respectively³⁴ (scheme 1 6). Reaction of (27a-c) with alkyl halides yielded TTF derivatives with four thioalkyl (28a), selenoalkyl (28b) or telluroalkyl (28c) chains. The tetrathiolate anion can also be formed by

ring opening of tetrathiapentalenedione (29)³⁵ or by deprotection of tetrakis(benzoylthio)TTF (30)³⁶ with sodium tert-butyl thiolate (scheme 1 7)



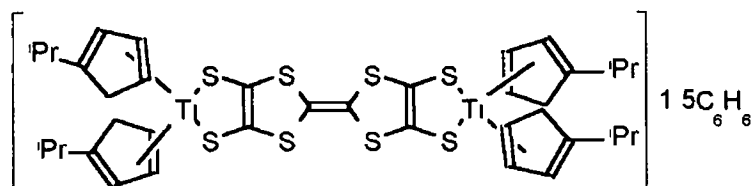
Scheme 1 6



Scheme 1 7

Coordination complexes of tetrathiafulvalene tetrathiolate salt (27a) that have potential as building blocks for new two-dimensional electrical conductors were recently investigated³⁷ The tetrathiafulvalene complex, $\{(i\text{-PrC}_5\text{H}_4)_2\text{Ti}[\text{S}_2\text{TTF}\text{S}_2]\text{Ti}(i\text{-PrC}_5\text{H}_4)_2\}1\text{ }5\text{C}_6\text{H}_6$ (31), formed two-dimensional stacks of a chain-link, fence-like structure (herringbone) and is representative of a new class of potential TTF-type building blocks These TTFs are of interest

because they can assemble into solid-state architectures which can function as organic superconductors

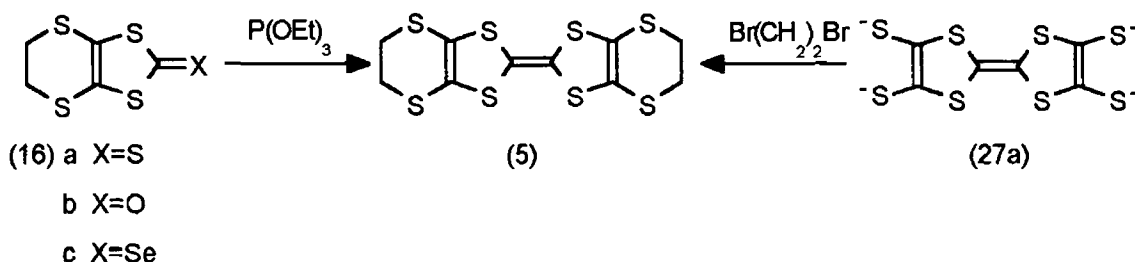


(31)

1 B 2 1 Bis(ethylenedithio)tetrathiafulvalene (BEDT-TTF)

The majority of organic conductors are unstable to periodic lattice distortions at low temperatures, leading to an insulating ground state. Over the past 20 years studies on a wide range of structural and chemical types of organic linear chain systems were carried out with the aim of suppressing these instabilities and stabilising a low-temperature metallic or superconducting state. New donor molecules which are capable of forming C-T complexes with increased dimensionality and thus suppress the metal-to-semiconductor or -insulator transition were needed for the design of new organic superconductors in order to understand the requirements for them.

One such molecule that was prepared was the tetrakis(alkylthio) substituted TTF derivative, BEDT-TTF (5) in which extension of the TTF moiety and the intermolecular interactions of the sulphur atoms, enhances the dimensionality. This permits the suppression of the metal-to-insulator transition and thus allows transitions to the superconducting state to occur. The most common method for the preparation of BEDT-TTF was the coupling of 4,5-bis-alkylthio-1,3-dithiol-2-thiones (16a),³³ or the corresponding -2-ones (16b)³⁸ or -2-selenones (16c) using trivalent phosphorus compounds (scheme 1.8). However this route sometimes fails to give the desired product or gives it in low yield. Alternatively, reaction of the tetrathiolate anion (27a) with 1,2-dibromoethane can be used³⁶ (scheme 1.8).



Scheme 1.8

The discovery that the TMTSF donor system containing monovalent anions was superconducting at low temperature¹⁰ stimulated interest in the synthesis of analogous BEDT-TTF systems. A new family of electrical conductors was synthesised, having the stoichiometry of $(\text{BEDT-TTF})_2\text{X}$ ³⁹. These salts were similar to the $(\text{TMTSF})_2\text{X}$ salts (section 1 B 4 1) where X is a charge-compensating monovalent anion. The $(\text{BEDT-TTF})_2\text{X}$ salts were prepared by electrocrystallisation, similar to the $(\text{TMTSF})_2\text{X}$ salts but in contrast to the TMTSF systems which only yield single phase crystals, the BEDT-TTF system produces two to five different phases all with different crystallographic and electrical properties and often the same stoichiometry. Two of the more common phases are β and κ -phase salts which are characterised by different structural packing motifs i.e. corrugated-sheet networks of BEDT-TTF molecules and orthogonally arranged BEDT-TTF molecular dimers respectively (figure 1 11).

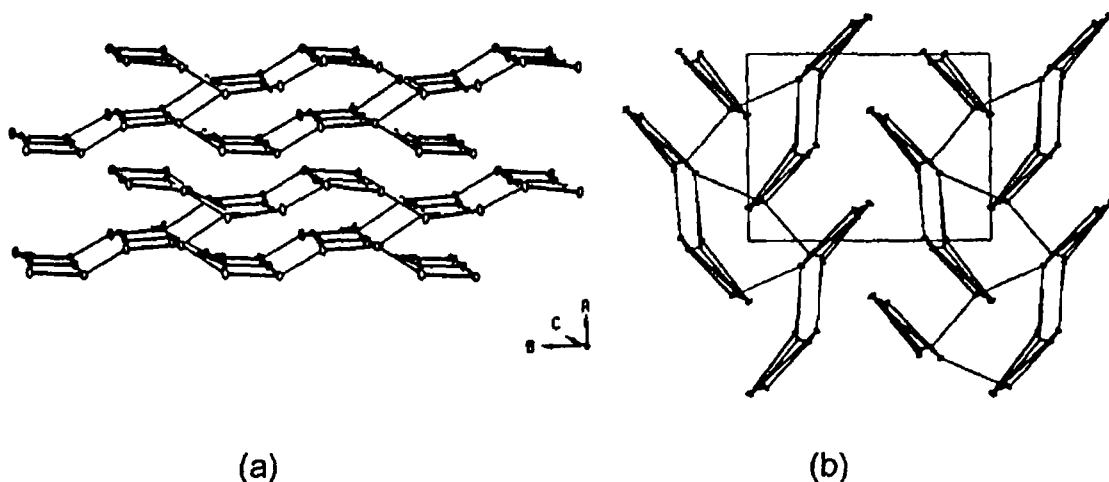


Figure 1 11 Structural packing motifs in BEDT-TTF salts, (a) "corrugated sheet network" of BEDT-TTF molecules in β -(BEDT-TTF)₂ReO₄ and (b) orthogonally arranged BEDT-TTF molecular dimers in κ -(BEDT-TTF)₂Cu(NCS)₂. Thin lines indicate short sulphur-sulphur interactions (<3.60 Å).

In the β -phase salts, the stacks of cations are replaced with orthogonally arranged dimers of BEDT-TTF cations which results in strong sulphur-sulphur (S-S) interactions whereas in the κ -phase salts the crystal has two BEDT-TTF molecules forming a dimerized pair. The pairs are linked to each other by short S-S contacts almost perpendicular, forming two-dimensional conducting sheets in the *bc* plane. All the S-S intermolecular contacts within the dimer are longer

than the sum of the van der Waals radii (3.6 Å) but shorter contacts exist between the dimers

The first BEDT-TTF salt that showed interesting properties was the perchlorate salt, $(\text{BEDT-TTF})_2\text{ClO}_4(1,1,2\text{-trichloroethane})_{0.5}$ ^{39a}. This salt remained metallic over the temperature range 300-1.4 K and showed no evidence of a metal-to-semiconductor transition. It also showed low conductivity in the stacking axis (because the overlap of neighbouring molecules was very small) and in the direction perpendicular to the stacking axis. This BEDT-TTF salt was more conductive than the corresponding TMTSF salt by a factor of >10. The first sulphur superconductor, $(\text{BEDT-TTF})_2\text{ReO}_4$, followed soon after¹¹ and this became superconducting below 2 K for pressures above 4 kbar. Williams and co-workers reported^{39b} that $(\text{BEDT-TTF})_2\text{ReO}_4$ was isostructural with $(\text{BEDT-TTF})_2\text{BrO}_4$ but structurally different to $(\text{TMTSF})_2\text{X}$ systems. The BEDT-TTF moiety in $(\text{BEDT-TTF})_2\text{ReO}_4$ was nonplanar, with the methylene groups protruding out of the molecular plane. In addition to this, the ReO_4^- anions were ordered at room temperature but this did not happen in the corresponding TMTSF salt.

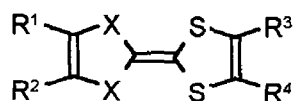
The structural feature of the $(\text{BEDT-TTF})_2\text{X}$ salts compared to the $(\text{TMTSF})_2\text{X}$ salts that is surprising is that there are short interstack S-S interactions instead of short intrastack S-S interactions with little or no columnar stacking^{39b, 40}. The interstack S-S interactions are sufficiently strong that the TMTSF-like (face-to-face) columnar stacking is not favoured and the BEDT-TTF molecules are arranged in side-by-side fashion to form two-dimensional sheets (figure 1.11). This two-dimensionality originates from the short intermolecular contacts between the sulphur atoms of the donor.⁴⁰ The S-S network is the pathway for electrical conduction in all $(\text{BEDT-TTF})_2\text{X}$ systems. The BEDT-TTF molecules are nonparallel and nonplanar in structure and in contrast to $(\text{TMTSF})_2\text{X}$ systems, the loosely connected zigzag stacks are not equally spaced. Williams and co-workers suggested^{39b} that the suppression of the metal-to-insulator transition by applying pressure reduces both the intra- and inter-stack S-S distances. This in turn increases the S-S overlap and dimensionality of the systems. At ambient pressure and low temperature the primary S-S interactions are those between the molecular stacks compared to those within a stack in $(\text{TMTSF})_2\text{X}$ salts.

Several conducting β - $(\text{BEDT-TTF})_2\text{X}$ ($\text{X}=\text{AuI}_2^-, \text{I}_3^-$) salts have also been synthesised. The linear symmetric AuI_2^- salt had the highest superconducting transition temperature $T_c=3.24$ ⁴¹ or 4.9 K⁴² at ambient pressure and the I_3^- salt, the first ambient pressure BEDT-TTF superconductor, had $T_c=8$ K under a

pressure of 1.3 kbar⁴³ As before, superconductivity was correlated to the observation of a sheetlike network of BEDT-TTF stacks linked through extensive S-S interactions giving two-dimensional behaviour Anion disorder appears to inhibit the onset of superconductivity in the β -(BEDT-TTF)₂X systems similar to that in (TMTSF)₂ClO₄

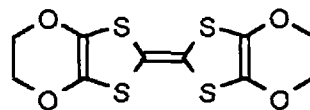
The length of the counteranion also influences the solid-state structure and so by increasing the length of the anion, the intermolecular interactions and T_c increase Thus the need for a longer anion resulted in the preparation of κ -(BEDT-TTF)₂Cu(NCS)₂ which was the first ambient pressure organic superconductor based on BEDT-TTF with $T_c=10.4\text{ K}$ ⁴⁴ κ -(BEDT-TTF)₂Cu(NCS)₂ was superconducting up to 10.4 K at atmospheric pressure and led to the development of κ -(BEDT-TTF)₂Cu[N(CN)₂]X salts (X=Br, $T_c=11.6\text{ K}$ ⁴⁵ and X=Cl, $T_c=12.5\text{ K}$ at 0.3 kbar¹²)

Superconductivity has also been discovered in cation radical salts of the unsymmetrical BEDT-TTF derivatives, dimethyl(ethylenedithio)diselenodithiafulvalene (DMET, 32a)⁴⁶ and methylenedithiotetrathiafulvalene (MDT-TTF, 32b)⁴⁷ The salts of these donors exhibit similar packing to that of κ -(BEDT-TTF)₂Cu(NCS)₂



(32) a X=Se, R¹=R²=Me, R³-R⁴=-S(CH₂)₂S-

b X=S, R¹=R²=H, R³-R⁴=-SCH₂S-



(33)

Within the TTF family the organic metallic state has been achieved with unsubstituted and various substituted sulphur, selenium and tellurium heterocycles The superconducting state however, has only been achieved with derivatives like TMTSF and BEDT-TTF with the highest superconducting transition temperature ($T_c=12.5\text{ K}$) recorded for (BEDT-TTF)₂Cu[N(CN)₂]Cl¹² Therefore electron donors that are structurally similar to BEDT-TTF were investigated This led to the first oxygen-containing donor, BEDO-TTF (33)⁴⁸

The stabilisation of the superconducting state depends on the inter- and intra-stack chalcogen interactions, and it was thought that changing a sulphur atom to a smaller, less polarizable oxygen atom would affect these interactions Also if organic superconductors were BCS superconductors it was expected that a change to a lower atomic mass chalcogen would raise the T_c (BCS isotope effect) and decrease the bandwidth, the density of states near the

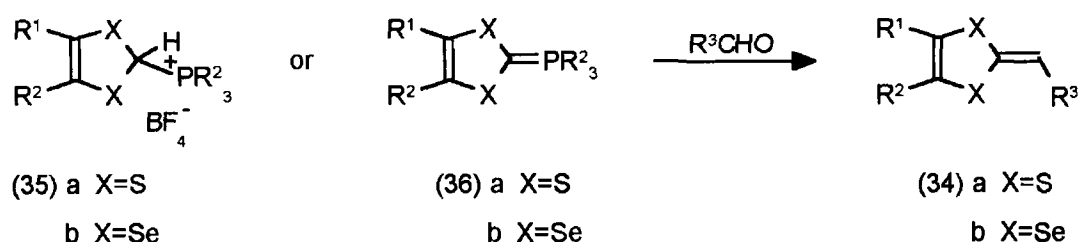
Fermi level would go up and T_c would be raised. Thus the discovery of an oxygen containing superconductor would expand the range of organic superconductors available and establish a link with high temperature oxide superconductors. But in contrast to this the $(BEDO-TTF)_2 4I_3$ salt increases the bandwidth and stabilises the metallic state down to low temperatures,⁴⁹ the stability being due to enhanced overlap between the fulvalene sulphur atoms [analogous to the $(TMTSF)_2X$ fulvalene chalcogens] and decreased steric bulk of the ethylenedioxo relative to the ethylenedithio functionality. Therefore the oxygen atom enhances the intermolecular interaction through electronic and steric factors. Radical salts of BEDT-TTF have the highest superconducting transition temperature (T_c) and it was expected that similar radical salts with superconducting properties could be prepared electrochemically from BEDO-TTF. BEDO-TTF forms many metallic salts with inorganic anions but only $\beta-(BEDO-TTF)_3Cu_2(NCS)_3$ and $(BEDO-TTF)_2ReO_4(H_2O)$ are superconducting at ambient pressure and below 1K and 2.5K respectively.⁵⁰

In conclusion, BEDT-TTF has the ability to form two-dimensional electrical conductors and superconductors and in contrast with other electron donors it has formed the largest number of superconducting and metallic cation-radical salts.

1 B 3 π -Extended TTF Derivatives

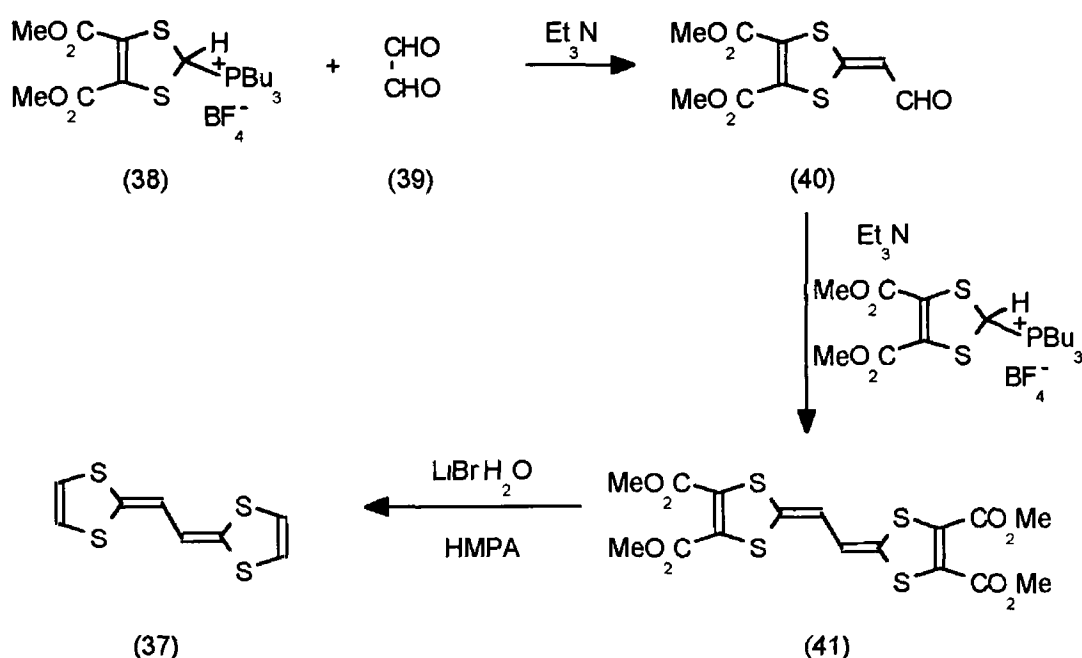
The design of highly conductive organic materials requires (i) radical ions based on chalcogenfulvalenoids, for example TTF-TCNQ and $(TMTSF)_2PF_6$, and (ii) minimisation of the Coulombic repulsion in the doubly ionised state.⁵¹ Considering these two conditions, the possibility of synthesising alternative donors by introducing heterocyclic or vinylic spacer groups between the two 1,3-dithiole rings in TTF in an attempt to increase its electron-donating ability was investigated. Extending the π -conjugation between the two 1,3-dithiole rings lowers the oxidation potential of the donor due to increased delocalisation of the positive charge and stabilises the dication state (relative to TTF) by reducing the intramolecular Coulombic repulsion (smaller ΔE values). These systems are of interest because they should display different redox and conformational properties compared to TTF.

Extended TTF derivatives (34) have been prepared by either the Wittig or Wittig-Horner reaction of a 1,3-dithiole (35a) or a 1,3-diselenole phosphonium salt (35b) or phosphorane (36) with an aldehyde (scheme 1.9).



Scheme 1 9

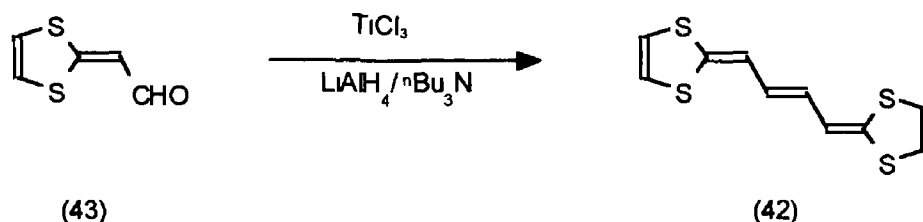
The first vinylogue of TTF, ethanedithiolene-2,2'-bis(1,3-dithiole) (EDBDT, 37), in which the two 1,3-dithiole rings were connected by sp^2 hybridised carbons was synthesised in 1983 by Yoshida and co-workers⁵² The phosphonium salt (38) was reacted with glyoxal (39) in the presence of triethylamine to give aldehyde (40) which was subsequently reacted with another molecule of (38) and triethylamine to give the carbomethoxy derivative (41) (scheme 1 10) Subsequent demethoxycarbonylation using lithium bromide/hexamethylphosphoramide treatment (HMPA) yielded EDBDT (37)



Scheme 1 10

Soon after the preparation of EDBDT, an analogous donor, 1,4-butenedithiolene-2,2'-bis(1,3-dithiole) (BDBDT, 42), in which four sp^2 carbons separate the two dithiole rings was prepared similarly by the same group⁵³ via reductive coupling of an aldehyde (McMurry-type coupling) (scheme 1 11) Contrary to TTF [first half-wave reduction potential ($E^1_{1/2}$)=+0.34 V, second half-wave reduction potential ($E^2_{1/2}$)=+0.71 V] and EDBDT ($E^1_{1/2}$ =+0.20 V,

$E^2_{1/2}=+0.36$ V), BDBDT has only one reversible redox wave (+0.22 V) attributed to a one-step two-electron oxidation probably due to the larger decrease of the Coulombic repulsion [smaller ΔE ($E^1_{1/2}-E^2_{1/2}$) value] of the doubly ionised state of BDBDT compared to TTF (+0.37 V) and EDBDT (+0.16 V)

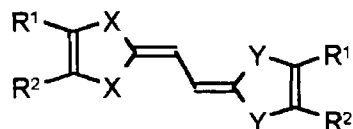
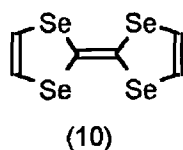


Scheme 1.11

Tetraselenafulvalene (TSF, 10) forms a much higher electrically conducting complex with TCNQ (σ_{IT} 800 Scm^{-1}) than TTF (σ_{IT} 500 Scm^{-1}) and it has a metal-to-semiconductor transition at 40K, 18K lower than TTF-TCNQ. Therefore it was expected that π -extended selenium analogues would be stronger donors than their TTF counterparts. Thus, the first selenium vinylologues of TTF, ethanedithiolene-2-(1,3-dithiole)-2'-(1,3-diselenole) (44a, $E^1_{1/2}=+0.26$ V, $E^2_{1/2}=+0.40$ V) and ethanedithiolene-2,2'-bis(1,3-diselenole) (44b, $E^1_{1/2}=+0.33$ V, $E^2_{1/2}=+0.47$ V) were prepared⁵⁴ by the same synthetic sequence shown in scheme 1.10. Compared to EDBDT, (44a) and (44b) have more positive oxidation values, the order being EDBDT < (44a) < (44b) which implies that oxidation is more difficult as the number of selenium atoms is increased. However the ΔE value remains almost unchanged with selenium replacement. Both of these donors form 2:3 (D:A) C-T complexes with TCNQ, i.e. (44b)₂-TCNQ₃, 0.24 Scm^{-1} and (44a)₂-TCNQ₃, 0.072 Scm^{-1} .

The EDBDT skeleton has been modified by the attachment of peripheral chalcogen atoms (e.g. sulphur and selenium) in the search for new electron donors. The TTF derivative, BEDT-TTF forms organic superconductors with increased dimensionality and so, by increasing π -conjugation between the 1,3-dithiole rings, higher T_c organic superconductors may be possible. The BEDT-TTF vinylologue (44c) was prepared simultaneously by three groups⁵⁵ by reacting a vinylous aldehyde with a 1,3-dithiole phosphonate anion. Extending the π -conjugation in BEDT-TTF reduces the difference (ΔE) between the two redox waves (i.e. there is reduced intramolecular repulsion) and lowers the first and second oxidation potentials of (44c) which indicates that it is a stronger donor than BEDT-TTF. In addition to this a range of vinylous donors

(45a-c) which contain two or four sulphur atoms at the periphery of the EDBDT system have been prepared⁵⁶ and were shown to have lower $E^1_{1/2}$ and $E^2_{1/2}$ values compared to the parent fulvalene EDBDT with the separation between these values reduced to ca 0.2 V in the vinylogues



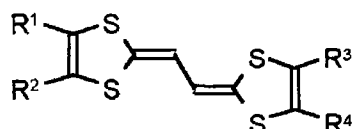
(44) a X=S, Y=Se, R¹=R²=H

b X=Y=Se, R¹=R²=H

c X=Y=S, R¹-R²=-S(CH₂)₂S-

d X=Y=S, R¹-R²=-Se(CH₂)₂Se-

π -Extended TTF derivatives (45d-f) with peripheral alkyl/seleno substituents on the EDBDT system have been prepared also,⁵⁷ the key step being the Wittig-Horner reaction of a vinylogous aldehyde with a phosphonate anion.^{52, 55} All the compounds exhibited two one-electron oxidations (sequential formation of the radical cation and the dication species). The selenium donor (44d) in contrast to compounds (45d-f) showed a single two-electron reduction (dication to neutral species). Similar to the other vinylogues (44c, 45d-f), these show a reduction in $E^1_{1/2}$ and $E^2_{1/2}$ values as well as a reduction in ΔE . All of these compounds formed C-T complexes with TCNQ.



(45) a R¹=R²=SMe, R³=R⁴=H

b R¹=R²=SMe, R³=R⁴=Me

c R¹-R²=-S(CH₂)₃S-, R³=R⁴=H

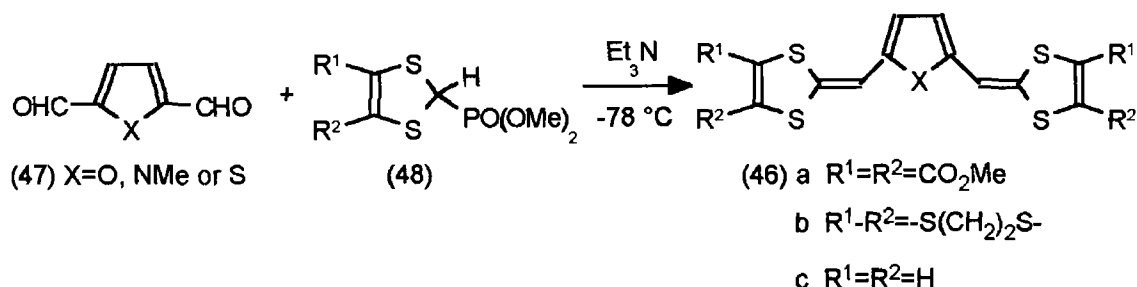
d R¹=R²=R³=R⁴=SeMe

e R¹-R²=-Se(CH₂)₂Se-, R³=R⁴=Me

f R¹-R²=-Se(CH₂)₂Se-, R³=R⁴=SeMe

Modification of the BDBDT skeleton by replacing the central double bond of BDBDT with a heterocyclic ring system (furan, pyrrole or thiophene) gave the π -extended TTF analogues (46). These analogues were prepared via the Wittig-Horner reaction of the appropriate dialdehyde (47) with the corresponding phosphonates (48) in the presence of triethylamine⁵⁸ and have

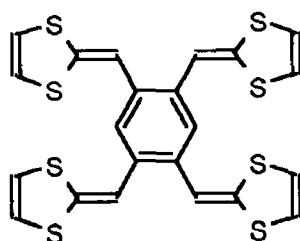
low oxidation potentials and reduced symmetry, desirable properties for the preparation of organic donors (scheme 1 12)



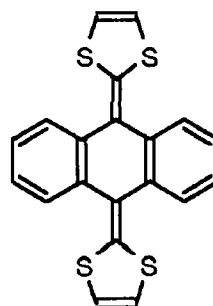
Scheme 1 12

These TTF derivatives are viewed as two dithiole rings separated by four carbon-carbon double bonds. There should be no difference between the $E^1_{1/2}$ and $E^2_{1/2}$ values as is seen in the furan derivative ($E^1_{1/2}-E^2_{1/2}=0.0\text{ V}$). Except for the furan derivative, all the compounds showed two oxidation waves. The pyrrole derivative has the highest value for ΔE because in the cation radical, the nitrogen atom bears the positive charge better than the oxygen or sulphur atom of the furan and thiophene derivatives respectively. The redox properties of these donors is strongly influenced by the heterocyclic spacer leading to separate one-electron oxidations. Therefore from the results the heteroatom and the heterocyclic ring has a strong influence on the oxidation process.

Many more TTF derivatives, prepared by Wittig or Wittig-Horner reaction⁵⁹ yielded extended TTFs which are hybrids of TTF and vinylogous TTFs (i.e. they consist of three or four 1,3-dithiole rings). Examples of these include (49) and (50). These donors showed a decrease in the on-site Coulombic repulsion due to a greater separation of the charges in the oxidised states of the donor in addition to increasing their dimensionality through S-S intra- and inter-chain contacts. Compound (49) formed C-T complexes with TCNQ and inorganic anions $Bu_4N^+X^-$ ($X=ClO_4, BF_4, I_3$).



(49)



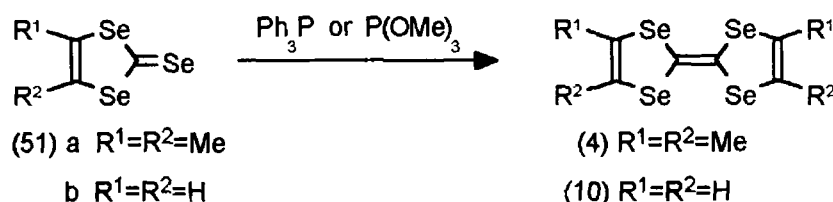
(50)

1 B 4 Selenium and Tellurium Organic Metals

The discovery of TTF-TCNQ as the first organic metal stimulated increased interest in the preparation of analogous derivatives that have improved metallic properties. One area which has been investigated is the replacement of the sulphur atom in TTF with a heavier chalcogen atom (i.e. selenium or tellurium) and its effect on the solid state structure, electrical conductivity and optical properties of complex salts derived from these donors. It was envisaged that this replacement would (i) increase the dimensionality of these systems due to the spatial increase of the chalcogen orbitals in the intrastack direction in order to circumvent the metal-to-insulator transition present in quasi-one-dimensional conductors, (ii) increase the intrachain interaction to produce a wider bandwidth metal (because of the increased overlap of the larger and more diffuse p_z π -orbitals and d orbitals on the chalcogen) and higher electrical conductivity but give a lower transition temperature to a superconducting state than the corresponding sulphur compound and (iii) reduce the on-site Coulombic repulsion due to the more polarizable selenium or tellurium atom and change the ionisation potential of the donor which thus changes the band filling.

1 B 4 1 Selenium derivatives

Since the preparation of TTF-TCNQ, attempts have been made to enhance the metallic properties of the tetrathiafulvalenium radical cation by replacing the hydrogen atoms on TTF with electron-donating substituents but such substitution distorted the original TTF-TCNQ crystal structure. Therefore to improve the metallic properties and hence the electron donating properties, the selenium analogues, tetraselenafulvalene (TSF, 10)⁶⁰ and tetramethyltetraselenafulvalene (TMTSF, 4)⁶¹ were synthesised by phosphine or phosphite coupling of the appropriate selenone (51) (scheme 1 13).

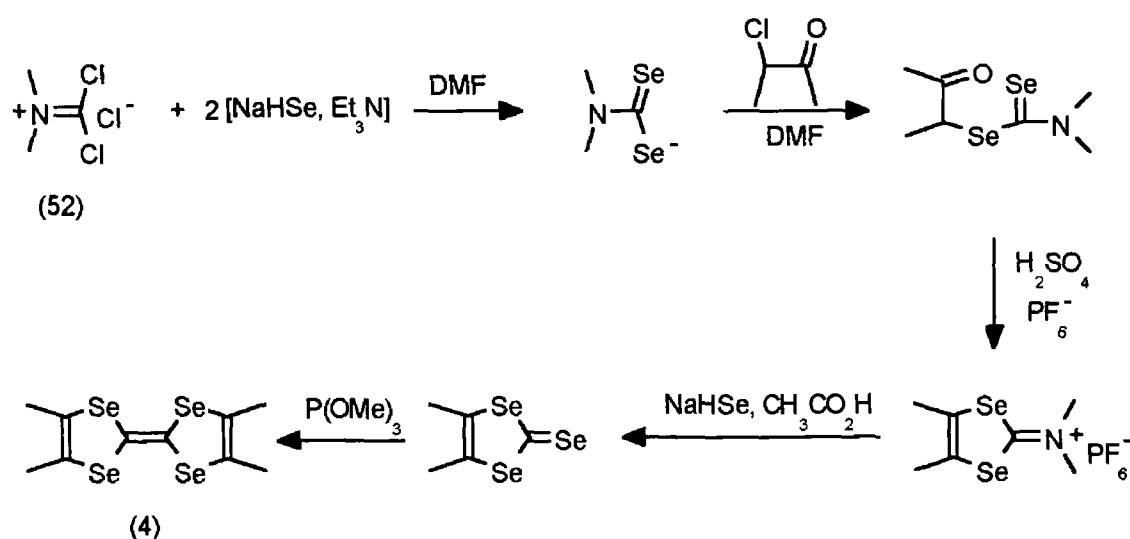


Scheme 1 13

The larger and more polarizable selenium atom reduces the Coulombic repulsions and increases electronic interactions possibly by enhanced overlap

between the cation radicals. The selenium compounds also have higher oxidation potentials than the corresponding sulphur analogues. This modification has kept the steric requirements of the original TTF-TCNQ structure constant.

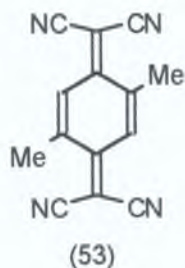
However, this method of preparation⁶¹ uses malodorous carbon diselenide. An alternative method for the preparation of TMTSF (4) was the reaction of *N,N*-dimethylphosgene iminium chloride (52) with piperidinium hydrogen selenide in the presence of base.⁶² But this involved the use of highly toxic hydrogen selenide. A modification of this procedure was found,⁶³ using (52) and elemental selenium (scheme 1 14). This is the preferred route to TMTSF (4).



Scheme 1 14

TSF, TMTSF and HMTSF form C-T complexes with TCNQ^{60, 61, 64} which were more metallic ($\sigma_{\text{IT}} \sim 800\text{--}2000 \text{ Scm}^{-1}$) than TTF-TCNQ ($\sigma_{\text{IT}} 500 \text{ Scm}^{-1}$). The TSF C-T complex had a metal-to-semiconductor transition at 40K, 18K lower than TTF-TCNQ but the HMTSF C-T complex was the most interesting because it behaved like a semimetal and did not become an insulator at low temperature.

Another milestone in the development of organic metals was the discovery that conductivity in the C-T complex between TMTSF and 2,5-dimethyl-tetracyano-*p*-quinodimethane (DMTCNQ, 53) was stabilised under pressure (13 kbar) down to 1K and at ambient pressure a sharp metal-to-insulator transition occurs at 42K.⁶⁵



However, results from magnetic measurements suggested⁶⁶ that the driving force for this transition resided on the TMTSF stacks. As a result of this, Bechgaard and co-workers synthesised a family of C-T salts based on TMTSF (Bechgaard salts),¹⁰ containing monovalent charge-compensating anions. These $(\text{TMTSF})_2\text{X}$ salts were prepared by electrochemical oxidation according to equation (5):



The $(\text{TMTSF})_2\text{X}$ salts ($\text{X}=\text{NO}_3^-$, PF_6^- , AsF_6^- , SbF_6^-) exhibited high electrical conductivities (at temperatures $<20\text{K}$) of $\sim 10^5 \text{ Scm}^{-1}$ and low temperature metal-to-insulator transitions ($12\text{-}18\text{K}$) whereas the BF_4^- salt had a metal-to-insulator transition at 40K . The application of hydrostatic pressure (12 kbar) to suppress the metal-to-insulator transition (Peierls-type transition) led to the discovery⁶⁷ of the first organic superconductor $[(\text{TMTSF})_2\text{PF}_6]$, $T_c \sim 0.9\text{K}$. This was followed soon after by the first zero pressure organic superconductor $(\text{TMTSF})_2\text{ClO}_4$ ($T_c \sim 1.2\text{K}$).²³

In the $(\text{TMTSF})_2\text{X}$ salts there was no evidence of a Peierls transition typical of one-dimensional conductors.⁶⁸ Instead a SDW distortion causes the metal-to-insulator transition. The reason for the existence of SDW instead of CDW is not clear but Wudl⁶⁹ explained it on the basis of the "spin-charge separation and charge-localisation" hypothesis. This hypothesis was based on two premises: (i) separation of spin and charge in the radical ion (inhomogeneous charge and spin distribution in TMTSF and a decrease in conjugation due to mismatch of carbon-selenium orbital size), and (ii) polarisation of the positively charged π -molecular orbital of TMTSF molecules in one crystallographic direction by adjacent anions. This hypothesis was further substantiated by comparing the isostructural $(\text{TMTSF})_2\text{X}$ and $(\text{TMTTF})_2\text{X}$ salts.^{68, 70} The $(\text{TMTSF})_2\text{X}$ salts have higher room temperature conductivities and lower metal-to-insulator transition temperatures than their sulphur counterparts.

The crystal and molecular structures of $(\text{TMTSF})_2\text{X}$ conductors were important in understanding their electrical properties and providing information regarding the design constraints for new conducting materials. The salts of this series are isostructural, with the same uniform stack of planar TMTSF molecules which stack in a characteristic zigzag pattern forming quasi-one-dimensional chains that parallel the axis of highest conductivity (a axis) (figure 1.12). In contrast to TCNQ-based organic metals, the metallic properties and superconductivity in the $(\text{TMTSF})_2\text{X}$ salts are due to selenium intermolecular orbital overlap.

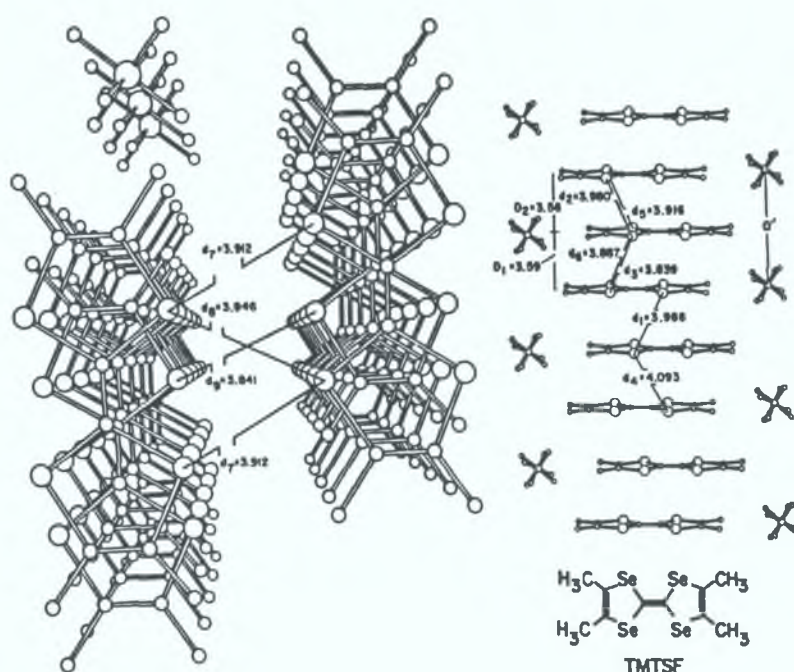


Figure 1.12 Crystal structure of $(\text{TMTSF})_2\text{BrO}_4$ salt, viewed down the stacking direction (left) and showing the zigzag stacking of TMTSF molecules (right).

The TMTSF stacks are arranged in two-dimensional molecular sheets which extend in the ab plane and the selenium atoms have fairly close interstack contact [less than the sum of the van der Waals radii for selenium (4.0 Å)]. Crystallographic studies also revealed the existence of an infinite sheet network of selenium-selenium interactions between the TMTSF molecules within which there are short ($d < 4.0$ Å) interstack selenium-selenium interactions (figure 1.12). In $(\text{TMTSF})_2\text{X}$ compounds intra- and inter-stack selenium-selenium distances are similar at room temperature (~ 3.9 – 4.0 Å compared to 4.0 Å for van der Waals radius sum). As the temperature is lowered from 298K to 125K, the ratio of decrease of the selenium-selenium

distances in the interstack direction is approximately twice that compared to the intrastack direction. This leads to increased interchain bonding and electronic delocalisation through the selenium atom network as the temperature is lowered.⁷¹ The interchain coupling is important in understanding the properties of the $(\text{TMTSF})_2\text{X}$ salts.

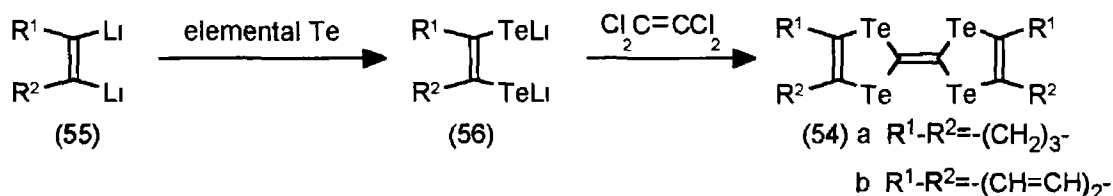
The TMTSF molecules do not form a complete three-dimensional network because the sheets are separated along the c axis by anions. The anions appear to have no role in the conduction process but influence the properties by controlling the band filling. The origin of the insulating state seems to be related to the symmetry of the anion. When the anion is highly symmetric (octahedral or tetrahedral) the network of selenium-selenium distances expands and contracts as the size of the anion is varied. This expansion is accompanied by changes in the crystallographic unit cell volume, V_c , which controls the average selenium-selenium distances and so pronounced changes in the electrical properties occur. The tetrahedral anions are smaller than the octahedral anions and this results in closer packing of the solid. The tetrahedral anion can either introduce anion order which may open a gap at the Fermi level or anion disorder which may prevent metal-to-insulator transition. In $(\text{TMTSF})_2\text{ClO}_4$ there is no evidence for ordering and it remains metallic down to $\sim 1.2\text{ K}$ where the material becomes superconducting. The suppression of the metal-to-insulator transition is ascribed to close packing and disorder effects.

An unusual aspect of the crystal structures of $(\text{TMTSF})_2\text{X}$ systems is the contact between peripheral atoms of the anions and the hydrogen atoms of the methyl groups of TMTSF and this may be related to the anion-ordering transitions.⁷² The anions in these systems reside in a "methyl group hydrogen atom cavity". Therefore the synthesis of new superconducting materials requires anions that interact with the methyl groups in such a fashion that they produce anion-ordered derivatives.

1 B 4 2 Tellurium derivatives

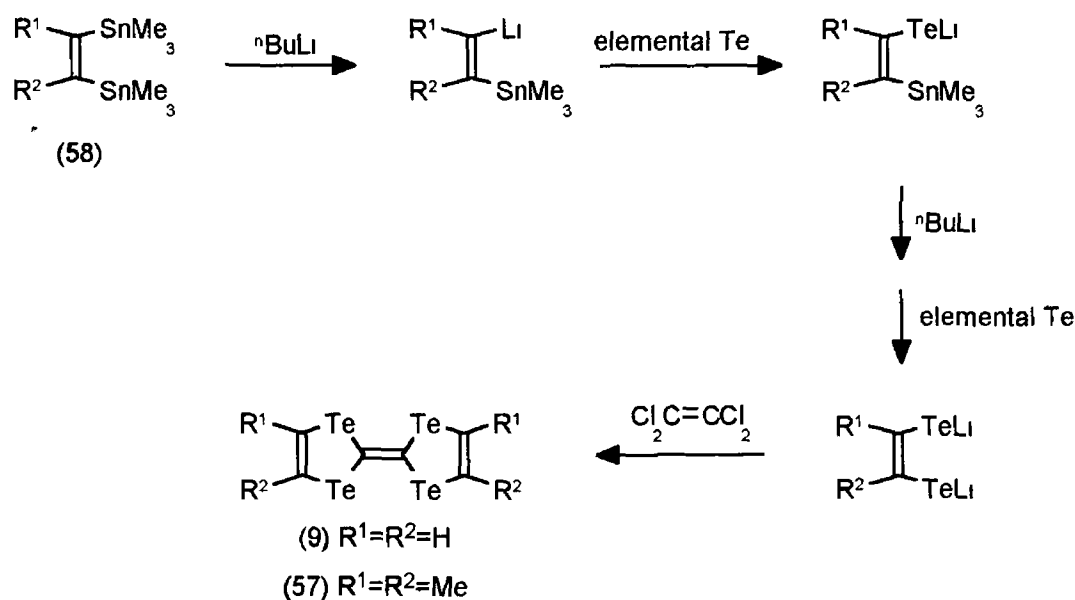
Tellurium analogues of TTF are of synthetic interest because the metals formed from tellurium donors have wider bandwidths and lower density of states (same number of levels spread over a larger energy) than the corresponding selenium or sulphur analogues and it was thought that the tellurium analogues might also expect to have lower superconducting transition temperatures. However, compared to sulphur and selenium derivatives, the number of derivatives containing tellurium atoms is limited due to synthetic difficulties encountered with tellurium chemistry.

The first tellurium electron donors, hexamethylenetetratellurafulvalene (HMTTeF, 54a)⁷³ and dibenzotetratellurafulvalene (DBTTeF, 54b)⁷⁴ were prepared similarly in 1982 by reacting a 1,2-dilithio compound (55) with elemental tellurium to give 1,2-dilithioditelluride (56). Compound (56) was reacted with tetrachloroethylene at -78 °C to give DBTTeF and HMTTeF in 36% and 10% yield respectively (scheme 1 15)



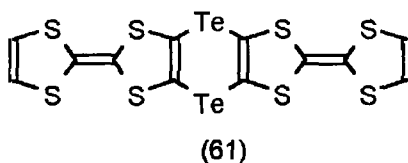
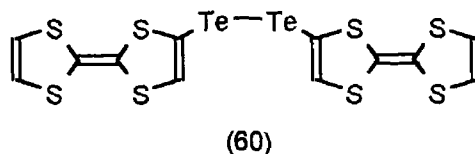
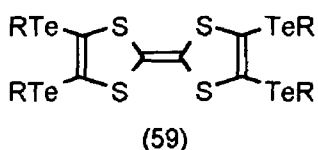
Scheme 1 15

However, this method was not useful for the synthesis of tetratellurafulvalene (TTeF, 9) or TMTTeF (57). In contrast to TMTTeF (which is still unknown), TTeF has been prepared⁷⁵ via a transmetallation reaction using a distannylalkene, 1,2-bis(trimethylstannyl)ethylene (58), to yield TTeF in 36% yield (scheme 1 16). The yield of TTeF was limited by the equilibrium of the transmetallation reaction and also by the reaction of tetrachloroethylene which gives polymeric products. However, a recent synthetic study of TTeF⁷⁶ has resulted in an optimized preparation and a reduction in by-product formation. TMTTeF, on the other hand, could not be prepared from an acyclic dibromide because metal halogen exchange yields an acetylene due to the elimination of lithium bromide.



Scheme 1 16

In addition to these tellurium containing donors, tetraalkyltellurium (59)^{34a} and ditelluride derivatives (60)^{77a} and (61)^{77b} have also been synthesised. Compound (59) forms a mixed stack complex with TCNQ, having a room temperature conductivity of $\sim 10^{-2} \text{ Scm}^{-1}$.



HMTTeF, DBTTeF and TTeF all exhibited two reversible one-electron oxidations of ($E^1_{1/2}=+0.40 \text{ V}$, $E^2_{1/2}=+0.69 \text{ V}$), ($E^1_{1/2}=+0.71 \text{ V}$, $E^2_{1/2}=+1.05 \text{ V}$) and ($E^1_{1/2}=+0.59 \text{ V}$, $E^2_{1/2}=+0.84 \text{ V}$) respectively. Compared to their sulphur and selenium counterparts these tellurium analogues have the smallest ΔE values, the order being $\text{S} > \text{Se} > \text{Te}$ and so there was no correlation between the oxidation potential and the size of the heteroatom. Thus Wudl and Aharon-Shalom suggested⁷³ that the ionisation of the sulphur fulvalene occurs primarily from the π -bonded network and that in the tellurium fulvalene it originates from the tellurium lone pairs. However, this explanation seems less likely than the one given by Lerstrup and co-workers who suggested⁷⁴ that the ionisation was influenced by two factors which have opposite effects in the series sulphur, selenium, tellurium. These are the valence state ionisation potentials and the differences in their orbital interactions with carbon. Thus the resonance integral $\beta_{\text{C-X}}$ becomes smaller due to larger C-X bond distances ($\text{X}=\text{S}$, Se or Te), and this stabilises the HOMO making it harder to remove an electron. However, the valence state ionisation potentials decrease in the series S , Se , Te and has the opposite effect to that caused by β , i.e. it is easy to remove an electron and this may account for the unusual trend in $E_{1/2}$ values. The value of ΔE decreases in the series $\text{S} > \text{Se} > \text{Te}$ which suggests that the intramolecular Coulomb repulsion energy decreases in the order $\text{Te} < \text{Se} < \text{S}$.⁷⁸

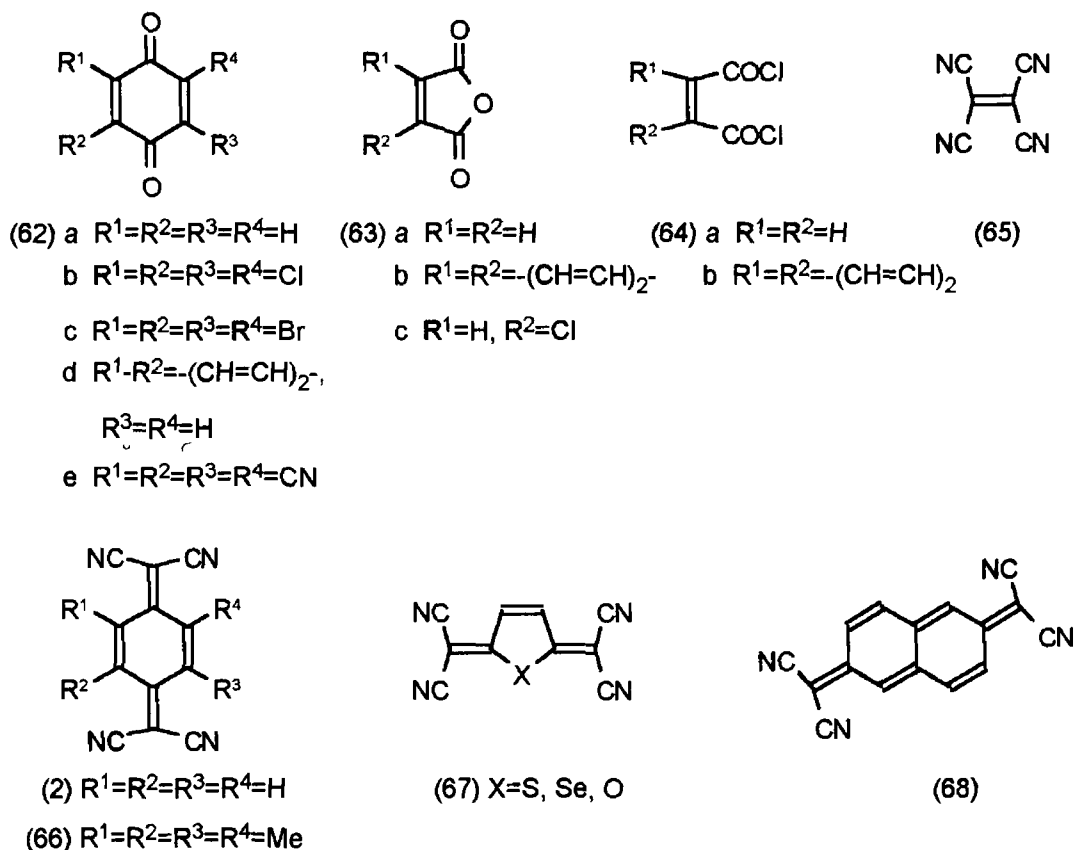
In contrast to DBTTeF and TTeF, for which few metallic complexes have been prepared, HMTTeF has formed C-T complex salts $[(\text{HMTTeF})_n\text{X}]$ with inorganic anions ($\text{X}=\text{Cl}^-$, Br^- , I^- , PF_6^- , AsF_6^- and ClO_4^-) and with TCNQ.⁷³ The PF_6^- , AsF_6^- and ClO_4^- salts were semiconductors whereas the TCNQ complexes form both conducting and semiconducting crystals.⁷⁹

As seen from the above information numerous TTF derivatives are now available. These derivatives offer a wide range of steric and electronic variations on the TTF molecule ranging from substitution of sulphur atoms with selenium or tellurium to derivatives with fused heterocyclic rings and extended π -orbital frameworks. The search for new organic conductors and superconductors is still active with the main emphasis on the solid state properties of TTF salts and ultimately higher temperature organic superconductors.

1 C Electron Acceptors

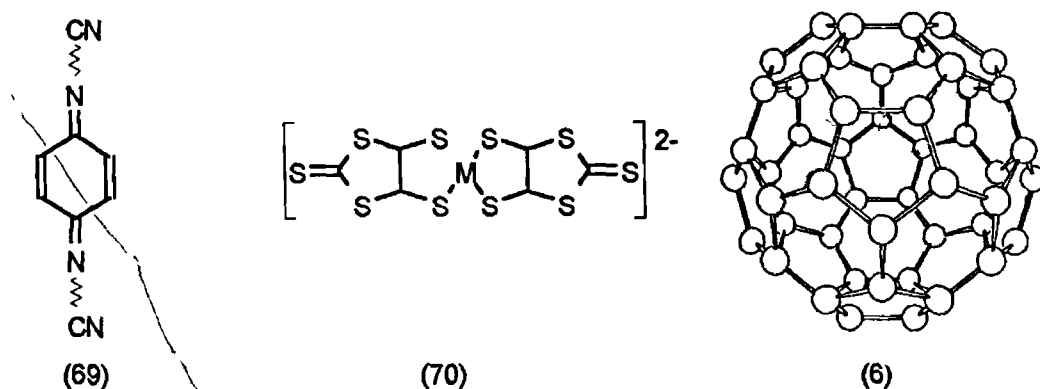
1 C 1 Introduction

The development of electron acceptors with planar geometry and a delocalised π -electron system is a prerequisite for the formation of C-T complexes. Many organic compounds function as acceptors in C-T complexes, among the most common being *p*-benzoquinone and its derivatives (62),⁸⁰ anhydrides of carboxylic acids and their halogenated derivatives (63)^{80b} and acid chlorides (64).^{80b} However, it was the presence of the powerful electron-withdrawing cyano group and its inferred high electron affinity that led to cyano-containing molecules being investigated as potential electron acceptors. The cyano-alkene, tetracyanoethylene (TCNE, 65) was one of the first to be investigated.⁸¹ It formed C-T complexes with a variety of donors and was the precursor to cyano-based acceptor molecules of today. Extending the conjugation between the cyano groups of TCNE led to the discovery of 7,7,8,8-tetracyano-*p*-quinodimethane (TCNQ, 2)⁷ which was one of the most extensively studied electron acceptors.²⁰



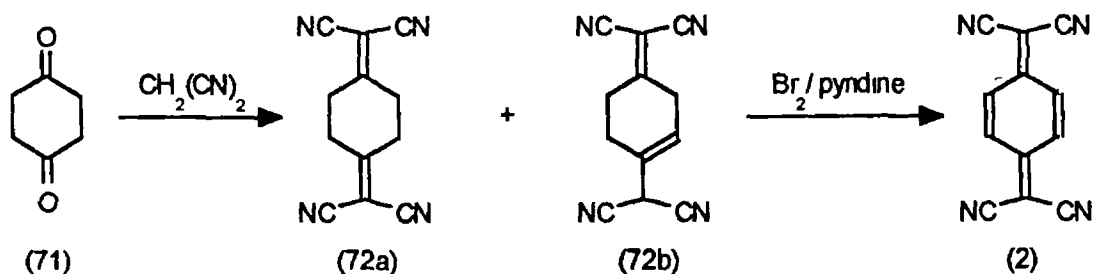
In addition to TCNE and TCNQ a large variety of electron acceptors containing the cyano group have been prepared. These include substituted (66), heterocyclic (67) and π -extended (68) TCNQ derivatives along with

N,N'-dicyanoquinonediimines (69) In recent years two other families of organic π -acceptor molecules, metal(DMIT)₂ (70) and buckminsterfullerenes (6), have been prepared Both of these form superconducting C-T salts



1 C 2 Synthesis and Properties of TCNQ

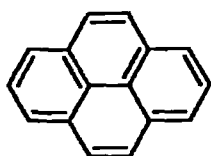
TCNQ was initially synthesised in 1960⁷ It was prepared by the condensation of cyclohexane-1,4-dione (71) with malononitrile followed by bromination/dehydrobromination of 1,4-bis(dicyanomethylene)cyclohexane (72a) in the presence of pyridine (scheme 1 17) Condensation in benzene solution in the presence of a small amount of acetic acid and ammonium acetate afforded a mixture of isomers (72a) and (72b) but condensation in aqueous solution in the presence of β -alanine afforded (72a) only



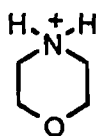
Scheme 1 17

The presence of four electron-withdrawing cyano groups and the planarity of TCNQ is responsible for its unique π -acid character It undergoes 1,6-addition⁷ as well as substitution reactions with nucleophiles⁸² In some cases the substitution reactions proceed via a one-electron transfer from donor to acceptor with the formation of an intermediate radical ion salt TCNQ also forms stable radical anions⁸³ and gives rise to C-T complexes with many organic and inorganic electron donors²⁰ These C-T complexes exhibit a wide range of electrical properties from insulators, pyrene-TCNQ,²⁰ to

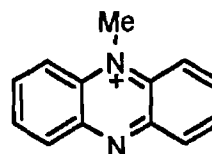
semiconductors, morpholinium-TCNQ,²⁰ to even metals, *N*-methylphenazinium-TCNQ⁸⁴



Pyrene



Morpholinium



N-Methylphenazinium

In the early 1960s conductivities as high as 10^2 Scm^{-1} were reported for C-T complexes of TCNQ²⁰ but it wasn't until the discovery of TTF-TCNQ⁹ that a major breakthrough in the field of C-T complexes occurred. The TTF-TCNQ C-T complex showed metallic conductivity ($\sigma_H=500 \text{ Scm}^{-1}$) with a maximum of $\text{ca } 10^4 \text{ Scm}^{-1}$ at 59K, where it undergoes a metal-to-insulator transition. The typical structural features that makes the TTF-TCNQ C-T complex so highly conducting is the planarity and high degree of symmetry of both molecules with π -delocalisation extending throughout. Both the ionisation potential of TTF and the electron affinity of TCNQ favour incomplete charge-transfer (0.59). The crystal structure of TTF-TCNQ¹⁷ consists of parallel columns of segregated stacked TTF and TCNQ molecules which are uniformly spaced (figure 1.13). Both TTF and TCNQ stack face-to-face with considerable π overlap. The strength of this overlap is indicated by a 3.17 Å stacking distance in the TCNQ \cdot^- column compared with 3.45 Å in neutral TCNQ and a 3.47 Å stacking distance in the TTF \cdot^+ column compared with 3.62 Å in neutral TTF. Within the TTF and TCNQ columns there is a 'ring-over-bond' overlap, i.e. the exocyclic carbon-carbon double bond lies over the ring of the molecule adjacent to it in the stack.¹⁷

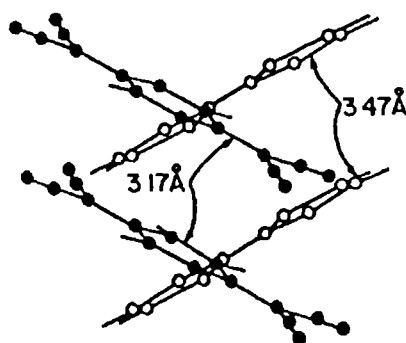
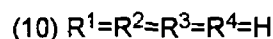
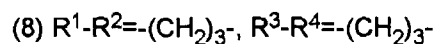
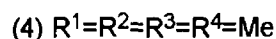
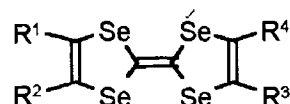
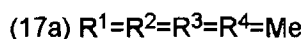
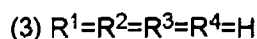
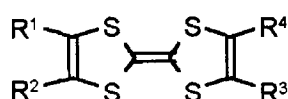


Figure 1.13 Crystal structure of TTF-TCNQ

C-T complexes of the electron donors tetramethyltetrafulvalene (TMTTF, 17a),²⁵ tetraselenafulvalene (TSF, 10),⁶⁰ tetramethyltetraselenafulvalene (TMTSF, 4)⁶¹ and hexamethylenetetraselenafulvalene (HMTSF, 8)⁶⁴ with TCNQ have also been prepared. These C-T complexes exhibited room temperature conductivities of ca. 10^3 , 800, 800 and 2000 Scm^{-1} respectively. The conductivity of the TSF-TCNQ complex rises to 10^5 Scm^{-1} at 40K and thus is a better conductor than the corresponding TTF complex. The HMTSF-TCNQ complex remains metallic as the temperature approaches zero.



Since the preparation of the TTF-TCNQ C-T complex and the discovery that TCNQ radical anions are semiconductors,^{7a} a lot of research has been devoted to the synthesis of new electron acceptors with enhanced electrical properties. The synthesis of TCNQ derivatives has followed three main routes:

(i) substitution of the hydrogen atoms on the parent TCNQ molecule with alkyl, alkoxy, thioalkyl, halogeno and cyano groups. This allows variation of band filling as well as interstack interactions and so the redox properties of TCNQ can be finely tuned.

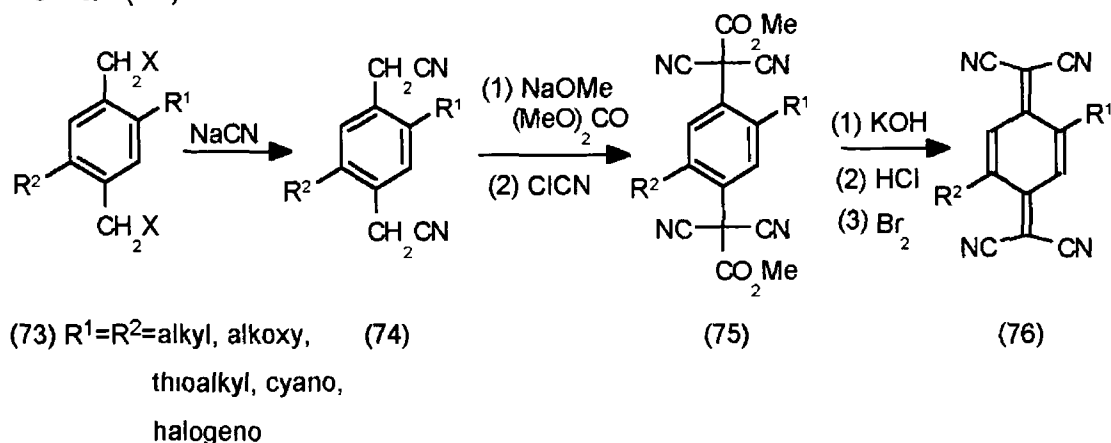
(ii) extension of the π system. This reduces the on-site Coulomb repulsion, thus leading to more stable radical anions and is important for attaining high electrical conductivity.

(iii) introduction of heteroatoms into the TCNQ moiety (heterocyclic-TCNQs). The heteroatoms reduce the on-site Coulomb repulsion and also participate in interheteroatom interactions which suppress the metal-to-insulator transition, leading to superior electrical conductivities in organic metals.

1 C 3 Substituted TCNQ Derivatives

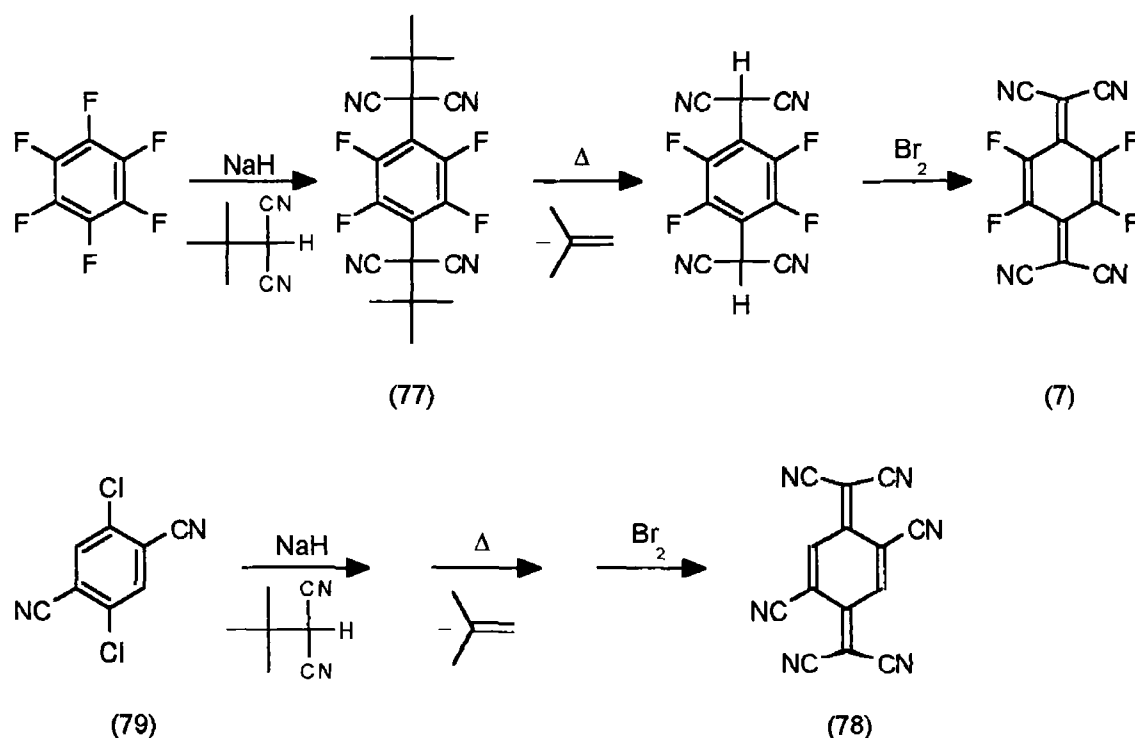
One of the early routes to substituted TCNQs proceeded from *p*-xylylene dihalides (73) via 1,4-di(cyanomethyl)benzene derivatives (74).⁸⁵

(scheme 1 18) This procedure involved the conversion of (74) into dimethyltetracyano-*p*-phenylenediacetate derivatives (75) followed by hydrolysis, decarboxylation and bromine oxidation to afford the substituted TCNQs (76)



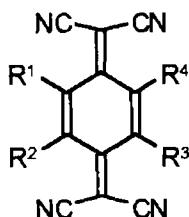
Scheme 1 18

TCNQ derivatives with alkyl, alkoxy, thioalkyl, halogeno and cyano substituents in the ring have been synthesised using this procedure^{85a} For example, tetrafluoro-TCNQ (7) was prepared by reacting hexafluorobenzene with *t*-butyl malononitrile in the presence of sodium hydride Thermolysis of the resulting product (77) followed by bromine oxidation gave compound (7) (scheme 1 19) 2,5-Dicyano-TCNQ (78) was similarly prepared from 2,5-dichloro-terephthalonitrile (79) (scheme 1 19)



Scheme 1 19

An alternative route to substituted TCNQs involved the condensation of alkyl cyclohexane-1,4-dione derivatives with malononitrile^{86, 85b} analogous to that used for the preparation of TCNQ. This procedure has been used for the synthesis of methyl-, 2,5-dimethyl- and 2,5-diethyl-TCNQ derivatives (80a-c). Derivatives (80d-f)^{85a} along with tetramethyl-TCNQ (80g) are also known.⁸⁷



(80) a $R^1=R^2=R^3=H$, $R^4=Me$

b $R^1=R^3=H$, $R^2=R^4=Me$

c $R^1=R^3=H$, $R^2=R^4=Et$

d $R^1=R^3=H$, $R^2=R^4=iPr$

e $R^1=R^3=H$, $R^2=OEt$, $R^4=OMe$

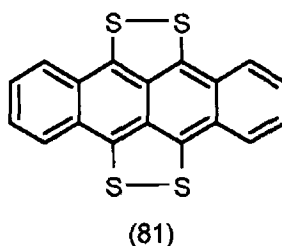
f $R^1=R^3=H$, $R^2=OPr$, $R^4=OMe$

g $R^1=R^2=R^3=R^4=Me$

1 C 3 1 C-T Complexes of Substituted TCNQ Derivatives

Wheland and Gillson prepared over eighty C-T complexes to investigate the factors required for high conductivity.¹⁸ The majority of acceptors in these C-T complexes were TCNQ derivatives and the electrical conductivity was correlated with redox potentials, heavy atom substitution and steric factors.⁸⁸ It was found that stronger acceptors (e.g. TCNQF₄, 7) for which complete electron transfer is most likely, gave poorly conductive complexes whereas the weaker electron acceptors (e.g. TCNQEt₂, 80c) gave highly conductive complexes. High conductivity was shown to be associated with moderately strong electron acceptors ($-0.02 \text{ V} < E_{1/2}^1 < +0.35 \text{ V}$) in combination with moderately strong donors ($-0.1 \text{ V} < E_{1/2}^1 < +0.4 \text{ V}$) such that the redox potentials are closely matched [$E_{1/2}^1(A) - E_{1/2}^1(D) < 0.25 \text{ V}$]. This correlation was subject to the strict requirements of crystal structure. High conductivity also required the anion or cation radical to stack on top of itself closer than van der Waals radii. Substitution of the TCNQ moiety with increasingly large groups appears to have only a minor effect until five to six side chain carbons or oxygens have been added. Beyond this point a breakdown in conductivity occurs. For example, the resistivities of the TTF complexes with diethyl- and diisopropyl-TCNQ derivatives (80c and d) increase from $0.1 \text{ } \Omega\text{cm}$ to $2.10 \text{ } \Omega\text{cm}$. Tetrathiatetracene (TTT, 81) forms a C-T complex with TCNQ(OMe)(OEt) (80e).

but does not complex with TCNQ(OMe)(ⁱOPr) (80f) Tetramethyl-TCNQ (80g), on the other hand, does not form C-T complexes with TTF, TMTTF or TMTSF ⁸⁷ This is due to distortion from planarity as a result of steric interaction of the methyl groups ⁸⁹



A comparison of the reduction potentials of the substituted TCNQs (table 1 1) shows that replacing the hydrogen atoms of TCNQ with alkyl groups results in poorer electron acceptors TMTCNQ (80g), in contrast to the mono- and 2,5-substituted derivatives, shows a single redox wave ($E^1_{1/2} = -0.405$ V) corresponding to a two electron process This coalescence of the first and second reduction potentials was attributed to its distortion from planarity ⁸⁷

Table 1 1 Cyclic Voltammetry Data for Substituted TCNQ Derivatives (measured in acetonitrile)

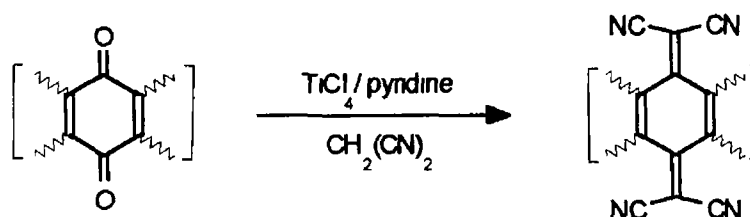
Compound	R ¹	R ²	R ³	R ⁴	$E^1_{1/2}/V$	$E^2_{1/2}/V$	Ref
	H	H	H	H	+0.19	-0.35	85b
	H	H	H	Me	+0.17	-0.34	85b
	H	Me	H	Me	+0.11	-0.35	85b
	H	Et	H	Et	+0.12	-0.365	85b
	Me	Me	Me	Me	-0.405 (2e ⁻)		87

1 C 4 Alternative Routes to TCNQ Derivatives

TCNQ derivatives have been synthesised from either cyclohexane-1,4-dione⁸⁶ or 1,4-di(cyanomethyl)benzene derivatives ^{85a} The latter procedure was tedious and used the electrophilic cyanating agent, cyanogen chloride for the formation of the dicyanomethylene group Thus alternative approaches to TCNQ derivatives were required, and the new methods subsequently developed were

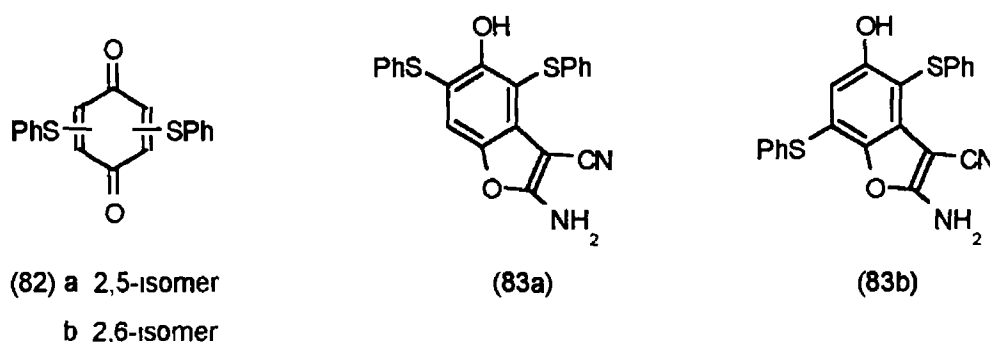
(i) *Bis(dicyanomethylenation) of 1,4-quinones using malononitrile and Lehnert's reagent (titanium tetrachloride and pyridine)*⁹⁰ (scheme 1 20)

This method affords ready replacement of the carbonyl group with a dicyanomethylene and is generally applicable^{87, 91} to tetrasubstituted derivatives. The titanium tetrachloride promotes nucleophilic addition specifically to the carbonyl by complexing with carbonyl oxygen and in doing so inhibits 1,4-additions to the carbon-carbon double bond.

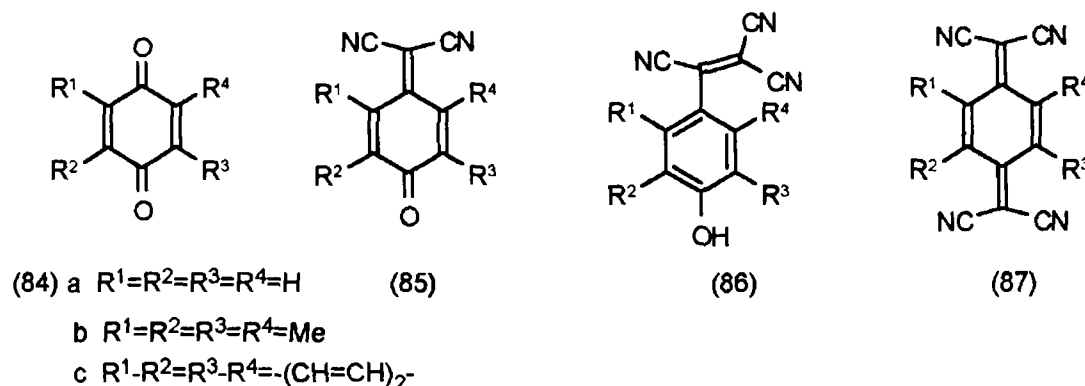


Scheme 1 20

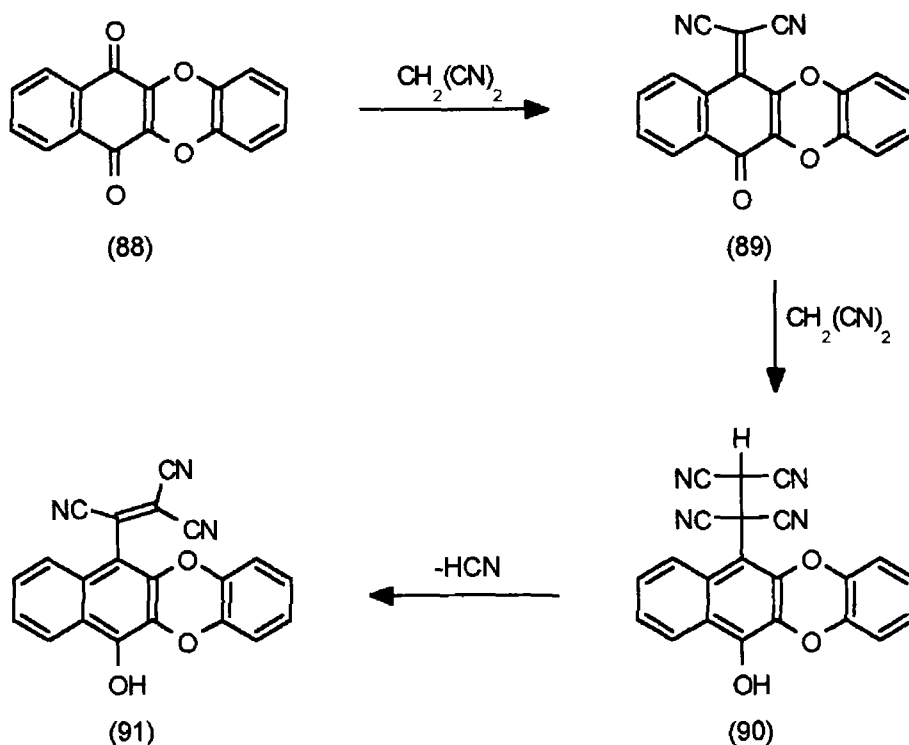
However, this method failed with bis(phenylthio)benzoquinones (82a) and (82b) affording the 1,4-addition products followed by cyclisation to yield (83a) and (83b) respectively⁹²



Recent investigations by Bryce and co-workers⁹³ showed that reaction of quinones (84) with malononitrile in the presence of Lehnert's reagent afforded mono-dicyanomethylated products (85) along with phenol products (86). This differs from previously reported data^{87, 94} which yielded TCNQ derivatives (87).



The phenolic products arise by 1,6-addition of malononitrile to quinomethanide system followed by 1,2 elimination of hydrogen cyanide. In the presence of Lehnert's reagent TCNQ formation (1,2-addition) is usually the major or sole pathway. However, Kini and co-workers⁸⁷ obtained phenolic products (86) along with TCNQ derivatives (87). Other workers also reported⁹⁵ that several derivatives of quinone (88) could not be converted into TCNQ derivatives using Lehnert's reagent. Instead, quinomethanides (90) and phenolic products (91) were isolated (scheme 1 21)

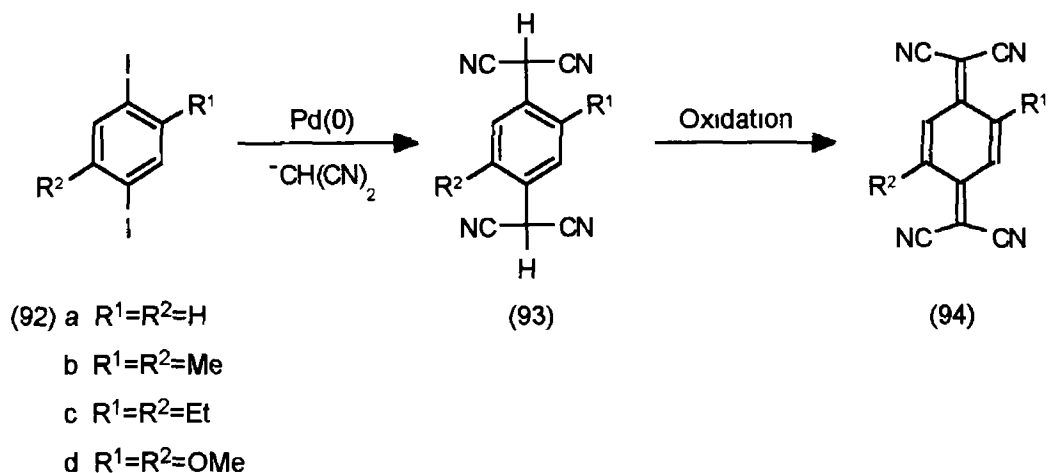


Scheme 1 21

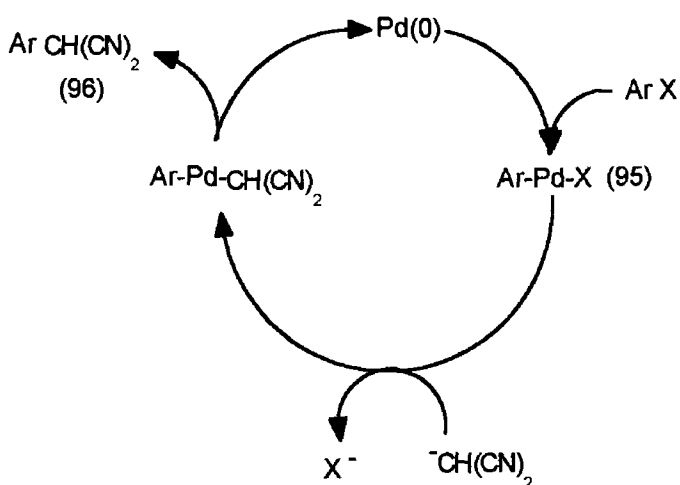
(ii) Palladium(0)-Catalysed Substitution of Dihaloarenes

1,4-Dihodobenzenes (92) react with malononitrile anion in the presence of a palladium catalyst to yield phenylenedimalononitrile derivatives (93) which are readily oxidised to yield the TCNQ system (94)^{89, 96a} (scheme 1 22). Heterocyclic-TCNQs have also been synthesised by this method.

The reaction pathway is postulated^{96b} as proceeding via the initially formed arylpalladium intermediate (95) which can undergo displacement of the halide when reacted with malononitrile anion. Rearrangement affords the coupled product (96) (scheme 1 23).



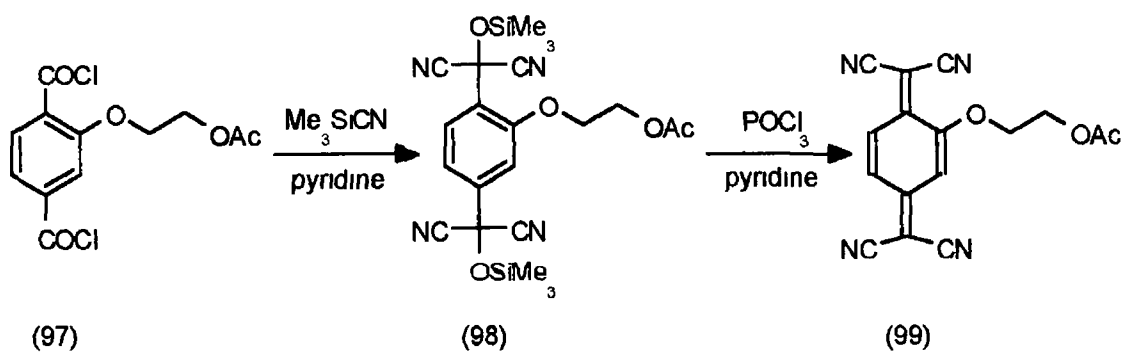
Scheme 1 22



Scheme 1 23

(iii) Cyanotrimethylsilylation/Desiloxylation of Terephthaloyl Chlorides

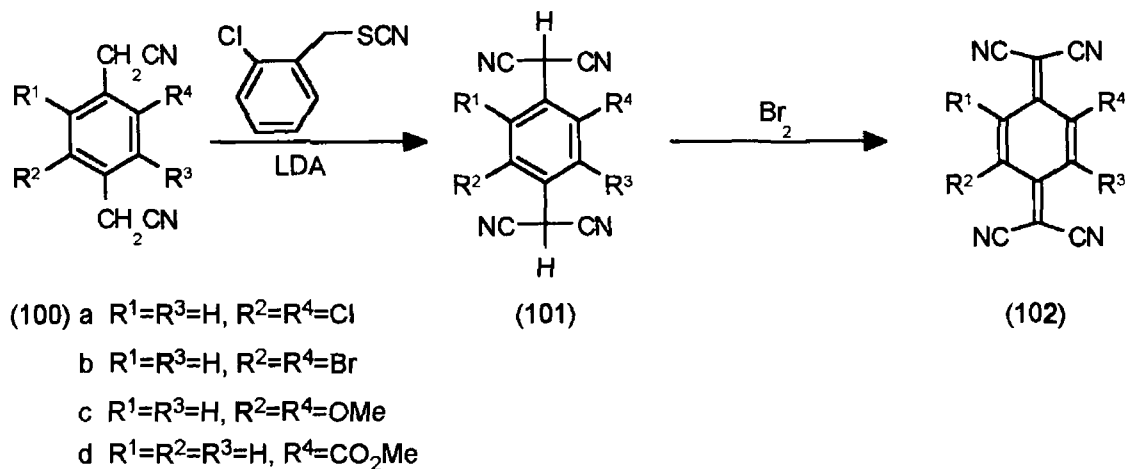
Terephthaloyl chlorides (97) react with an excess of cyanotrimethylsilane in the presence of pyridine to produce 1,4-bis[dicyano(trimethylsiloxy)methyl]benzenes (98) ⁹⁷ Treatment of (98) with phosphorus oxychloride yields the TCNQ derivatives (99) (scheme 1 24)



Scheme 1 24

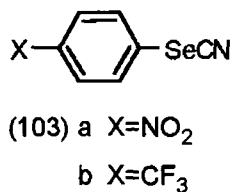
(iv) *Reaction of Arylacetonitrile Anions with an Electrophilic Cyanating Agent*

Reaction of 1,4-di(cyanomethyl)benzenes (100) with 2-chlorobenzyl thiocyanate in the presence of lithium diisopropylamine followed by bromine oxidation of (101) afforded the TCNQ derivatives (102)^{89, 98} (scheme 1 25)



Scheme 1 25

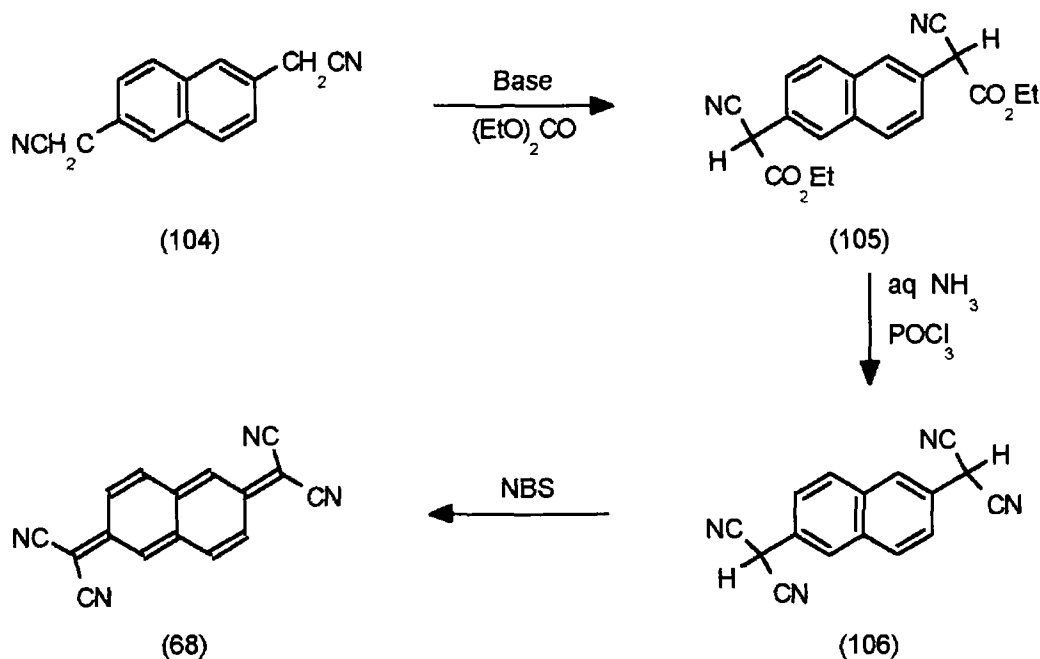
2-Chlorobenzyl thiocyanate in contrast to the other electrophilic cyanating agent, cyanogen chloride, does not react with the phenylmalononitrile anion to form the tricyanomethyl group. Thus there is no need to insert and then remove the ester groups (i.e. proceed via dimethyl tetracyano-*p*-phenylenediacetate derivatives) as was previously necessary^{85a}. In addition to this, electron-withdrawing, electron-donating and ring-fused TCNQ derivatives can be prepared in a one-pot procedure using 2-chlorobenzyl thiocyanate. Arylselenocyanates (103a) and (103b) also function as electrophilic cyanating agents^{98b}.



1 C 5 π -Extended TCNQ Derivatives

Minimum Coulomb interaction is required to achieve a metallic state⁹⁹. The difference, ΔE , between the first and second reduction potentials ($\Delta E=E^1_{1/2}-E^2_{1/2}$) is a measure of the Coulomb interaction, with smaller values of ΔE being desirable. Theoretical studies suggested⁹⁹ that extension of the π -system of TCNQ would lower the intramolecular Coulomb repulsion and thus

maintain a metallic state in organic systems. The first π -extended TCNQ derivative prepared was 11,11,12,12-tetracyano-2,6-naphthoquinodimethane (TNAP, 68), which was synthesised⁸⁶ from 2,6-dicyanomethylnaphthalene (104) in several synthetic steps (scheme 1 26)

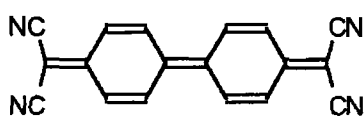


Scheme 1 26

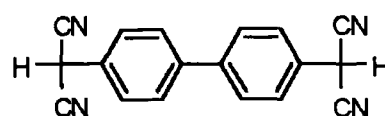
This synthetic route was hampered by the fact that 2,6-naphthalenediacetonitrile (106), the precursor to (68), was only obtained in 25% yield. However, an improved synthesis of (106) and subsequently TNAP was reported soon after,¹⁰⁰ and recently Bryce and co-workers reported its synthesis in three steps from 2,6-dicyanomethylnaphthalene (104) and 2-chlorobenzyl thiocyanate but lower yields were obtained.^{98c} TNAP undergoes two, one-electron reductions ($E^1_{1/2}=+0.21$ V, $E^2_{1/2}=-0.17$ V) to the corresponding radical anion and dianion.¹⁰¹ It readily undergoes chemical reduction to give anion radical salts of TNAP^{-•} and also forms C-T complexes with HMTSF and TTF. The HMTSF complex exhibits high conductivity at ambient pressure and low temperature ($\sigma_{300K}=2400\pm600$ Scm⁻¹, $\sigma_{50K}=15,000$ Scm⁻¹)^{102a} whereas the TTF complex has room temperature conductivity of 40 Scm⁻¹ and virtually no temperature dependence down to 185K where a sharp metal-to-insulator transition takes place.^{102b}

Soon after the preparation of TNAP, and in keeping with the desirable features of extended π conjugation and high degree of symmetry, the synthesis of the electron acceptor, tetracyanodiphenylquinodimethane (TCNDQ, 107) was investigated.^{100, 103} However, initial attempts to isolate TCNDQ failed,¹⁰¹ due

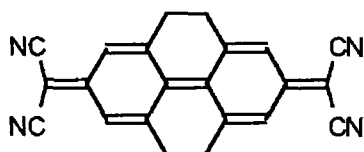
to its instability. This instability was attributed to the repulsive interactions of the biphenylic hydrogens. Formation of a polymeric material resulted but dianion salts with alkali metals and tetraalkylammonium counterions were prepared.¹⁰¹ TCNDQ was eventually synthesised by deprotonation of dihydro-TCNDQ (108) followed by electrochemical oxidation of the resultant dianion.¹⁰⁴ The tetrahydropyrene analogue, TCNTP (109) was similarly prepared but can also be chemically synthesised.^{104, 105} Catalytic dehydrogenation of TCNTP followed by 2,3-dichloro-5,6-dicyano-1,4-benzoquinone (DDQ) oxidation afforded the pyrene analogue TCNP (110).¹⁰⁶



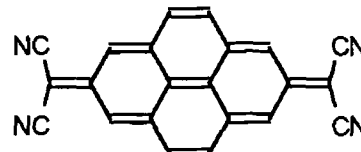
(107)



(108)



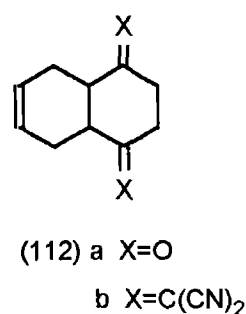
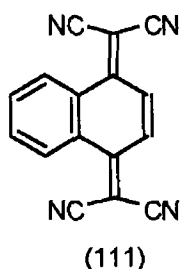
(109)



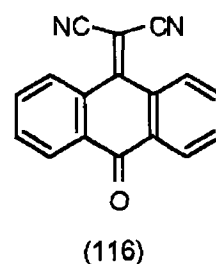
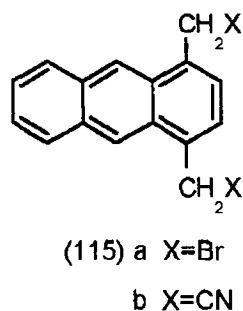
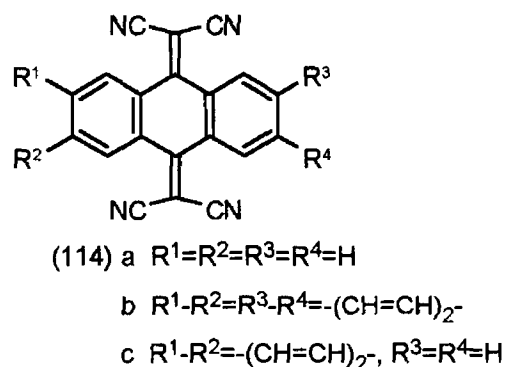
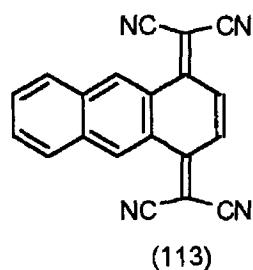
(110)

C-T complexes of TCNDQ with TTF, and TCNTP with TTF and TMTTF have been isolated,¹⁰⁴ the latter complex showing a room temperature conductivity of 0.2 Scm^{-1} .¹⁰⁵ Cyclic voltammetry studies showed that TCNDQ and TCNTP undergo two one-electron reductions.^{104, 105} The difference, ΔE , between the first and second half wave potentials for TCNDQ ($\Delta E = 0.16 \text{ V}$), TCNTP ($\Delta E = 0.23 \text{ V}$) and TCNP ($\Delta E = 0.30 \text{ V}$) is smaller than that found for TCNQ ($\Delta E = 0.42 \text{ V}$) or TNAP ($\Delta E = 0.38 \text{ V}$). Therefore there is a reduction in the intramolecular Coulomb repulsions resulting from π conjugation.

The synthesis of the first TCNQ-fused aromatic system, 11,11,12,12-tetracyano-1,4-naphthaquinodimethane (TCNNQ, 111), usually named benzo-TCNQ was reported in 1967.¹⁰⁷ This was prepared by Knoevenagel condensation of *cis*-2,3,5,8,9,10-hexahydro-1,4-naphthoquinone (112a) with malononitrile followed by bromination/dehydrobromination of the resulting product (112b).



However, it wasn't until the early 1980s that the synthesis of ring-fused TCNQs was extensively studied. The first TCNQ analogues fused to two benzene rings, 11,11,12,12-tetracyano-1,4-anthraquinodimethane (1,4-TCAQ, 113) and 11,11,12,12-tetracyano-9,10-anthraquinodimethane (9,10-TCAQ, 114a) were synthesised by Yamaguchi and co-workers¹⁰⁸. 9,10-TCAQ was simultaneously prepared by the Matsushita Electric Industrial Co. in Japan,¹⁰⁹ Aumuller and Hunig^{94a} and Kini and co-workers¹¹⁰. Extending the π structure of 9,10-TCAQ both symmetrically and asymmetrically by benzannulation afforded TCPQ (114b) and its analogue (114c)^{91, 111}. 1,4-TCAQ was prepared in low yield (5.4%) from 1,4-bis(bromomethyl)anthracene (115a) using a multistep procedure¹⁰⁸ but recently an improved one-step synthesis (58% yield) from the corresponding quinone using Lehnert's reagent was reported¹¹².

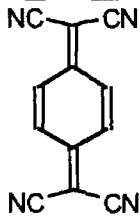
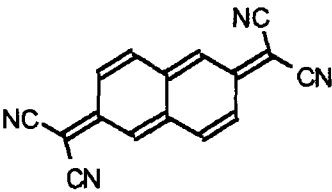
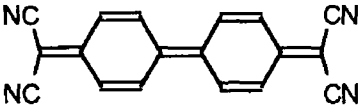
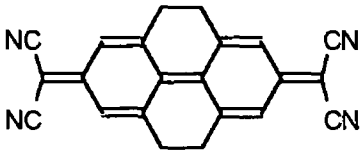
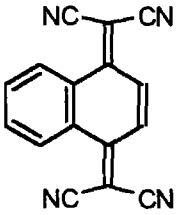
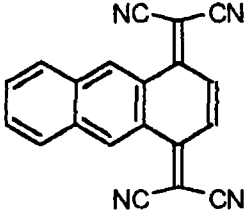


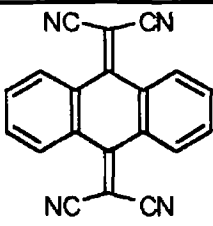
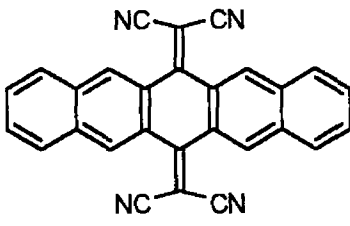
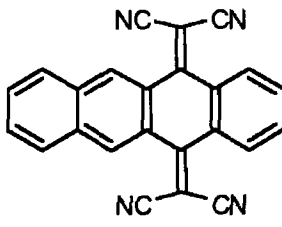
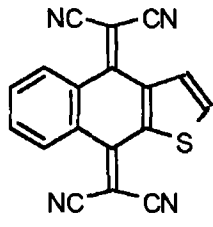
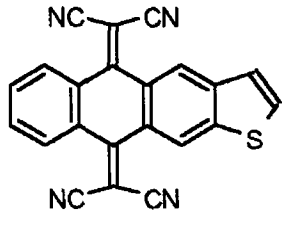
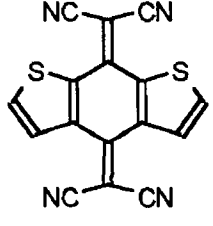
1.C.5.1 Electrochemical Properties of π -Extended TCNQ Derivatives

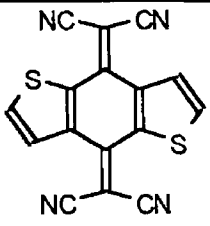
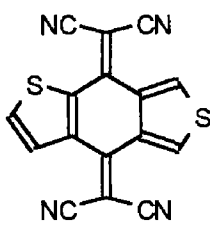
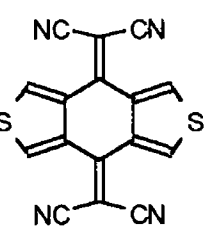
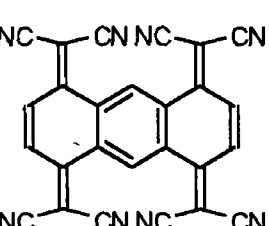
The electrochemical data (table 1.2) reveals that in general the first and second half-wave reduction potentials of the π -extended TCNQ derivatives have more negative values compared to TCNQ which implies that they are poorer electron acceptors. In addition to this, as the number of fused benzene rings is increased, the strength of the acceptor is lowered *i.e.* TCNQ > benzo-TCNQ > 9,10-TCAQ. This decrease in redox potentials was attributed to the distortion of the TCNQ moiety which on extension of the π system adopts a butterfly-like conformation *i.e.* the dicyanomethylene groups fold in opposite directions and a boat conformation is obtained for the TCNQ ring. This molecular deformation occurs to avoid the steric interactions between the dicyanomethylene groups and the *peri*-hydrogens. This was confirmed by X-ray crystal structures of benzo-TCNQ (111),¹¹³ 9,10-TCAQ (114a)¹¹⁴ and 10-(dicyanomethylene)anthrone (116).¹¹⁵

In an attempt to overcome this deformation, a thiophene ring was fused to the TCNQ system. The sulphur-containing TCNQs (117a) and (117b) were prepared from the corresponding quinone and Lehnert's reagent.¹¹⁶ The sulphur atom can participate in inter- and intra-stack interactions and consequently the conductivity and stabilisation of the metallic state are enhanced. The presence of a π -system in these molecules lowers the Coulomb repulsion energies in the dianion species. However, the X-ray crystal structure of (117a) shows a highly distorted non-planar structure and its cyclic voltammogram reveals a two-electron single wave reduction to the dianion.^{116a} This is in agreement with the previously described two-electron reduction observed for 9,10-TCAQ (114a) (table 1.2) but contrasts to previously reported thiophene-TCNQs (118-121) which show two single electron waves.¹¹⁷ The data obtained shows that (117a and b) are not as good electron acceptors as TCNQ but (117a) is a better acceptor than 9,10-TCAQ (114a). This could be accounted for by the more planar structure of (117a) compared to 9,10-TCAQ. The presence of an additional fused ring on (114a) and (117a) leads to a more severe deviation from planarity as confirmed by UV/visible spectroscopy and the shifting of the conjugated cyano group vibration in the IR spectrum. Coalescence of the first and second reduction potentials has been observed for the closely related 9,10-TCAQ (114a), TCPQ (114b) and TMTCNQ (80g) and is attributed to the lower stability of the anion radicals of the tetrasubstituted TCNQ rings. Some of the π -extended derivatives form radical trianions. It was suggested¹¹⁸ that the third electron enters the central arenediyl fragment which is the next LUMO (NLUMO).

Table 1 2 Cyclic Voltammetry Data for π -Extended TCNQ Derivatives
(measured in acetonitrile unless otherwise stated)

Compound	Solvent	$E^1_{1/2}$ volts	$E^2_{1/2}$ volts	ΔE	$E^3_{1/2}$ volts	$E^4_{1/2}$ volts	Ref
 (2) TCNQ		+0 08	-0 48	0 56			108
 (68) TNAP		+0 21	-0 17	0 38			87
 (107) TCNDQ		+0 13	-0 03	0 16			101
 (109) TCNTP		+0 012	-0 214	0 23			105
 (111) Benzo-TCNQ		-0 04	-0 41	0 37			108
 (113) Naphto-TCNQ		-0 18	-0 48	0 30			108

 <p>(114a) 9,10-TCAQ</p>	-0.285 (2e ⁻)	-2.06	110		
 <p>(114b) TCPQ</p>	-0.57	-0.91	0.34	-1.61	111
 <p>(114c)</p>	-0.44	-0.93	0.49	-1.85	111
 <p>(117a)</p>	-0.18 (2e ⁻)				116b
 <p>(117b)</p>	-0.37 (2e ⁻)				116b
 <p>(118)</p>	+0.13	-0.19	0.32		117
DMF					

 (119)	DMF	+0.13	-0.21	0.34			117
 (120)	DMF	-0.14	-0.41	0.27			117
 (121)	DMF	-0.47	-0.73	0.24			117
 (122)		+0.26	+0.05	0.21	-0.44	-0.53	119

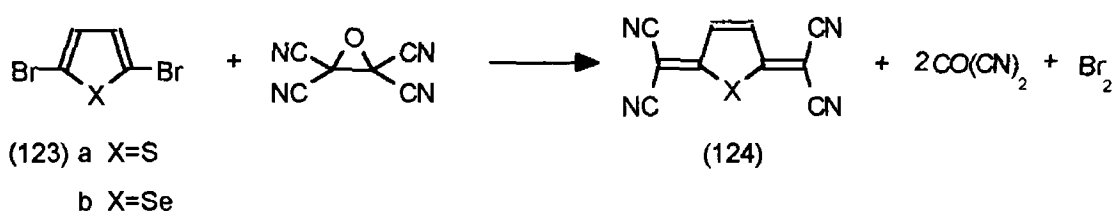
Attempts to prepare C-T complexes of the π -extended TCNQs with strong donors such as TTF was unsuccessful probably due to distortion of the benzene rings. However, the heterocyclic compounds (118) and (119) form C-T complexes with TTF which are conducting ($\sigma_{\text{f}}=0.9-4.8 \text{ Scm}^{-1}$) and OCNAQ (122) forms a semiconducting complex with TTF which has a conductivity of 10^{-2} Scm^{-1} .¹¹⁹

1 C 6 Heterocyclic-TCNQs

The development of new electron acceptors with small on-site Coulomb repulsion and better overlap have been extensively studied in an attempt to obtain new TCNQ analogues. This has already been exemplified in the last

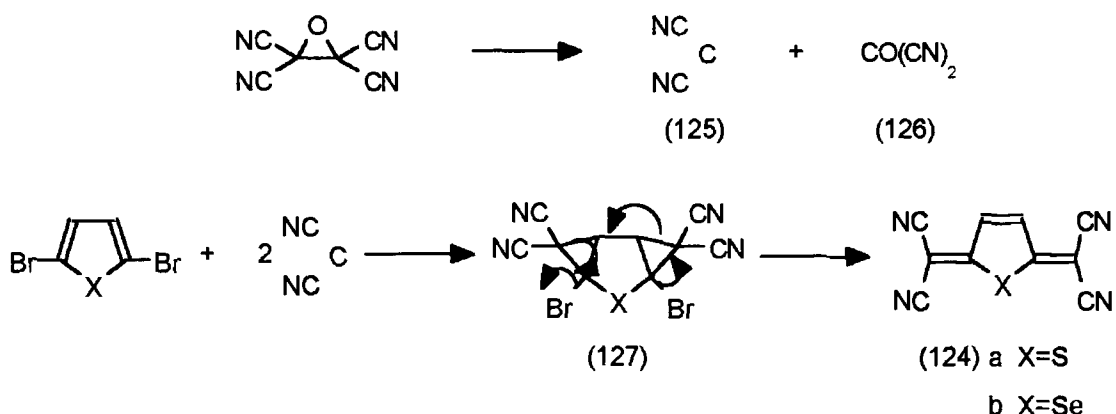
section with the π -extended TCNQs. However, another way in which the on-site Coulomb repulsion may be reduced is by introducing heteroatoms into the TCNQ system. These heteroatoms can participate in interheteroatom interactions and in contrast to benzenoid systems they can prevent the unfavourable steric interaction between the cyano groups and the *peri*-hydrogens. Therefore they can influence the metallic properties. Heterocyclic-TCNQs, or hetero-TCNQs as they are commonly called, are very stable and avoid the steric interactions in linearly conjugated systems [e.g. compound (128)] by taking the *trans* conformation. Hetero-TCNQs are synthesised by two methods

(i) Gronowitz and Uppstrom reaction of tetracyanoethylene oxide (TCNEO) with heteroaromatic halides (123) (scheme 1 27) ¹²⁰



Scheme 1 27

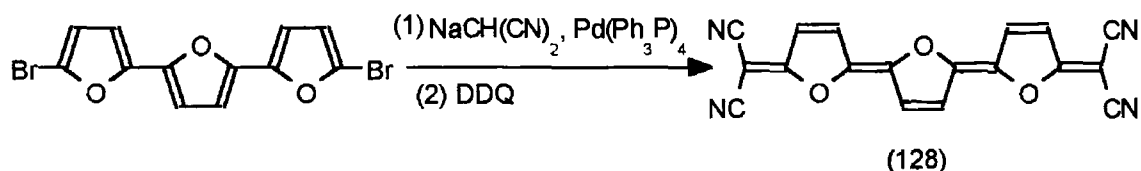
The mechanism is thought to be rather complex and is likely to involve the thermal dissociation of TCNEO into dicyanomethylene (125) and carbonyl cyanide (126) (scheme 1 28) followed by cycloaddition of carbene (125) to the 2,3 and 4,5 double bonds affording (127). This product rearranges yielding (124). Support for the mechanism was the fact that tetracyanoethylene was observed as a minor by-product in the reaction.



Scheme 1 28

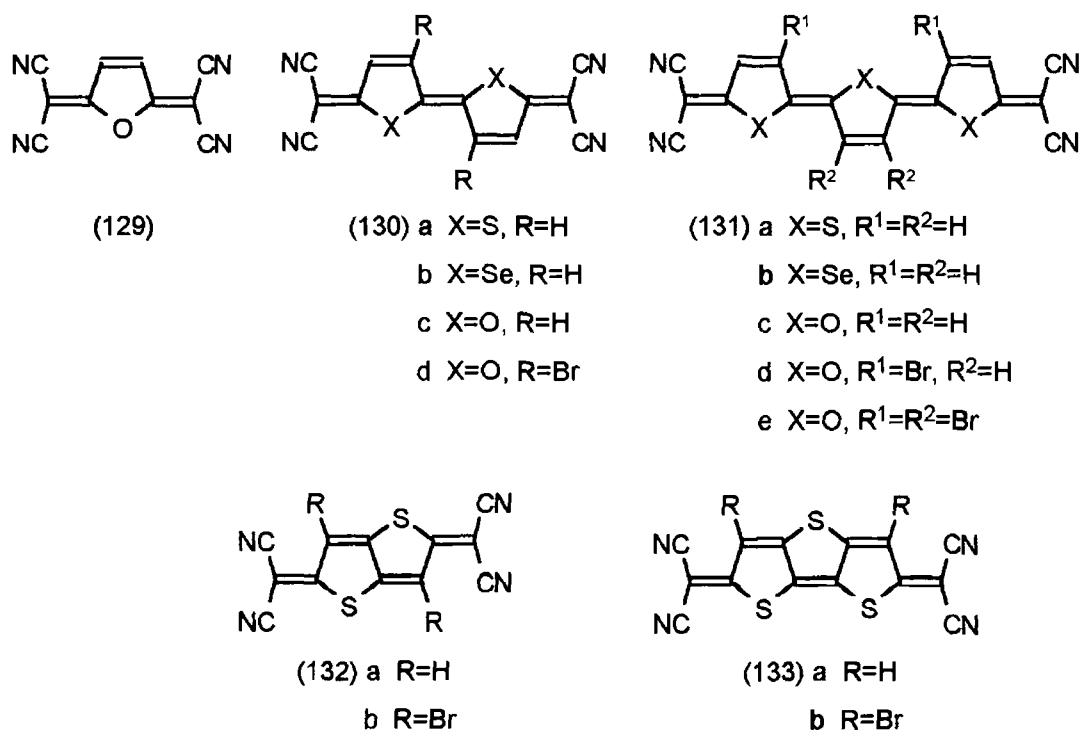
(ii) Palladium(0)-catalysed substitution of aromatic halides with sodium dicyanomethanide and successive oxidation 96b, 121

The malononitrile anion reacts with aryl halides in the presence of a palladium catalyst to give product (128) (scheme 1 29) The mechanism of this reaction was previously shown in section 1 C 4 and involves the initial formation of an arylpalladium intermediate The final dehydrogenation step was accomplished using bromine, DDQ or lead tetraacetate

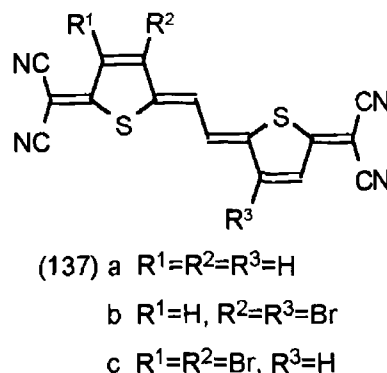
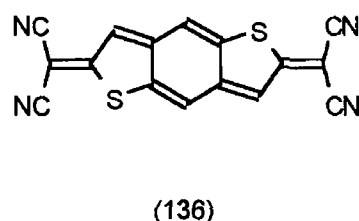
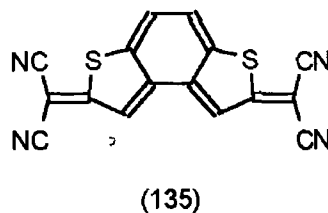
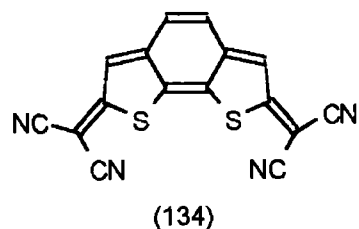


Scheme 1 29

2,5-Bis(dicyanomethylene)-2,5-dihydro-thiophene (124a) and -selenophene (124b) were the first heterocyclic TCNQs to be prepared ¹²⁰ This was achieved by heating 2,5-dibromo-thiophene or -selenophene and tetracyanoethylene oxide under reflux in 1,2-dibromoethane Distillation of carbonyl cyanide from the reaction followed by work-up procedures afforded the required products (124a) and (124b) respectively Similarly prepared using this procedure was the furanoquinoid analogue (129),¹²² the extensively conjugated homologues (130)¹²³ and (131a and b)^{123b} and the fused homologues (132a) and (133) ¹²⁴



The heteroquinoid TCNQs (131c-e),¹²² (134) to (136)¹²⁵ and the vinylogous hetero-TCNQ (137)¹²⁶ were prepared by palladium (0)-catalysed substitution of aromatic halides with sodium dicyanomethanide



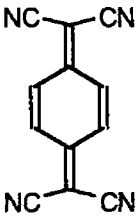
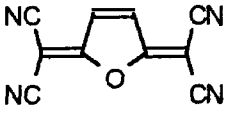
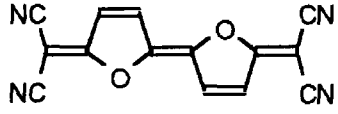
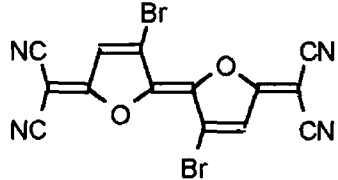
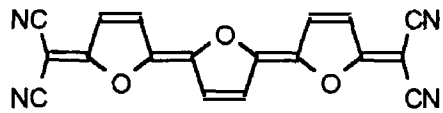
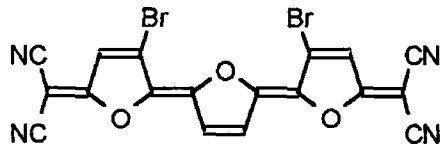
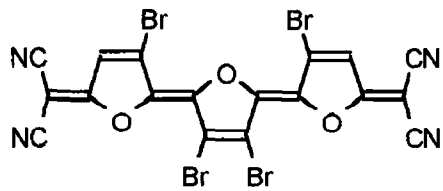
1 C 6 1 Electrochemical Properties of Heterocyclic-TCNQs

From the cyclic voltammetry data (table 1 3) of heterocyclic-TCNQs it can be seen that they are generally weaker electron acceptors than TCNQ. This reflects the decrease in aromaticity of the central heterocyclic moieties formed upon reduction.¹²⁷ For the same reason, within the furan, thiophene and selenophene series the electron accepting ability increases in the order thiophene>selenophene>oxygen. However, the differences between the first and second reduction potentials (ΔE) become smaller when the conjugation is expanded, i.e. ΔE of (131a-c) is almost zero. Therefore they have the attractive features of strong electron affinities and reduction of on-site Coulombic repulsion which is a requisite for components of C-T complexes. The acceptor abilities may be improved by the introduction of additional electron-withdrawing groups.^{124b}

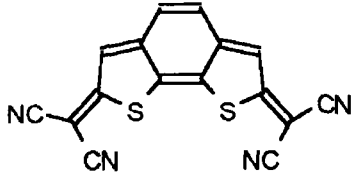
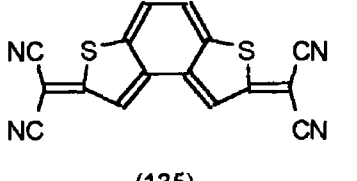
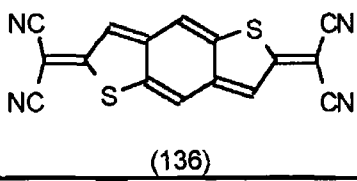
1 C 6 2 C-T Complexes of Heterocyclic-TCNQs

Contrary to the fact that the heteroquinoid analogues (124) and (129) and their conjugated and fused homologues (130-133) have poor electron accepting abilities compared to TCNQ, they form C-T complexes with TTF. The thiophene-fused derivative (132a), which is isoelectronic with TNAP, also forms C-T complexes with HMTTeF^{124b} and BEDT-TTF.¹²⁸ The dibromo derivative (132b) also formed a C-T complex with HMTTeF exhibiting a room temperature

Table 1.3 Cyclic Voltammetry Data for Heterocyclic-TCNQs (measured in acetonitrile unless otherwise stated)

Compound	Solvent	$E^1_{1/2}/V$	$E^2_{1/2}/V$	ΔE	Ref
 (2) TCNQ		+0.08	-0.48	0.56	108
 (129)		+0.03	-0.55	0.58	122
 (130c)		-0.09	-0.31	0.22	122
 (130d)		+0.08	-0.12	0.20	122
 (131c)		-0.09 ($2e^-$)			122
 (131d)		-0.01 ($2e^-$)			122
 (131e)		+0.14 ($2e^-$)			122

 (124a)	+0 068	-0 259	0 612	123a
 (130a)	-0 026	-0 259	0 285	123a
 (131a)	-0 028 (2e ⁻)			123a
 (124b)	+0 03	-0 54	0 57	123b
 (130b)	-0 05	-0 25	0 20	123b
 (131b)	-0 07 (2e ⁻)			123b
 (132a)	+0 058	-0 355	0 413	124a
 (133a)	+0 048	-0 288	0 336	124a

 <p>(134)</p>	DMF	+0.26	-0.01	0.27	125a
 <p>(135)</p>	DMF	+0.32	+0.09	0.23	125a
 <p>(136)</p>	DMF	+0.20	-0.05	0.25	125a

conductivity of 170 Scm^{-1} ^{124b} The C-T complex of BEDT-TTF exhibited a room temperature conductivity of $6.9 \times 10^{-10} \text{ Scm}^{-1}$. The X-ray crystal structure of (132a)-BEDT-TTF C-T complex¹²⁸ (figure 1.14) shows segregate stacking columns along the *a* axis with the sulphur-sulphur distances (3.73 and 3.82 Å) between the stacked components slightly longer than the sum of the van der Waals radius (3.70 Å). The sulphur atoms of BEDT-TTF also interact with atoms of the adjacent BEDT-TTF molecules (3.64 and 3.59 Å) and with the nitrogen atoms of the acceptor, with a van der Waals contact of 3.33 Å. In addition to this there are strong sulphur-sulphur interactions between the acceptors (3.48 Å) which indicates that this system is capable of inducing multi-dimensionality in molecular complexes.

In contrast to the selenium and thiophene analogues, complexation of furanoquinoid acceptors with donors was difficult due to weak electron affinities as well as weak nonbonded interaction of oxygen relative to sulphur and selenium. Derivatives (129) and (130c) formed complexes with TTF which were nearly insulating but no C-T occurred. The dibromo analogue (130d) was a better acceptor and afforded a C-T complex with TTF whereas (131e) gave a highly conductive complex with TTT (81).¹²²

TCNQs fused with 1,2,5-thiadiazole (138a, 139a and 140) and 1,2,5-selenadiazole (138b and 139b) rings were also synthesised and were shown to be planar molecules by X-ray crystallography.¹²⁹

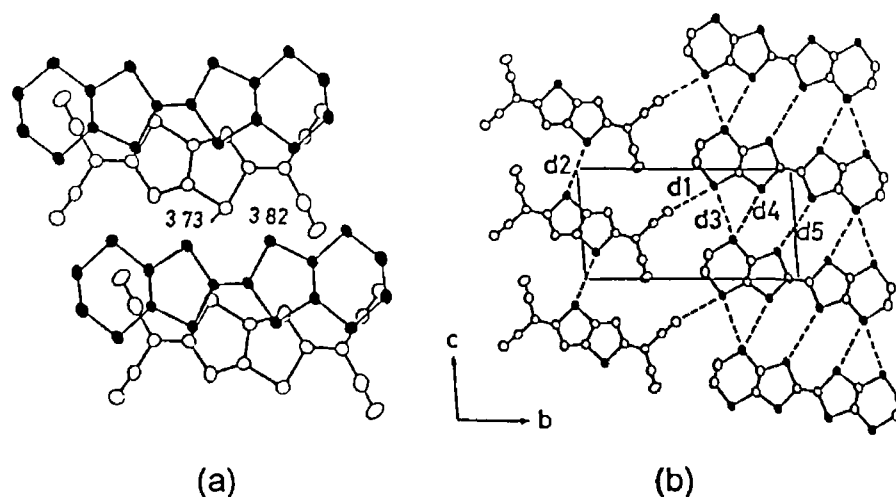
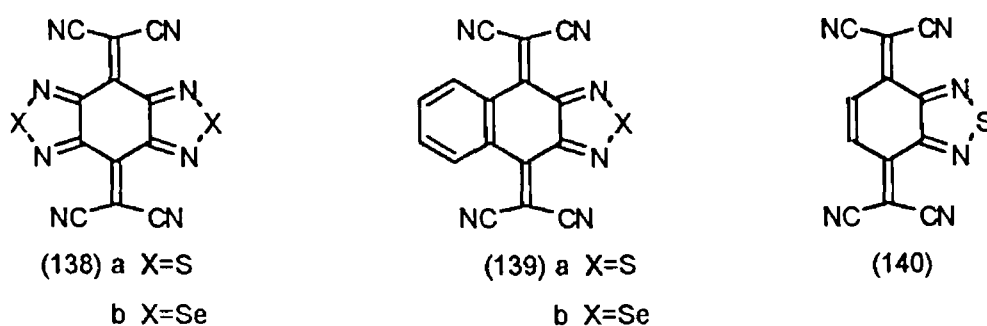


Figure 1 14 Crystal structure of (132a)-BEDT-TTF C-T complex showing (a) the mode of molecular overlap and (b) sulphur-sulphur and sulphur-nitrogen interactions between the donor and acceptor molecules



Derivatives (138) and (139) possess short sulphur-cyano or selenium-cyano contacts forming a coplanar "sheetlike" network. The sheets stack to form infinite layers with face-to-face overlapping between heterocycles. Compounds (138) and (139) show strong intermolecular interactions. This interaction is one of the sources of directionality in the crystal packing of organic molecules and causes the formation of inclusion lattices in the C-T complexes of (138).^{129b} In contrast, 1,2,5-thiadiazolotetracyano-*p*-quinodimethane (TDA-TCNQ, 140) shows no sulphur-sulphur or sulphur-nitrogen interactions in the crystal but forms a coplanar dyad by hydrogen bonding of the cyano groups (2.35 Å) with the hydrogens on the adjacent quinodimethane ring (figure 1 15).^{129a} The dyad formation shows the possibility that the negative charge can be delocalised over the two molecules in the anion radical salts. This is another way of reducing the on-site Coulomb repulsion. Contrary to BTDA-TCNQ (138a), TDA-TCNQ is a stronger acceptor and it forms highly conducting complexes.

with TTF and its derivatives indicating that the inclusion behaviour of (138a) is diminished by eliminating one of the heterocyclic rings ^{129a}

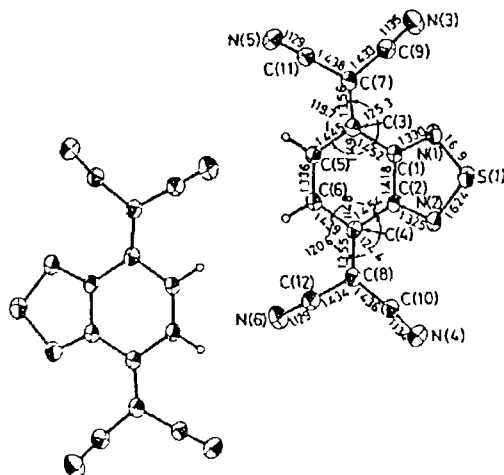
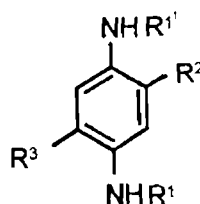
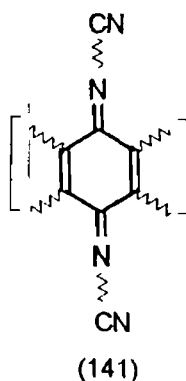


Figure 1 15 Crystal structure of TDA-TCNQ (140) showing dyad formation

1 C 7 *N,N'*-Dicyanoquinonediimines

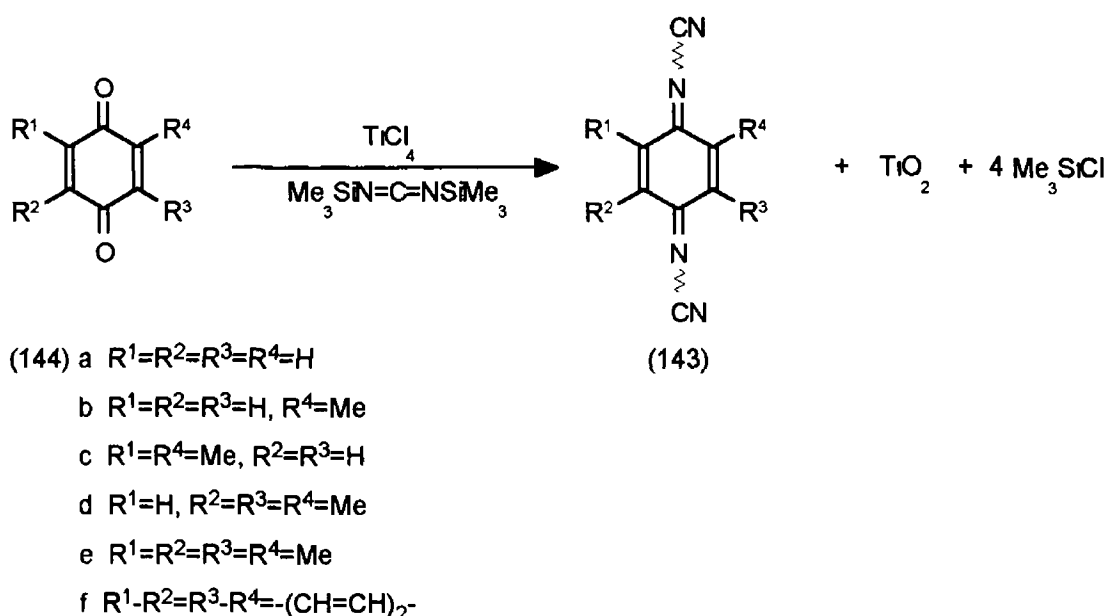
The planarity of the donor and acceptor molecules has been suggested as one of the prerequisites required to form C-T complexes. However, in order to preserve the planarity, only TCNQ derivatives with small substituents are tolerated in the ring. To remove the steric drawbacks of the Y-shaped dicyanomethylene [=C(CN)₂] group, replacing it with a smaller, flexible and less sterically demanding cyanoimine (=NCN) group led to the preparation of the DCNQI family of acceptors. The =NCN group does not alter the planarity even on tetrasubstitution of the molecule ¹¹⁴ *N,N'*-Dicyanoquinonediimines (141) were initially prepared from substituted *p*-phenylenediamines (142a) via the *N,N'*-dicyanodiamines (142b). However, this synthetic route was limited because only a few substituted phenylenediamines were easily accessible ¹³⁰



(142) a $R^1=H$, $R^2=R^3=H$ Me or Cl

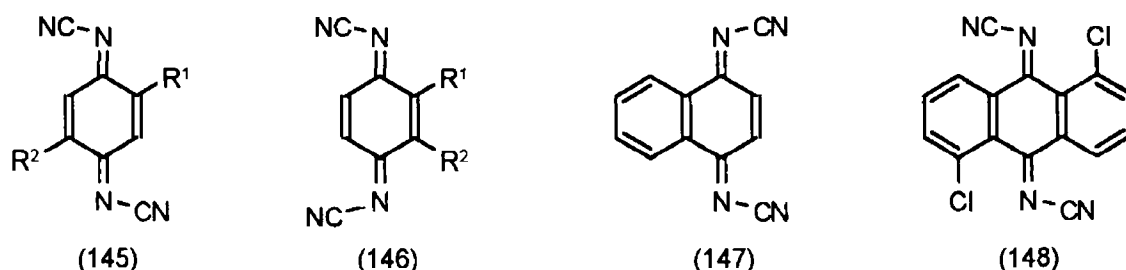
b $R^1=CN$, $R^2=R^3=H$ Me or Cl

However, an alternative preparation of (141) was discovered from non-enolising ketones using bis(trimethylsilyl)carbodiimide (BTC) in the presence of fluoride or cyanide catalysts¹³¹ But when this reaction was applied to *p*-benzoquinones only 1,4-addition products were isolated This problem was overcome by using titanium tetrachloride as a Lewis acid catalyst in the reaction The use of Lewis acids aluminium trichloride, boron trifluoroetherate and tin (IV) chloride were found to be either inactive or led to the decomposition of the *p*-benzoquinone The highest yields are obtained when titanium tetrachloride is added first to the quinone Thus Aumuller and Hunig prepared *N,N'*-dicyanoquinonediimine (DCNQI, 143) derivatives in one step from the corresponding quinones (144) by reacting with titanium tetrachloride and bis(trimethylsilyl)carbodiimide (BTC)¹³¹ (scheme 1 30)



Scheme 1 30

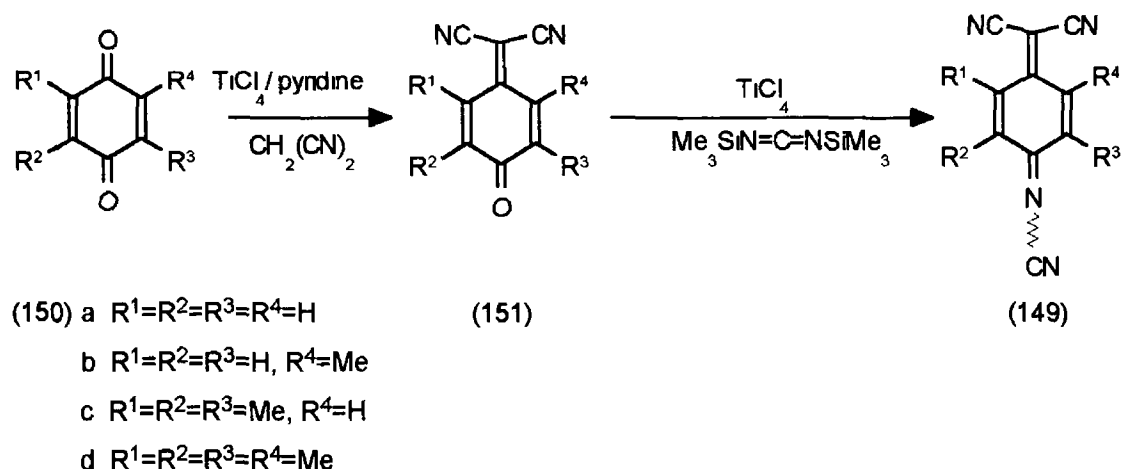
The parent compound (143a) showed redox potentials ($E^1_{1/2}=-0.25$ V, $E^2_{1/2}=+0.39$ V) similar to those of TCNQ ($E^1_{1/2}=-0.28$ V, $E^2_{1/2}=+0.39$ V)¹³² A variety of substituted DCNQIs have been prepared Examples of these are (145-148)



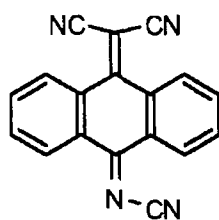
R^1 and R^2 can be alkyl, alkoxy, thioalkyl, aryl halogeno

The =NCN groups of the DCNQI derivatives can exist as *syn* and *anti* isomers with respect to the neighbouring ring atoms so that in total four isomers may exist. However, only one *syn* and/or *anti* isomer has been observed by ^{13}C and ^1H NMR spectroscopy of these imines. Generally the 2,3- and 2,5-substituted dicyanoimine derivatives exist only in that configuration in which the cyano group prefers the *anti* position to the ring substituents. Accordingly the *anti* configuration is observed in compounds (145) and (148) and the *syn* configuration in (146) and (147). The monosubstituted derivative (143b) also exists as a mixture of *syn/anti* isomers since only one cyano group is fixed in the "*anti*" position. In contrast, only one of the cyano groups of the 2,6-disubstituted dicyanoimines (143c) and trisubstituted derivative (143d) is configurationally stable (*anti*) while the other one undergoes rapid *syn/anti* isomerisation at room temperature. As a result the signals of the α -carbon atoms are broadened and are hard to detect. In the tetrasubstituted dicyanoimine (143e) both cyano groups isomerise so rapidly that the number of NMR signals is diminished.

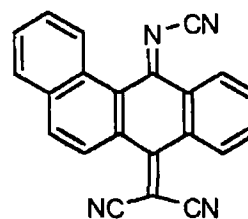
The hybrid acceptor molecules, *N*,7,7-tricyanoquinomethanimines (TCNQI, 149) in which the dicyanomethylene and cyanoimine groups are present in the same structure have also been synthesised.¹³³ These compounds were prepared by titanium tetrachloride-mediated Knoevenagel condensation of quinone (150) with malononitrile followed by reaction of compound (151) with BTC in the presence of titanium tetrachloride (scheme 1.31). In addition to these alkyl substituted derivatives π -extended TCNQIs (152) and (153) have also been synthesised.¹³³



Scheme 1.31



(152)



(153)

Tetramethyl-TCNQ (80g) and other tetrasubstituted TCNQ derivatives (e.g. 9,10-TCAQ, 114a) are non-planar as shown^{89, 114} by X-ray crystallography. However, in contrast the tetrasubstituted DCNQI derivatives are essentially planar. This is due to the $=\text{NCN}$ groups being smaller than the $=\text{C}(\text{CN})_2$ groups and therefore they can bend with the DCNQI molecular plane while the latter are forced out of the plane thus distorting the tetrasubstituted TCNQ ring into a boat conformation. The X-ray crystal structure of tetramethyl-TCNQI (149d) shows that the ring is strongly distorted into a boat conformation with greater deformation about the bulkier $=\text{C}(\text{CN})_2$ group than about the $=\text{NCN}$ group⁹³. Contrary to this, trimethyl derivative (149c) is essentially planar. Hybrid molecule (153) shows similar distortion to the tetramethyl-TCNQI (149d) and analogously exhibits greater deformation about the $=\text{C}(\text{CN})_2$ group than the $=\text{NCN}$ group.

The cyclic voltammetric data of the DCNQI and TCNQI derivatives exhibit two one-electron reduction waves to the corresponding radical anion and dianion except for derivatives (152) and (153). Molecule (153) shows a single two electron reduction whereas compound (152) the second reduction potential is not observable. The latter result contrasts with the results obtained for the corresponding TCNQ and DCNQI derivatives in which dianion formation is observed. Increasing the benzannulation of DCNQI results in poorer electron acceptors (i.e. decrease in first reduction potentials with an increase in benzannulation). This is mainly due to steric factors¹³² and a smaller difference, ΔE , between the first and second reduction potentials compared with that of the parent DCNQI. This suggests a reduction in the intramolecular Coulomb repulsion due to π -system extension. A similar situation is found in the TCNQ system. The acceptor ability of DCNQI derivatives can be improved by the presence of chlorine or bromine groups or the replacement of a benzene ring with a sulphur heterocycle.^{116b, 134}

1 C 7 1 C-T Complexes of DCNQI Acceptors

Substituted DCNQIs form C-T complexes with TTF and TMTSF many of which show powder conductivities of ca. 0.1 Scm^{-1} . This is indicative of

segregated stacking between the donor and acceptor molecules. The first DCNQI-type C-T complex obtained was the C-T complex of *N,N'*-dicyano-1,4-naphthoquinodiimine (DCNNI, 147) with TTF.¹³⁵ This contrasts with the tetracyano analogue, benzo-TCNQ (111) which does not form a C-T complex with TTF. The C-T complex of TTF and DCNNI consists of separated oblique stacks of almost planar donor and acceptor moieties which are equidistant at room temperature [figure 1.16(a)]. The crystal packing in TTF-DCNNI C-T complex was due to the electrostatic interaction between the *syn*-configured cyanoimine group and the sulphur atoms of TTF (318-324 pm). This interaction causes two stacks of the acceptor to crystallise in 'dimers' with the unsubstituted part of the naphthalene ring oriented towards each other with two parallel rows of TTF on the other side.¹³⁵ The conductivity of the TTF-DCNNI C-T complex increases with decreasing temperature down to a phase transition temperature of 140K. A similar stacking arrangement is also seen in TTF-DCNQI.2H₂O. The X-ray crystal structure of TTF-DCNQI.2H₂O [figure 1.16(b)] shows the segregated stacks of TTF and DCNQI molecules to have chess-board-like arrangement with both stacks skewed to the same side.¹³⁶ This contrasts with the TTF-TCNQ C-T complex in which the donors and acceptors form alternating rows and the two components are skewed in a cross-like manner.¹⁷

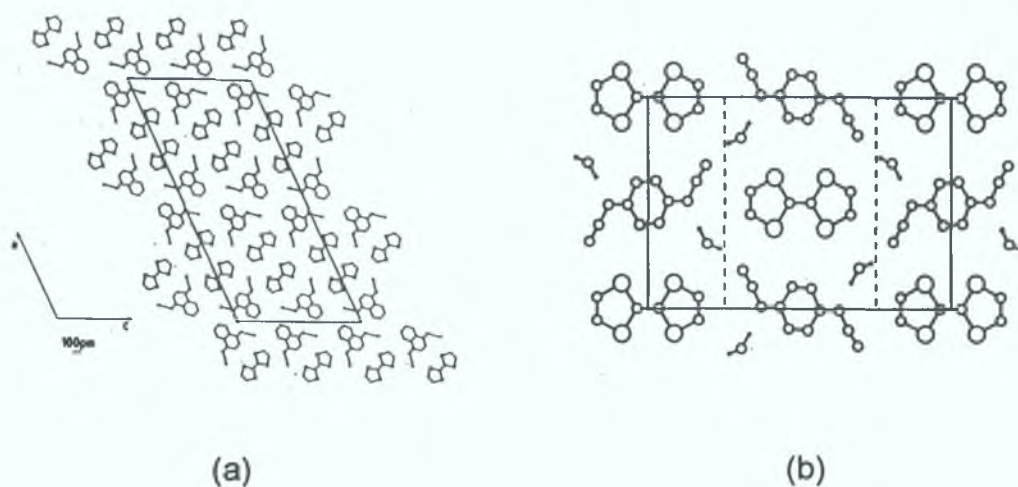
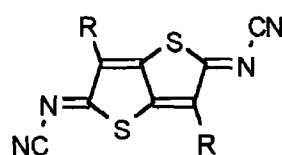


Figure 1.16 Stacking modes of (a) TTF-DCNNI and (b) TTF-DCNQI.2H₂O.

The first example of a heteroquinoid system containing the =NCN group, 2,5-bis(cyanoimino)-2,5-dihydrothieno[3,2-b]thiophenes (DCNTT, 154) were prepared in 1990.¹³⁷ Derivative (154b) formed C-T complexes with TTF, TMTTF, BEDT-TTF and TMTSF. The TMTSF complex exhibited the highest

conductivity ($\sigma=200 \text{ Scm}^{-1}$) The crystal structure of the (154b)-TTF C-T complex shows segregated stacks of planar donor and acceptor molecules which are almost equidistant at room temperature with a stack separation of 348 pm This C-T complex undergoes a metal-to-semiconductor phase transition at 160K



(154) a R=H

b R=Br

1 C 7 2 DCNQI Radical Anion Salts

The DCNQI acceptors, in addition to forming C-T complexes with TTF, also form conducting radical anion salts with monovalent metals in a 2:1 stoichiometry of which the 2,5-disubstituted were the most important. These salts, $(2,5\text{-R}^1, \text{R}^2\text{-DCNQI})_2\text{M}$ ($\text{R}^1, \text{R}^2 = \text{Hal}, \text{Me}, \text{MeO}$, $\text{M} = \text{Li}, \text{Na}, \text{K}, \text{NH}_4, \text{Cu}, \text{Ag}, \text{Ti}$), have the unique feature of having the same space group ($I4_1/a$) or a very similar one ($C2/c$ or $P4/n$). Therefore the effects of either the substituents or metal ions on the electronic properties can be evaluated. The metal-nitrogen distances in the alkali-metal salts are close to the sum of the van der Waals radius of nitrogen and the ionic radii of the metal ions indicating that mainly Coulomb interactions are present. All of these radical anion salts behave as one-dimensional metal-like semiconductors except for the copper salts which display metallic properties.

The first radical-anion salt to be prepared was the copper salt of 2,5-dimethyl-*N,N'*-dicyanoquinonediimine $(2,5\text{-Me}_2\text{DCNQI})_2\text{Cu}$ ¹³⁸. This salt exhibited a single crystal conductivity of $\text{ca } 500,000 \text{ Scm}^{-1}$ at 3.5 K. Previously radical anions with such high conductivity were unknown. The crystal structure of $(2,5\text{-Me}_2\text{DCNQI})_2\text{Cu}$ (figure 1.17) shows that each copper atom is surrounded by four DCNQI molecules in a slightly distorted tetrahedron arrangement with strong Cu-N interactions ($d=1.99 \text{ \AA}$). The acceptor forms one-dimensional columns with an intrastack distance of 3.2 \AA ¹³⁸. Many of the $(2,5\text{-R}^1, \text{R}^2\text{-DCNQI})_2\text{M}$ salts possess this structure. Electrical conductivity along the copper atoms is unlikely because of the large copper-copper distance (388 pm) and thus occurs through the stacks of the acceptor molecules along the *c* axis. The copper ions function as a conductivity bridge between the individual stacks, i.e. the electrons migrate between the stacks via the copper ions which possess an average charge of $\text{Cu}^{1.33+}$ ($\text{Cu}^+, \text{Cu}^+, \text{Cu}^{2+}$).

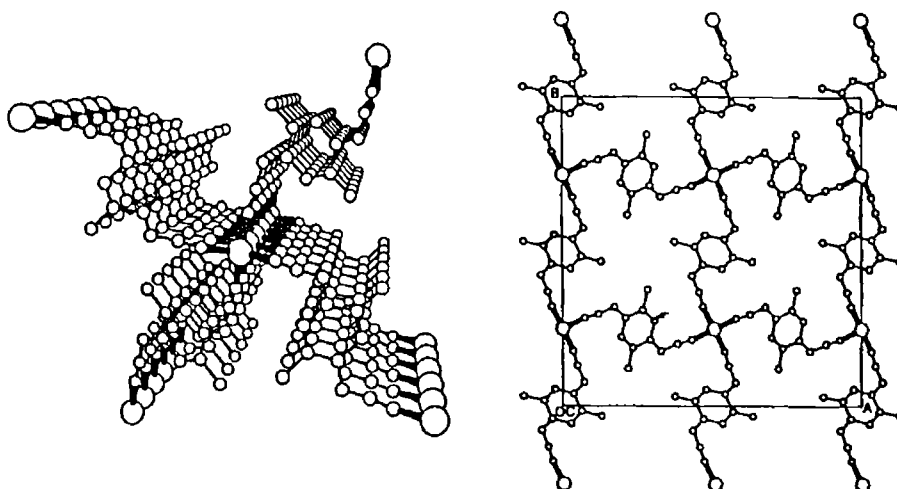
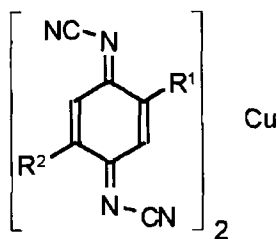


Figure 1 17 Crystal Structure of $(2,5\text{-Me}_2\text{DCNQI})_2\text{Cu}$

Although all of the copper salts derived from 2,5-disubstituted DCNQIs are isostructural (space group $I4_1/a$) and show metallic properties, they behave differently on cooling. One group of compounds (Group I, 155a-i) exhibits metallic conductivities which increase down to low temperatures and the other group (Group II, 155j-o) exhibit decreasing conductivities with decreasing temperature i.e. they undergo a metal-to-insulator phase transition between 160-230K.¹³⁹ The size of the substituents is an essential factor governing the occurrence of a phase transition on cooling i.e. combinations of small substituents (e.g. Cl and Br) induce phase transitions (Group II) whereas large substituents (e.g. MeO) remain metallic to the lowest temperatures (Group I). However, the $(2,5\text{-Me}_2\text{DCNQI})_2\text{Cu}$ salt is an exception and no phase transition is found although the van der Waals volume of the methyl group (22.7 Å³) is smaller than that of bromine (25.1 Å³). The electron donating properties of the methyl group are probably responsible for suppressing the phase transition. In both types of salt the distorted tetrahedral coordination around the copper cation and the $p\pi$ - d band mixing between DCNQI and the copper cation are associated with their peculiar properties.¹⁴⁰ Coordination of the $=\text{NCN}$ groups to the copper ions plays an important role in achieving three-dimensional conductivity required for a metal. The $(2,5\text{-R}^1, \text{R}^2\text{-DCNQI})_2\text{Cu}$ salts display conductivities both parallel and perpendicular to the c axis i.e. electron transport occurs through the stacks as well as through infinite arrays of $-\text{Cu-DCNQI}-$ moieties.



(155)

Group I

- a $R^1=R^2=Me$
- b $R^1=Cl, R^2=I$
- c $R^1=Me, R^2=I$
- d $R^1=Br, R^2=I$
- e $R^1=R^2=I$
- f $R^1=Me, R^2=OMe$
- g $R^1=Br, R^2=OMe$
- h $R^1=I, R^2=OMe$
- i $R^1=R^2=OMe$

Group II

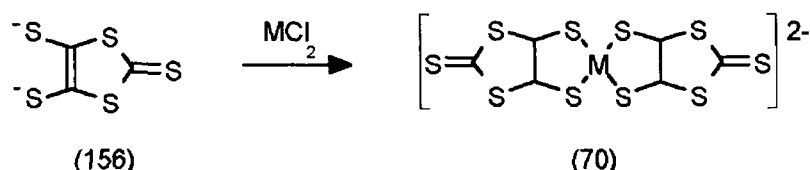
- j $R^1=R^2=Cl$
- k $R^1=Cl, R^2=Me$
- l $R^1=Cl, R^2=Br$
- m $R^1=Br, R^2=Me$
- n $R^1=R^2=Br$
- o $R^1=Cl, R^2=OMe$

The conductivity brought about by the copper ions implies mixing of the copper 3d orbitals with the organic π electrons near the Fermi level. This turns the original one-dimensional character of the DCNQI chain into a multi-Fermi surface one and is responsible for the suppression of the metal-to-insulator transition in $(2,5-Me_2DCNQI)_2Cu$. For this transition a threshold coordination angle N-Cu-N (α_{CO}) is found. The α_{CO} angle reflects the distortion of the tetrahedral geometry around the copper ion. The distortion of the coordination tetrahedron decreases the number of d orbitals participating in the $p\pi$ -d mixing and weakens the multi-Fermi surface nature, which leads to the gap formation by a charge density wave (CDW) on DCNQI columns.¹³⁹

1 C 8 Metal(DMIT)₂ Acceptors

The desire to prepare conducting organic materials with increased dimensionality has been prevalent in the work of many groups. This was achieved by enhancing the interstack interactions and thus the metal-to-insulator phase transition associated with one-dimensional metals is avoided. The majority of work in this area has concentrated on π donor molecules but has also been applied to metal(DMIT)₂ π acceptors. Metal(DMIT)₂ (70) or M(DMIT)₂ for short, were prepared¹⁴¹ from 1,3-dithiole-2-thione-4,5-dithiolate (DMIT, 156) by reacting with the appropriate metal dichloride and counterion (scheme 1 32). The M(DMIT)₂ system is attractive as a π -acceptor molecule because it is planar, it contains ten sulphur atoms which can participate in

intra- and inter-stack interactions and also its redox properties can be tuned by varying the metal atom. $M(\text{DMIT})_2$ anions have formed complexes with TTF and tetraalkylammonium salts, both of which are superconducting.



Scheme 1 32

These complexes are prepared by diffusion of solutions of the appropriate $[\text{n-Bu}_4\text{N}][\text{M}(\text{DMIT})_2]$ with, for example, $(\text{TTF})_3(\text{BF}_4)_2$ in the case of the TTF complexes. The stoichiometry of the $\text{TTF}[\text{M}(\text{DMIT})_2]_x$ complexes depends on the nature of the metal / e when the metal is nickel or palladium, $x=2$ and when it is platinum, $x=3$ ¹⁴². However, a disadvantage with this technique is the possibility of obtaining a heterogeneous sample. An alternative is to synthesise the complexes electrochemically in a U-tube. This method is more selective and yields a homogeneous sample.

The first superconducting M(DMIT)₂ complex, TTF[Ni(DMIT)₂]₂, was synthesised by Bousseau and co-workers¹⁴³ and provided the first example of superconductivity in a π -anion molecule with a π -counterion. This salt exhibited superconductivity at 1.6 K on the application of 7 kbar of pressure.¹⁴⁴ TTF[Ni(DMIT)₂]₂ exhibited a metal-like conductivity temperature dependence down to 4 K, with a conductivity at room temperature of ca. 300 Scm⁻¹ and at 4 K of over 10⁵ Scm⁻¹ without undergoing a metal-to-insulator phase transition. The crystal structure of TTF[Ni(DMIT)₂]₂ (figure 1.18) consists of segregated stacks of essentially planar donors and acceptors with intermolecular intrastack sulphur-sulphur distances between molecules in either the TTF or Ni(DMIT)₂ stacks not larger than the sum of van der Waals radii. On the other hand, a number of intermolecular interstack sulphur-sulphur interactions are shorter (3.45–3.54 Å) than the van der Waals separation (3.70 Å) between the Ni(DMIT)₂ groups or between the Ni(DMIT)₂ and TTF units.¹⁴⁴ Shorter sulphur-sulphur interactions (3.38 Å) are found between the terminal sulphur atoms of the Ni(DMIT)₂ units and the sulphur atoms in the TTF thus extending the range of interactions in the third direction.

Based on these observations, $\text{TTF}[\text{Ni}(\text{DMIT})_2]_2$ appears to have a quasi-three-dimensional network of intermolecular sulphur-sulphur interactions. Soon after the preparation of the nickel TTF complex both palladium and platinum

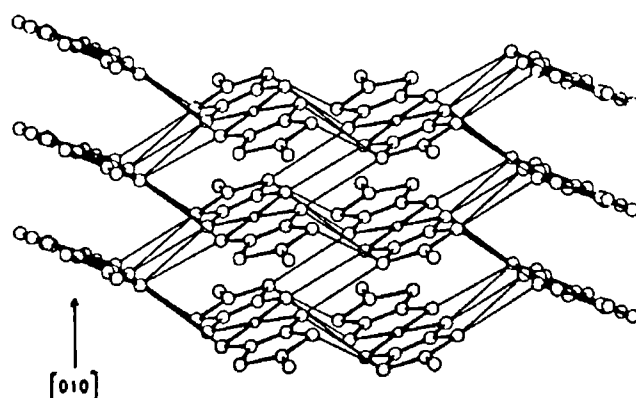


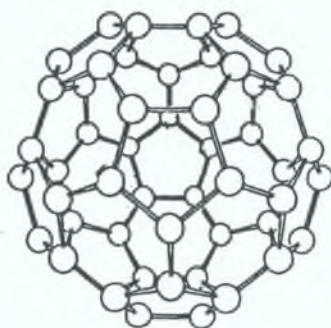
Figure 1 18 Crystal structure of TTF[Ni(DMIT)₂]₂ Parallel view of entities slacked along [010] Thin lines indicate sulphur-sulphur distances shorter than 3 70 Å

complexes with TTF were prepared¹⁴² The TTF[Pd(DMIT)₂]₂ complex, which is isomorphous with the nickel derivative, exhibits a room-temperature conductivity of ca 750 Scm⁻¹ and undergoes a metal-to-insulator transition below ca 220K The TTF[Pt(DMIT)₂]₃, unlike the nickel and palladium derivatives, is a semiconductor throughout the 300-100K range with a room temperature conductivity of ca 20 Scm⁻¹¹⁴² Its unit cell consists of one TTF molecule, one monomer Pt(DMIT)₂ molecule and two Pt(DMIT)₂ molecules connected by a platinum-platinum bond thus forming a dimer The X-ray crystal structure shows TTF[Pt(DMIT)₂]₃ to consist of alternate layers of donor and acceptor molecules The acceptor layer contains Pt(DMIT)₂ monomers and [Pt(DMIT)₂]₂ dimers stacked in columns Within a column, the monomers and dimers alternate The two Pt(DMIT)₂ dimer units are distorted from planarity as evidenced by the dihedral angle value (112 °) between the two Pt(DMIT) moieties in each Pt(DMIT)₂ unit Intermolecular sulphur-sulphur contacts shorter (3 23-3 66 Å) than the sum of the van der Waals radii (3 70 Å) are observed within a stack and within a dimer as well as between dimers and monomers and between Pt(DMIT)₂ units of either monomers or dimers belonging to adjacent stacks (3 45-3 65 Å) Therefore these sulphur-sulphur interactions form a two-dimensional network Short intermolecular sulphur-sulphur separations also occur between two TTF sulphur atoms and the terminal sulphur atoms of the monomeric Pt(DMIT)₂ units There are no short sulphur-sulphur separations between TTF molecules in a layer

The first molecular superconductor based on the π acceptor $M(\text{DMIT})_2$ and closed-shell cations was the salt $[(\text{CH}_3)_4\text{N}][\text{Ni}(\text{DMIT})_2]_2$.¹⁴⁵ This salt exhibits a superconducting transition at 5K under 7 kbar of pressure and its X-ray crystal structure consists of planar $\text{Ni}(\text{DMIT})_2$ anions separated by channels containing the tetramethylammonium cations. The palladium analogue, $[(\text{CH}_3)_4\text{N}][\text{Pd}(\text{DMIT})_2]_2$ was obtained in two different forms, α and β , whose crystal structures were similar to $[(\text{CH}_3)_4\text{N}][\text{Ni}(\text{DMIT})_2]_2$. The $\text{Pd}(\text{DMIT})_2$ dimers form segregated one-dimensional stacks. Within the dimers the $\text{Pd}(\text{DMIT})_2$ anions are eclipsed but between the dimers the anions are displaced sideways with respect to each other by 0.07 Å. β - $[(\text{CH}_3)_4\text{N}][\text{Pd}(\text{DMIT})_2]_2$ exhibited a transition temperature of 6.2K at 6.5kbar¹⁴⁶ whereas the α form showed no sign of a superconducting transition up to 12 kbar.¹⁴⁷

1.C.9 Buckminsterfullerene Electron Acceptors

Buckminsterfullerene, C_{60} (6), and its derivatives are the latest type of electron acceptors to be discovered. These acceptors are the first three-dimensional molecular conductors *i.e.* unlike traditional molecular conductors which are planar, C_{60} has radially oriented π orbitals in all three dimensions.



(6)

C_{60} has icosahedral symmetry which places each carbon atom in an identical environment. There are 20 six-membered hexagonal rings and 12 five-membered pentagonal rings on the surface of the sphere. It is the non-planarity and sp -orbital hybridisation that allows C_{60} to accept electrons. Curving the surface of conjugated organic molecules causes the σ -bonds of the carbon atoms to deviate from planarity. Rehybridisation of the carbon atom occurs so that the π orbital is no longer of purely p -orbital character and the σ orbitals no longer contain all of the s -orbital character. Thus the fullerenes are of intermediate hybridisation ($sp^{2.28}$), between that of graphite (sp^2) and diamond

(sp³) The 2s-orbital lies at a much lower energy than the 2p orbital therefore the molecular orbitals which form from these rehybridised orbitals will have enhanced electron affinity relative to the usual type of molecular orbitals derived from pure carbon 2p atomic orbitals

The high electron affinity of C₆₀ allows the addition of up to six electrons in solution ¹⁴⁸ Its electron accepting ability was measured electrochemically with respect to the 9,10-diphenylanthracene/9,10-diphenylanthracene radical cation reference redox couple and then referenced to saturated calomel electrode (SCE) This gave a first reduction potential $E_{1/2}^1 = -0.59$ V in dichloromethane (vs SCE) ¹⁴⁹ The first half-wave reduction potential of C₆₀ has also been given as $E_{1/2}^1 = -0.422$ V in acetonitrile ¹⁵⁰ Although it is a weak electron acceptor, C₆₀ formed C-T salts with alkali and alkaline-earth metals some of which exhibited superconductivity e.g. the C-T salt K₃C₆₀ exhibited superconductivity at 18K ¹⁵¹ Higher values for onset of superconductivity were subsequently obtained and currently the highest temperatures at which superconductivity is observed is 40K under a pressure of 15 kbar for Cs₃C₆₀ ¹³ C₆₀ also formed a C-T complex with the strong electron donor tetrakis(dimethylamino)ethylene which exhibits ferromagnetic properties and an ambient temperature conductivity of 10⁻² Scm⁻¹ ¹⁵² However, it failed to form C-T complexes with TTF and its derivatives ¹⁵⁰ As a result of these findings, novel fullerene derivatives with better acceptor abilities were investigated At present only two derivatives, (C₆₀F₄₈)¹⁴⁹ and a quinone-type methanofullerene¹⁵³ exhibited more positive first half wave reduction potentials than C₆₀ The first reduction potential of C₆₀F₄₈, $E_{1/2}^1 = 0.79$ V (vs SCE) in dichloromethane is more positive than that of most neutral organic electron acceptors known The reduction potential of the quinone-type methanofullerenes on the other hand can be tuned depending on the substituents on the cyclohexadienone moiety and are thus precursors for organic metals

Chapter 2

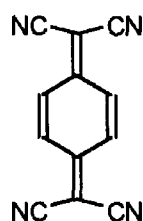
RESULTS AND DISCUSSION

Synthesis of Dicyanomethylene Electron Acceptors

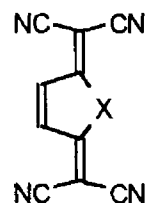
2 1 Introduction

As outlined in the previous chapter there has been considerable interest in the synthesis of derivatives of TCNQ (2) that have potential as novel electron acceptors in the formation of charge-transfer complexes and radical-ion salts. Interest in these materials arises from their electrically conducting properties and the fact that at low temperatures many such salts exhibit superconductivity. New electron acceptors are sought in an attempt to raise the temperature at which onset of superconductivity is observed.

Our approach has been to investigate the synthesis of heterocyclic analogues of TCNQ, (157), in which isoelectronic replacement of a double bond π -electron pair has been achieved by a heteroatom carrying a lone pair of electrons capable of π -type conjugation.



(2)



(124a) X=S

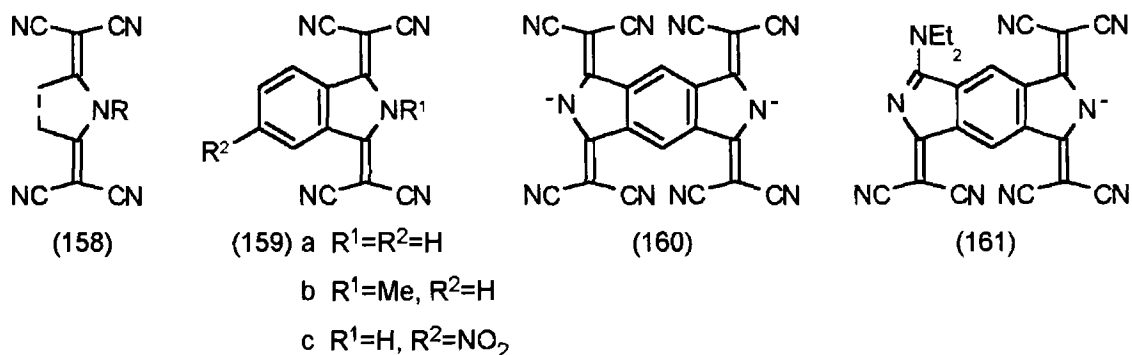
(124b) X=Se

(129) X=O

(157) X=NR, R=H, alkyl, aryl

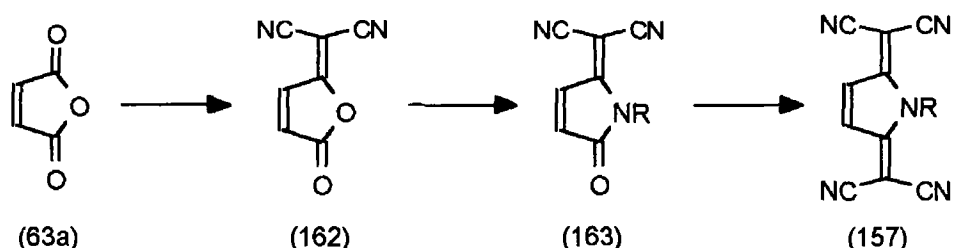
A comprehensive structural search of the literature showed that only four closely related examples of compounds containing the structural unit (158) had been synthesised. Thus compound (159a) and some of its salts are known,¹⁵⁴ as are the nitro derivative (159c),¹⁵⁵ the dianion (160),¹⁵⁶ and the anion (161).¹⁵⁶ No tetracyano *N*-substituted derivatives required as precursors to the potential organic metals were known at the outset of this work, but the thiophene, selenophene and furan analogues (124a), (124b) and (129) have been prepared.^{120, 122} These derivatives, upon one- or two-electron reduction, should form an aromatic sextet resulting in a planar cyclic system. Since the aromaticity decreases in the order thiophene>selenophene \approx pyrrole>furan, it is expected that the reduction potentials of the pyrroline system (157) will be between that of the thiophene and furan systems. The pyrroline ring system, in contrast to (124a), (124b) and (129) has the ability to tune its electron accepting properties by varying the substituent on the nitrogen atom. This

would also allow a variety of functional groups to attach which should lead to increased solubilities for these compounds



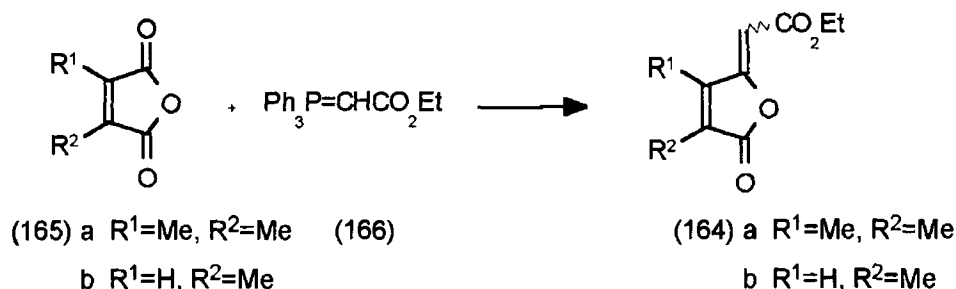
Recently work in our laboratory aimed at the synthesis of the *N*-substituted derivative (159b) was successful in achieving this objective¹⁵⁷ It was also found¹⁵⁷ that reaction of (159a) or its ammonium salt with a variety of acylating and alkylating agents did not yield the desired compounds This was probably due to the non-nucleophilicity of the anion as a result of stabilisation granted by the dicyanomethylene $[=C(CN)_2]$ group The *N*-substituted derivatives are of interest in order to examine their ability to form radical anion salts and charge-transfer complexes and their potential as conducting organic materials

It was decided to investigate the synthesis and chemistry of 4-dicyanomethylene-2-butenolide (162) as a potential precursor to (157) starting from the readily available compound maleic anhydride (63a) (scheme 2 1)



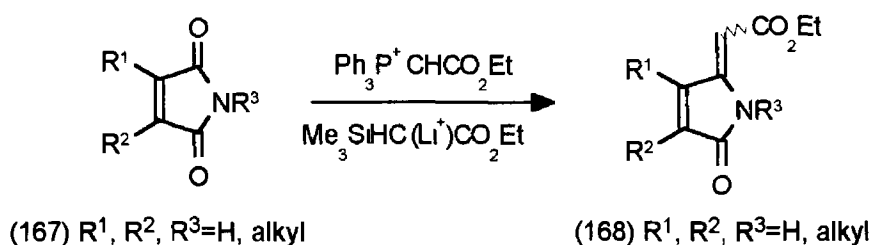
Scheme 2 1

It has been shown that *Z* and *E* isomers of lactones (164) can be prepared¹⁵⁸ by reacting substituted maleic anhydrides (165) with ethoxycarbonylmethylene(triphenyl)phosphorane (166) via the Wittig reaction (scheme 2 2)



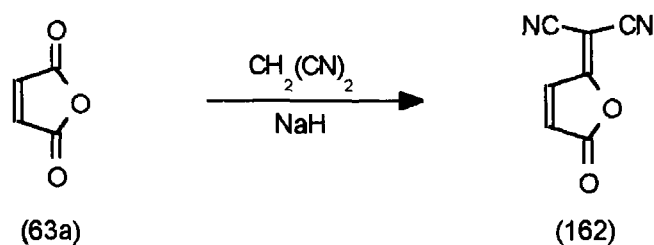
Scheme 2 2

Analogous reactions of maleimides with stabilised phosphoranes have received scant attention despite the fact that the reactions of phosphoranes with both cyclic and acyclic imides are known to give ylide derivatives ^{158b}. This is because forceful conditions are required and also maleimide itself undergoes nucleophilic attack at the carbon-carbon double bond rather than at the carbonyl group. But maleimides (167) have been shown to undergo Wittig and Peterson olefination reactions to form 5-ylidenepyrrol-2(5*H*)-ones (168)¹⁵⁹ (scheme 2 3)



Scheme 2 3

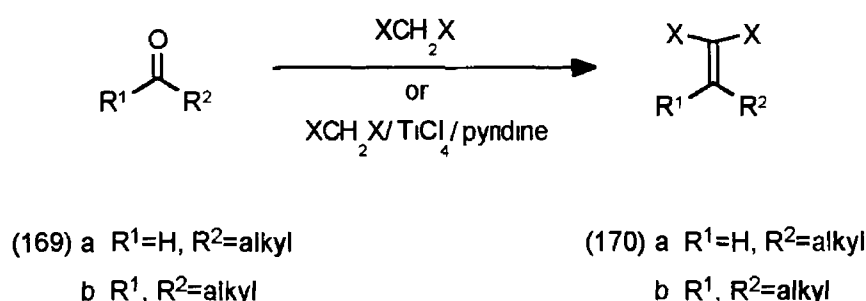
It was of interest to see whether an analogous nucleophilic substitution would occur at the carbonyl group of maleic anhydride (63a) using malononitrile, via Knoevenagel condensation (scheme 2 4)



Scheme 2 4

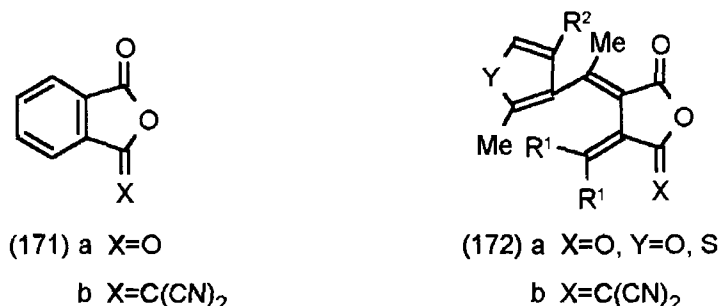
Knoevenagel condensation involves the reaction of an active methylene compound of the form XCH_2X (where $X=CO_2Et, CN, CO_2H$) with an aldehyde

(169a) or ketone (169b) to afford an alkene (170) (scheme 2 5) The aldehyde or ketone does not contain an α hydrogen usually In contrast to ketones, aldehydes react much better with active methylene compounds and few successful reactions with ketones have been reported However, Lehnert has shown⁹⁰ that good yields of alkene (170, $X=CO_2Et$) result from the condensation of diethyl malonate with aldehydes and ketones when the Lewis acid titanium tetrachloride is used with pyridine in tetrahydrofuran (scheme 2 5)



Scheme 2 5

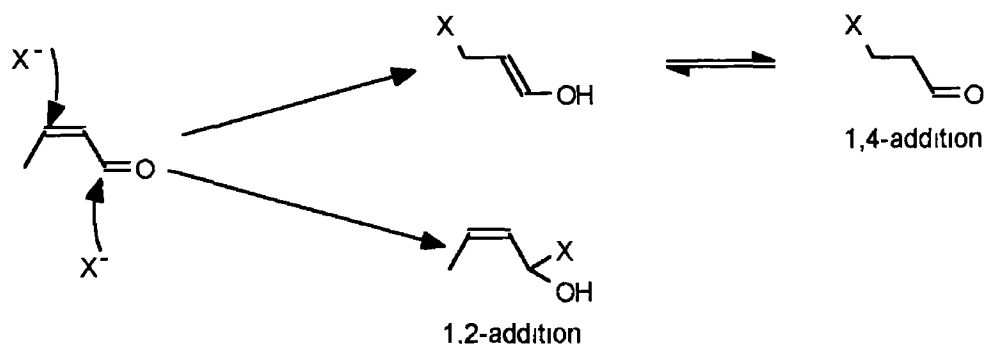
At the outset of this work Knoevenagel condensation of maleic anhydride with the active methylene compound malononitrile had not been reported However, 3-dicyanomethylenephthalide (171b) had previously been synthesised¹⁶⁰ by base-catalysed condensation of phthalic anhydride (171a) with malononitrile and more recently Heller and co-workers condensed malononitrile with a substituted succinic anhydride (172a) to afford a new class of photochromic fulgides (172b) ¹⁶¹



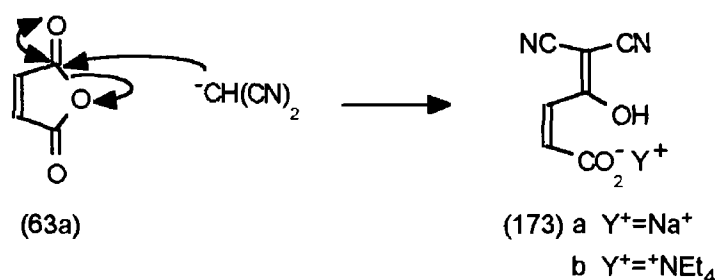
2 2 Synthesis of Sodium (Z)-4-Dicyanomethylene-4-hydroxy-2-butenate (173a), Tetraethylammonium (Z)-4-Dicyanomethylene-4-hydroxy-2-butenate (173b) and (Z)-4-Dicyanomethylene-4-hydroxy-2-butenic acid (179)

Nucleophilic addition to α,β -unsaturated carbonyl compounds is well documented in the literature and can occur either at the carbon-carbon double

bond or at the carbonyl group resulting in 1,4- (Michael addition) or 1,2-addition respectively (scheme 2 6) However, during the course of our work nucleophilic attack occurred predominantly at the carbonyl group of maleic anhydride (63a) (scheme 2 7) Thus reaction of maleic anhydride with malononitrile in tetrahydrofuran afforded sodium (Z)-4-dicyanomethylene-4-hydroxy-2-butenolate (173a) as a yellow solid which was isolated by filtration This solid was found to be insoluble in most organic solvents but did dissolve in water



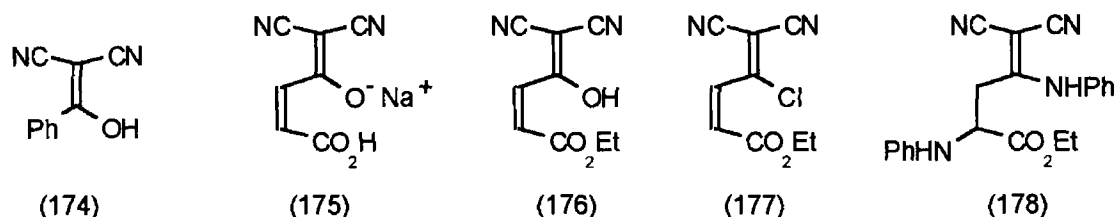
Scheme 2 6



Scheme 2 7

The IR spectrum of (173a) showed a broad hydroxyl band at 3460 cm^{-1} , two strong nitrile bands at 2216 and 2191 cm^{-1} and a strong carbonyl band at 1550 cm^{-1} . The 1H NMR spectrum displayed one proton doublets at δ 6.11 and 6.74 ppm (vinylic protons) with a coupling constant of 12.8 Hz consistent with the expected Z geometry of the molecule and a broad singlet at δ 17.46 ppm (hydroxyl proton). The presence of the hydroxyl proton was confirmed by its disappearance from the 1H NMR spectrum on shaking with deuterium oxide. The ^{13}C NMR spectrum exhibited seven signals, a signal at δ 57.47 ppm due to the dicyano substituted carbon, two nitrile absorptions at δ 116.97 and 117.81 ppm, two vinylic absorptions at δ 133.02 and 133.59 ppm and two absorptions at δ 165.54 and 182.30 ppm due to the carbonyl and dicyanomethylene substituted carbons. The carbon absorption at δ 57.47 ppm

was assigned as the dicyano substituted carbon by comparison with the ^{13}C NMR spectral data of (174) ¹⁶²



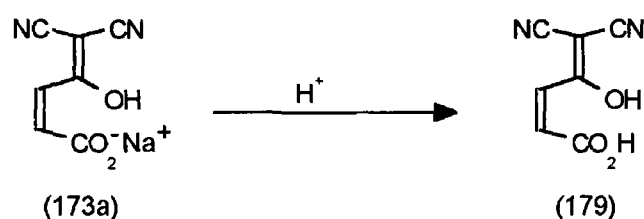
On the basis of the IR and NMR data it was also possible that the isomeric compound (175) had been formed. However, heating (173a) under reflux in ethanol containing a catalytic amount of sulphuric acid afforded the ethyl ester (176). Comparison of the melting point, IR and NMR spectra of (176) with an authentic sample, prepared by treating lactone (162) with ethanol, section 2.3.1, showed that they were identical. Conversion of the ethyl ester (176) to the corresponding chloroester (177) and subsequent reaction of (177) with aniline, as discussed in section 2.4, afforded (178) as the major product. An X-ray crystal structure of (178) (figure 2.1) confirmed the structure thus providing conclusive evidence that the yellow solid isolated was the sodium salt (173a) rather than the isomeric compound (175).

The sodium salt (173a) was difficult to recrystallise so it was converted to the corresponding tetraethylammonium salt (173b) by reaction with tetraethylammonium bromide under aqueous conditions. Compound (173b) was isolated as a yellow solid after work up (scheme 2.7). The IR spectrum of (173b) contained many spectral similarities to the sodium salt (173a). For example, it showed a hydroxy band at 3440 cm^{-1} , a nitrile absorption at 2202 cm^{-1} and a carbonyl absorption at 1695 cm^{-1} . The ^1H and ^{13}C NMR spectra of (173b) corresponded to those expected and were also very similar to those for the sodium salt. However, the methyl protons β to the nitrogen atom exhibited a twelve proton triplet of triplets at $\delta\ 1.30\text{ ppm}$ ($J\ 2.0, 7.4\text{ Hz}$) in the ^1H NMR, the splitting of the methyl protons being due to hydrogen coupling with the methylene protons (7.4 Hz) and also coupling with the ^{14}N nucleus ($J\ 2.0\text{ Hz}$). The methylene protons showed an eight proton quartet due to its coupling with the methyl protons at $\delta\ 3.38\text{ ppm}$ ($J\ 7.4\text{ Hz}$). Similarly in the ^{13}C NMR spectrum the methylene carbon showed a 1:1:1 triplet at $\delta\ 52.18\text{ ppm}$ ($J\ 3.05\text{ Hz}$) due to carbon-nitrogen coupling. This is as expected from the literature¹⁶³ and was confirmed by comparison with the ^1H and ^{13}C NMR spectra of an authentic sample of tetraethylammonium bromide. The ^1H NMR spectrum of tetraethylammonium bromide showed a twelve proton triplet of triplets at $\delta\ 0.73\text{ ppm}$ ($J\ 2.0, 7.4\text{ Hz}$) due to the methyl group and an eight

proton quartet at δ 2.83 ppm (J 7.4 Hz) due to the methylene protons. The ^{13}C NMR spectrum showed a singlet at δ 6.45 ppm (methyl carbon) and a 1:1:1 triplet at δ 51.23 ppm (J 3.05 Hz, methylene carbon).

The observed coupling between $^{14}\text{N}/^1\text{H}$ and $^{14}\text{N}/^{13}\text{C}$ in the NMR spectra is attributed to the slow transition of the spin states of nitrogen compared to that of the proton or carbon transition. The proton or carbon only "sees" the spin of nitrogen in one state or another during their transitions. ^{14}N has three possible spin states (+1, 0, -1) due to its spin of 1 rather than a half. Nuclei with spin greater than a half have larger electric quadrupole moments than those with spin of a half and are much more sensitive to interactions with the magnetic field of the NMR spectrometer and to magnetic and electric perturbations of the valence electrons and/or their environment.

Treatment of the sodium salt (173a) with dilute hydrochloric acid afforded, after work up, (Z)-4-dicyanomethylene-4-hydroxy-2-butenolide (179) as a yellow solid (scheme 2.8). The IR, ^1H and ^{13}C NMR spectra were consistent with the assigned structure and contained many spectral similarities to the sodium salt. The IR spectrum contained two strong hydroxyl bands at 3441 and 3370 cm^{-1} , two strong nitrile bands at 2250 and 2236 cm^{-1} and a strong carbonyl band at 1690 cm^{-1} . The ^1H NMR spectrum showed one proton doublets at δ 6.64 and 7.12 ppm (vinyl protons) with a *cis* coupling constant of 12.8 Hz and a one proton broad singlet (hydroxyl proton) at δ 10.96 ppm. It is possible that the second hydroxyl proton exchanged with the acetone- d_6 used as the NMR solvent to give a water signal at δ 2.75 ppm in the ^1H NMR spectrum. The ^{13}C NMR spectrum showed seven signals, one at δ 68.71 ppm corresponding to the dicyano substituted carbon, signals at δ 111.87 and 112.87 ppm corresponding to the nitrile carbons and four signals between δ 130.93 and 175.12 ppm due to vinyl, carbonyl and dicyanomethylene substituted carbons.

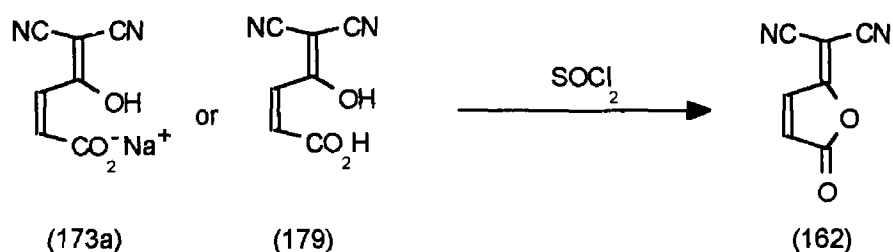


Scheme 2.8

2.3 Synthesis and Chemistry of 4-Dicyanomethylene-2-butenolide (162)

As was mentioned in the introduction (section 2.1) it was decided to investigate the synthesis and chemistry of 4-dicyanomethylene-2-butenolide

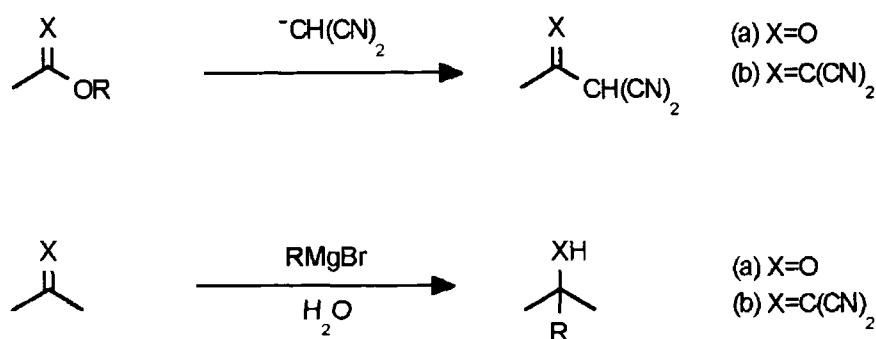
(162) as a potential precursor to the potential organic metals. Initially the previously unknown 4-dicyanomethylene-2-butenolide (162) was prepared in reasonable yield (~53%) by heating sodium (Z)-4-dicyanomethylene-4-hydroxy-2-butenolate (173a) with thionyl chloride under reflux (scheme 2 9). The reason for the low yield of product obtained from this reaction may be due to the low solubility of (173a) in thionyl chloride. Alternatively (162) can be synthesised from (Z)-4-dicyanomethylene-4-hydroxy-2-butenic acid (179) in higher yield (~71%) using the same reaction conditions.



Scheme 2 9

The microanalytical, IR and NMR spectral data were consistent with the proposed structure of the γ -lactone (162). The IR spectrum showed a strong α,β -unsaturated- γ -lactone carbonyl band at 1819 cm⁻¹ and a strong nitrile band at 2241 cm⁻¹. The ¹H NMR spectrum showed one proton doublets at δ 7.23 and 8.27 ppm (vinyl protons) with a *cis* coupling constant of 5.9 Hz. The ¹³C NMR spectrum showed seven signals, one at δ 68.58 ppm corresponding to the dicyano substituted carbon, signals at δ 109.73 and 110.38 ppm corresponding to the nitrile carbons and four signals between δ 129.70 and 172.35 ppm corresponding to the vinylic, carbonyl and dicyanomethylene substituted carbons.

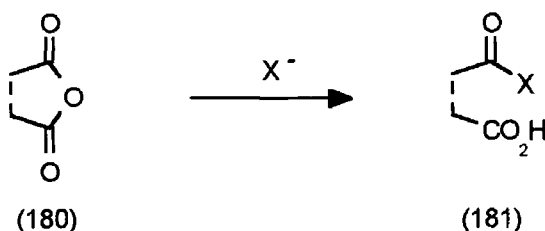
Now that 4-dicyanomethylene-2-butenolide (162) had been synthesised interest turned to its chemistry and whether it exhibited similar reactivity to that of maleic anhydride (63a). The analogy between the dicyanomethylene and carbonyl groups was previously observed by Wallenfels and co-workers.¹⁶⁴ They showed that the two groups have similar inductive and resonance effects and that many of the well-known reactions of the carbonyl group have close parallels with the dicyanomethylene group. Examples of these include the aldol condensation and Grignard addition reactions (scheme 2 10).



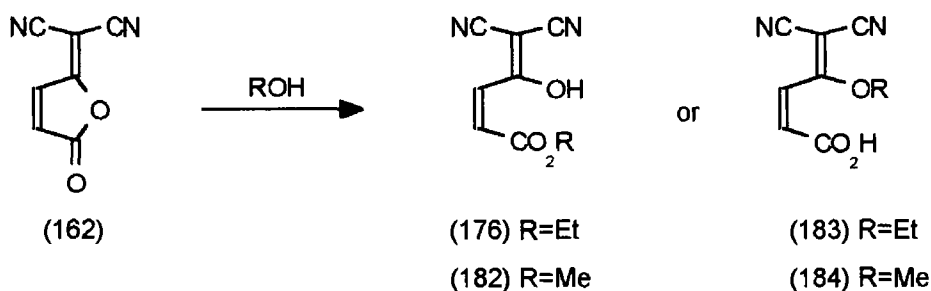
Scheme 2 10

2 3 1 Synthesis of Ethyl (Z)-4-Dicyanomethylene-4-hydroxy-2-butenate (176) and Methyl (Z)-4-Dicyanomethylene-4-hydroxy-2-butenate (182)

It is well known that cyclic anhydrides (180) react with nucleophiles (X^-) to yield monosubstituted carboxylic acids (181)¹⁶⁵ (scheme 2 11) Similarly it was anticipated that nucleophilic substitution of 4-dicyanomethylene-2-butenolide (162) with alcohols would afford the open-chain hydroxy compounds (176) and (182) or (183) and (184) (scheme 2 12)



Scheme 2 11

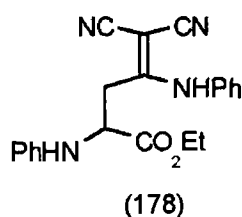
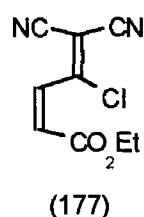


Scheme 2 12

Thus reaction of (162) with ethanol afforded the previously unknown ethyl (Z)-4-dicyanomethylene-4-hydroxy-2-butenate ester (176) in good yield. The IR, ^1H and ^{13}C NMR spectra were consistent with the proposed structure of the ethyl ester. The IR spectrum showed a strong α,β -unsaturated ester carbonyl band at 1660 cm^{-1} and a strong nitrile band at 2227 cm^{-1} . The ^1H NMR

spectrum showed a three proton triplet at δ 1.41 ppm (J 7.4 Hz) due to the methyl protons, a two proton quartet at δ 4.43 ppm (J 7.4 Hz) due to the methylene protons, one proton doublets at δ 6.43 and 7.06 ppm (vinylic protons) with a *cis* coupling constant of 12.8 Hz and a one proton broad signal at δ 14.55 ppm (hydroxyl proton). The ^{13}C NMR spectrum showed nine signals, two upfield signals at δ 13.43 and 64.64 ppm due to the saturated carbons of the ethyl group, a signal at δ 70.01 ppm corresponding to the dicyano substituted carbon, two signals at δ 111.35 and 112.47 ppm corresponding to the nitrile carbons and four signals between δ 129.54 and 173.83 ppm corresponding to the vinylic, carbonyl and dicyanomethylene substituted carbons.

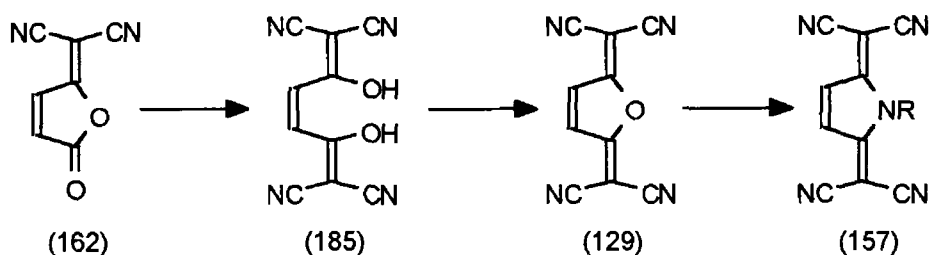
On the basis of the IR and NMR spectral data it was also possible that the isomeric compound (183) had been formed. The microanalytical data was also consistent with both structures. However, conversion of (176) to the chloroester (177) and subsequent reaction of (177) with aniline afforded (178) as the major product. X-ray crystallography of compound (178), (figure 2.1) confirmed that the product was the ethyl ester (176) rather than the isomeric compound (183).



Methyl (*Z*)-4-dicyanomethylene-4-hydroxy-2-butenolate (182) was similarly prepared by treating the lactone (162) with methanol. The IR, ^1H and ^{13}C NMR spectra for (182) corresponded to those expected and were very similar to those obtained for (176). For the same reasons given for (176), the compound isolated was (182) and not its isomer (184).

2.3.2 Attempted Synthesis of 1,4-Bis(dicyanomethylene)-1,4-dihydroxy-2-butene (185)

It was of interest to see if the reaction of another molecule of malononitrile with 4-dicyanomethylene-2-butenolide (162) would result in nucleophilic attack at the lactone carbonyl to generate intermediate (185) which might then undergo intramolecular cyclisation to form the known compound, 2,5-bis(dicyanomethylene)-2,5-dihydrofuran (129).¹²² This might provide a viable route to the desired *N*-substituted analogues (157) (scheme 2.13).

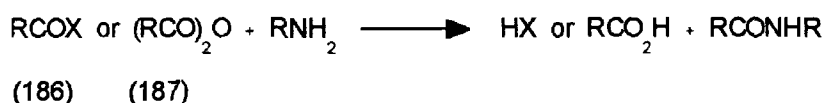


Scheme 2 13

Reaction of lactone (162) with sodiomalononitrile in tetrahydrofuran afforded a brown oil after work up ^1H NMR and IR spectral analysis of the brown oil was suggestive of a complex mixture of products and thus an alternative route to the desired *N*-substituted derivatives was necessary

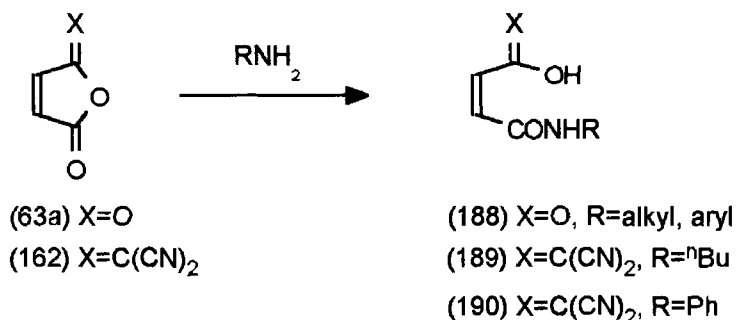
2 3 3 Synthesis of (*Z*)-*N*-Butyl-4-dicyanomethylene-4-hydroxy-2-butenamide (189) and (*Z*)-*N*-Phenyl-4-dicyanomethylene-4-hydroxy-2-butenamide (190)

The general method for the preparation of amides is by treatment of acyl halides (186) or anhydrides (187) with amines (scheme 2 14)



Scheme 2 14

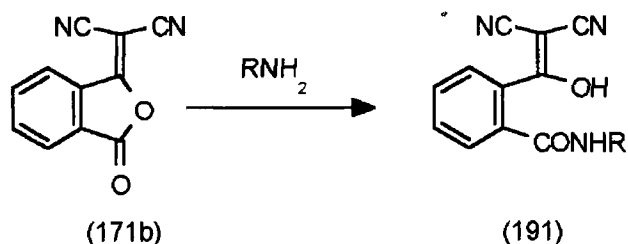
The analogous reaction of amines with maleic anhydride (63a) produces the corresponding maleamic acids (188) (scheme 2 15)



Scheme 2 15

It was anticipated that the reaction of lactone (162) with amines would afford the hydroxy amide (189) and (190) This was further supported by the discovery¹⁶⁰ that nucleophilic attack, by a series of aromatic and aliphatic

amines on the phthalic anhydride derivative (171b), occurs at the carbonyl carbon rather than at the dicyanomethylene substituted carbon affording the amic acid analogue (191) (scheme 2 16)



Scheme 2 16

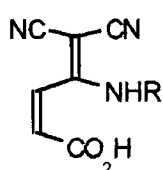
The synthesis of hydroxy amides (189) and (190) had not been previously reported Treatment of 4-dicyanomethylene-2-butenolide (162) with *N*-butylamine in tetrahydrofuran yielded (*Z*)-*N*-butyl-4-dicyanomethylene-4-hydroxy-2-butenamide (189) as yellow crystals The IR, ¹H and ¹³C NMR spectra were consistent with the assigned structure The IR spectrum showed a strong hydroxyl band at 3270 cm⁻¹, a strong NH band at 3120 cm⁻¹, a strong nitrile band at 2231 cm⁻¹ and two strong amide carbonyl bands at 1582 and 1517 cm⁻¹ respectively The ¹H NMR spectrum showed four signals between δ 0.90 and 3.40 ppm corresponding to the four different hydrogens of the butyl group, one proton doublets at δ 6.70 and 6.93 ppm (vinyl protons) with a *cis* coupling constant of 12.8 Hz and one proton broad signals at δ 9.36 and 14.45 ppm (amide and hydroxyl protons) The methylene group α to the nitrogen atom exhibits a quartet integrating for two protons at δ 3.40 ppm This is due to coupling of the methylene group with the amino proton and with the adjacent methylene group However, there is no observed coupling between the proton on nitrogen and the α methylene protons and thus the NH is shown as a one proton broad singlet The expected triplet for the amino proton is obscured by nuclear quadrupolar broadening i.e the rate of transitions of the spin states of nitrogen is similar to the time required for proton transitions The ¹³C NMR spectrum showed eleven signals, four between δ 13.05 and 40.33 ppm corresponding to the four carbons of the butyl group, one at δ 65.42 ppm corresponding to the dicyano substituted carbon, two at δ 112.96 and 113.98 ppm corresponding to the two nitrile carbons, two vinylic absorptions at δ 132.25 and 132.35 ppm and two signals at δ 166.73 and 177.28 ppm due to the carbonyl and dicyanomethylene substituted carbons

(*Z*)-*N*-Phenyl-4-dicyanomethylene-4-hydroxy-2-butenamide (190) was similarly synthesised by treating lactone (162) with aniline The IR, ¹H and ¹³C

NMR spectra were consistent with the assigned structure and were very similar to those of (189). The IR spectrum showed an NH band at 3277 cm^{-1} , aromatic and aliphatic carbon-hydrogen bands at 3119 and 3053 cm^{-1} and a nitrile band at 2228 cm^{-1} . The ^1H NMR spectrum showed one proton doublets at δ 6.59 and 6.94 ppm (vinylic protons) with a coupling constant of 12.8 Hz, a one proton aromatic multiplet at δ 7.19 ppm and a two proton aromatic multiplet at δ 7.39 ppm which were superimposed on a broad hydroxyl proton. A two proton aromatic multiplet at δ 7.62 ppm and a one proton amide singlet at δ 11.98 ppm were also observed. The presence of the amide and hydroxyl protons was confirmed by their disappearance from the ^1H NMR spectrum on shaking with deuterium oxide. In addition to this the ^{13}C NMR spectrum showed eleven signals, one at δ 61.96 ppm corresponding to the dicyano substituted carbon, two at δ 114.73 and 115.60 ppm corresponding to the nitrile carbons, eight between δ 120.72 and 179.38 ppm corresponding to the vinylic, aromatic, carbonyl and dicyanomethylene substituted carbons.

On standing, compound (190) precipitated from dimethyl sulfoxide- d_6 solution, thus some heating was required in order to redissolve it. As a result, when the NMR spectra were repeated, a number of additional carbon absorptions were observed in the ^{13}C NMR spectrum along with a complex ^1H NMR spectrum. TLC analysis of the heated sample showed that it was no longer just one product but several products indicating that the compound was unstable when heated in dimethyl sulfoxide- d_6 .

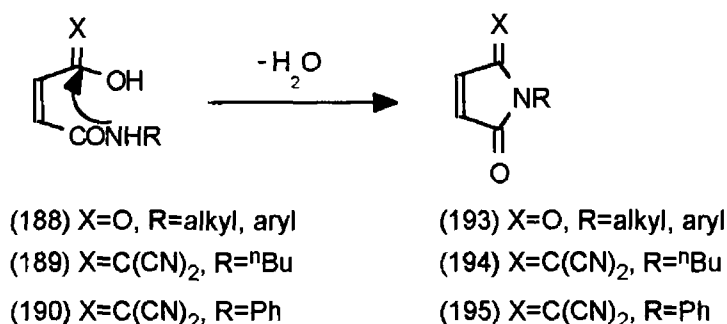
On the evidence of the microanalytical, IR and NMR spectral data it is also possible that the isomeric compound (192) could be the product formed in the reaction. However, treating ethyl ester (176) with *N*-butylamine under reflux afforded (189). The melting point, IR and NMR spectral data were identical with an authentic sample of (189). The evidence for the structure of (176) (X-ray crystal structure of its dianilide derivative) confirms that the product isolated was (189) and not the isomeric compound (192). Analogously it is assumed that aniline reacts at the carbonyl carbon to afford (190). These results were also supported by the results of Moore and Kim.¹⁶⁰ These workers showed that reaction of amines on (171b) afforded amic acid analogues (191) (scheme 2.16).



(192)

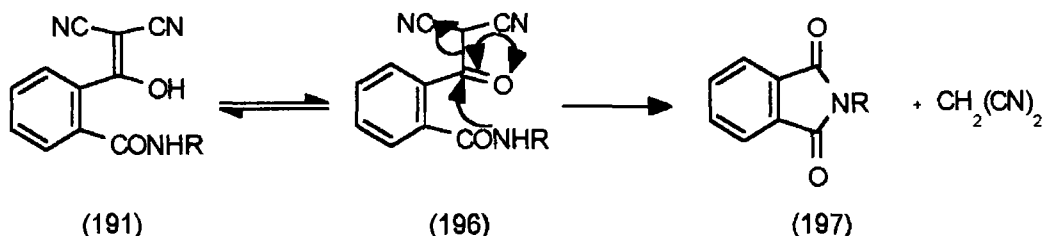
2 3 4 Attempted Cyclisation of (Z)-N-Butyl-4-dicyanomethylene-4-hydroxy-2-butenamide (189) and (Z)-N-Phenyl-4-dicyanomethylene-4-hydroxy-2-butenamide (190)

Maleic anhydride (63a) reacts with *N*-alkyl and *N*-aryl amines to form the corresponding maleamic acids (188) (scheme 2 15) These maleamic acid derivatives (188) can be dehydrated and cyclised with acetic anhydride, acetic acid or by heating above their melting points yielding *N*-substituted maleimides (193) (scheme 2 17)



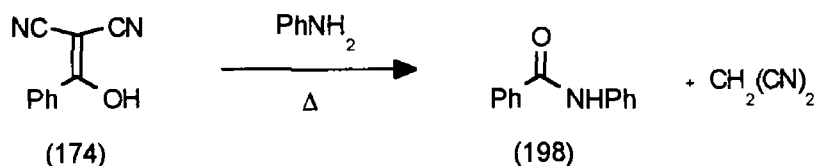
Scheme 2 17

It was of interest to see whether (Z)-*N*-butyl-4-dicyanomethylene-4-hydroxy-2-butenamide (189) or (Z)-*N*-phenyl-4-dicyanomethylene-4-hydroxy-2-butenamide (190) would undergo a similar cyclisation via intramolecular nucleophilic attack by the amide nitrogen on the dicyanomethylene group and thus yield (194) and (195) potential precursors to the desired analogues (157) (scheme 2 17) It has been shown previously by NMR spectroscopy¹⁶⁰ that the amic acid derivatives (191) slowly tautomerise to the intermediate (196) (scheme 2 18) Derivative (196) subsequently undergoes imidization to give (197) The elimination of malononitrile anion rather than hydroxide is favoured because of the enhanced stability granted by the two conjugated nitrile groups



Scheme 2 18

In addition to this, dehydration of the anilinium salt of (174), gave benzanilide (198) and malononitrile¹⁶² which was further support of this mechanism (scheme 2 19)



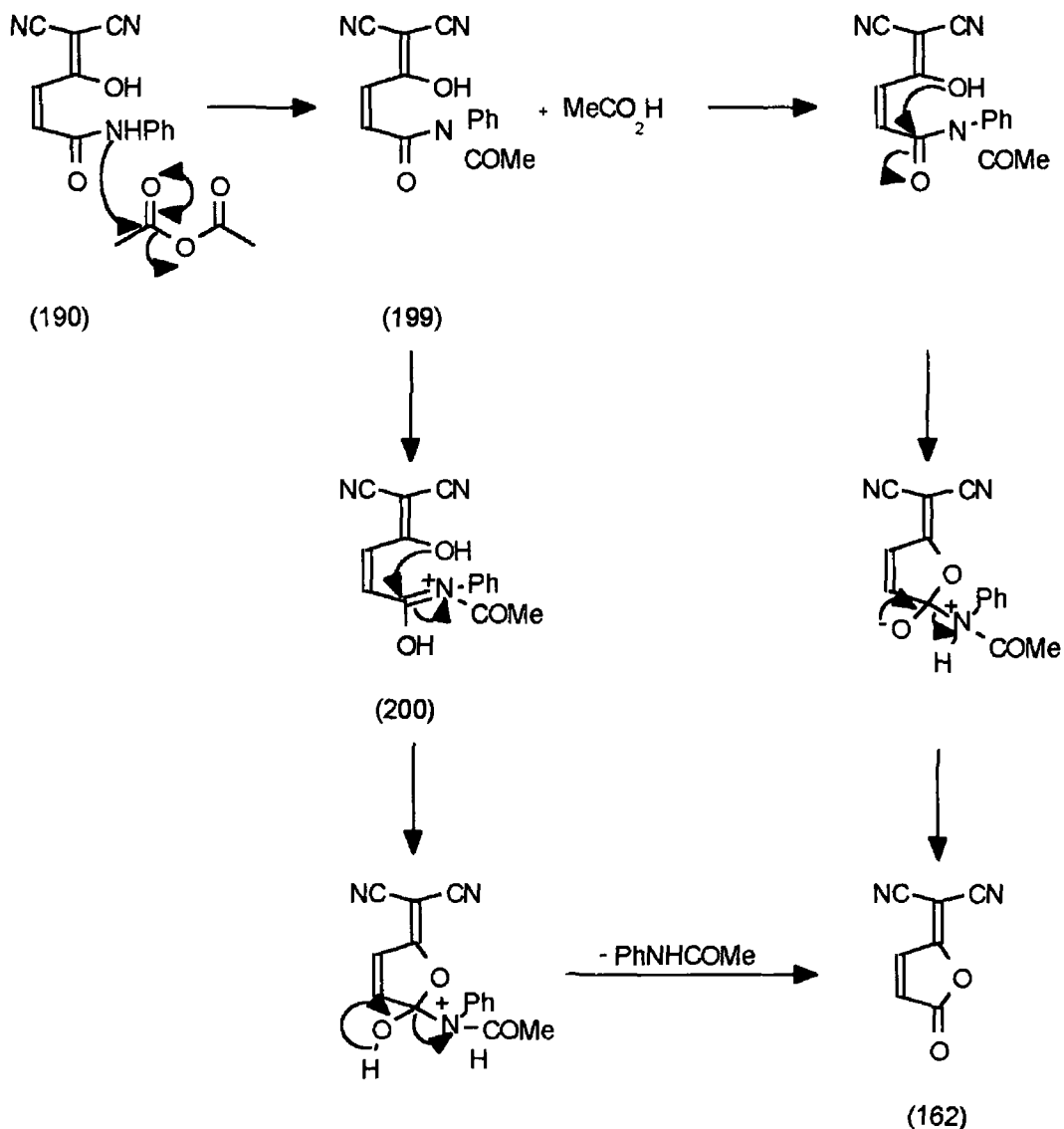
Scheme 2 19

Initially the cyclisation of (*Z*)-*N*-butyl-4-dicyanomethylene-4-hydroxy-2-butenamide (189) was attempted by heating (189) at 160 °C for 30 minutes. However, the resulting black solid isolated from this reaction gave complex ¹H and IR spectra suggestive of a multiplicity of decomposition products. Similar results using the same reaction conditions were obtained from the pyrolysis of (*Z*)-*N*-phenyl-4-dicyanomethylene-4-hydroxy-2-butenamide (190).

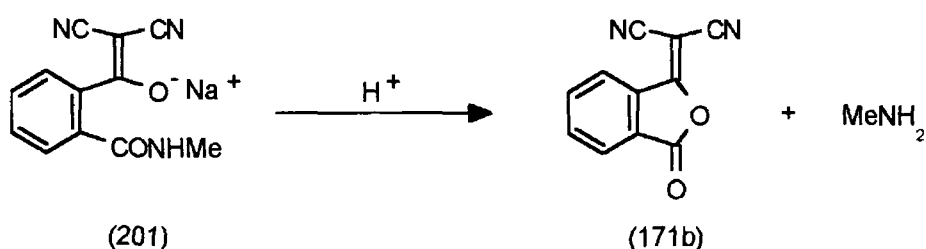
The cyclisation of (*Z*)-*N*-phenyl-4-dicyanomethylene-4-hydroxy-2-butenamide (190) was attempted by heating (190) with acetic anhydride under reflux. On following the reaction by TLC the formation of a faster eluting major product and some baseline material was observed. The major product was isolated as a white solid after work up. The ¹H NMR showed a three proton singlet at δ 2.12 ppm, a one proton aromatic triplet at δ 7.05 ppm, a two proton aromatic triplet at δ 7.29 ppm and a three proton doublet at δ 7.45 ppm. The ¹H NMR spectrum on shaking with deuterium oxide showed the disappearance of one proton from the triplet at δ 7.45 ppm (amide proton). The number of distinct signals and the absence of the vinylic protons indicated that this was not the expected *N*-phenyl-2-dicyanomethylene-pyrrol-5-one (195). The ¹³C NMR spectrum confirmed this with an aliphatic signal at δ 24.64 ppm, four aromatic signals between δ 119.92 and 137.87 ppm and a carbonyl signal at δ 168.49 ppm. Examination of the IR spectrum showed a strong amide band at 3250 cm⁻¹ and a strong carbonyl band at 1650 cm⁻¹. On the basis of this data the product was assigned as acetanilide. This was confirmed by comparing the spectra and melting point of the white solid with the IR, ¹H and ¹³C NMR spectra of an authentic sample of acetanilide. The possible mode of reaction is shown in scheme 2 20 in which the amide group of (190) becomes acylated to yield the *N*-acyl amide (199) and acetic acid. Derivative (199) is then probably intramolecularly attacked by the hydroxyl oxygen or alternatively under acidic conditions at the electron deficient iminium carbon of (200) to yield the lactone (162) and acetanilide. Lactone (162) was not isolated from the reaction mixture.

and was not detected on TLC due to its instability and probably hydrolysis to the hydroxy acid (179)

Our results show that an alternative ring closure with the elimination of acetanilide, affording lactone (162) can occur. These results were further substantiated by the discovery¹⁵⁷ that acidification of the sodium salt (201) gave 3-dicyanomethylenephthalide (171b) and methylamine (scheme 2 21)



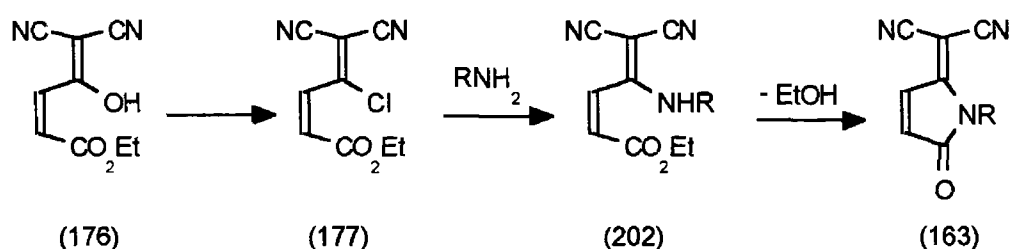
Scheme 2 20



Scheme 2 21

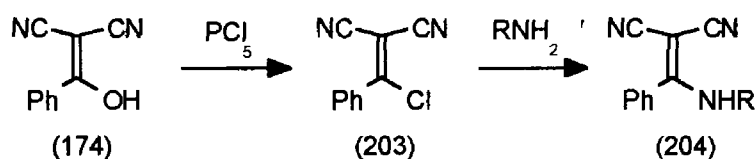
2.4 Synthesis and Reactions of Ethyl (Z)-4-Dicyanomethylene-4-chloro-2-butenate (177)

Since the dehydration of hydroxy amides (189) and (190) failed to give the desired imide derivative (163), it was decided to investigate an alternative route for the synthesis of these derivatives. An attractive route seemed to be the conversion of the hydroxyl group of ethyl (Z)-4-dicyanomethylene-4-hydroxy-2-butenate (176) to a chlorine atom affording (177), nucleophilic substitution of the chlorine atom with primary amines and ring closure of the resultant enamines (202) to yield the *N*-substituted derivatives (163) (scheme 2.22)



Scheme 2.22

An examination of the literature indicated that (hydroxyphenylmethylene)propanedinitrile (174) can be converted to the corresponding chloro compound (203) by heating under reflux with phosphorus pentachloride in dry dichloromethane.¹⁶² Subsequent reaction of (203) with aromatic amines was rapid and afforded the enaminnitriles (204) in good yield (scheme 2.23)



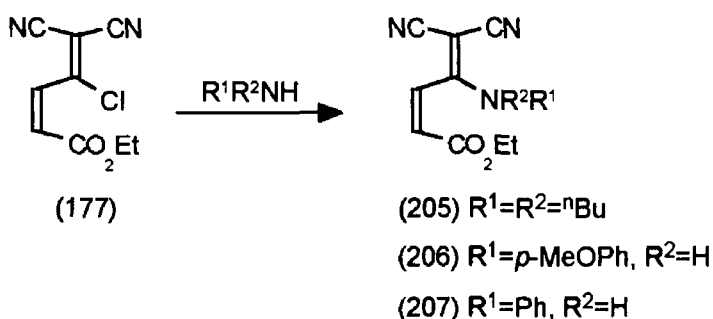
Scheme 2.23

Using this procedure ethyl (Z)-4-dicyanomethylene-4-chloro-2-butenate (177) was prepared from (176) and isolated after work up as a dark brown oil. TLC analysis of this oil indicated that it consisted of one major product and this was used in subsequent reactions without further purification. The IR, ¹H and ¹³C NMR spectra of (177) corresponded to those expected and were very similar to that obtained for (176) except for the absence of the hydroxyl group in the IR and ¹H NMR spectra and the downfield shift of the dicyano substituted

carbon to δ 90 86 ppm in the ^{13}C NMR spectrum Moore and Robello reported¹⁶² a similar downfield shift in the dicyano substituted carbon of (203)

2 4 1 Synthesis of Ethyl (Z)-4-Dicyanomethylene-4-dibutylamino-2-butenolate (205), Ethyl (Z)-4-Dicyanomethylene-4-*p*-anisidino-2-butenolate (206) and Ethyl (Z)-4-Dicyanomethylene-4-anilino-2-butenolate (207)

The reactions of ethyl (Z)-4-dicyanomethylene-4-chloro-2-butenolate (177) with primary and secondary amines were investigated Thus treatment of (177) with an excess of *N,N*-dibutylamine afforded a brown oil after work up TLC analysis of this oil indicated that it consisted of one major product Purification by column chromatography gave the anticipated product, ethyl (Z)-4-dicyanomethylene-4-dibutylamino-2-butenolate (205) as yellow crystals (scheme 2 24)



Scheme 2 24

The IR, ^1H and ^{13}C NMR spectra of (205) were consistent with the assigned structure The IR spectrum showed an aliphatic carbon-hydrogen band at 2963, 2937 and 2879 cm^{-1} , a strong ester carbonyl band at 1721 cm^{-1} and two strong nitrile bands at 2206 and 2189 cm^{-1} The ^1H NMR spectrum showed five signals between δ 0 96 and 4 27 ppm (alkyl protons), one proton doublets at δ 6 44 and 7 16 ppm (vinyl protons) with a coupling constant of 16 2 Hz The ^{13}C NMR spectrum showed seven upfield signals between δ 13 47 and 61 50 ppm corresponding to the saturated alkyl carbons and the dicyano substituted carbon, nitrile absorptions at δ 115 85 and 117 13 ppm, vinyl absorptions at δ 131 81 and 135 22 ppm and absorptions at δ 162 98 and 163 79 ppm corresponding to the carbonyl and dicyanomethylene substituted carbon atoms The C-H correlation spectrum confirmed the signals at δ 13 47, 13 86, 19 22, 29 93, 52 66 and 61 50 ppm to be alkyl carbons and in doing so confirms that the signal at δ 50 92 ppm corresponds to the dicyano substituted carbon

The addition of excess *p*-anisidine to (177) afforded a white precipitate from the reaction mixture which was filtered off and assigned as *p*-anisidine hydrochloride. This was confirmed by converting the hydrochloride salt to *p*-anisidine using aqueous sodium carbonate and comparing the IR, ^1H and ^{13}C NMR spectra and melting point of the resultant solid with an authentic sample of *p*-anisidine. In addition to this white solid, ethyl (*Z*)-4-dicyanomethylene-4-*p*-anisidino-2-butenolate (206) was isolated from the filtrate following column chromatography. Derivative (206) exhibited similar spectra to that of (205). The IR spectrum showed aromatic and aliphatic carbon-hydrogen bands at 3237, 2996 and 2839 cm^{-1} , two strong nitrile bands at 2219 and 2200 cm^{-1} , a strong carbonyl band at 1708 cm^{-1} and a carbon-carbon double bond absorption at 1642 cm^{-1} . The ^1H NMR spectrum showed a three proton triplet at δ 1.29 ppm (methyl protons, J 7.4 Hz), a singlet at δ 3.82 ppm (methoxy protons), a quartet at δ 4.22 ppm (methylene protons, J 7.4 Hz), a one proton doublet (vinylic proton, J 16.2 Hz) at δ 6.74 ppm, a two proton aromatic multiplet at δ 6.90 ppm, a three proton multiplet at δ 7.00 ppm and a one proton singlet (NH proton) at δ 8.25 ppm. The presence of the NH proton was confirmed by its disappearance from the ^1H NMR spectrum on shaking with deuterium oxide. Expansion of the multiplet at δ 7.00 ppm showed a two proton aromatic multiplet superimposed upon a one proton vinylic doublet (J 16.2 Hz). This second vinylic proton although superimposed by the absorptions from the aromatic protons could be assigned on the basis of its coupling constant of 16.2 Hz. The ^{13}C NMR spectrum contained fourteen signals, four signals between δ 13.98 and 61.73 ppm due to the aliphatic and dicyano substituted carbons, two nitrile absorptions at δ 114.29 and 114.64 ppm, six vinylic and aromatic absorptions between δ 114.94 and 159.35 ppm and two absorptions at δ 163.14 and 164.08 ppm due to the carbonyl and dicyanomethylene substituted carbons.

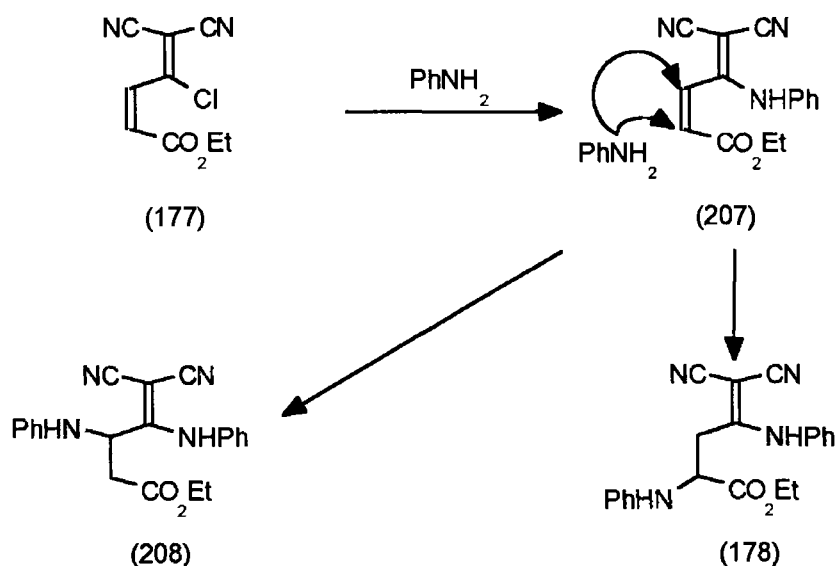
In contrast to *N,N*-dibutylamine and *p*-anisidine, addition of excess aniline to (177) deposited a white solid as the major product from the reaction mixture. This white solid was filtered off and TLC analysis of the filtrate showed that it contained one major product. Purification by column chromatography yielded the anticipated product ethyl (*Z*)-4-dicyanomethylene-4-anilino-2-butenolate (207), required as the potential precursor to (163), in low yield (~11%). The IR, ^1H and ^{13}C NMR spectra of (207) was consistent with the assigned structure and exhibited similar spectra to that of (205) and (206).

The ^1H NMR spectrum of the white solid contained a three proton triplet at δ 1.20 ppm (J 7.4 Hz), a two proton doublet at δ 3.07 ppm (J 8.37 Hz), a two proton multiplet at δ 4.14 ppm (J 7.4 and 8.37 Hz), a one proton broad signal at

δ 4.41 ppm, a one proton doublet at δ 6.15 ppm (J 8.37 Hz) and five signals between δ 6.60 and 7.43 ppm (aromatic protons) and a one proton singlet at δ 10.64 ppm (amino proton). The number of distinct signals and the disappearance of the vinylic doublets indicated that this was not the expected dicyanomethylene amide ester (207). The ^{13}C NMR spectrum confirmed this with four aliphatic signals at δ 14.09, 50.98, 52.11 and 61.16 ppm, a quaternary carbon at δ 54.59 ppm, ten signals between δ 112.74 and 146.91 ppm due to nitrile and aromatic carbons and two signals at δ 166.68 and 171.56 ppm due to the carbonyl and dicyanomethylene substituted carbons. The DEPT 135 spectrum showed ten carbons bearing hydrogen and combined with the C-H correlation spectrum confirmed the proton triplet at δ 1.20 ppm to be methyl protons of the ester group. The doublet at δ 3.07 ppm was assigned as methylene protons α to the dicyanomethylene group, the multiplet at δ 4.14 ppm was assigned as the methylene protons of the ester group, the broad signal at δ 4.41 ppm was assigned as an NH proton, the doublet at δ 6.15 ppm was assigned as a methine proton α to the ester group and the singlet at δ 10.64 ppm was assigned as an NH proton. The presence of the NH protons was confirmed by their disappearance from the ^1H NMR spectrum on shaking with deuterium oxide. The NMR data is consistent with the addition of two aniline molecules.

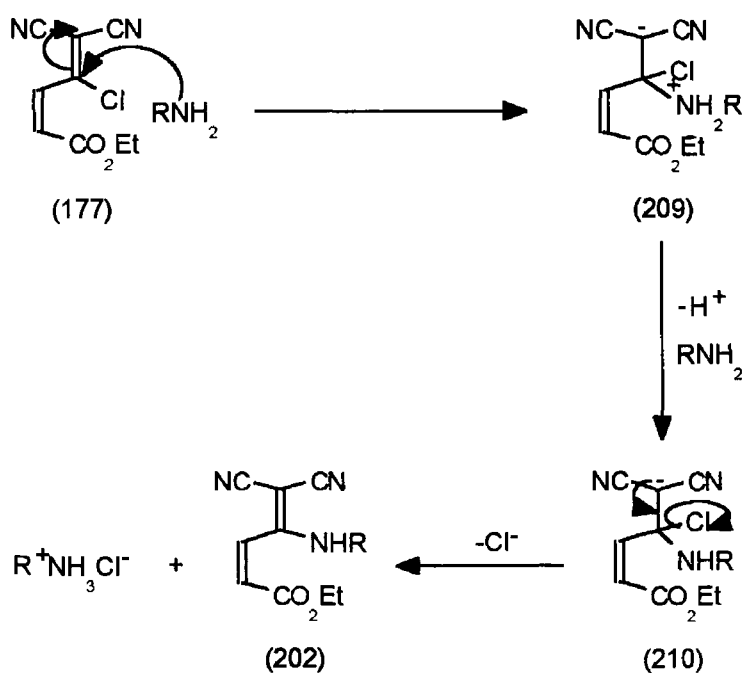
Examination of the IR spectrum showed two strong NH bands at 3377 and 3290 cm^{-1} , two strong nitrile bands at 2214 and 2198 cm^{-1} , a strong carbonyl band at 1725 cm^{-1} and aromatic carbon-hydrogen bands at 749 and 699 cm^{-1} . The microanalytical data was also consistent with the addition of two molecules of aniline. On the basis of this data two structures were considered possible for the major product observed in this system. The two possible modes of reaction considered for this system are attack at the carbon-carbon double bond α to the ester group to yield (178) and attack at the carbon-carbon double bond α to the dicyanomethylene group (scheme 2.25) to yield (208). Both products are consistent with the addition of two equivalents of aniline.

Suitable crystals for X-ray diffraction were grown and the structure is shown in figure 2.1. The relevant bond lengths and bond angles are given in table 2.1 and 2.2 respectively. This clearly shows that the product arises from addition of aniline to the carbon α to the ester group i.e. ethyl (Z)-4-dicyanomethylene-2,4-dianilinobutanoate (178).



Scheme 2 25

The probable mode of reaction of (177) with the aromatic amines *p*-anisidine and aniline is shown in scheme 2 26 and may be explained in terms of the basicities of the amines



Scheme 2 26

p-Anisidine is the stronger base and thus the more powerful nucleophile. However, it is the weaker base aniline, that gives the Michael addition product (178) as the major product. Two equivalents of amine were required, the first equivalent is involved in the formation of intermediate (209) and the second equivalent of amine deprotonates the ammonium ion affording carbanion (210).

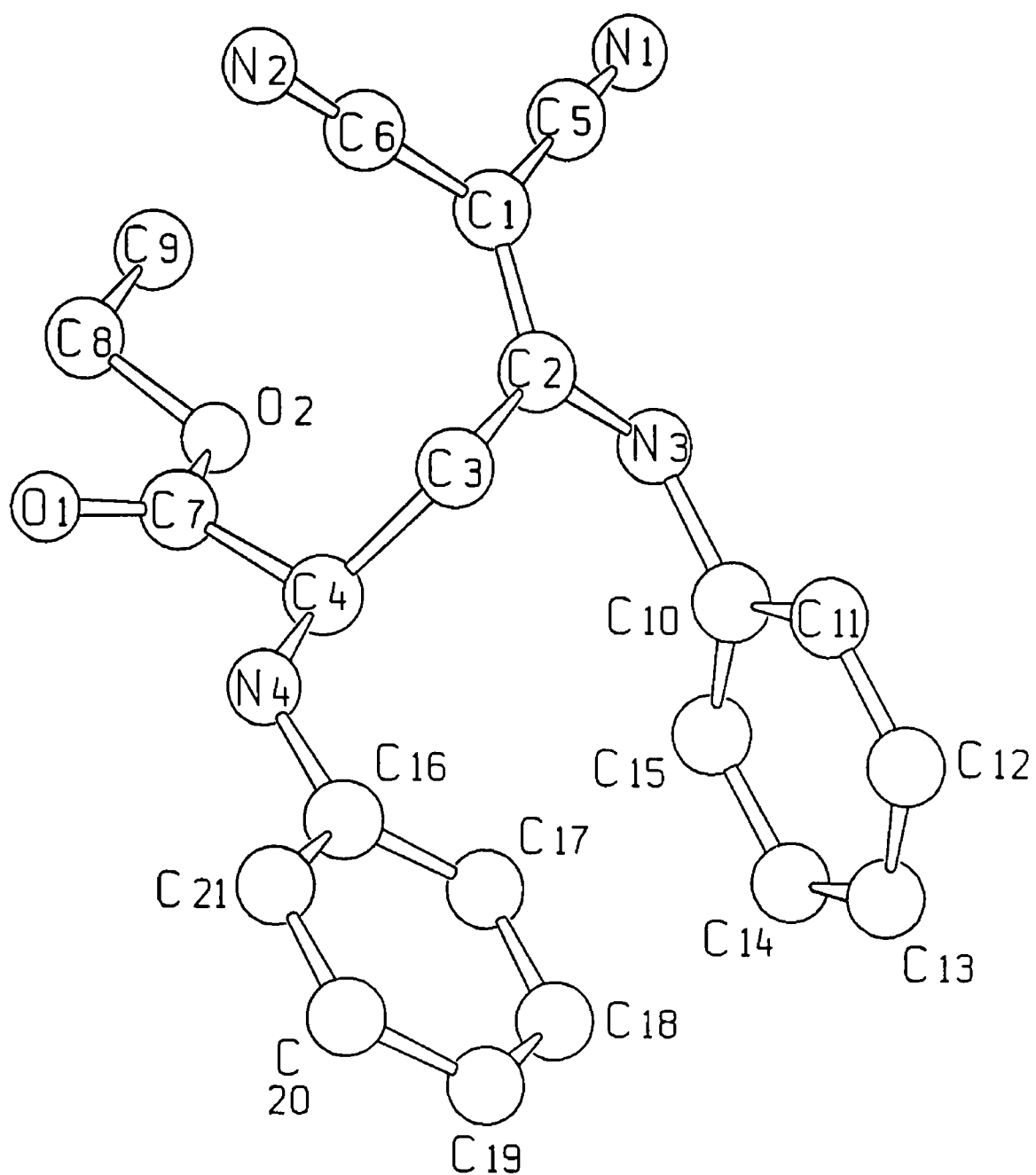


Figure 2 1 Schakal representation of X-ray crystal structure of dianilide (178)

Table 2 1 Bond lengths for (178)

Bond lengths [Å]			
O(1)-O(6)	1 197(2)	C(4)-C(7)	1 512(3)
O(2)-C(7)	1 313(2)	C(8)-C(9)	1 463(4)
O(2)-C(8)	1 476(3)	C(10)-C(15)	1 377(3)
N(1)-C(5)	1 145(3)	C(10)-C(11)	1 378(3)
N(2)-C(6)	1 142(3)	C(11)-C(12)	1 375(3)
N(3)-C(2)	1 338(3)	C(12)-C(13)	1 378(4)
N(3)-C(10)	1 433(3)	C(13)-C(14)	1 374(4)
N(4)-C(16)	1 380(3)	C(14)-C(15)	1 379(4)
N(4)-C(4)	1 432(3)	C(16)-C(17)	1 384(3)
C(1)-C(2)	1 384(3)	C(16)-C(21)	1 394(3)
C(1)-C(5)	1 416(3)	C(17)-C(18)	1 381(3)
C(1)-C(6)	1 422(3)	C(18)-C(19)	1 375(4)
C(2)-C(3)	1 501(3)	C(19)-C(20)	1 379(4)
C(3)-C(4)	1 561(3)	C(20)-C(21)	1 366(4)

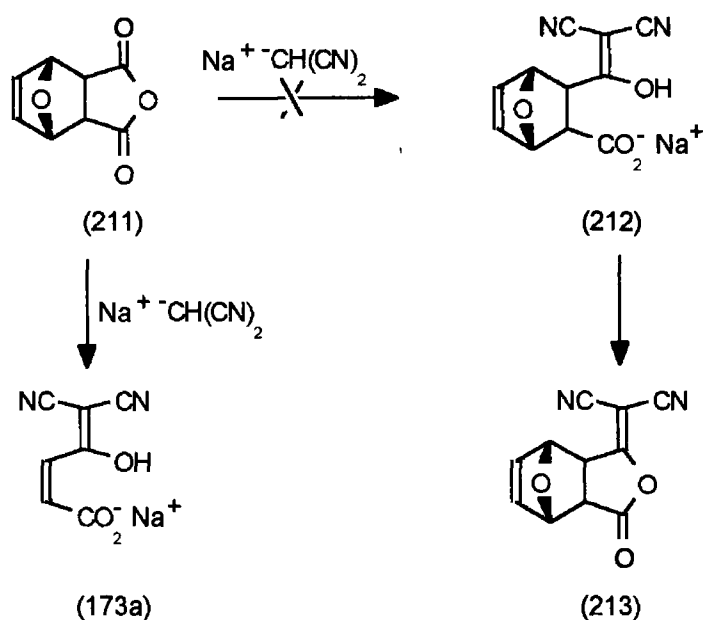
Table 2 2 Bond angles for (178)

Bond angles [deg]			
C(7)-O(2)-C(8)	115 6(2)	C(9)-C(8)-O(2)	107 8(2)
C(2)-N(3)-C(10)	126 2(2)	C(15)-C(10)-C(11)	120 5(2)
C(16)-N(4)-C(4)	125 5(2)	C(15)-C(10)-N(3)	119 3(2)
C(2)-C(1)-C(5)	120 7(2)	C(11)-C(10)-N(3)	120 1(2)
C(2)-C(1)-C(6)	121 3(2)	C(12)-C(11)-C(10)	119 8(2)
C(5)-C(1)-C(6)	118 0(2)	C(11)-C(12)-C(13)	119 8(3)
N(3)-C(2)-C(1)	120 3(2)	C(14)-C(13)-C(12)	120 3(3)
N(3)-C(2)-C(3)	119 2(2)	C(13)-C(14)-C(15)	120 1(3)
C(1)-C(2)-C(3)	120 4(2)	C(10)-C(15)-C(14)	119 4(2)
C(2)-C(3)-C(4)	116 6(2)	N(4)-C(16)-C(17)	123 5(2)
N(4)-C(4)-C(7)	107 6(2)	N(4)-C(16)-C(21)	118 0(2)
N(4)-C(4)-C(3)	110 2(2)	C(17)-C(16)-C(21)	118 5(2)
C(7)-C(4)-C(3)	111 7(2)	C(18)-C(17)-C(16)	120 5(2)
N(1)-C(5)-C(1)	177 3(2)	C(19)-C(18)-C(17)	120 5(3)
N(2)-C(6)-C(1)	179 8(3)	C(18)-C(19)-C(20)	119 1(2)
O(1)-C(7)-O(2)	123 6(2)	C(21)-C(20)-C(19)	120 9(3)
O(1)-C(7)-C(4)	123 7(2)	C(20)-C(21)-C(16)	120 5(3)
O(2)-C(7)-C(4)	112 6(2)		

Carbanion (210) subsequently leads to (202) and the amine hydrochloride by chloride ion elimination. It is the stabilities of the respective hydrochloride salts that gives an insight to the observed reaction differences.

The unshared pair of electrons on the nitrogen atom of the two amines, aniline and *p*-anisidine, can delocalise into the aromatic ring and thus they are stabilised. However, on protonation the lone pair of electrons on aniline are no longer available and so aniline is stabilised with respect to the anilinium cation. Therefore it is energetically unprofitable for aniline to take up a proton and so it is likely that the aniline hydrochloride that forms in the reaction readily dissociates into aniline and hydrochloric acid. This allows for a second molecule of aniline to add to the carbon-carbon double bond. *p*-Anisidine hydrochloride, in contrast, is stabilised by the electron releasing ability of the methoxy group and therefore it is isolated as a white solid from the reaction mixture.

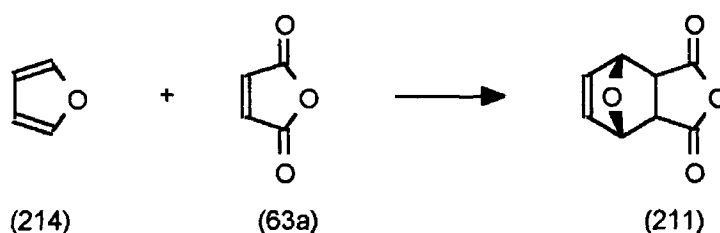
In attempting to circumvent the Michael addition, the reaction sequence in scheme 2.27 was attempted. It was hoped that reaction of 7-oxabicyclo[2.2.1]hept-5-ene-2,3-dicarboxylic anhydride (211) with sodium malononitrile would afford salt (212), a precursor to lactone (213). Compound (213) would subsequently lead to the desired *N*-alkyl derivatives.



Scheme 2.27

Treating the Diels-Alder adduct (211) with sodium malononitrile under reflux in anhydrous tetrahydrofuran for 1 hour afforded a yellow solid which was

isolated by filtration. This solid was identified as sodium (Z)-4-dicyanomethylene-4-hydroxy-2-butenolate (173a) by comparison of its IR and NMR spectra with those of an authentic sample of (173a). Compound (211) was synthesised according to a previously reported procedure¹⁶⁶ which involved adding furan (214) to an ethereal solution of maleic anhydride (63a) and its structure was confirmed by melting point, ¹H and ¹³C NMR and IR spectroscopy (scheme 2 28).

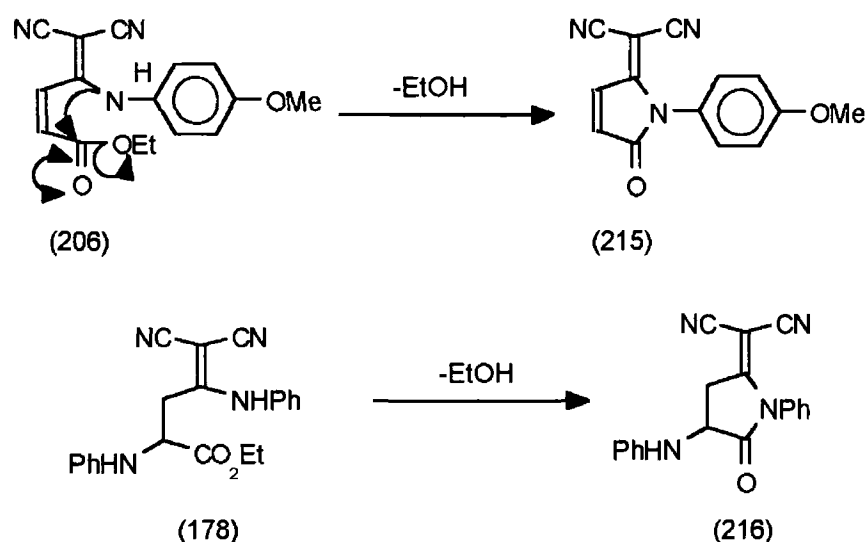


Scheme 2 28

However, from our results it is obvious that a retro Diels-Alder reaction has taken place. This occurs after the addition of malononitrile since heating (211) under reflux in anhydrous tetrahydrofuran for 1 hour afforded no new products. The spectral data and melting point of the white solid isolated from this reaction were consistent with those for (211). The failure to isolate (212) may be related to the greater stability of (173a) granted by its increased conjugation compared to (212).

2 4 2 Attempted Cyclisation of Ethyl (Z)-4-Dicyanomethylene-4-*p*-anisidino-2-butenolate (206) and Ethyl (Z)-4-Dicyanomethylene-2,4-dianilinobutanoate (178)

It was of interest to see whether intramolecular nucleophilic attack by the amide nitrogen on the ester carbonyl would lead to ring closure to form the pyrrolone derivative (215) or pyrrolidone derivative (216) (scheme 2 29). Ethyl (Z)-4-dicyanomethylene-4-*p*-anisidino-2-butenolate (206) was pyrolysed at 160 °C for 30 minutes. However the resulting solid gave complex ¹H and IR spectra suggestive of a multiplicity of decomposition products. Similar results were obtained when ethyl (Z)-4-dicyanomethylene-2,4-dianilinobutanoate (178) was pyrolysed under similar conditions and when (206) was heated in *N,N*-dimethylformamide.



Scheme 2 29

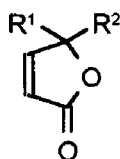
2 5 Discussion

Our approach to the synthesis of *N*-substituted TCNQ analogues via the dicyanomethylene lactone (162), proved to be a non-viable route for the synthesis of these derivatives. However, lactone (162) exhibits similar reactivity to its oxygen analogue, maleic anhydride. For example, it reacts with alcohols and amines under mild conditions to give hydroxy esters and amides respectively. Attempted cyclisation of the hydroxy amides by pyrolysis afforded, not the desired *N*-substituted derivatives, but a complex mixture of products. An alternative ring-closure to lactone (162) occurred when the *N*-phenyl hydroxy amide (190) was treated with acetic anhydride. This contrasts with the results obtained by Moore and Kim who showed¹⁶⁰ that ring closure of the dicyanomethylene amic acid derivative (191) under basic conditions afforded phthalimides and malononitrile. Our results may be attributed to presence of acid in the reaction mixture.

An alternative route to the desired *N*-substituted derivatives by treating chloroester (177) with primary amines and subsequent ring-closure of the resultant enamine esters also afforded a complex mixture of products. Our findings also showed that reaction of (177) with *N,N*-dibutylamine and *p*-anisidine gave the anticipated product whereas aniline afforded two products, one was the anticipated product (207) and the other product involved both Michael addition and nucleophilic displacement of the chlorine. Attempts to circumvent the Michael addition by protecting the carbon-carbon double bond of maleic anhydride with furan and reaction of the subsequent maleic anhydride-furan adduct with malononitrile gave the retro Diels-Alder product (173a).

The ease with which dicyanomethylene lactone (162) ring opens on nucleophilic attack by amines to give hydroxy amides, and the failure of these compounds and the enamine esters to undergo ring closure to (163), makes this route non-viable for the synthesis of the desired *N*-substituted derivatives (157)

Comparison of the ^1H NMR spectra of 4-dicyanomethylene-2-butenolide (162), (179) and the open-chain compounds showed not only chemical shift differences but also coupling constant differences (table 2.3). The coupling constant between the vinylic protons of (162), 5.9 Hz, is much lower than its corresponding open-chain analogues. This agrees well with literature coupling constant values of analogous butenolides (217)¹⁶⁷ which range from 5.6 to 6.0 Hz.



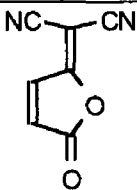
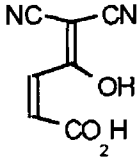
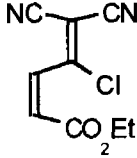
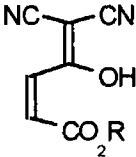
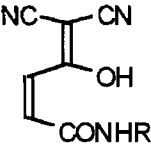
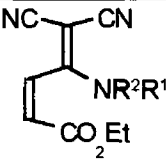
(217) a $\text{R}^1=\text{R}^2=\text{Me}$, $J_{\text{vinylic-H}}=6\text{ Hz}$

b $\text{R}^1=\text{Me}$, $\text{R}^2=\text{Ph}$, $J_{\text{vinylic-H}}=6\text{ Hz}$

c $\text{R}^1=\text{Me}$, $\text{R}^2=\text{CH}_2\text{CH}(\text{Me})_2$, $J_{\text{vinylic H}}=5.6\text{ Hz}$

The lower coupling constant value of (162) may be attributed to the smaller H-C=C bond angle of (162) compared to its open-chain derivatives. Also, a comparison of the coupling constants of the hydroxy esters (176) and (182), the chloroester (177) and the amide esters (205-207) in chloroform- d showed varying values (table 2.3). The coupling constant value increases in the order amide ester > chloroester > hydroxy ester. This may be explained by the electronic effect of the amide, chloro or hydroxyl group on the vinylic hydrogens.

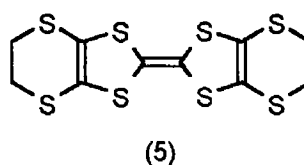
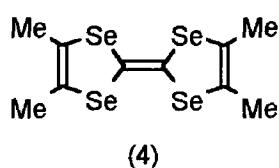
Table 2.3 Chemical Shift (ppm) and Coupling Constant (Hz) values of the Vinylic Protons of Dicyanomethylene Derivatives (in CDCl₃, unless otherwise stated)

Compound		δ_H	J
	(162)	7.23, 8.27 (acetone-d ₆)	5.9
	(179)	6.64, 7.12 (acetone-d ₆)	12.8
	(177)	6.86, 7.78	14.8
	(176) R=Et (182) R=Me	6.43, 7.06 6.39, 7.08	12.8 12.8
	(189) R= ⁿ Bu (190) R=Ph	6.70, 6.93 6.59, 6.94 (DMSO-d ₆)	12.8 12.8
	(205) R ¹ =R ² = ⁿ Bu (206) R ¹ = <i>p</i> -MeOPh R ² =H (207) R ¹ =Ph, R ² =H	6.44, 7.16 6.74, 7.00 6.76, 7.06	16.2 16.2 16.2

2.6 Future Work

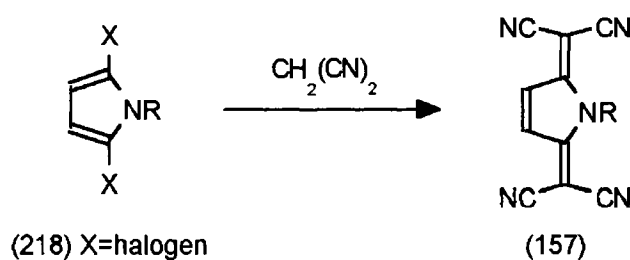
The design of organic metals is, in many cases, restricted to controlling the key properties of the individual component molecules or ions e.g. size, planarity, ionisation potential/electron affinity and extent of conjugation. When new donor and acceptor molecules are synthesised, it is necessary to prepare C-T salts and screen their properties to elucidate the effects of the new

C-T salts and screen their properties to elucidate the effects of the new structural modification on their electrical conductivities. C-T systems with increased dimensionality of structural, and therefore electrical, properties has been prevalent in the work of many groups. This stems from the fact that superconducting salts of TMTSF (4) and BEDT-TTF (5) were shown to have close inter- and intra-stack heteroatom interactions that stabilise the metallic state by suppressing Peierls distortion. This increase in dimensionality can be achieved by placing heteroatoms at peripheral sites in the donor or acceptor or alternatively by choosing an appropriate inorganic counterion for subsequent C-T salt formation.



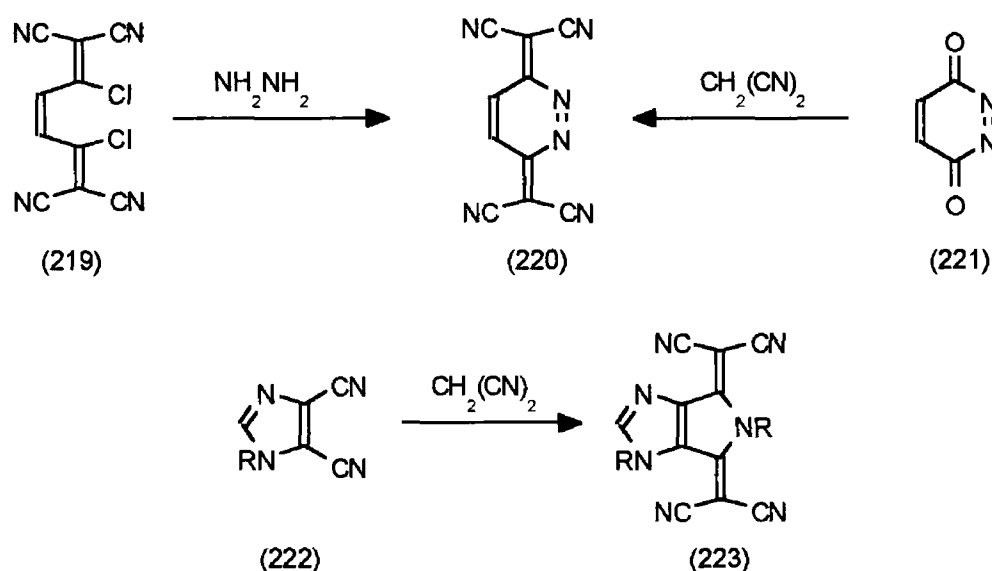
By analogy with the superconducting salts of TMTSF and BEDT-TTF, analogous superconducting salts of TCNQ would be attractive. Therefore, there is a need for the availability of a wide range of TCNQ analogues. The synthesis of TCNQ analogues that are structurally different from those already known are of interest so that their electron accepting abilities, C-T complex and radical-ion forming ability with appropriate electron donors could be investigated.

Our work was successful in synthesising dicyanomethylene electron acceptors but the ultimate, *N*-substituted pyrrole derivatives was not achieved. Alternative approaches to the design of these analogues are necessary and when available their C-T complex forming ability and electron accepting properties should be investigated. One alternative route may involve the construction of the heterocyclic ring prior to *N*-substitution, for example the reaction of 2,5-dihalogeno derivatives (218) with malononitrile (scheme 2.30).



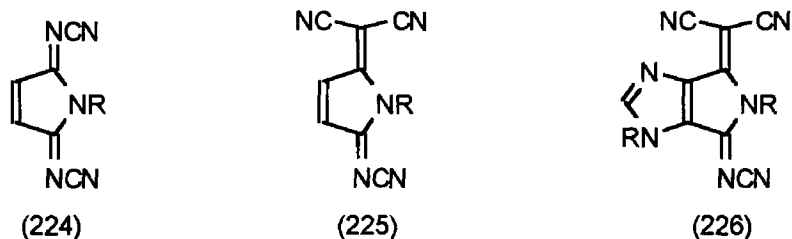
Scheme 2.30

Other systems that may also be useful are the heterocyclic TCNQ analogue (220) and the imidazole derivative (223). The presence of additional heteroatoms should lead to an increase in inter- and intra-stack heteroatom interactions and also a decrease in the on-site Coulomb repulsion. Compound (220) might possibly be synthesised from either the known compound, maleic hydrazide (221) or the unknown dichloride derivative (219) (scheme 2.31). Imidazole (223) may be prepared from the 4,5-dicyanoimidazole analogue (222).



Scheme 2.31

Alternatively the design and synthesis of organic acceptors containing the cyanoimine group ($=\text{NCN}$) opens up possibilities for the synthesis of DCNQI-type acceptors (224-226). The cyanoimine group has been shown to be a useful replacement for the dicyanomethylene group and has the advantage of being less sterically demanding than the dicyanomethylene group.

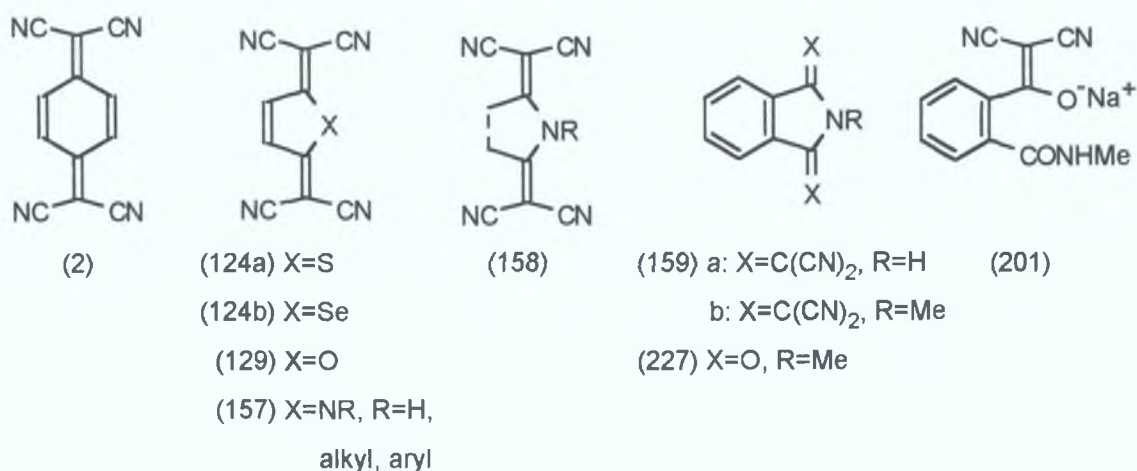


Chapter 3

Synthesis of Heterocyclic TCNQ Analogues

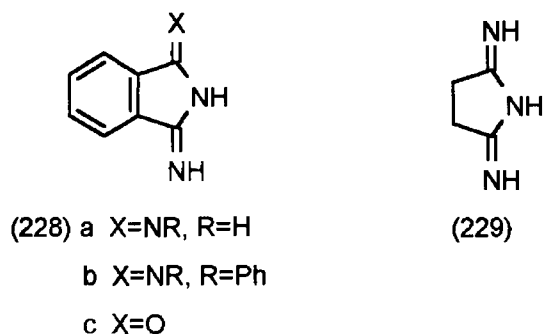
3.1 Introduction

It can be seen in chapter 1 that TCNQ (2) has been widely modified to improve its electrical properties. The majority of these modifications include extending its quinoid conjugation and introducing heteroatoms into the TCNQ ring. The introduction of heteroatoms into the component molecules of organic metals is one of the prerequisites to attain superior electrical conductivity. The heteroatoms can participate in inter- and intra-stack interactions thus suppressing the metal-to-insulator transition. The heterocyclic-TCNQ analogues (124a), (124b), (129) and (157) are isoelectronic with TCNQ and the lone pair of electrons on the heteroatom are capable of π -type conjugation. At the outset of this work only four closely related examples of compounds containing the structural unit (158) were known. Contrary to the traditional heterocyclic-TCNQs (124a), (124b) and (129) the acceptor properties of the pyrroline ring system (157) can be finely tuned by varying the substituents on the nitrogen atom. As a result, functionalisation is possible which can lead to increased solubilities for these compounds.

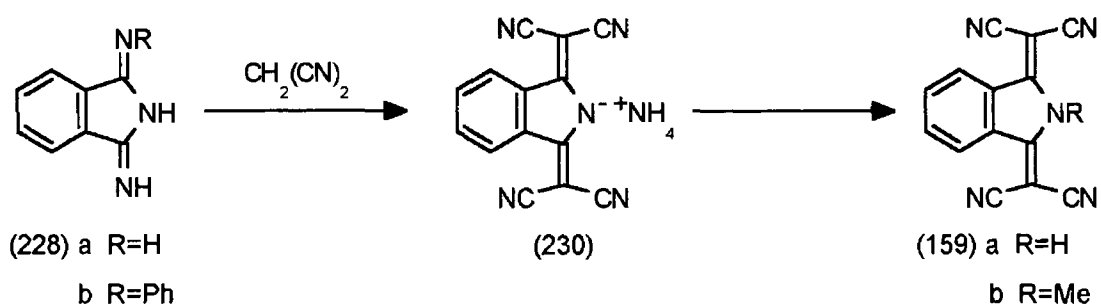


Previous work in our laboratory¹⁵⁷ investigated possible synthetic routes to the isoindoline analogues (159a and b). The first route involved the condensation of malononitrile with *N*-methylphthalimide (227). However, this gave the salt (201) which failed to undergo ring-closure to give the desired precursor to the *N*-substituted derivative. An alternative approach, which involved Knoevenagel condensation of malononitrile with (227) using Lehnert's reagent, was also investigated¹⁵⁷ but only resulted in unreacted *N*-methylphthalimide being recovered. Since these routes did not give the desired *N*-substituted derivatives, attention was focussed on the imidines (228a and b) as possible precursors to (159a and b). The condensation of imidines with active methylene compounds was extensively investigated by Elvidge and co-workers in the 1950s.¹⁶⁸ They found that the exocyclic imino

group of (228) and (229) reacted readily with a variety of active methylene compounds but the carbonyl group on (228c) showed no tendency to react with bases with the elimination of water

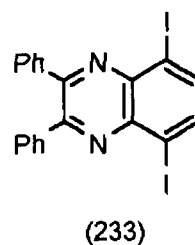
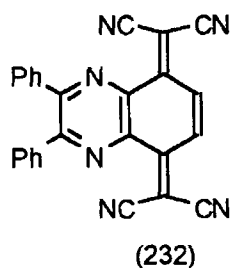
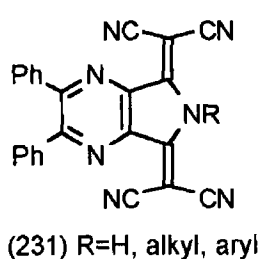


This approach provided a viable route to the isoindoline derivatives (159a and b), via the ammonium salt (230), by reacting malononitrile with either (228a) or (228b) in *N,N*-dimethylformamide at room temperature (scheme 3 1) 157



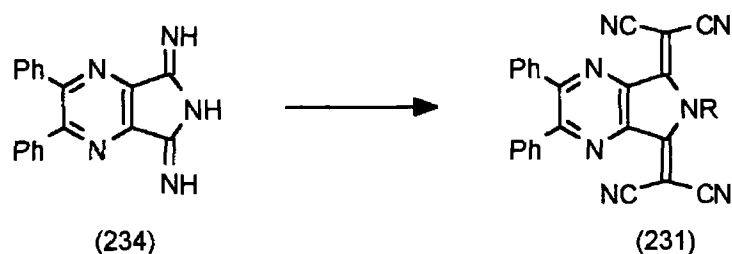
Scheme 3 1

With these considerations in mind it was intended to investigate the synthesis of *N*-substituted pyrazine derivatives (231). These derivatives are of interest in order to examine their electron accepting abilities and their potential to form C-T complexes with electron donors. The benzo analogue (232) was previously synthesised¹⁶⁹ and was shown to have very similar redox potentials ($E^1_{1/2}=+0.25\text{ V}$, $E^2_{1/2}=-0.29\text{ V}$) to TCNQ ($E^1_{1/2}=+0.28\text{ V}$, $E^2_{1/2}=-0.29\text{ V}$). Thus the presence of a bulky phenyl substituent does not affect the redox properties of the pyrazino-TCNQ skeleton. Compound (232) was synthesised from (233) in 81% yield by treating (233) with sodium dicyanomethanide in the presence of a palladium catalyst followed by appropriate oxidation.^{96a}



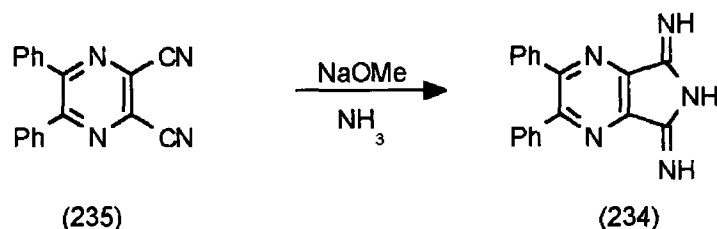
3 2 Reaction of Diimino-6H-5,7-dihydropyrrolo[3,4-b]pyrazine (234) with Malononitrile

Since the reaction of malononitrile with imidines (228a and b) yielded the isoindoline derivatives (159a and b) it was decided to synthesise the pyrazine analogues (231) by an analogous route (scheme 3 2) Condensation of imines with active methylene compounds is similar to that of aldehydes and ketones with active methylene compounds¹⁷⁰ The products are analogous and ammonia is lost instead of water



Scheme 3 2

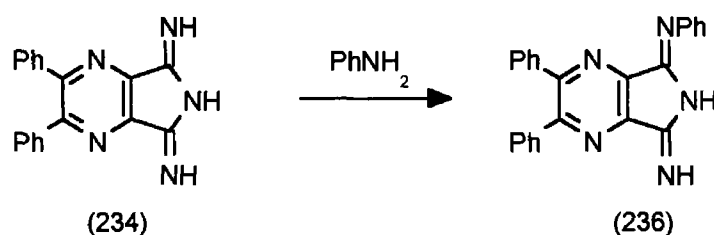
Compound (234) was synthesised¹⁷¹ by bubbling ammonia through a methanolic solution of (235) (scheme 3 3) 5,6-Diphenyl-2,3-dicyanopyrazine (235) was synthesised according to a previously reported procedure¹⁷² by reacting benzil with diaminomaleonitrile in the presence of acetic acid



Scheme 3 3

The IR, ¹H and ¹³C NMR spectra were consistent with the assigned structure of (234) The IR spectrum showed two NH absorptions at 3416 and 3259 cm⁻¹ and two imide carbon-nitrogen double bond absorptions at 1680 and

1644 cm^{-1} The ^1H NMR spectrum showed a three proton broad singlet (NH protons) at δ 3.07 ppm and a ten proton aromatic multiplet at δ 7.32 ppm. The ^{13}C NMR spectrum exhibited seven signals, six aromatic absorptions between δ 125.63 and 130.43 ppm and one signal at δ 139.04 ppm (imide carbon). However, the dimino derivative (234) proved very difficult to recrystallise so it was decided to derivatise it to the corresponding phenylimino analogue (236). An examination of the literature had shown that the isoindoline imine (228a) reacts readily with aniline to give the phenylimino derivative (228b).^{168b} Thus heating (234) under reflux for two hours with one equivalent of aniline in ethanol afforded (236) as yellow crystals (scheme 3.4).

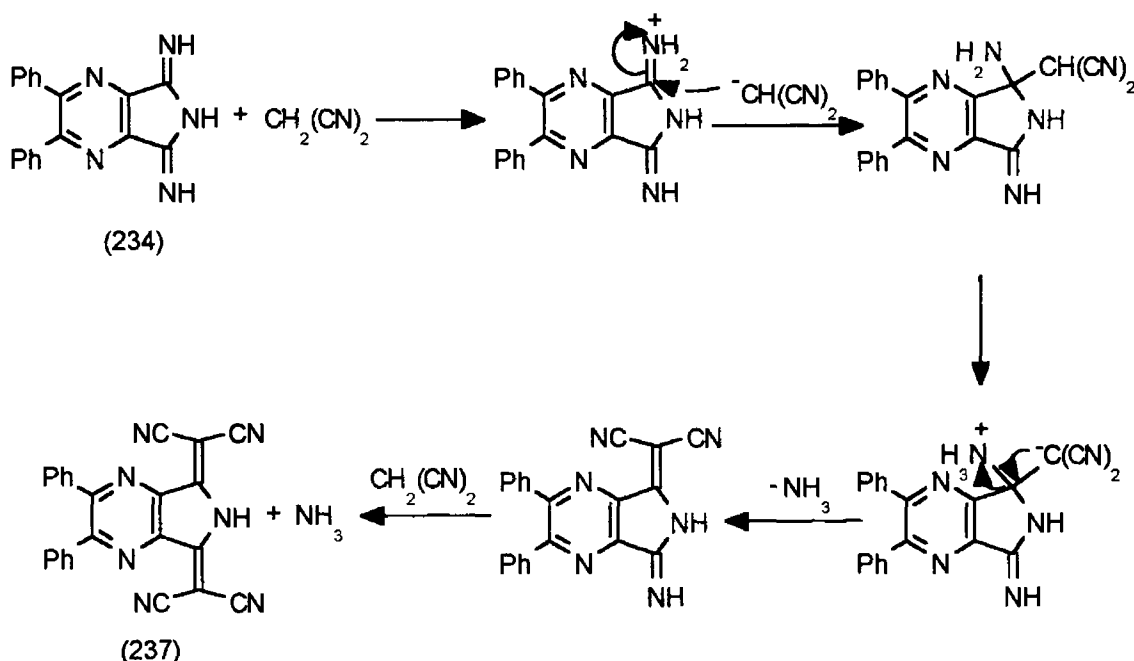


Scheme 3.4

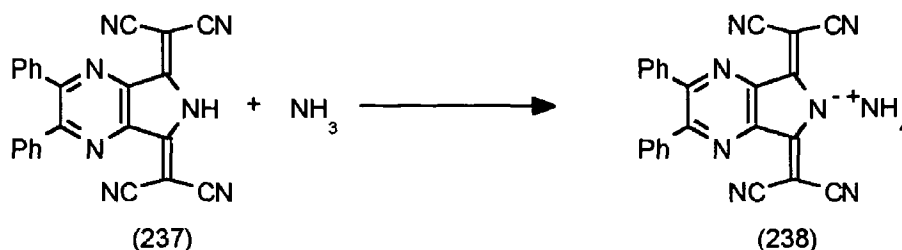
The ^1H NMR spectrum was consistent with the proposed structure of (236) showing three aromatic multiplets at δ 7.09, 7.36 and 7.45 ppm whose integrations were in the ratio of 1:10:4 respectively. Also present were two broad singlets at δ 8.81 and 8.99 ppm, whose integrations were in the ratio of 1:1 (NH protons). The presence of the NH protons was confirmed by their disappearance from ^1H NMR spectrum on shaking with deuterium oxide. The ^{13}C NMR spectrum supported the unsymmetrical structure of the molecule by showing the correct number of carbons for the proposed structure. Eighteen signals were observed, sixteen aromatic absorptions between δ 123.90 and 153.67 ppm and two absorptions at δ 160.46 and 168.05 ppm due to the imino carbons.

Treating 2,3-diphenyl-5,7-dimino-6H-5,7-dihydropyrrolo[3,4-b]pyrazine (234) with malononitrile in tetrahydrofuran at room temperature afforded, after work up, a red solid as the major product. The ^1H NMR spectrum showed a six proton aromatic multiplet at δ 7.35 ppm and a four proton aromatic multiplet at δ 7.60 ppm. The ^{13}C NMR spectrum showed ten signals, one at δ 55.86 ppm due to the dicyano substituted carbon, two nitrile signals at δ 114.35 and 115.34 ppm and seven signals between δ 127.56 and 166.91 ppm corresponding to the aromatic and dicyanomethylene substituted carbons. The IR spectrum showed an NH band at 3174 cm^{-1} and a strong nitrile band at

2214 cm^{-1} On the basis of this data two structures were considered possible for the product observed in this reaction. The possible mode of reaction is attack at the imino carbons of (234) to afford compound (237) and ammonia (scheme 3 5). However, it is also possible that the acidic hydrogen on (237) could be deprotonated by the ammonia formed in the reaction to yield the ammonium salt (238) (scheme 3 6). The red solid was soluble in most common organic solvents but attempts to recrystallise it for elemental analysis were unsuccessful.



Scheme 3 5



Scheme 3 6

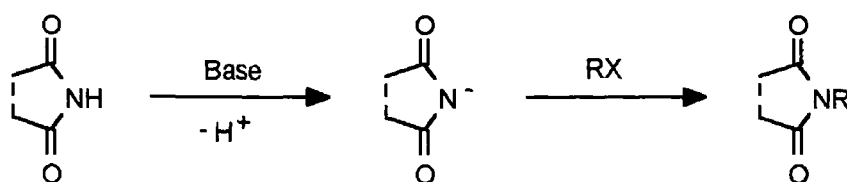
It has been shown¹⁵⁷ that addition of malononitrile to the isoindoline derivatives (228a and b) gave the ammonium salt (230). Therefore it was expected that the red solid isolated was the analogous pyrazine salt (238). However, in contrast to (230), which showed a four proton 1 1 1 triplet for the ammonium cation in the ^1H NMR spectrum due to $^{14}\text{N}/^1\text{H}$ coupling, protons due

to the ammonium cation of (238) were not observed. This may be attributed to the fact that nitrogen-hydrogen coupling in the NH resonance has been decoupled or broadened by the large electric quadrupole moment of nitrogen. Acidification of (238) and work up gave a yellow solid whose IR, NMR and microanalytical data were consistent with the structure of 2,3-diphenyl-5,7-bis(dicyanomethylene)-6H-5,7-dihydropyrrolo[3,4-b]pyrazine (237). Thus, the ^{13}C NMR spectrum showed only ten signals and was consistent with the presence of a dicyano substituted carbon (peaks at δ 63.03, 111.54 and 112.08 ppm) and its expected symmetry. The ^1H NMR spectrum confirmed the presence of an exchangeable proton at δ 3.53 ppm as expected for (237) and the IR spectrum showed a number of absorptions (2240, 2224 and 2214 cm^{-1}) consistent with a number of nitrile absorptions. The isolation of (237) by acidification of (238) is consistent with (238) being the ammonium salt. This was confirmed by its conversion to the tetraalkylammonium salts as discussed in the next section.

3.3 Synthesis of *N*-Substituted Pyrazine Derivatives

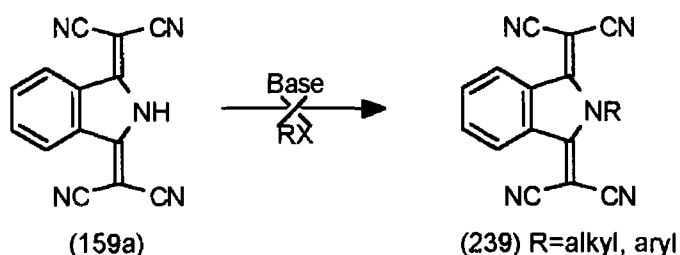
The synthesis of *N*-substituted pyrazine derivatives (231) was investigated so that the redox properties of (237) can be finely tuned by varying the substituents on the nitrogen atom. Therefore it is possible to introduce a variety of functional groups leading to increased solubilities for these compounds. The ability of these *N*-substituted derivatives to form C-T complexes with appropriate donor molecules would then be investigated.

It was of interest to find an efficient synthetic route to the *N*-substituted pyrazine derivatives from readily available starting materials. It has been shown¹⁶⁴ that there are similarities between the dicyanomethylene and carbonyl groups and that they have similar inductive and resonance effects. It was also shown that the pK_a values of $\text{C}(\text{CN})_2\text{-H}$ acids are 3.7 to 4.5 units smaller than those of the corresponding O-H acids. Thus a likely route to the *N*-alkyl pyrazine analogues seemed to be a route analogous to that used for the Gabriel synthesis of imides (scheme 3.7).



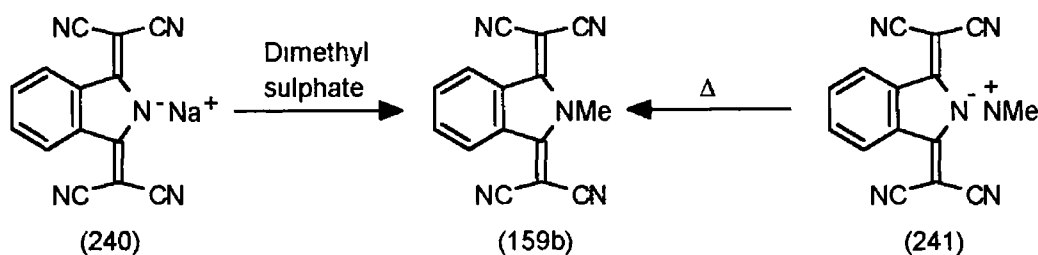
Scheme 3.7

The electron-withdrawing cyano groups are more electronegative than the oxygen atom and thus the hydrogen on (237) is expected to be more acidic than the analogous oxygen analogue. The acidity of (237) was verified by the addition of sodium carbonate to a tetrahydrofuran solution of (237) with the evolution of carbon dioxide gas. However, Gabriel-type *N*-substitution reactions of the isoindoline analogue (159a) has been unsuccessful¹⁵⁷ in achieving direct alkylation because of the poor nucleophilicity of (159a) (scheme 3 8). As a result of these findings analogous Gabriel-type alkylations with the ammonium salt (238) were not investigated in the present work.



Scheme 3 8

Successful *N*-methylation of (159a) was finally achieved in poor yield when the sodium salt of (159a), compound (240), was treated with dimethyl sulphate¹⁵⁷. However, a more modest yield was obtained by pyrolysis of its tetramethylammonium salt (241) (scheme 3 9). Contrary to this, little success resulted from analogous treatment of other *N*-alkylammonium salts of (159a).

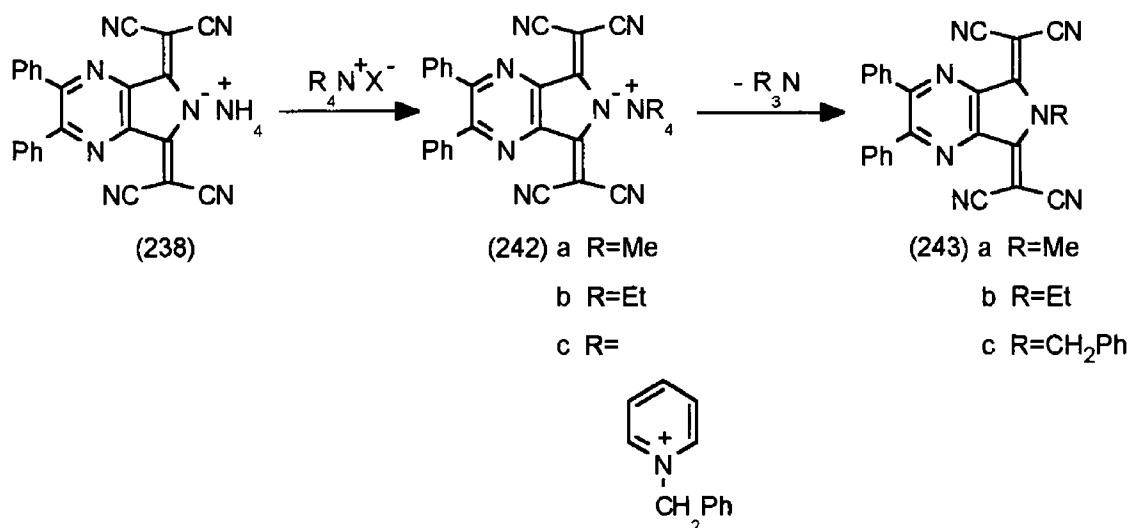


Scheme 3 9

3 3 1 Synthesis of Tetraalkylammonium Salts (242a-c)

Since the pyrolysis of tetramethylammonium salt (241) in 1,2-dichlorobenzene gave the desired *N*-methyl derivative (159b) it was decided to investigate the synthesis of *N*-alkyl pyrazine derivatives (243) from their tetraalkylammonium salts (242a-c). The synthesis of these salts had not previously been reported in the literature. The ammonium salt (238) was

treated with tetramethylammonium chloride in methanol to yield (242a) (scheme 3 10)



Scheme 3 10

The IR, ¹H and ¹³C spectra and microanalysis were consistent with the assigned structure of (242a). The ¹H NMR spectrum confirmed the presence of a tetramethylammonium group with a twelve proton singlet at δ 3.07 ppm. Two aromatic multiplets at δ 7.36 and 7.48 ppm in the ratio 6:4 were also observed. The ¹³C NMR spectrum was consistent with the symmetry of the molecule showing a total of eleven signals, a 1:1:1 triplet at δ 54.38 ppm (J 4.05 Hz) corresponding to the methyl carbons, one signal at δ 55.65 ppm corresponding to the dicyano substituted carbon, two nitrile absorptions at δ 115.28 and 166.0 ppm and seven absorptions between δ 128.27 and 167.71 ppm due to the aromatic and dicyanomethylene substituted carbons. The IR spectrum showed a strong nitrile band at 2209 cm⁻¹. The 1:1:1 triplet at δ 54.38 ppm observed for the methyl carbon is due to the coupling of this carbon with the ¹⁴N nucleus.

The tetraethylammonium salt (242b) was similarly prepared by treatment of (238) with tetraethylammonium bromide. The IR spectrum of (242b) showed a strong nitrile band at 2205 cm⁻¹. The ¹H NMR spectrum of (242b) was analogous to that of the tetramethylammonium salt (242a) showing two aromatic multiplets at δ 7.36 and 7.47 ppm in a 6:4 ratio. The only difference between the two proton NMR spectra was the difference in the ammonium cation. The tetraethylammonium cation showed a twelve proton triplet of triplets at δ 1.14 ppm (methyl protons β to the nitrogen atom) and an eight proton

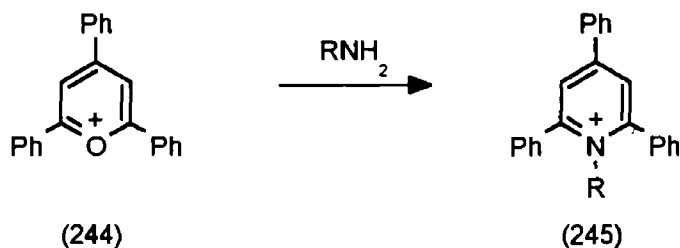
quartet at δ 3.18 ppm (methylene protons α to the nitrogen atom). The unusual triplet of triplet splitting of the methyl protons β to the nitrogen atom in the ^1H NMR spectrum of the tetraethylammonium salt (242b) is due to hydrogen coupling of these protons with the ^{14}N nucleus and the methylene protons. The ^{13}C NMR spectrum showed twelve signals and was consistent with the presence of a tetraethylammonium group. The main difference, on comparing the ^{13}C NMR spectrum of (242b) with that of (242a) was the difference in the number of carbon absorptions observed for the tetraalkylammonium cation. The tetraethylammonium cation showed one signal at δ 7.06 ppm due to the methyl carbon β to the nitrogen atom and a 1:1:1 triplet at δ 51.34 (J 3.05 Hz) due to the methylene carbon α to the nitrogen. The unusual splitting of the methyl protons β to the nitrogen atom in the ^1H NMR spectrum and the methylene carbon α to the nitrogen atom in the ^{13}C NMR spectrum is due to hydrogen and carbon coupling with the ^{14}N nucleus respectively. This is as expected¹⁶³ and was confirmed by comparison with the ^1H and ^{13}C NMR spectra of an authentic sample of tetraethylammonium bromide.

N-Benzylpyridinium salt (242c) was similarly prepared by treating the ammonium salt (238) with benzylpyridinium chloride, synthesised by heating benzyl chloride and pyridine together. The ^1H NMR spectrum of (242c) was analogous to those of (242a) and (242b) the main difference being the expected difference in the quaternary cation group. The benzylpyridinium cation showed a two proton singlet at δ 5.83 ppm (methylene protons), and four aromatic multiplets at δ 7.42, 8.16, 8.60 and 9.17 ppm whose integrations were in the ratio 1:5:2:1:2 respectively. The last three aromatic multiplets were assigned as the pyridyl aromatic protons. The ^{13}C NMR spectrum showed eighteen signals which was consistent with the expected symmetry and the presence of a benzylpyridinium cation (peak at δ 63.32 ppm due to the methylene carbon). The presence of a dicyano substituted carbon (peaks at δ 55.66, 115.26 and 115.97 ppm) was also observed.

3.3.2 *N*-Alkylation using the Tetraalkylammonium Salts (242a-c)

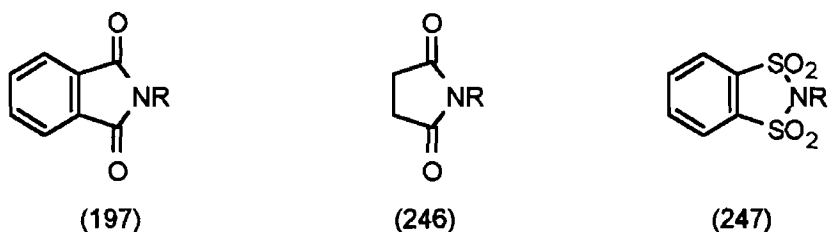
The use of alkylammonium salts in nucleophilic displacement reactions has been reported but is problematic in terms of side-reactions and poor yields. Examples include the pyrolysis of tetramethylammonium hydroxide affording trimethylamine and dimethyl ether¹⁷³. In addition to this Katritzky and co-workers have investigated the transformation of primary aliphatic amino groups into other functional groups¹⁷⁴. This involved the reaction of an amine with a 2,4,6-triarylpyrylium (244) to afford the corresponding pyridinium salt (245) (scheme 3.11). The *N*-substituent on the pyridinium cation can undergo

nucleophilic displacement when reacted with halogens, oxygen, sulphur, nitrogen, carbon or hydrogen nucleophiles ^{174b}



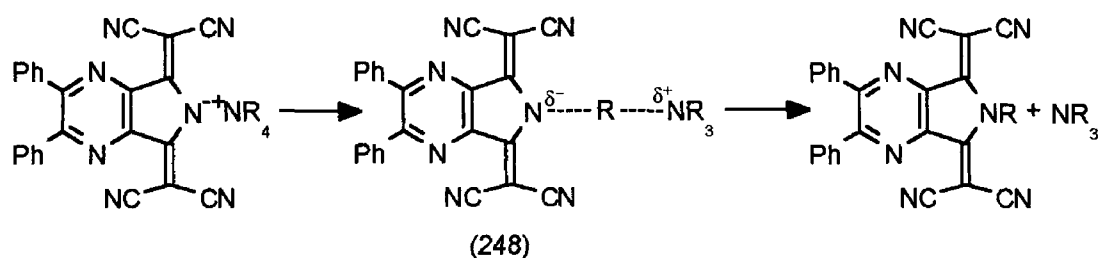
Scheme 3 11

These workers have also developed a method^{174b} for synthesising *N*-substituted phthalimides (197) by reacting the appropriate 2,4,6-triarylpyridinium salt with potassium phthalimide in *N,N*-dimethylformamide. This synthetic route has been successful in preparing succinimide (246) and sulphonamide (247) analogues also and is a widely applicable two-step sequence for the conversion of primary amino groups into other functionalities under mild conditions in high yields.



N-Ethylation of (237) was initially attempted by heating the tetraethylammonium salt (242b) under a variety of different reaction conditions. Heating salt (242b) at 300 °C for 30 minutes under an atmosphere of nitrogen gas changed the salt to a black solid. TLC analysis of the black solid showed that it consisted of one main product which had a similar *R_f* value as the salt (242b). The spectral data of the black solid was consistent with that of (242b). An alternative method reported,¹⁵⁷ which involved pyrolysing the tetramethylammonium isoindoline salt (241) in 1,2-dichlorobenzene, was also attempted for the tetraethylammonium pyrazine salt (242b). However, treating the salt (242b) with 1,2-dichlorobenzene under reflux for 30 hours, showed no new products on following the reaction by TLC. Dark orange crystals were obtained on filtering the solution, the spectral data of which were consistent with that of (242b).

In an effort to synthesise the *N*-alkyl pyrazine derivatives (243a-c) from the corresponding tetraalkylammonium salts it was decided to change the reaction solvent. For S_N2 reactions a decrease in polarity of the solvent (decrease in dielectric constant) and/or its ion-solvating ability results in an increase in reaction rate. This is because in the transition state (248) the charge is dispersed compared to the starting material thus solvation of the transition state is likely to be more effective than the initial nucleophile hence the slight increase (scheme 3 12)



Scheme 3 12

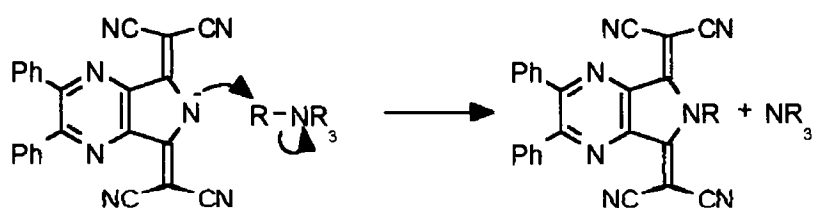
The tetraethylammonium salt (242b) was heated under reflux for 20 hours in 1,2,4-trichlorobenzene as a higher boiling non-polar solvent. The progress of the reaction was monitored by TLC and slow formation of a yellow spot was observed, increasing in intensity as the reaction progressed. Column chromatography and recrystallisation afforded 2,3-diphenyl-5,7-bis(dicyanomethylene)-6-ethyl-5,7-dihydropyrrolo[3,4-*b*]pyrazine (243b) as a yellow crystalline solid. The IR, ^1H and ^{13}C NMR spectra were consistent with the assigned structure. The ^{13}C NMR spectrum showed only twelve signals and was consistent with the presence of an ethyl group (signals at δ 16.11 and 41.85 ppm) and a dicyano substituted carbon (signals at δ 63.51, 110.80 and 111.95 ppm). This was also consistent with its expected symmetry. The ^1H NMR spectrum confirmed the presence of the ethyl group with a three proton triplet at δ 1.69 ppm (methyl protons) and a two proton quartet at δ 4.79 ppm (methylene protons) as expected. Three symmetrical aromatic multiplets at δ 7.37, 7.45 and 7.69 ppm in the ratio 4:2:4 respectively were also observed. The IR spectrum showed aliphatic and aromatic carbon-hydrogen bands at 3070 and 2934 cm^{-1} and a strong nitrile band at 2220 cm^{-1} .

The *N*-methyl derivative (243a) was similarly prepared as a yellow crystalline material from the tetramethylammonium salt (242a). The IR, ^1H and ^{13}C NMR spectra were consistent with the assigned structure. The ^1H NMR

spectrum of (243a) was consistent with that of the *N*-ethyl derivative (243b) showing the same symmetry in the aromatic region of 4.2-4.4 ppm with similar chemical shift values. The main difference between the two proton NMR spectra was the expected difference in the *N*-substituent, i.e. (243a) showed a three proton singlet at δ 4.29 ppm (methyl protons). The ^{13}C NMR spectrum of (243a) was also consistent with the *N*-ethyl derivative showing the correct number of carbons (eleven) and the same symmetry. The main difference was the observation of a carbon corresponding to a methyl group at δ 35.56 ppm. The aromatic and dicyanomethylene absorptions occur at similar chemical shifts as (243b). The IR spectrum showed a strong nitrile absorption at 2222 cm^{-1} .

Treatment of the *N*-benzylpyridinium salt (242c) with 1,2,4-trichlorobenzene under the same reaction conditions as salts (242a) and (242b) afforded (243c) as a yellow solid after column chromatography. The IR, ^1H and ^{13}C NMR spectra were consistent with the assigned structure. The ^{13}C NMR spectrum showed the correct number of carbons (fifteen) for the assigned structure. The presence of a methylene carbon at δ 49.19 ppm and a dicyano substituted carbon (peaks at δ 64.56, 110.74 and 111.66 ppm) was consistent with the expected symmetry of the molecule. The ^1H NMR spectrum of (243c) was similar to that of (243a) and (243b) and was also consistent with the symmetrical nature of the molecule. This was confirmed by the presence of a two proton singlet at δ 6.05 ppm (methylene protons) and fifteen aromatic protons. The aromatic protons were observed as three aromatic multiplets at δ 7.15, 7.42 and 7.72 ppm in the ratio of 2:9:4 respectively. The IR spectrum showed a strong nitrile absorption at 2221 cm^{-1} .

The formation of the *N*-alkyl derivatives is thought to have occurred by nucleophilic attack of the nitrogen anion on the alkyl group of the tetraalkylammonium cation affording the *N*-alkyl derivative and trialkylamine (scheme 3.13).



Scheme 3.13

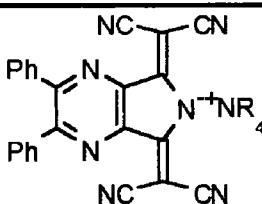
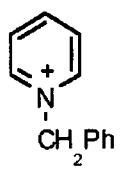
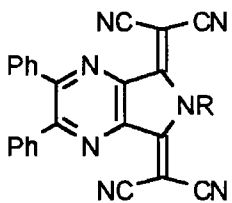
3 3 3 Electronic Absorption Spectra of *N*-Substituted Heterocyclic TCNQ Analogues

UV/visible spectroscopy has been used to gain an insight into the electronic properties of the *N*-substituted pyrazine derivatives (237) and (243) which are highly coloured solids. The UV/visible absorbance maxima for the *N*-substituted derivatives are listed in table 3 1 along with those for the corresponding ammonium salts.

Comparison of the UV/visible spectra of the ammonium and tetralkylammonium salts (238) and (242) in acetonitrile were found to be essentially the same (table 3 1). The UV/visible spectra of one of these salts, (242a), and the ammonium salt (238) are shown in figure 3 1 for comparison. However, comparison of the spectra of (242a), (238) and the protonated compound (237) with those of the *N*-alkyl derivatives (243), exemplified by the spectrum of the *N*-methyl analogue (243a) (figure 3 1), shows that λ_{\max} for the latter compounds occurs at much shorter wavelengths, ~390 and 414 nm compared with ~481 and 511 nm (table 3 1). This difference may be attributed to greater conjugation within the anion compared to the *N*-alkyl derivatives. In compound (237) this difference may possibly be attributed to the partial ionisation of (237) to its anion in acetonitrile. Thus its UV/visible spectrum is a composite of the protonated compound and its anion and both absorb strongly in this region. This was confirmed by comparison of the UV/visible spectrum of (237) and its ammonium salt (238) (figure 3 1) which shows that they have similar λ_{\max} values. This result contrasts with the data obtained for the analogous isoindoline compounds (159a) and (159b), in which the λ_{\max} value of (159b) occurs at slightly longer wavelengths in acetonitrile.¹⁵⁷

In conclusion, pyrolysis of the quaternary ammonium salts (242a-c) was successful in providing a route to the desired *N*-alkyl substituted pyrazine derivatives (243a-c) which were obtained in moderate to good yields. The conversion of these *N*-substituted pyrazines into appropriate C-T complexes was investigated, the results of which are reported in chapter 4. The electrochemical properties of these derivatives are outlined in chapter 5.

Table 3 1 Electronic Absorption Data for Heterocyclic TCNQ Analogues

Compound		$\lambda_{\text{max}}/\text{nm}$ (ϵ_{max})
	(238) R=H	220sh (25,750), 330 (20,100), 481 (23,000) and 511 (22,650)
	(242) a R=Me	221 (22,674), 270 (17,914), 318 (17,540), 331 (18,396), 370sh (12,834), 481 (21,765) and 511 (21,551)
	b R=Et	222 (29,500), 271 (16,100), 318 (23,100), 332 (24,050), 374sh (18,100), 482 (28,000) and 512 (27,500)
	c $^+\text{NR}_4 =$ 	222sh (31,466), 262 (23,314), 318 (21,956), 330 (22,429), 372sh (15,121), 482 (26,054) and 510 (25,655)
	(237) R=H	223 (32,250), 327 (21,200), 387 (34,500), 410 (32,000), 481 (6,650) and 511 (6,660)
	(243) a R=Me	222 (28,100), 250sh (16,500), 332 (19,100), 392 (29,700) and 414 (28,400)
	b R=Et	218sh (26,492), 248sh (10,801), 330 (16,480), 394 (29,183) and 414 (28,365)
	c R=CH ₂ Ph	224sh (21,127), 250sh (11,737), 331 (13,146), 389 (22,066) and 412 (21,268)

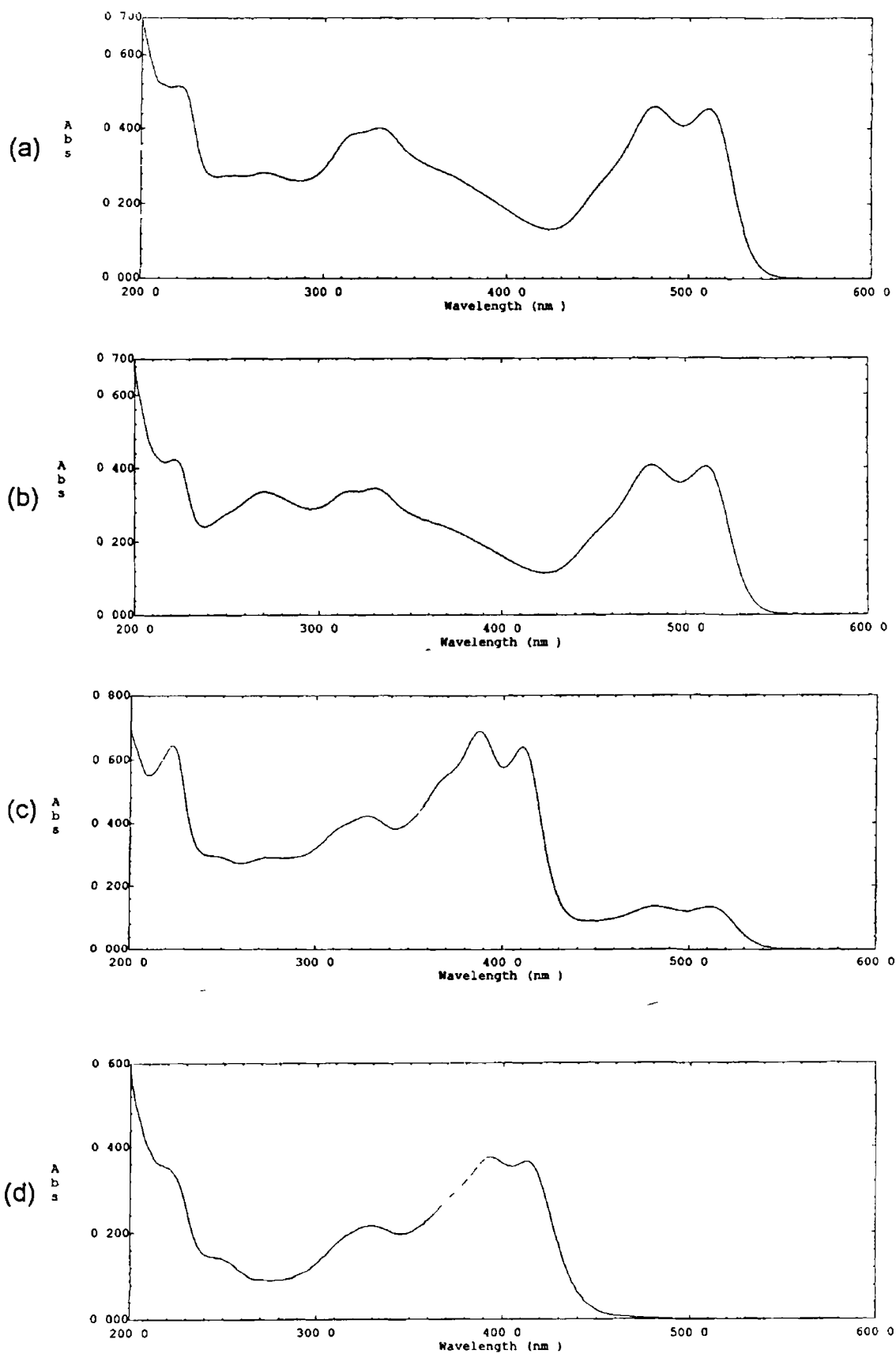
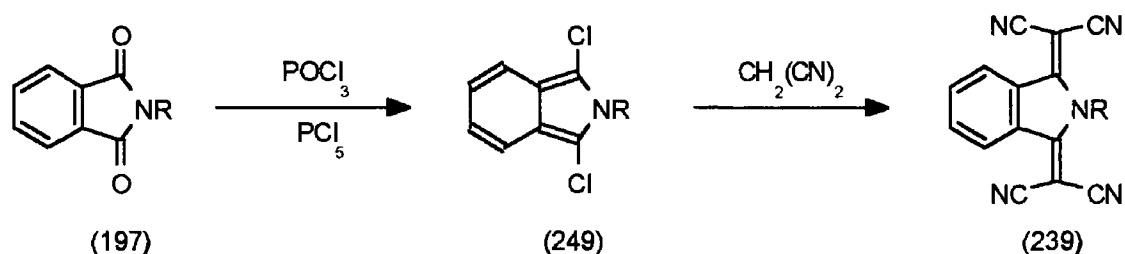


Figure 3.1 UV/visible spectrum of (a) (238), (b) (242a), (c) (237) and (d) (243a)

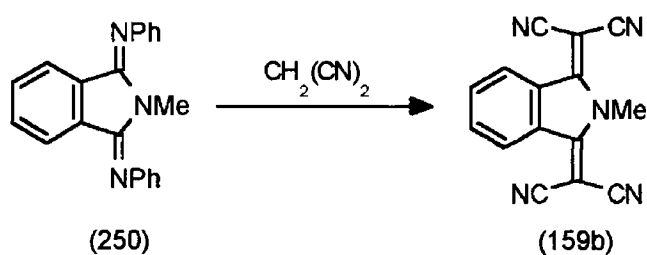
3.4 Future Work

Although *N*-substitution of the pyrazine analogue (237) was achieved by pyrolysis of the tetraalkylammonium salts in 1,2,4-trichlorobenzene, reaction times are long and the overall synthetic route requires five steps. Alternative approaches to the design of TCNQ analogues containing the structural unit (158) are required. One such route that may be useful is the reaction of dihalogeno precursors (249) with sodiomalononitrile (scheme 3.14). The dihalogeno derivatives (249) may be easily prepared from the imide analogues (197) by treating (197) with phosphorus pentachloride and phosphorus oxychloride. This procedure was previously used¹⁷⁵ to convert thiophthalic anhydride to its 1,3-dichloro derivative.

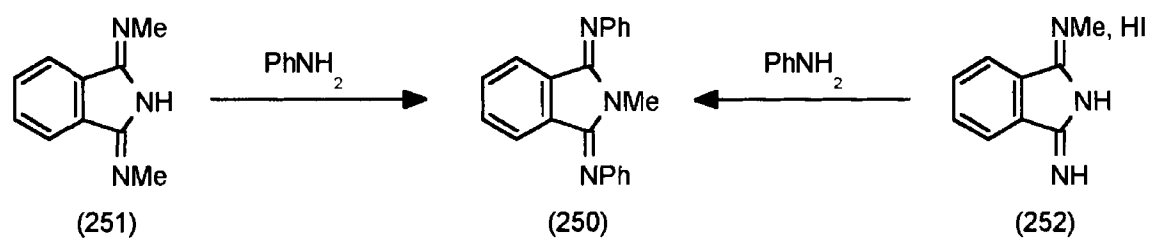


Scheme 3.14

Another alternative may be the Knoevenagel condensation of malononitrile with *N*-substituted imidines (250) (scheme 3.15). It has been shown that 2-methyl-1,3-diphenyliminoisoindoline (250) can be prepared¹⁷⁶ by reacting 1,3-dimethyliminoisoindoline (251) or 1-imino-3-methyliminoisoindoline hydride (252) with aniline (scheme 3.16).



Scheme 3.15



Scheme 3 16

Compound (251) can be synthesised by reacting (228a) with methylamine¹⁷⁶ This may be a possible synthetic route for the preparation of analogous pyrazine analogues and would be attractive since a variety of *N*-substitutents can be attached by varying the amine

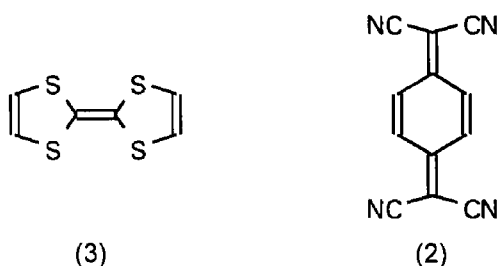
Chapter 4

Charge-Transfer Studies

4 1 Introduction

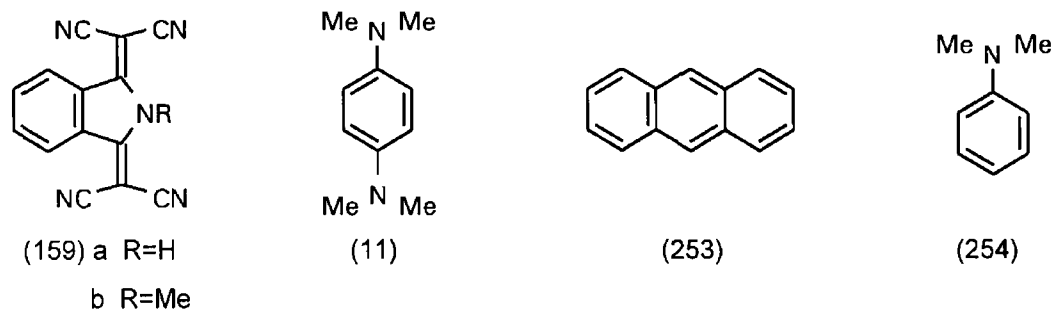
It has been reported in Chapter 1 that intense colours frequently form instantly when mixing an electron donor and an electron acceptor results in the formation of C-T complexes. These complexes are characterised by an intense electronic absorption in the visible or near UV that is attributable to neither component of the complex alone, but to a new molecular species, the C-T complex itself. As a result, UV/visible spectroscopy has been widely used in the study of C-T complexes. Mulliken¹⁴ considered these to arise from a Lewis acid-base type of interaction, the bond between the components arising from partial electron transfer from donor to acceptor (section 1 A 4). Retaining the metallic character of these C-T complexes down to very low temperatures, and thus achieving high conductivities has been a major goal for organic chemists.

C-T complexes have been extensively investigated since the discovery⁹ that crystals of a complex between TTF (3) and TCNQ (2) were produced by mixing solutions of the two components. Crystals of this complex exhibited a



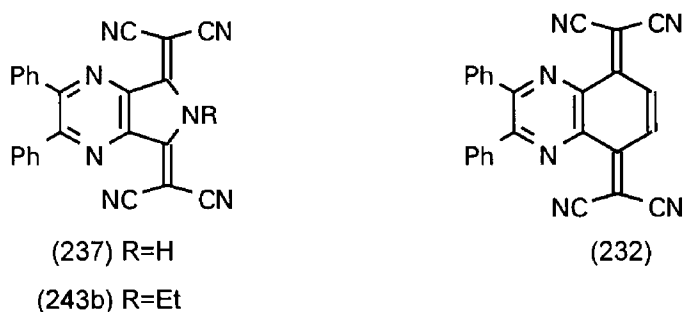
room temperature conductivity (500 Scm^{-1}), much lower than metals like copper and silver (10^6 Scm^{-1}) but higher than that of a typical semiconductor (10^{-5} - 10^{-2} Scm^{-1}) and considerably higher than an insulator (10^{-14} - $10^{-18} \text{ Scm}^{-1}$). The ability of C-T complexes to conduct electricity depends on the arrangement of molecules in the crystal. For example, in the TTF-TCNQ C-T complex the molecules stack on top of each other resulting in a structure with two types of stack (segregated stacks), one consisting of electron donors and one of electron acceptors. Within each stack the orbitals of one molecule overlap with those of the molecules above and below. In the crystal an electron can transfer from the donor to the acceptor to form a salt. High electrical conductivity in C-T complexes is associated with segregated stacks of donor and acceptor molecules which have extensive π -electron delocalisation in the stacking direction. One of the prerequisites for the formation of C-T complexes is that at least one of the molecular components must be planar with a delocalised π electron system.

It has been reported¹⁵⁷ that the isoindoline analogues (159) are capable of forming C-T complexes with the electron donors TTF (3), *N,N,N',N'*-tetramethyl-*p*-phenylenediamine (TMPD, 11) and anthracene (253) but not *N,N*-dimethylaniline (254)



The X-ray crystal structure of the 1:1 (159a)-TMPD C-T complex exhibited a mixed stacking arrangement of the donor and acceptor, as a result of which it is anticipated that this complex is probably semiconducting

The *N*-substituted heterocyclic TCNQ analogues (237) and (243b) were investigated as to their C-T complex-forming behaviour with electron donors TTF (3) and TMPD (11)



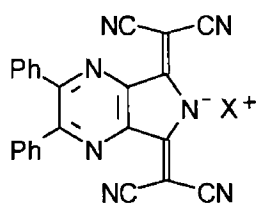
The benzo analogue (232) has previously been shown to form C-T complexes with TTF and TMTSF, both of which exhibited low conductivities¹⁶⁹

4.2 Charge-Transfer Studies with 2,3-Diphenyl-5,7-bis(dicyanomethylene)-6*H*-5,7-dihydropyrrolo[3,4-*b*]pyrazine (237)

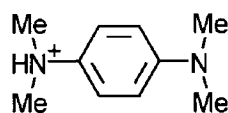
4.2.1 Attempted C-T Complex formation between (237) and TMPD (11)

Treatment of a hot solution of (237) in acetonitrile with one equivalent of TMPD afforded dark red crystals. TLC analysis showed that it consisted of two

individual components with the same R_f values as (237) and (11). Examination of the IR spectrum of these red crystals showed two strong nitrile bands at 2219 and 2204 cm^{-1} . The microanalytical data was consistent with a 1:1 composition. On the basis of this, two structures were considered possible for the product observed in this system. These were the 1:1 C-T complex or the salt (255).



(255) $X^+ =$



(242a) $X^+ = ^+NMe_4$

The UV/visible spectrum of the red crystals was essentially identical to that of the tetramethylammonium salt (242a) (figure 4.1). The only difference in the spectra, which was due to the absorption difference of the cationic components, occurred below 300 nm. The UV/visible spectrum and X-ray crystallography (figure 4.2) confirmed that the solid was in fact the ammonium salt (255). The crystal structure shows that the *N,N,N',N'*-tetramethyl-*p*-phenylenediaminium cation is essentially planar except for the two methyl groups attached to N(8). These methyl groups are twisted out of the plane with the bond angles around N(8) ($\sim 112^\circ$) being close to the regular tetrahedral angle of 109.5° . In contrast, the two methyl groups attached to N(9) have bond angles of $\sim 120^\circ$, consistent with the regular trigonal planar angle (120°). The relevant bond lengths and bond angles are given in tables 4.1 and 4.2 respectively.

4.2.2 C-T Complex formation between (237) and TTF (3)

The C-T complex-forming ability of (237) with TTF (3) was also investigated. The addition of an equimolar amount of TTF to (237) in acetonitrile resulted in the almost immediate formation of a black/dark green solution from which unreacted (237) deposited as a yellow solid. Recrystallisation of the solid obtained on evaporating the filtrate gave dark purple crystals from acetonitrile.

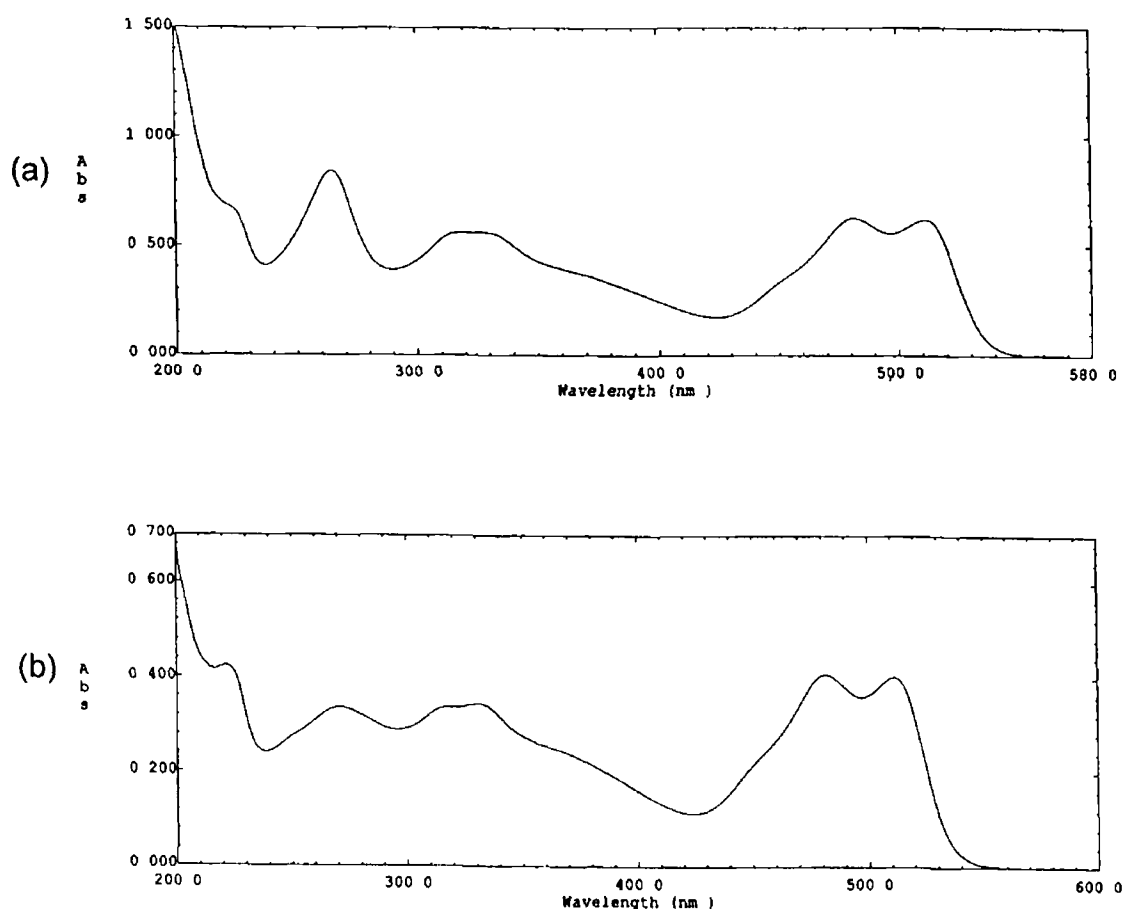


Figure 4.1 UV/Visible spectra of (a) (255) and (b) tetramethylammonium salt (242a)

TLC analysis of the crystals showed that they consisted of two individual components with the same R_f values as (237) and (3). The IR spectrum showed only one nitrile group absorption at 2225 cm^{-1} compared with three nitrile group absorptions in (237) (2240 , 2224 and 2214 cm^{-1}) and the melting point was also different from those of (237) and (3). The UV/visible spectrum of the purple solid showed absorption values similar to those of (237) (figure 4.3). On the basis of this data it is possible that a C-T complex had been formed. This was confirmed by microanalytical data, which was consistent with a 2:1 [(237) TTF] stoichiometry for the complex. Unfortunately, all attempts to prepare crystals suitable for X-ray diffraction have been unsuccessful.

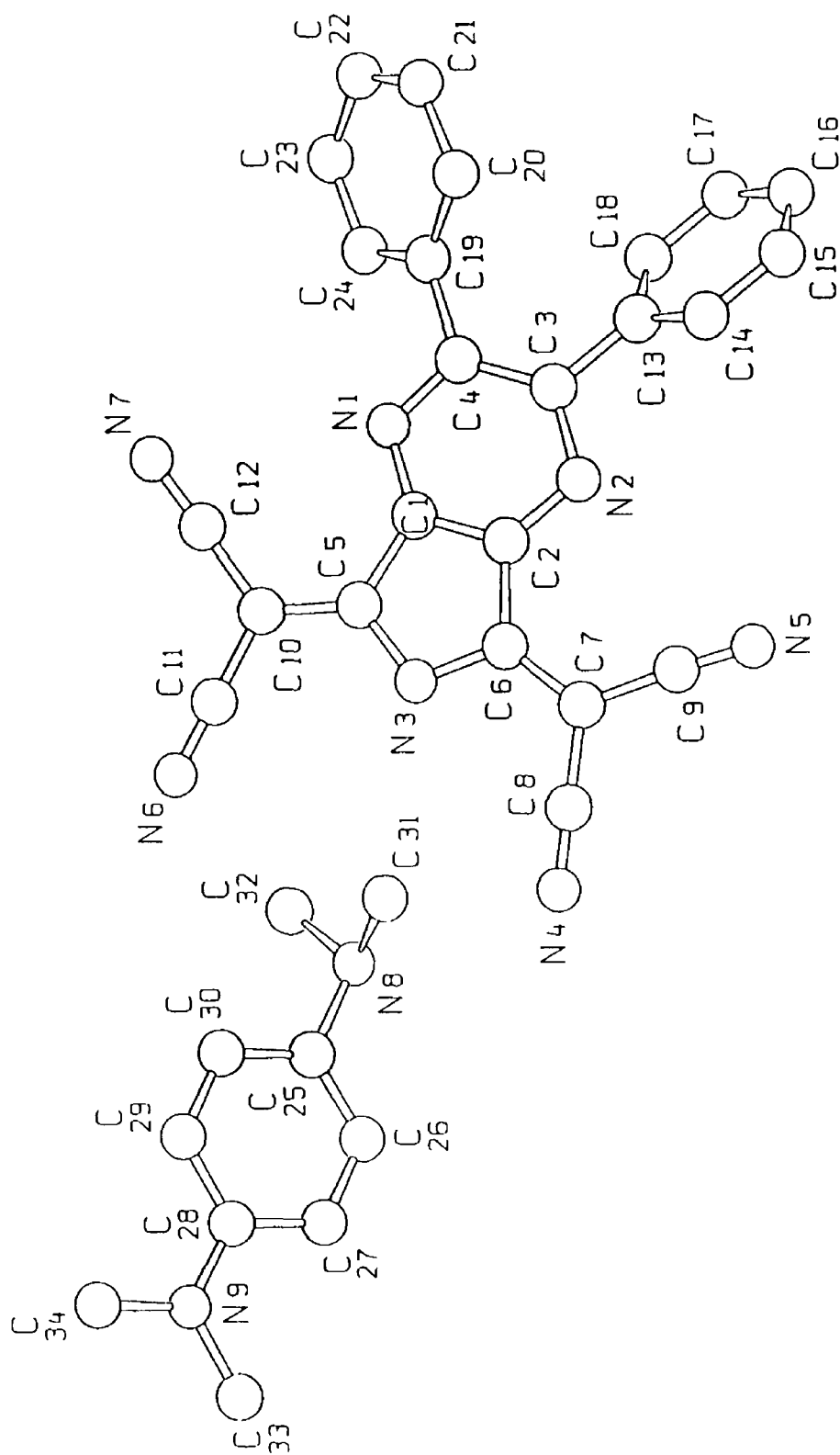


Figure 4 2 Schakal representation of X-ray crystal structure of salt (255)

Table 4 1 Bond lengths for (255)

Bond lengths [Å]			
N(1)-C(1)	1 325(3)	C(6)-C(7)	1 374(3)
N(1)-C(4)	1 352(3)	C(7)-C(9)	1 422(3)
N(2)-C(2)	1 330(2)	C(7)-C(8)	1 424(3)
N(3)-C(3)	1 352(3)	C(10)-C(12)	1 419(3)
N(3)-C(5)	1 353(3)	C(10)-C(11)	1 418(3)
N(3)-C(6)	1 368(3)	C(13)-C(14)	1 387(3)
N(4)-C(8)	1 142(3)	C(13)-C(18)	1 393(3)
N(5)-C(9)	1 148(3)	C(14)-C(15)	1 379(3)
N(6)-C(11)	1 144(3)	C(15)-C(16)	1 378(4)
N(7)-C(12)	1 150(3)	C(16)-C(17)	1 367(4)
N(8)-C(25)	1 479(3)	C(17)-C(18)	1 379(3)
N(8)-C(31)	1 487(3)	C(19)-C(20)	1 388(3)
N(8)-C(32)	1 495(4)	C(19)-C(24)	1 393(3)
N(9)-C(28)	1 367(3)	C(20)-C(21)	1 386(3)
N(9)-C(33)	1 431(4)	C(21)-C(22)	1 377(4)
N(9)-C(34)	1 445(4)	C(22)-C(23)	1 375(4)
C(1)-C(2)	1 378(3)	C(23)-C(24)	1 376(4)
C(1)-C(5)	1 473(3)	C(25)-C(26)	1 369(3)
C(2)-C(6)	1 472(3)	C(25)-C(30)	1 377(3)
C(3)-C(4)	1 419(3)	C(26)-C(27)	1 379(3)
C(3)-C(13)	1 485(3)	C(27)-C(28)	1 401(3)
C(4)-C(19)	1 486(3)	C(28)-C(29)	1 396(3)
C(5)-C(10)	1 382(3)	C(29)-C(30)	1 370(3)

Table 4 2 Bond angles [deg] for (255)

Bond angles [deg]			
C(1)-N(1)-C(4)	114 9(2)	C(5)-C(10)-C(12)	121 8(2)
C(2)-N(1)-C(3)	114 6(2)	C(5)-C(10)-C(11)	121 4(2)
C(5)-N(3)-C(6)	107 7(2)	C(12)-C(10)-C(11)	116 5(2)
C(25)-N(8)-C(31)	112 2(2)	N(6)-C(11)-C(10)	178 3(3)
C(25)-N(8)-C(32)	112 2(2)	N(7)-C(12)-C(10)	175 5(2)
C(31)-N(8)-C(32)	112 0(2)	C(14)-C(13)-C(18)	118 9(2)
C(28)-N(9)-C(33)	120 5(2)	C(14)-C(13)-C(3)	119 1(2)
C(28)-N(9)-C(34)	120 8(2)	C(18)-C(13)-C(3)	122 1(2)
C(33)-N(9)-C(34)	118 6(2)	C(15)-C(14)-C(13)	120 2(2)
N(1)-C(1)-C(2)	123 5(2)	C(16)-C(15)-C(14)	120 3(3)
N(1)-C(1)-C(5)	130 2(2)	C(17)-C(16)-C(15)	119 9(2)
C(2)-C(1)-C(5)	106 3(2)	C(16)-C(17)-C(18)	120 5(2)
N(2)-C(2)-C(1)	123 5(2)	C(17)-C(18)-C(13)	120 2(2)
N(2)-C(2)-C(6)	130 4(2)	C(20)-C(19)-C(24)	119 0(2)
C(1)-C(2)-C(6)	105 9(2)	C(20)-C(19)-C(4)	122 2(2)
N(2)-C(3)-C(4)	122 0(2)	C(24)-C(19)-C(24)	118 7(2)
N(2)-C(3)-C(13)	114 5(2)	C(21)-C(20)-C(19)	120 2(3)
C(4)-C(3)-C(13)	123 6(2)	C(22)-C(21)-C(20)	119 9(3)
N(1)-C(4)-C(3)	121 6(2)	C(23)-C(22)-C(21)	120 4(2)
N(1)-C(4)-C(19)	114 1(2)	C(24)-C(23)-C(22)	120 0(3)
C(3)-C(4)-C(19)	124 3(2)	C(23)-C(24)-C(19)	120 5(3)
N(3)-C(5)-C(10)	124 2(2)	C(26)-C(25)-C(30)	119 8(2)
N(3)-C(5)-C(1)	110 0(2)	C(26)-C(25)-N(8)	119 8(2)
C(10)-C(5)-C(1)	125 8(2)	C(30)-C(25)-N(8)	120 4(2)
N(3)-C(6)-C(7)	122 9(2)	C(25)-C(26)-C(27)	120 1(2)
N(3)-C(6)-C(2)	110 0(2)	C(26)-C(27)-C(28)	121 6(2)
C(7)-C(6)-C(2)	127 1(2)	N(9)-C(28)-C(29)	121 1(2)
C(6)-C(7)-C(9)	124 1(2)	N(9)-C(28)-C(27)	122 5(2)
C(6)-C(7)-C(8)	119 5(2)	C(29)-C(28)-C(27)	116 5(2)
C(9)-C(7)-C(8)	116 4(2)	C(30)-C(29)-C(28)	121 9(2)
N(4)-C(8)-C(7)	178 9(2)	C(29)-C(30)-C(25)	120 2(2)
N(5)-C(9)-C(7)	175 5(2)		

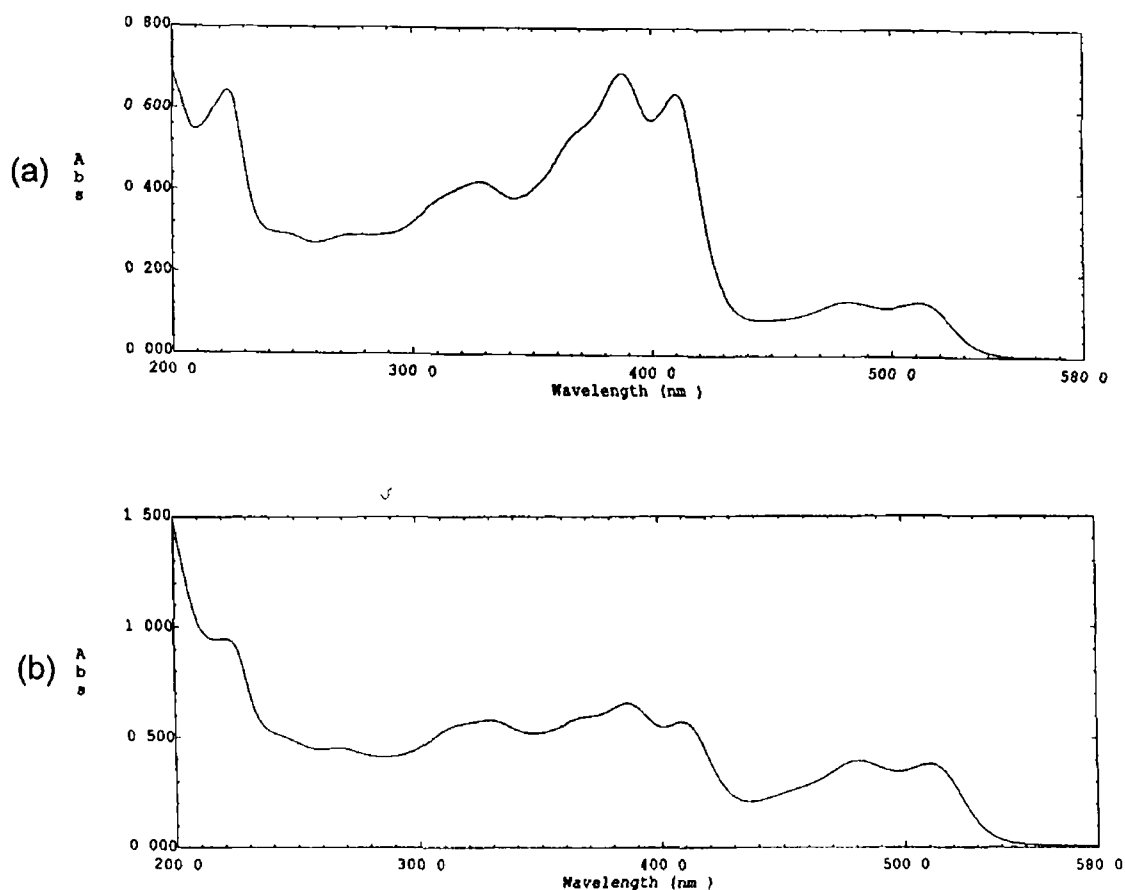


Figure 4.3 UV/visible spectra of (a) (237) and (b) (237)-TTF

4.3 Charge Transfer Studies with 2,3-Diphenyl-5,7-bis(dicyanomethylene)-6-ethyl-5,7-dihydropyrrolo[3,4-b]pyrazine (243b)

4.3.1 C-T Complex formation between (243b) and TMPD

Mixing equimolar acetonitrile solutions of (243b) and TMPD gave a dark purple coloured solution from which dark purple crystals deposited. The IR and UV/visible spectra of the crystals were identical to that of (243b) but its melting point was different to those of either (243b) or TMPD. Figure 4.4 shows the UV/visible absorption spectra of (243b) and (243b)-TMPD C-T complex. TLC analysis of the crystals showed two components with R_f values similar to those of (243b) and TMPD, consistent with the formation of a C-T complex. An exact stoichiometric ratio of the two components in the complex could not be elucidated from the microanalytical data and crystals suitable for X-ray diffraction could not be obtained. The microanalytical data however could be

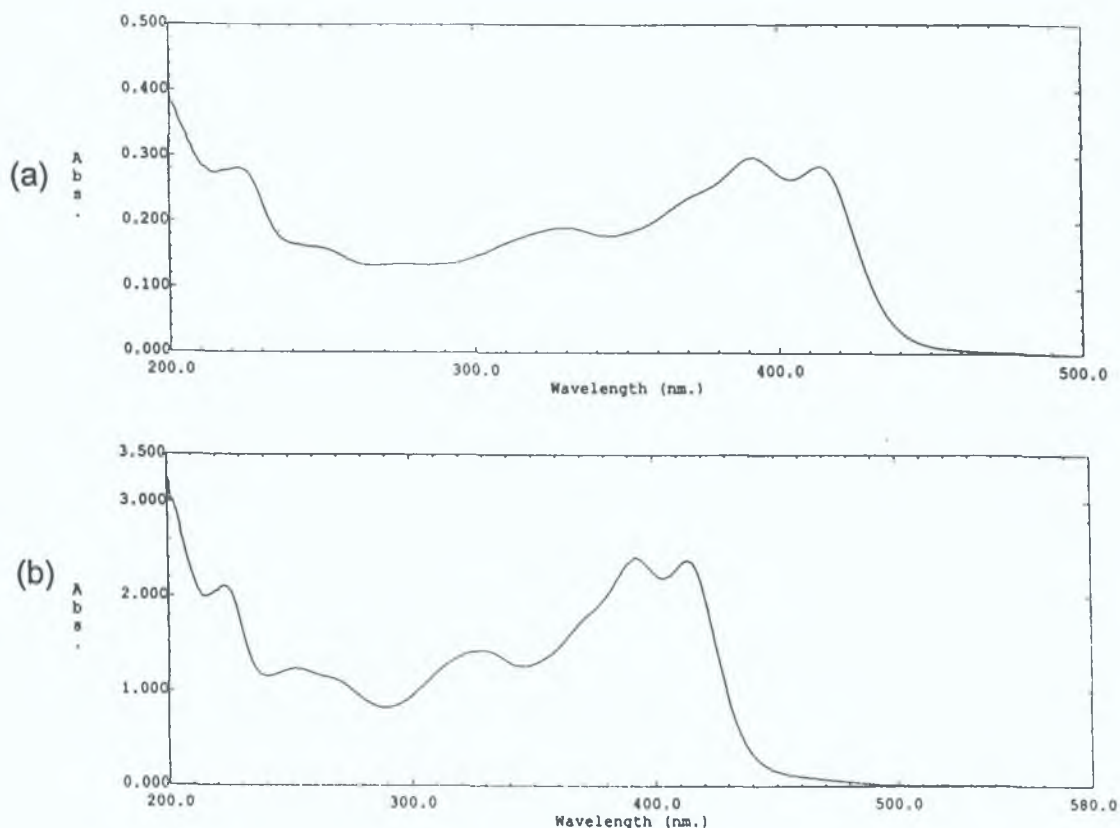


Figure 4.4 UV/visible spectra of (a) (243b) and (b) (243b)-TMPD.

better understood if it were assumed that the crystals contained either water or acetonitrile of crystallisation. However, more direct evidence for this was unavailable. The ^1H NMR spectrum showed a water signal in chloroform- d at δ 1.56 ppm; however this may have been due to the presence of water in the chloroform- d itself. In contrast there was no evidence for the presence of acetonitrile in the NMR spectrum.

Examination of the microanalytical data calculated for different stoichiometric acceptor:donor:water and acceptor:donor:acetonitrile compositions (table 4.3) shows that a 2:1:1 ratio for (243b):TMPD:H₂O provides the best fit for the experimental carbon, hydrogen and nitrogen compositions obtained from two independent samples (table 4.4). A 3:1:1 ratio for (243b):TMPD:H₂O and a 2:1:2 ratio for (243b):TMPD:CH₃CN were also consistent with the experimental composition of the second sample.

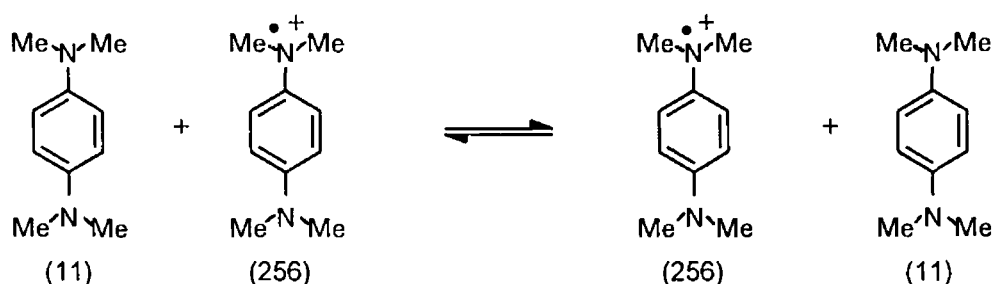
Table 4.3 Carbon, Hydrogen and Nitrogen Values for different stoichiometries of (243b)-TMPD C-T Complex

Acceptor Donor Ratio	Carbon (%)	Hydrogen (%)	Nitrogen (%)
1 1 (C ₃₆ H ₃₁ N ₉)	73.32	5.29	21.37
2 1 (C ₆₂ H ₄₆ N ₁₆)	73.35	4.56	22.07
3 1 (C ₈₈ H ₆₁ N ₂₃)	73.37	4.27	22.36
4 1 (C ₁₁₄ H ₇₆ N ₃₀)	73.37	4.10	22.51
1 1 + H ₂ O (C ₃₆ H ₃₃ N ₉ O)	71.15	5.47	20.74
2 1 + H ₂ O (C ₆₂ H ₄₈ N ₁₆ O)	72.07	4.68	21.69
3 1 + H ₂ O (C ₈₈ H ₆₃ N ₂₃ O)	72.46	4.35	22.08
4 1 + H ₂ O (C ₁₁₄ H ₇₈ N ₃₀ O)	72.67	4.17	22.30
1 2 + H ₂ O (C ₄₆ H ₄₇ N ₁₁ O)	71.75	6.15	20.01
1 3 + H ₂ O (C ₅₆ H ₆₅ N ₁₃ O)	71.84	6.99	19.44
1 4 + H ₂ O (C ₆₆ H ₈₁ N ₁₅ O)	72.03	7.41	19.09
1 1 + 2H ₂ O (C ₃₆ H ₃₅ N ₉ O ₂)	69.10	5.63	20.14
2 1 + 2H ₂ O (C ₆₂ H ₅₀ N ₁₆ O ₂)	70.84	4.79	21.31
3 1 + 2H ₂ O (C ₈₈ H ₆₅ N ₂₃ O ₂)	71.58	4.43	21.81
4 1 + 2H ₂ O (C ₁₁₄ H ₈₀ N ₃₀ O ₂)	71.98	4.24	22.09
1 2 + 2H ₂ O (C ₄₆ H ₅₁ N ₁₁ O ₂)	69.94	6.50	19.50
1 3 + 2H ₂ O (C ₅₆ H ₆₇ N ₁₃ O ₂)	70.48	7.07	19.08
1 4 + 2H ₂ O (C ₆₆ H ₈₃ N ₁₅ O ₂)	70.87	7.48	18.78
1 1 + CH ₃ CN (C ₃₈ H ₃₄ N ₁₀)	72.36	5.43	22.20
1 2 + CH ₃ CN (C ₄₈ H ₅₀ N ₁₂)	72.52	6.34	21.14
1 3 + CH ₃ CN (C ₅₈ H ₆₆ N ₁₄)	72.62	6.93	20.44
1 4 + CH ₃ CN (C ₆₈ H ₈₂ N ₁₆)	72.69	7.25	19.94
2 1 + CH ₃ CN (C ₆₄ H ₄₉ N ₁₇)	72.78	4.67	22.54
3 1 + CH ₃ CN (C ₉₀ H ₆₄ N ₂₄)	72.95	4.35	22.68
4 1 + CH ₃ CN (C ₁₁₆ H ₇₉ N ₃₁)	73.05	4.17	22.76
1 1 + 2CH ₃ CN (C ₄₀ H ₃₇ N ₁₁)	71.15	5.55	22.93
1 2 + 2CH ₃ CN (C ₅₀ H ₅₃ N ₁₃)	71.83	6.39	21.78
1 3 + 2CH ₃ CN (C ₆₀ H ₆₉ N ₁₅)	72.04	6.95	21.00
1 4 + 2CH ₃ CN (C ₇₀ H ₈₅ N ₁₇)	72.19	7.35	20.44
2 1 + 2CH ₃ CN (C ₆₆ H ₅₂ N ₁₈)	72.24	4.77	22.97
3 1 + 2CH ₃ CN (C ₉₂ H ₆₇ N ₂₅)	72.56	4.43	22.99
4 1 + 2CH ₃ CN (C ₁₁₈ H ₈₂ N ₃₂)	72.75	4.24	23.00

Table 4 4 Carbon, Hydrogen and Nitrogen Values obtained for (243b)-TMPD C-T Complex

	Carbon (%)	Hydrogen (%)	Nitrogen (%)
Sample 1	71 41	4 61	22 30
	71 80	4 68	21 66
Sample 2	72 30	4 73	23 43
	72 17	4 82	22 07
	72 14	4 74	22 67

The ^1H NMR spectrum of the (243b)-TMPD C-T complex in chloroform-d was examined in an attempt to establish the ratio of the individual components present. However, at room temperature the aromatic and *N*-methyl protons of TMPD were not observed due to peak broadening. Peak broadening of TMPD in NMR spectroscopy is well known¹⁷⁷ and is caused by the electron exchange reaction (scheme 4 1) between neutral TMPD, which is diamagnetic, and its one electron oxidation product (256), which is paramagnetic. Formation of the cation radical (256) is due to air oxidation of neutral TMPD^{177b}.



Scheme 4 1

Therefore in order to observe the TMPD protons, the ^1H NMR spectrum over the temperature range 20 °C to -30 °C was investigated (figure 4 5). Some of the peaks remain unchanged as the temperature is lowered whereas others that were initially broad became more distinct. The peaks that became more distinct included a broad signal at δ 2.91 ppm (*N*-methyl protons of TMPD) and a broad signal at δ 6.79 ppm (aromatic protons of TMPD), consistent with the presence of TMPD in the C-T complex. The exact stoichiometric ratio of the complex however could not be elucidated from the ^1H NMR spectrum.

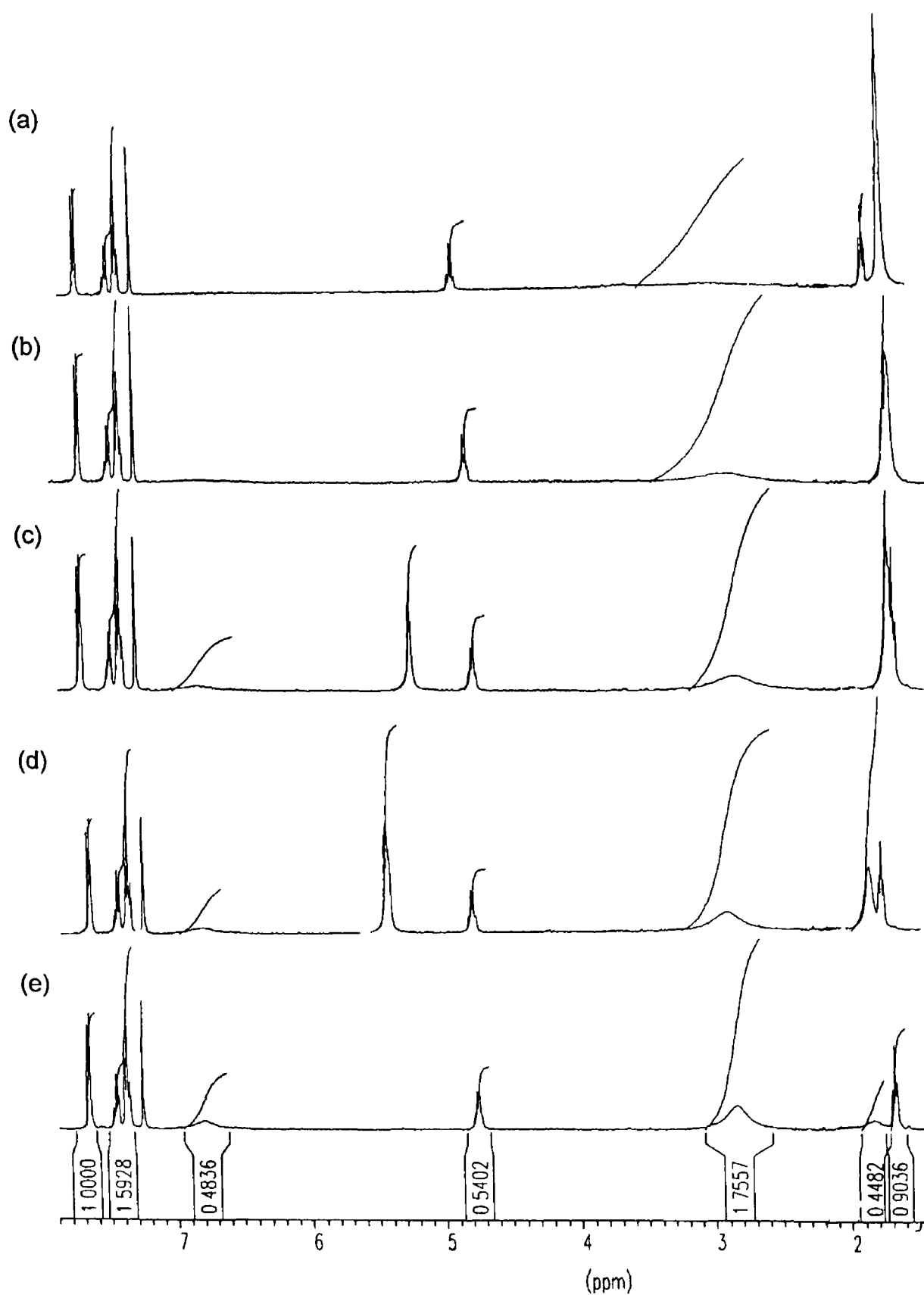


Figure 4.5 ^1H NMR spectrum of (243b)-TMPD C-T complex at (a) room temperature (20 °C), (b) 0 °C, (c) -10 °C, (d) -20 °C and (e) -30 °C

1

In addition to the TMPD signals a broad peak was observed at -10 °C and -20 °C which was not observed at either 0 °C, 20 °C or -30 °C. At -10 °C this peak occurred at δ 5.24 ppm but was shifted downfield to δ 5.42 ppm at -20 °C. It is unknown whether this signal is real, reproducible or reversible.

The only rational conclusion that can be deduced from the data is that the crystals of the C-T complex contain water of crystallisation.

4.3.2 Attempted C-T Complex formation between (243b) and TTF (3)

Treatment of a hot solution of (243b) in acetonitrile with an equimolar amount of TTF afforded a yellow solution, which on cooling deposited crystals of unreacted (243b). Recrystallisation in acetonitrile of the yellow solid, obtained on evaporating the filtrate, afforded additional quantities of (243b). The UV/visible spectrum recorded after the addition of TTF to one equivalent of (243b) in acetonitrile (figure 4.6) did not show the formation of a new C-T band.

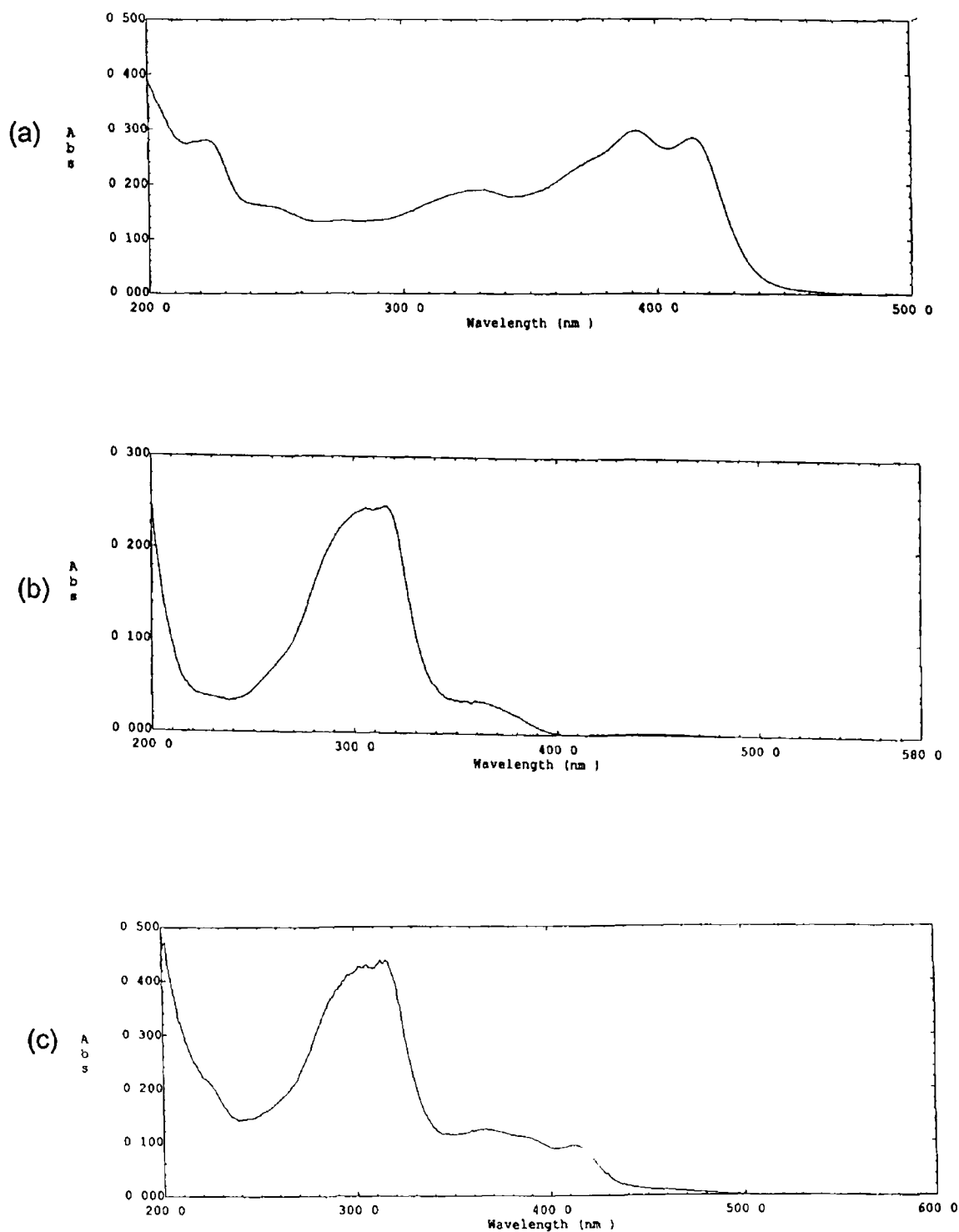


Figure 4.6 UV/Visible spectra of (a) (243b), (b) TTF and (c) (243b) and TTF

Chapter 5

Cyclic Voltammetry Studies

5 1 Introduction

Cyclic voltammetry has been extensively used by organic chemists in the search for new organic conducting materials ^{110, 125a} The potential of a given molecule as a possible candidate for a constituent in a C-T complex or organic conductor can be inferred from the energy changes accompanying the half reactions



A convenient method is to measure the half-wave potentials ($E_{1/2}$) under similar solvent, electrolyte and reference electrode conditions The energy change, ΔE ($\Delta E = E_{1/2}^1 - E_{1/2}^2$), corresponding to the disproportionation reaction



may be regarded as a figure of merit with smaller ΔE values being desirable Thus cyclic voltammetry provides a quantitative means of determining likely conditions for organic conducting materials

5 2 Cyclic Voltammetry

Cyclic voltammetry involves the measurement of cell current as a function of the electrode potential In a cyclic voltammetric experiment one has an unstirred solution containing a supporting electrolyte and a redox species (in solution or on the surface) ¹⁷⁸ The potential of the working electrode is cycled and the resulting current is measured, with the potential of the working electrode controlled versus the reference electrode A redox system can be characterised by the peaks on the cyclic voltammogram and from changes caused by variations in the scan rate The potential that is applied across the electrode for a cyclic voltammogram is considered as an excitation signal (linear potential scan with triangular waveform) (figure 5 1)

The triangular potential excitation signal sweeps the electrode potential between two values (switching potentials) The excitation signal causes potential first to scan negatively versus the reference electrode The scan direction is then reversed (point 5, figure 5 1), causing a positive scan back to the original potential Single or multiple scans may be used and the potential

scan rate can also be varied. The current evolved at the working electrode is measured throughout the potential scan.

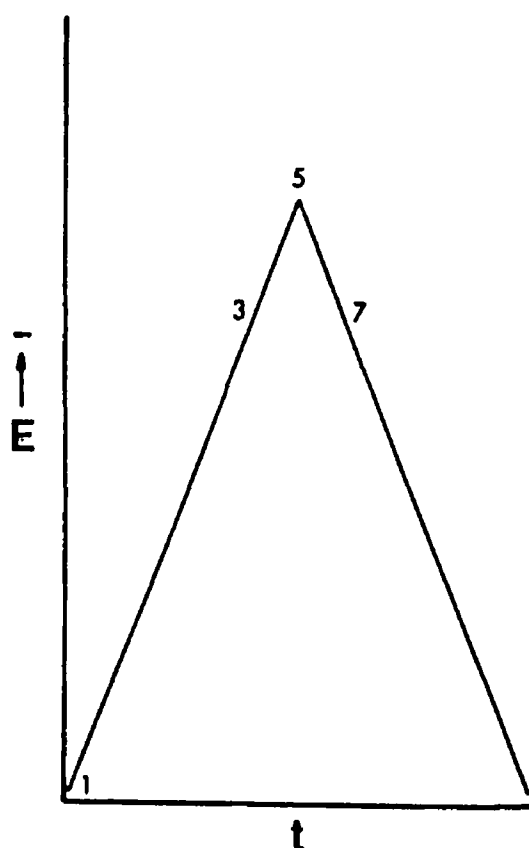
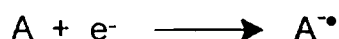


Figure 5.1 Triangular potential 'Excitation Signal' for a cyclic voltammogram

The typical response curve (cyclic voltammogram) to the potential excitation signal for the reversible reduction of A to its stable anion radical $A^{\bullet-}$ having a characteristic potential E^0 for the process is shown in figure 5.2. The cyclic voltammetric scan is initiated from a positive potential (point 1) and proceeds in the negative direction. When the working electrode eventually attains sufficient negative potential to reduce A, the cathodic current (point 2) occurs due to the process:



The cathodic current increases rapidly (point 2 \rightarrow point 3) until the concentration of A at the electrode surface is diminished, causing the current to peak (point 3). The current then decays (point 3 \rightarrow point 5) as the solution

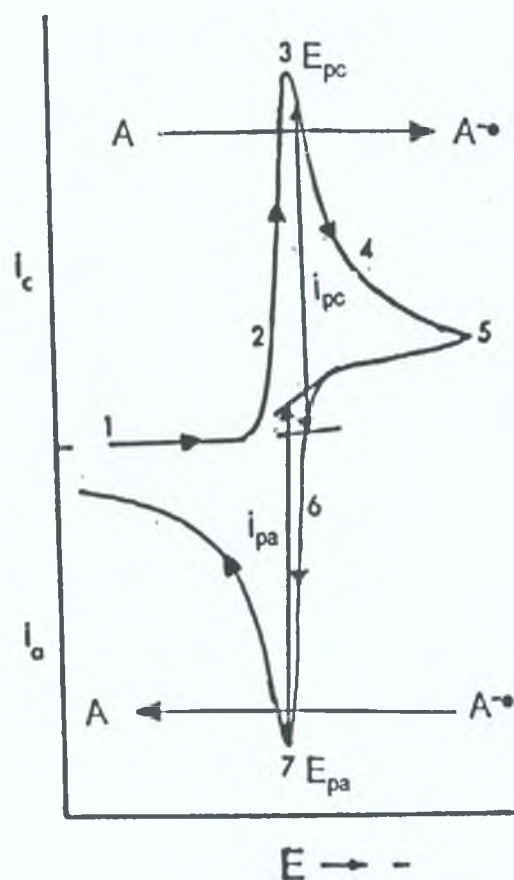


Figure 5.2 Cyclic Voltammogram for a freely diffusing species.

around the electrode is depleted of A due to its reduction to $A^{\bullet-}$. The scan direction is reversed or 'cycled' at point 5 and the reverse scan is analogous to the forward scan. The potential is still sufficiently negative to reduce A, so the cathodic current continues even though potential is now scanning in the positive direction. When the electrode becomes a sufficiently strong oxidant (sufficiently positive), $A^{\bullet-}$ which has been accumulating near the electrode can now be oxidised *i.e.*



This causes the anodic current (point 6 \rightarrow point 7). The anodic current rapidly increases until the surface concentration of $A^{\bullet-}$ is diminished, causing the current to peak (point 7). Current then decays as the solution around the electrode is depleted of $A^{\bullet-}$. From figure 5.2, $A^{\bullet-}$ is generated electrochemically

from A in the forward scan and in the reverse scan A^\bullet is oxidised back to A as indicated by the anodic current

A more detailed understanding can be gained by considering the Nernst equation (equation 6) and the changes in concentration that occur in solution 'adjacent' to the electrode during electrolysis. The potential excitation signal exerts control on the ratio $[\text{conc } A / \text{conc } A^\bullet]$ at the electrode surface as described by the Nernst equation for a reversible system

$$E = E^0 + RT/nF \ln[\text{conc } A / \text{conc } A^\bullet] \quad (6)$$

where E is the peak potential ($=E_{\text{initial}} - \nu t$ where E_{initial} is the initial potential, ν is the scan rate in volts per second and t is the elapsed time), E^0 is the formal reduction potential of the couple A/A^\bullet , R is the gas constant, T is the absolute temperature, F is the Faraday constant and n is the number of electrons in the half reactions. The half-wave potential ($E_{1/2}$) is related to E^0 by

$$E_{1/2} = E^0 + RT/nF \ln(D_R/D_O)^{1/2}$$

$E_{1/2}$ is exactly (within $2/n$ mV) midway between the anodic peak potential (E_{pa}) and the cathodic peak potential (E_{pc}) and D_R and D_O are diffusion coefficients of the oxidised and reduced forms

The location of the peak potential (E) can be used in the qualitative identification of the electroactive species while the peak current (i) can be used in its quantitative determination. For electrochemically reversible reactions the anodic peak potential (E_{pa}) is equal to the cathodic peak potential (E_{pc}). Reversibility occurs when both species rapidly exchange electrons with the working electrode. The criterion for reversibility is two-fold

(1) the peak separation (ΔE_p) is equal to the difference between the anodic peak potential (E_{pa}) and the cathodic peak potential (E_{pc}) i.e.

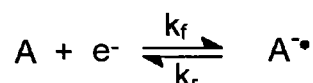
$$\Delta E_p = E_{pa} - E_{pc} = 59/n \text{ mV}$$

and (2) the difference between the cathodic half-peak potential ($E_{p/2}$) and the cathodic potential (E_{pc}) is equal to $59/n$ mV

$$E_{p/2} - E_{pc} = 59/n \text{ mV}$$

Both (1) and (2) are independent of concentration and scan rate

Irreversibility, on the other hand is due to slow exchange of the redox species with the working electrode / e the rate constant for the forward reaction (k_f) is much greater than the rate constant for the reverse reaction (k_r) for the cathodic peak and the opposite holds for the anodic peak ($k_r \gg k_f$)



Also

$$\Delta E_p > 59/n \text{ mV}$$

and

$$E_{p/2} - E_{pc} > 59/n \text{ mV}$$

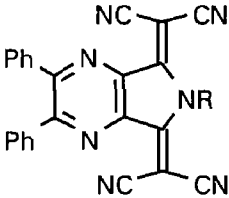
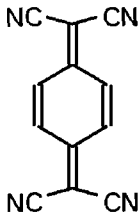
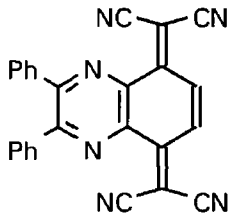
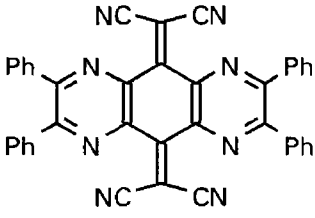
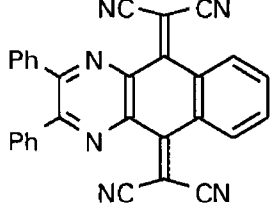
A quasi-reversible reaction results if k_f and k_r are the same order of magnitude over most of the potential range

5 3 Electrochemical studies of Bis(dicyanomethylene)-5,7-dihydropyrrolo-[3,4-b]pyrazines (237) and (243)

The electrochemical properties of 2,3-diphenyl-5,7-bis(dicyanomethylene)-6H-5,7-dihydropyrrolo[3,4-b]pyrazine (237) and the 2,3-diphenyl-5,7-bis(dicyanomethylene)-6-alkyl-5,7-dihydropyrrolo[3,4-b]pyrazine derivatives (243) were studied by cyclic voltammetry at room temperature. The half-wave ($E_{1/2}$) potentials are shown in table 5 1 along with those of TCNQ (2),¹⁰⁸ and pyrazino-TCNQs (232),¹⁶⁹ (257)¹⁷⁹ and (258)¹⁷⁹ measured under similar conditions

The reduction potentials of (237) and (243) were measured in acetonitrile at room temperature using lithium perchlorate as supporting electrolyte to establish their potential as electron acceptors. The cyclic voltammogram of (237) exhibits a single reversible redox wave corresponding to a one electron reduction at the potential $E_{1/2} = -0.84 \text{ V}$ (figure 5 3). The separation of the cathodic and anodic peaks amounts to 0.063 V, consistent with a one electron transfer.

Table 5.1 Cyclic Voltammetry Data for Heterocyclic TCNQ Analogues
(measured in acetonitrile unless otherwise stated)

Compound	Solvent	$E^1_{1/2}/V$	$E^2_{1/2}/V$	$\Delta E/V$
(237) R=H		-0.84		
	(243a) R=Me	-0.36	-0.51	0.15
	(243b) R=Et	-0.37	-0.53	0.16
	(243c) R=CH ₂ Ph	-0.34	-0.49	0.15
 (2)		+0.08	-0.48	0.56
 (232)	DMF	+0.25	-0.29	0.54
 (257)		+0.10	-0.38	0.48
 (258)		-0.22	-0.31	0.09

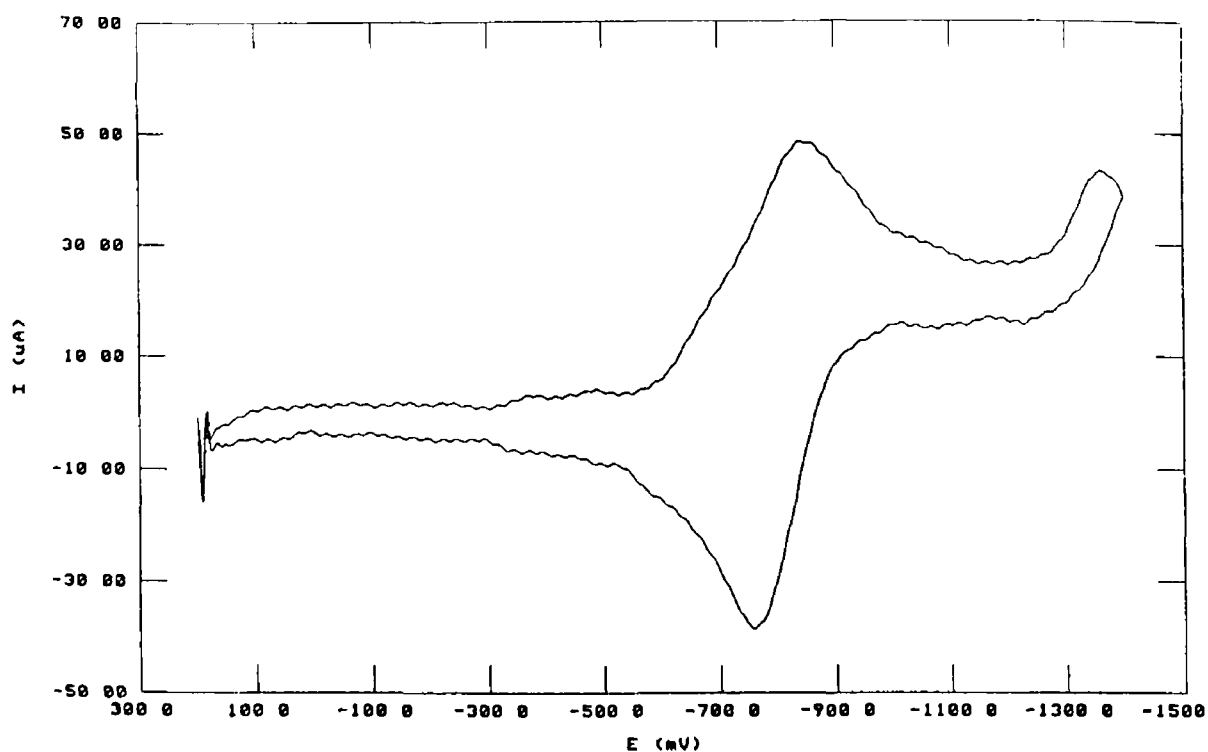
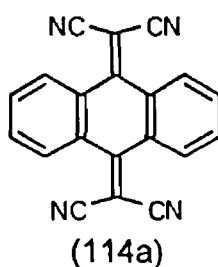
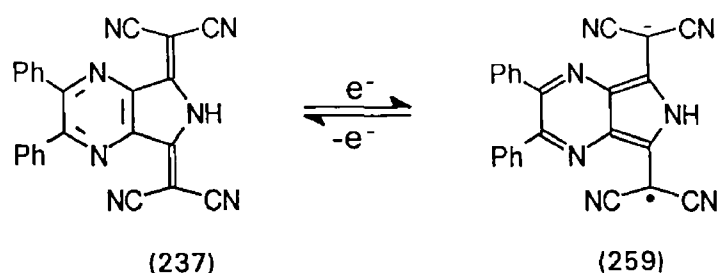


Figure 5.3 Cyclic Voltammogram of (237) in 0.25 M lithium perchlorate/acetonitrile solution Mercury electrode Scan rate 100 mV s⁻¹

Huckel molecular orbital calculations by Gerson and co-workers showed¹¹⁸ that the negative charges in the radical anion and dianion of 9,10-TCAQ (114a) are located on the two dicyanomethylene carbon atoms



This is because the LUMO i.e. the orbital where the extra electrons are placed is located in this moiety. Analogously it is expected that reduction of (237) mainly affects the tetracyanopyrrolidine ring moiety. Therefore, the reversible redox wave in the cyclic voltammogram of (237) may correspond to a one electron reduction to radical anion (259) (scheme 5.1).



Scheme 5 1

In contrast to 2,3-diphenyl-5,7-bis(dicyanomethylene)-6H-5,7-dihydro-pyrrolo[3,4-b]pyrazine (237) which shows a single wave one-electron reduction to the anion radical, the *N*-alkyl derivatives (243) exhibit two reversible single wave reductions (figures 5 4-5 6). The first reversible redox wave ($E_{1/2}^1$) in the cyclic voltammograms of (243) corresponds to a one electron reduction to the anion radicals (260) and the second reversible redox wave corresponds to a one electron reduction of the anion radicals (260) to the dianions (261) (scheme 5 2) the potentials of which are shown in table 5 1. The separations of the cathodic and anodic peaks are consistent with a one electron reduction for both waves.

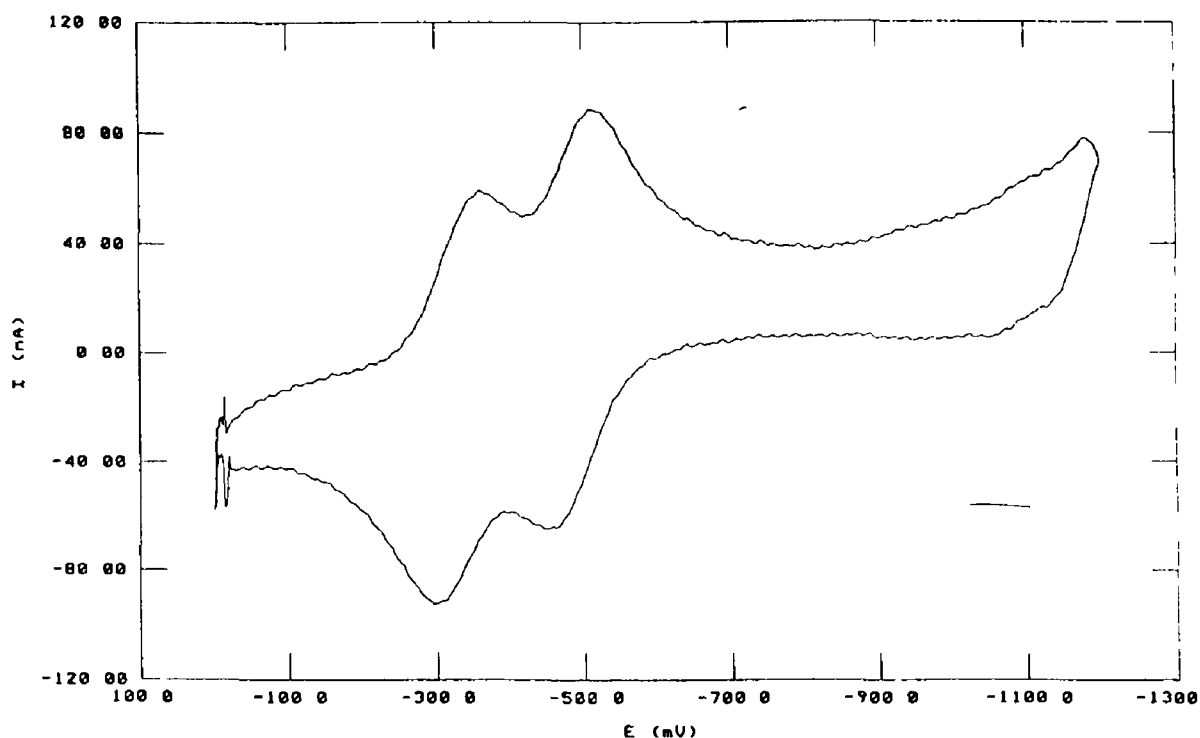


Figure 5 4 Cyclic Voltammogram of (243a) in 0.25 M lithium perchlorate/acetonitrile solution. Mercury electrode. Scan rate 100 mV s⁻¹.

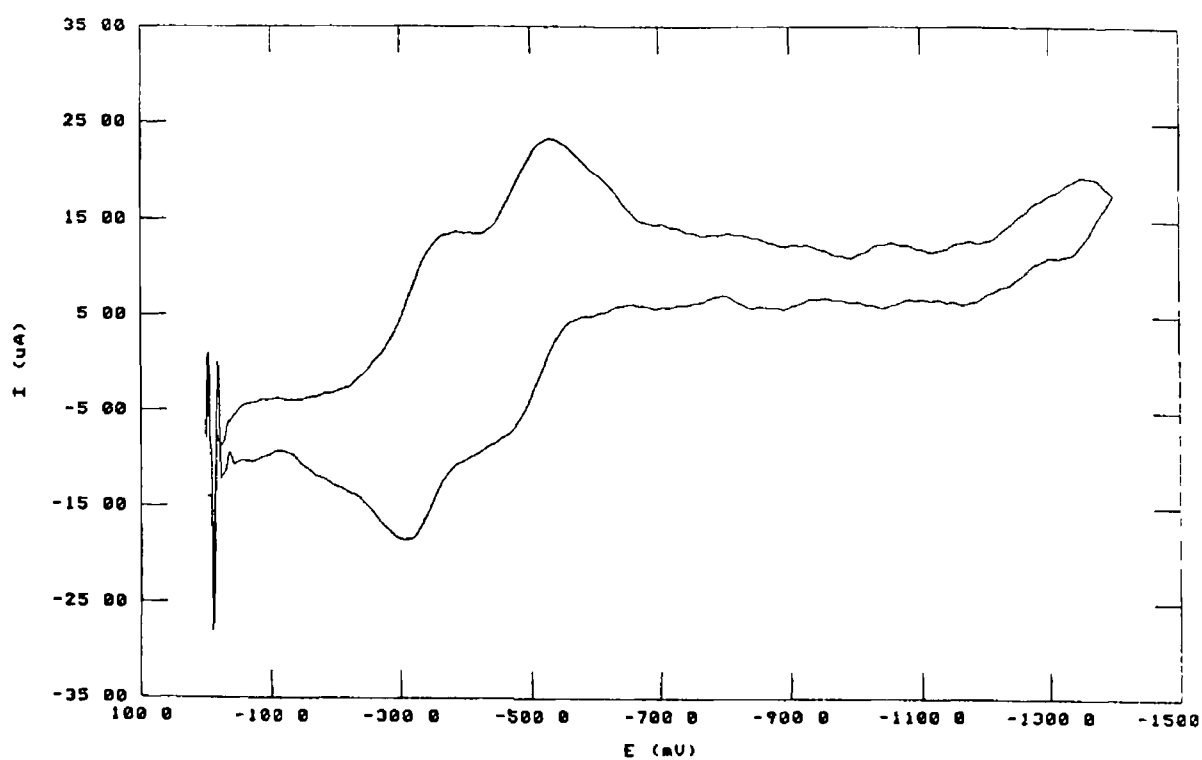


Figure 5.5 Cyclic Voltammogram of (243b) in 0.25 M lithium perchlorate/acetonitrile solution Mercury electrode Scan rate 100 mV s⁻¹

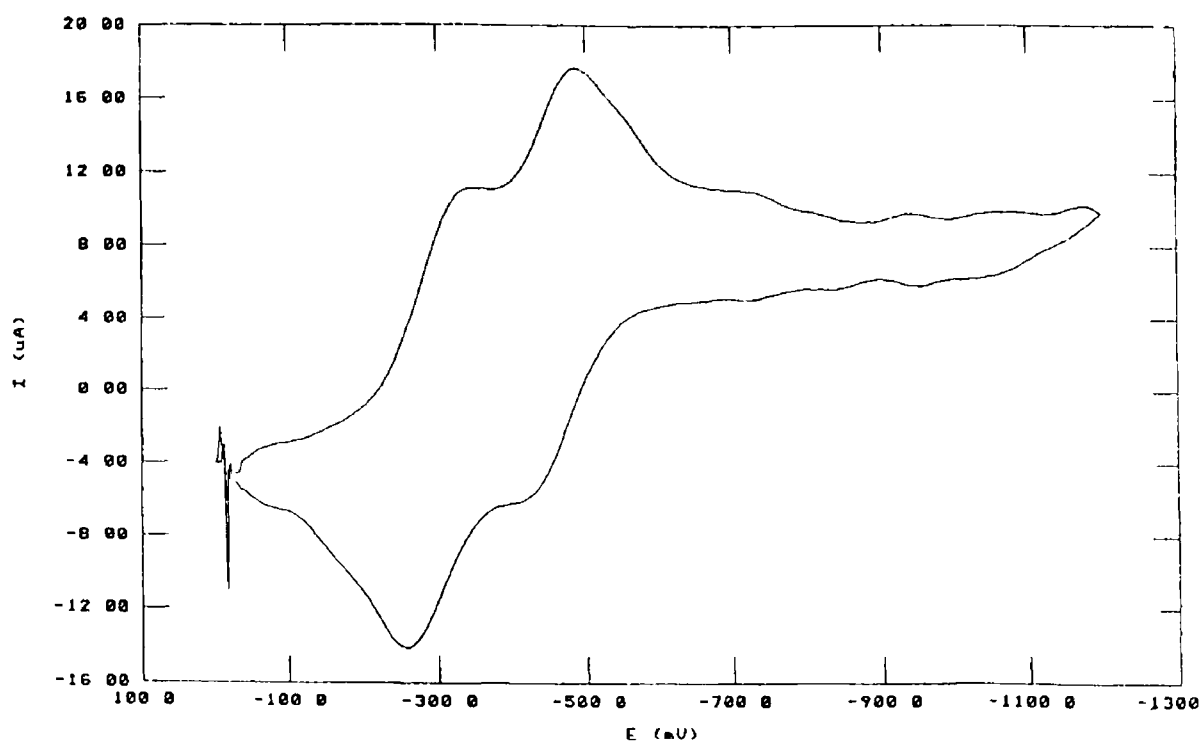
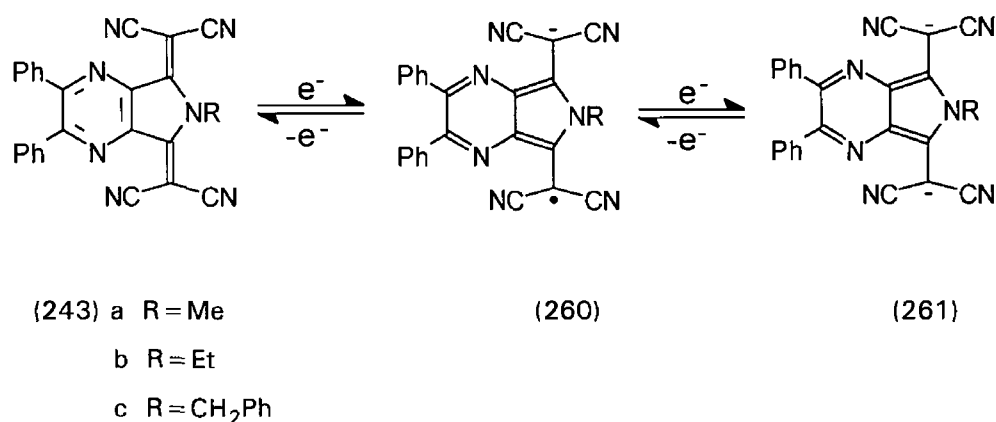


Figure 5.6 Cyclic Voltammogram of (243c) in 0.25 M lithium perchlorate/acetonitrile solution Mercury electrode Scan rate 100 mV s⁻¹



Scheme 5 2

5 3 1 Discussion

Cyclic voltammetry measurements reveal that compound (237) forms a stable anion radical and compounds (243) form stable anions and dianions. Substitution on the nitrogen atom of the tetracyanopyrrolidine ring allows tuning of the acceptor ability depending on the electronic behaviour of the substituents. The first half-wave reduction potentials of (243a, $E^1_{1/2} = -0.36$ V), (243b, $E^1_{1/2} = -0.37$ V) and (243c, $E^1_{1/2} = -0.34$ V) are similar and have a more positive value than (237, $E^1_{1/2} = -0.84$ V). This indicates that replacing the hydrogen atom with an alkyl group enhances the electron accepting ability.

The first reduction potentials of (237) and (243) are higher than that of TCNQ (2, $E^1_{1/2} = +0.08$ V),¹⁰⁸ and the pyrazino-TCNQs (232, $E^1_{1/2} = +0.25$ V),¹⁶⁹ (257, $E^1_{1/2} = +0.10$ V)¹⁷⁹ and (258, $E^1_{1/2} = -0.237$ V).¹⁷⁹ This indicates that (237) and (243) are poorer electron acceptors than the latter compounds. However, the smaller difference between $E^1_{1/2}$ and $E^2_{1/2}$ (i.e. ΔE value) of (243a, $\Delta E = 0.15$ V), (243b, $\Delta E = 0.16$ V) and (243c, $\Delta E = 0.15$ V) compared to TCNQ ($\Delta E = 0.56$ V) suggests that the intramolecular Coulomb repulsion is reduced in the electron acceptors (237) and (243) owing to the extension of the π -system. Reduction of the intramolecular on-site Coulombic repulsion is one of the prerequisites for attaining high electrical conductivity. These heterocyclic TCNQ analogues, as reported in chapter 4, have potential as electron acceptor constituents in C-T complexes.

Chapter 6

EXPERIMENTAL

Introductory Remarks

Nuclear Magnetic Resonance (NMR) spectra were recorded on a Bruker AC 400 instrument operating at 400 MHz for ^1H NMR and 100 MHz for ^{13}C NMR. All spectra were recorded using deuteriochloroform (CDCl_3) as solvent unless otherwise stated (s=singlet, d=doublet, t=triplet, q=quartet, m=multiplet and br=broad). Coupling constants (J) are given in Hertz (Hz).

Infra-red (IR) spectra were recorded on a Perkin-Elmer 983G IR spectrophotometer, a Nicolet 205 FT-IR spectrometer or a Perkin-Elmer FT-IR spectrometer for KBr pellets unless otherwise stated (s=strong, m=medium).

Ultraviolet (UV) spectra were recorded on a Hewlett-Packard 8452A diode array or a Shimadzu 3100 UV/visible spectrophotometer. The units for ϵ are $\text{dm}^3 \text{mol}^{-1} \text{cm}^{-1}$. HPLC grade acetonitrile was used as the solvent unless otherwise stated.

Melting point determinations were recorded using a Griffin or Gallenkamp melting point apparatus and are uncorrected.

Elemental analyses were carried out by the Microanalytical Laboratory at University College Dublin.

Thin Layer Chromatography (TLC) was carried out using silica gel TLC plates containing a fluorescent indicator (Riedel de Haen, DC cards SiF, layer thickness 0.2 mm).

High Resolution Mass Spectra (HRMS) were carried out by the Department of Chemistry, The University, Dundee, DD1 4HN, Scotland, UK.

Radial centrifugal chromatography (RCC) was carried out using a Harrison Research model 7924T Chromatotron system using rotors coated with Kieselgel 60 PF₂₅₄ containing 5% calcium sulphate as binder.

Tetrahydrofuran was dried prior to use by heating under reflux over benzophenone and sodium metal until the mixture developed a deep purple colour (sodium benzophenone ketyl) followed by distillation. Dichloromethane was dried prior to use by distillation from calcium hydride. Light petroleum (40–60 °C) was used unless otherwise stated.

Sodium hydride (60% oil dispersion) was washed with light petroleum prior to use. The light petroleum was removed using a Pasteur pipette and the remaining suspension was dried by applying a flow of nitrogen gas.

Synthesis of Sodium (Z)-4-Dicyanomethylene-4-hydroxy-2-butenolate (173a)

Sodium hydride (15.0 g, 800 mmol) and anhydrous tetrahydrofuran (800 cm³) were placed in a round-bottom flask fitted with a magnetic stirrer and a dropping funnel. Malononitrile (59.2 g, 900 mmol), dissolved in anhydrous tetrahydrofuran (400 cm³) was added dropwise with stirring at room temperature. Maleic anhydride (63a) (78.4 g, 800 mmol) in anhydrous tetrahydrofuran (600 cm³) was added to the sodiummalononitrile solution. A yellow solid precipitated and the mixture was stirred at room temperature for 1 hour after which the yellow solid was filtered off, washed with tetrahydrofuran (2x50 cm³) and dried under vacuum to yield sodium (Z)-4-dicyanomethylene-4-hydroxy-2-butenolate (173a) (118.0 g, 90%), m.p. 90 °C (decomp.), IR ν_{\max} 3460 (broad OH), 2216, 2191 (s, CN), 1550 (s, C=O), 1500, 1440, 1386, 1314, 1210, 970 and 805 cm⁻¹, ¹H-NMR (DMSO-d₆) δ 6.11 (1H, d, J 12.8, vinylic-H), 6.74 (1H, d, J 12.8, vinylic-H) and 17.46 (1H, br s, OH, exchanges with D₂O) ppm, ¹³C-NMR (DMSO-d₆) δ 57.47 [C(CN)₂], 116.97, 117.81 (CN), 133.02, 133.59 (HC=CH), 165.54 and 182.30 [C=O and C=C(CN)₂] ppm

Synthesis of Tetraethylammonium (Z)-4-Dicyanomethylene-4-hydroxy-2-butenolate (173b)

Tetraethylammonium bromide (1.9 g, 9 mmol), dissolved in water (20 cm³), was added dropwise with stirring at room temperature to sodium (Z)-4-dicyanomethylene-4-hydroxy-2-butenolate (173a) (1.5 g, 9 mmol) dissolved in water (50 cm³). The reaction mixture was stirred at room temperature for 1 hour. The product was extracted with dichloromethane (3x25 cm³) and the combined organic extracts were dried over anhydrous magnesium sulphate. Removal of dichloromethane by rotary evaporation yielded tetraethylammonium (Z)-4-dicyanomethylene-4-hydroxy-2-butenolate (173b) as a yellow solid (1.1 g, 43%). Recrystallisation from ethanol gave yellow crystals, m.p. 95-96 °C, Microanalysis Found C, 60.91, H, 7.91, N, 14.03% C₁₅H₂₃N₃O₃ requires C, 61.41, H, 7.90, N, 14.32%, UV λ_{\max} 232 (ϵ 12,228) and 344 (ϵ 10,988) nm, IR ν_{\max} 3440 (OH), 2987, 2958 (aliphatic C-H), 2202 (s, CN), 1695 (s, C=O), 1611 (s, conj C=C), 1478 (s), 1391 (s), 1356 (s), 1254, 1240, 1220, 1174, 1069, 1052, 998, 838 (s), 814 (m), 787 (m) and 640 cm⁻¹, ¹H-NMR δ 1.30 (12H, t of t, J 2.0, 7.4, CH₃), 3.38 (8H, q, J 7.4, CH₂), 6.06 (1H, d, J 12.8, vinylic-H), 6.75 (1H, d, J 12.8, vinylic-H) and 14.09 (1H, br s, OH) ppm, ¹³C-NMR δ 6.94 (CH₃), 52.18 (1.1.1 t, J 3.05 Hz, CH₂), 58.20 [C(CN)₂], 117.01, 117.83 (CN), 133.03, 133.68 (HC=CH), 165.65 and 182.56 [C=O and C=C(CN)₂] ppm

Synthesis of (Z)-4-Dicyanomethylene-4-hydroxy-2-butenic acid (179)

Sodium (Z)-4-dicyanomethylene-4-hydroxy-2-butenate (173a) (30.0 g, 160 mmol) and 1% v/v dilute hydrochloric acid (600 cm³) were placed in a round-bottom flask and the reaction was stirred at room temperature for 1 hour. The product was extracted exhaustively with diethyl ether and the combined ethereal extracts were dried over anhydrous magnesium sulphate. Removal of diethyl ether by rotary evaporation yielded (Z)-4-dicyanomethylene-4-hydroxy-2-butenic acid (179) (19.0 g, 72%) as a yellow solid. Recrystallisation from toluene gave yellow crystals, m.p. 130-132 °C. Microanalysis Found C, 51.04, H, 2.51, N, 17.15%. C₇H₄N₂O₃ requires C, 51.22, H, 2.45, N, 17.06%, UV λ_{\max} 236 (ϵ 7,933) and 330 (ϵ 10,450) nm, IR ν_{\max} 3441, 3370 (s, OH), 2250, 2236 (s, CN), 1690 (s, C=O), 1640, 1508, 1355 (s), 1294 (s), 1224 (s) and 847 (s) cm⁻¹, ¹H-NMR (Acetone-d₆) δ 2.75 (4H, br s, H₂O), 6.64 (1H, d, J 12.8, vinylic-H), 7.12 (1H, d, J 12.8, vinylic-H) and 10.96 (1H, br s, OH) ppm, ¹³C-NMR (Acetone-d₆) δ 68.71 [C(CN)₂], 111.87, 112.87 (CN), 130.93, 134.65 (HC=CH), 170.97 and 175.12 [C=O and C=C(CN)₂] ppm.

Synthesis of 4-Dicyanomethylene-2-butenolide (162)

(i) From (Z)-4-Dicyanomethylene-4-hydroxy-2-butenic acid (179)

(Z)-4-Dicyanomethylene-4-hydroxy-2-butenic acid (179) (36.0 g, 220 mmol) and toluene (150 cm³) were added to a round-bottom flask fitted with a magnetic stirrer, reflux condenser and a dropping funnel. A solution containing thionyl chloride (21 cm³, 290 mmol) and toluene (150 cm³) was placed in the dropping funnel and added dropwise with stirring at room temperature. The reaction was heated under reflux for 3 hours (until the evolution of gases ceased) after which a small amount of insoluble material was filtered off. The thionyl chloride and toluene were removed from the filtrate by ambient pressure distillation to yield a brown oil which, on cooling, solidified to give 4-dicyanomethylene-2-butenolide (162) (22.9 g, 71%). Recrystallisation from light petroleum (60-80 °C) gave off-white crystals, m.p. 101-102 °C. Microanalysis Found C, 57.56, H, 1.36, N, 19.39%. C₇H₂N₂O₂ requires C, 57.54, H, 1.37, N, 19.17%, UV λ_{\max} 300 (ϵ 17,902) nm, IR ν_{\max} 3146 (s), 3112 (s), 3089 (s, aliphatic C-H), 2241 (s, CN), 1819 (s, C=O), 1628 (s, conj C=C), 1561 (s), 1350 (m), 1304 (m), 1200 (s), 1094 (s), 1073 (s), 1010 (s), 859 (s), 830 (s) and 820 (s) cm⁻¹, ¹H-NMR (Acetone-d₆) δ 7.23 (1H, d, J 5.9, vinylic-H) and 8.27 (1H, d, J 5.9, vinylic-H) ppm, ¹³C-NMR (Acetone-d₆) δ 68.58 [C(CN)₂], 109.73, 110.38 (CN), 129.70, 141.21 (HC=CH), 165.09 and 172.35 [C=O and C=C(CN)₂] ppm.

(ii) *From Sodium (Z)-4-Dicyanomethylene-4-hydroxy-2-butenolate (173a)*

Sodium (Z)-4-dicyanomethylene-4-hydroxy-2-butenolate (173a) (44.0 g, 258 mmol) and toluene (200 cm³) were placed in a round-bottom flask fitted with a magnetic stirrer, reflux condenser and a dropping funnel. A solution containing thionyl chloride (20 cm³, 274 mmol) and toluene (50 cm³) was placed in the dropping funnel and added dropwise with stirring at room temperature. The reaction mixture was heated under reflux for 3 hours (until the evolution of gas ceased) and the insoluble black solid which precipitated was filtered off. The thionyl chloride and toluene were removed from the filtrate by ambient pressure distillation to yield a brown oil which on cooling, solidified to give 4-dicyanomethylene-2-butenolide (162) (20.0 g, 53%). Recrystallisation from light petroleum (60-80 °C) gave off-white crystals, m.p. 101-102 °C. The IR and NMR spectral data were identical to those reported for (162) by route (i).

Synthesis of Ethyl (Z)-4-Dicyanomethylene-4-hydroxy-2-butenolate (176)

(i) *From 4-Dicyanomethylene-2-butenolide (162)*

Ethanol (200 cm³) was added to 4-dicyanomethylene-2-butenolide (162) (15.0 g, 100 mmol) in a round-bottom flask and the solution was stirred at room temperature for 30 minutes. The yellow crystalline solid which precipitated was filtered off on a Buchner funnel, washed with ethanol (2x25 cm³) and dried under vacuum to yield ethyl (Z)-4-dicyanomethylene-4-hydroxy-2-butenolate (176) (9.8 g, 50%). Complete removal of ethanol from the filtrate by rotary evaporation gave additional quantities of the crude ester (4.8 g, 24%). This was confirmed by ¹H, ¹³C and IR spectroscopic data, (overall yield 14.6 g, 74%). Recrystallisation from chloroform/light petroleum (60-80 °C) gave yellow crystals, m.p. 108-110 °C. Microanalysis. Found: C, 55.81, H, 4.27, N, 14.50%. C₉H₈N₂O₃ requires: C, 56.25, H, 4.19, N, 14.57%. UV λ_{max} 238 (ε 13,037), 326 (ε 16,746) and 334sh (ε 16,226) nm, IR ν_{max} 3420 (OH), 3020, 3006 (C-H), 2227 (s, CN), 1660 (s, C=O), 1629 (s), 1620 (s, conj C=C), 1568 (s), 1468, 1438 (s), 1418 (s), 1391, 1277 (s), 1233 (s), 1218 (s), 921 (s), 846 (s) and 834 cm⁻¹, ¹H-NMR δ 1.41 (3H, t, J 7.4, CH₃), 4.43 (2H, q, J 7.4, CH₂), 6.43 (1H, d, J 12.8, vinylic-H), 7.06 (1H, d, J 12.8, vinylic-H) and 14.55 (1H, br s, OH) ppm, ¹³C-NMR δ 13.43 (CH₃), 64.64 (CH₂), 70.01 [C(CN)₂], 111.35, 112.47 (CN), 129.54, 134.25 (HC=CH), 169.13 and 173.83 [C=O and C=C(CN)₂] ppm.

(ii) *From Sodium (Z)-4-Dicyanomethylene-4-hydroxy-2-butenolate (173a)*

Ethanol (25 cm³) and concentrated sulphuric acid (0.5 cm³) was added to sodium (Z)-4-dicyanomethylene-4-hydroxy-2-butenolate (173a) (0.5 g, 3 mmol)

and the solution was heated under reflux for 30 minutes. The reaction solution was allowed to cool and the ethanol was removed by rotary evaporation. The product was extracted from the resulting oil with diethyl ether (3x25 cm³). The ethereal extract was washed with water (2x25 cm³) and dried over anhydrous magnesium sulphate to yield ethyl (Z)-4-dicyanomethylene-4-hydroxy-2-butenolate (176) (0.3 g, 56%). Recrystallisation from chloroform/light petroleum (60-80 °C) gave yellow crystals, m.p. 108-110 °C. The IR and NMR spectral data were identical to those reported for (176) by route (i).

Synthesis of Methyl (Z)-4-Dicyanomethylene-4-hydroxy-2-butenolate (182)

Methanol (200 cm³) was added to 4-dicyanomethylene-2-butenolide (162) (15.0 g, 100 mmol) in a round-bottom flask and the solution was stirred at room temperature for 30 minutes. The yellow crystalline solid which precipitated was filtered off on a Buchner funnel, washed with methanol (2x25 cm³) and dried under vacuum to yield methyl (Z)-4-dicyanomethylene-4-hydroxy-2-butenolate (182) (9.3 g, 51%). Complete removal of methanol from the filtrate by rotary evaporation gave additional quantities of the crude ester (3.2 g, 17%). This was confirmed by ¹H, ¹³C and IR spectroscopic data, (overall yield 12.5 g, 68%). Recrystallisation from chloroform/light petroleum (60-80 °C) gave yellow crystals, m.p. 110-111 °C. Microanalysis. Found C, 53.63, H, 3.43, N, 15.57%. C₈H₆N₂O₃ requires C, 53.93, H, 3.39, N, 15.72%, UV λ_{max} 236 (ε 19,558) and 328 (ε 20,888) nm, IR ν_{max} 3050, 3004 (aliphatic C-H), 2225 (s, CN), 1655 (s, C=O), 1630 (s, C=C), 1560 (s), 1465 (s), 1420 (s), 1355, 1280 (s), 1220 (s), 955 (s), 935 (s), 849 (s) and 675 cm⁻¹, ¹H-NMR δ 3.98 (3H, s, CH₃), 6.39 (1H, d, J 12.8, vinylic-H), 7.08 (1H, d, J 12.8, vinylic-H) and 14.15 (1H, br s, OH) ppm, ¹³C-NMR δ 54.82 (CH₃), 70.94 [C(CN)₂], 111.30, 112.56 (CN), 128.77, 134.80 (HC=CH), 169.63 and 173.57 [C=O and C=C(CN)₂] ppm.

Attempted Synthesis of 1,4-Bis(dicyanomethylene)-1,4-dihydroxy-2-butene (185)

To sodium hydride (0.1 g, 4 mmol) in anhydrous tetrahydrofuran (10 cm³) was added malononitrile (0.27 g, 4 mmol) in anhydrous tetrahydrofuran (20 cm³), followed by 4-dicyanomethylene-2-butenolide (162) (0.58 g, 4 mmol) in anhydrous tetrahydrofuran (20 cm³). The reaction mixture was stirred at room temperature for 30 minutes after which the tetrahydrofuran was removed by rotary evaporation to yield a brown oil. ¹H NMR and IR gave complex spectra suggestive of a complex mixture of products.

Synthesis of (Z)-N-Butyl-4-dicyanomethylene-4-hydroxy-2-butenamide (189)

(i) From 4-Dicyanomethylene-2-butenolide (162)

4-Dicyanomethylene-2-butenolide (162) (2.3 g, 16 mmol) in tetrahydrofuran (40 cm³) was placed in a round-bottom flask fitted with a magnetic stirrer and a dropping funnel. N-Butylamine (1.8 cm³, 18 mmol) in tetrahydrofuran (30 cm³) was added dropwise with stirring at room temperature for 1 hour. The solvent was removed by rotary evaporation and the product was extracted with dichloromethane (3x25 cm³). The extract was washed with 1% v/v dilute hydrochloric acid (2x25 cm³) and water (2x25 cm³) and dried over anhydrous magnesium sulphate. The dichloromethane was removed by rotary evaporation to yield (Z)-N-butyl-4-dicyanomethylene-4-hydroxy-2-butenamide (189) (1.6 g, 46%). Recrystallisation from toluene gave yellow crystals, m.p. 149-150 °C, Microanalysis. Found C, 60.15, H, 6.09, N, 18.93%. C₁₁H₁₃N₃O₂ requires C, 60.26, H, 5.97, N, 19.16%, UV λ_{max} 238 (ϵ 8,250) and 330 (ϵ 11,820) nm, IR ν_{max} 3270 (s, OH), 3120 (s, NH), 2962 (s, aliphatic C-H), 2231 (s, CN), 1582 (s), 1517 (s, C=O), 1470 (s), 1455 (s), 1380 (s), 1312, 1266, 1125, 952 (s), 839 (s), 760 (s), 745 (s) and 690 (s) cm⁻¹, ¹H-NMR (Acetone-d₆) δ 0.90 (3H, t, J 7.4, CH₃), 1.37 (2H, sextet, J 7.4, CH₃CH₂CH₂CH₂), 1.59 (2H, quintet, J 7.4, CH₃CH₂CH₂CH₂), 3.40 (2H, q, J 7.4, CH₃CH₂CH₂CH₂), 6.70 (1H, d, J 12.8, vinylic-H), 6.93 (1H, d, J 12.8, vinylic-H), 9.36 (1H, br s) and 14.45 (1H, br s) (NH and OH) ppm, ¹³C-NMR (Acetone-d₆) δ 13.05 (CH₃), 19.75 (CH₂), 30.28 (CH₂), 40.33 (CH₂), 65.42 [C(CN)₂], 112.96, 113.98 (CN), 132.25, 132.35 (HC=CH), 166.73 and 177.28 [C=O and C=C(CN)₂] ppm.

(ii) From Ethyl (Z)-4-Dicyanomethylene-4-hydroxy-2-butenolate (176)

N-Butylamine (1.28 cm³, 13 mmol) was added to a solution of ethyl (Z)-4-dicyanomethylene-4-hydroxy-2-butenolate (176) (1.0 g, 5.2 mmol) in tetrahydrofuran (40 cm³). The solution was heated under reflux for 4 hours and then allowed to cool. The solvent was removed by rotary evaporation and the product was extracted with dichloromethane (3x20 cm³). The extract was washed with 1% v/v dilute hydrochloric acid (2x25 cm³) and water (2x25 cm³) and dried over anhydrous magnesium sulphate. The dichloromethane was removed by rotary evaporation to yield (Z)-N-butyl-4-dicyanomethylene-4-hydroxy-2-butenamide (189). The melting point, IR and NMR spectral data were identical to those reported for (189) by route (i).

Synthesis of (Z)-N-Phenyl-4-dicyanomethylene-4-hydroxy-2-butenamide (190)

4-Dicyanomethylene-2-butenolide (162) (2.9 g, 20 mmol) in tetrahydrofuran (50 cm³) was placed in a round-bottom flask fitted with a magnetic stirrer and a dropping funnel. Aniline (2.1 cm³, 23 mmol) in tetrahydrofuran (50 cm³) was added dropwise with stirring at room temperature. Stirring was continued for 1 hour, after which the yellow solid that precipitated was filtered off, washed with tetrahydrofuran (2x20 cm³) and dried under vacuum to yield (Z)-N-phenyl-4-dicyanomethylene-4-hydroxy-2-butenamide (190) (2.5 g, 61%). Recrystallisation from acetonitrile gave yellow crystals, m.p. 219-220 °C (darkens 206 °C), Microanalysis Found C, 65.38, H, 3.76, N, 17.65%. C₁₃H₉N₃O₂ requires C, 65.26, H, 3.79, N, 17.56%, UV λ_{max} 230 (ϵ 14,252) and 348 (ϵ 18,989) nm, IR ν_{max} 3277, 3206, 3162, 3119, 3053 (aromatic and aliphatic C-H), 2228 (CN), 1609, 1561, 1468, 1390, 1332, 1232, 1202, 1058, 961, 831, 754 and 689 cm⁻¹, ¹H-NMR (DMSO-d₆) δ 6.59 (1H, d, J 12.8, vinylic-H), 6.94 (1H, d, J 12.8, vinylic-H), 7.19-7.50 [4H, m, OH (exchanges with D₂O) and aromatic protons], 7.62 (2H, m, aromatic protons) and 11.98 (1H, s, NH, exchanges with D₂O) ppm, ¹³C-NMR (DMSO-d₆) δ 61.96 [C(CN)₂], 114.73, 115.60 (CN), 120.72, 125.60, 129.12, 132.38, 133.67, 137.10 (vinylic and aromatic carbons), 164.16 and 179.38 [C=O and C=C(CN)₂] ppm.

Attempted Cyclisation of (Z)-N-Butyl-4-dicyanomethylene-4-hydroxy-2-butenamide (189) and (Z)-N-Phenyl-4-dicyanomethylene-4-hydroxy-2-butenamide (190)

(i) (Z)-N-Butyl-4-dicyanomethylene-4-hydroxy-2-butenamide (189) (0.05 g, 2.3 mmol) was placed in a boiling tube connected to a nitrogen supply and a bubbler. A continuous stream of nitrogen gas was passed through the apparatus for 10 minutes after which the nitrogen supply was turned off. The solid was heated at 160 °C for 30 minutes using an oil bath, then allowed to cool and the resulting black solid which resulted was collected (0.02 g). ¹H NMR and IR spectral analysis of the crude product gave complex spectra suggestive of a multiplicity of decomposition products.

(ii) (Z)-N-Phenyl-4-dicyanomethylene-4-hydroxy-2-butenamide (190) (0.1 g, 0.42 mmol) and acetic anhydride (10 cm³) were placed in a round-bottom flask. The mixture was heated under reflux for 30 minutes, allowed to cool, then poured into a separating funnel and the product extracted with diethyl ether (3x25 cm³). The extracts were combined, washed with water (3x30 cm³) and

10% sodium carbonate (3x30 cm³) and dried over anhydrous magnesium sulphate. The diethyl ether was removed by rotary evaporation to yield a white solid (0.05 g), m.p. 113-114 °C, IR ν_{\max} 3250, 3198, 2950, 1650 (s, C=O), 1600 (s), 1555 (s), 1500, 1495, 1451 (s), 1402, 1348, 1298, 768 and 700 cm⁻¹, ¹H-NMR δ 2.12 (3H, s, CH₃), 7.05 (1H, t, aromatic proton), 7.29 (2H, t, aromatic protons) and 7.45 [3H, d, aromatic and NH (exchanges with D₂O) protons], ¹³C-NMR δ 24.64 (CH₃), 119.92, 124.32, 128.98, 137.87 (aromatic carbons) and 168.49 (C=O) ppm. This product was assigned as acetanilide by comparing the melting point, IR and NMR spectral data with those of an authentic sample.

Synthesis of Ethyl (Z)-4-Dicyanomethylene-4-chloro-2-butenate (177)

Phosphorous pentachloride (21.6 g, 100 mmol), dissolved in anhydrous dichloromethane (400 cm³), was added dropwise with stirring to a solution of ethyl (Z)-4-dicyanomethylene-4-hydroxy-2-butenate (176) (10 g, 50 mmol) in anhydrous dichloromethane (50 cm³). The solution was heated under reflux for 4 hours and then allowed to cool. Phosphorous oxychloride and dichloromethane were removed completely by ambient pressure distillation to yield ethyl (Z)-4-dicyanomethylene-4-chloro-2-butenate (177) (7.5 g, 68%) as a dark brown oil. This was used in subsequent reactions without further purification. An analytically pure sample was obtained by chromatography using a 4 mm Chromatotron plate with dichloromethane/light petroleum (3:1) as eluent, followed by reduced pressure distillation of the yellow oil onto a cold finger (b.p. 85-87 °C, 1.5 mbar). Microanalysis Found C, 51.52, H, 3.36, N, 13.36, Cl, 16.61%. C₉H₇N₂O₂Cl requires C, 51.32, H, 3.35, N, 13.30, Cl, 16.83%, UV λ_{\max} 288 (ϵ 14,597) nm, IR (NaCl) ν_{\max} 3072, 2986 (aliphatic C-H), 2941, 2907, 2234 (s, CN), 1722 (s, C=O), 1541 (C=C), 1466, 1395, 1368, 1310, 1286, 1239, 1188, 1146, 1095, 1030, 981, 887, 665 and 625 cm⁻¹, ¹H-NMR δ 1.36 (3H, t, J 7.4, CH₃), 4.33 (2H, q, J 7.4, CH₂), 6.86 (1H, d, J 14.8, vinylic-H) and 7.78 (1H, d, J 14.8, vinylic-H) ppm, ¹³C-NMR δ 14.07 (CH₃), 62.26 (CH₂), 90.86 [C(CN)₂], 109.73, 110.44 (CN), 133.18, 136.04 (HC=CH), 160.69 and 163.47 [C=O and C=C(CN)₂] ppm.

Synthesis of Ethyl (Z)-4-Dicyanomethylene-4-dibutylamino-2-butenate (205)

N,N-Dibutylamine (0.47 cm³, 2.8 mmol) in diethyl ether (30 cm³) was added dropwise with stirring to a solution of ethyl (Z)-4-dicyanomethylene-4-chloro-2-butenate (177) (0.3 g, 1.4 mmol) in diethyl ether (30 cm³). Stirring was

continued at room temperature for 1 hour, after which the solution was placed in a separating funnel, washed with 1% v/v dilute hydrochloric acid (2x25 cm³) and water (2x25 cm³) and dried over anhydrous magnesium sulphate. Removal of diethyl ether by rotary evaporation yielded ethyl (Z)-4-dicyanomethylene-4-dibutylamino-2-butenolate (205) (0.3 g, 78%) as a brown oil. An analytically pure sample was obtained following column chromatography on silica gel using diethyl ether/light petroleum (3:1) as eluent. The yellow fraction was collected and removal of diethyl ether and light petroleum by rotary evaporation yielded a yellow oil which on standing solidified to give ethyl (Z)-4-dicyanomethylene-4-dibutylamino-2-butenolate (205). Recrystallisation from light petroleum gave yellow crystals, m.p. 64-65 °C. Microanalysis. Found: C, 67.42, H, 8.24, N, 13.97%. C₁₇H₂₅N₃O₂ requires: C, 67.29, H, 8.30, N, 13.85%. UV λ_{max} 278 (ε 11,320) nm, IR ν_{max} 2963, 2937, 2879 (aliphatic C-H), 2206, 2189 (s, CN), 1721 (s, C=O), 1660, 1567 (s, C=C), 1470 (s), 1436 (s), 1370, 1308 (s), 1266, 1182 (s), 1111, 1066, 1027, 980, 892 and 735 cm⁻¹, ¹H-NMR δ 0.96 (6H, t, J 7.9, CH₃CH₂CH₂CH₂), 1.36 (7H, m, CH₃CH₂, J 7.4, CH₃CH₂CH₂CH₂, J 7.9), 1.65 (4H, quintet, J 7.9, CH₃CH₂CH₂CH₂), 3.49 (4H, t, J 7.9, CH₃CH₂CH₂CH₂), 4.27 (2H, q, J 7.4, OCH₂), 6.44 (1H, d, J 16.2, vinylic-H) and 7.16 (1H, d, J 16.2, vinylic-H) ppm, ¹³C-NMR δ 13.47 (CH₃), 13.86 (CH₃), 19.22 (CH₂), 29.93 (CH₂), 50.92 [C(CN)₂], 52.66 (NCH₂), 61.50 (OCH₂), 115.85, 117.13 (CN), 131.81, 135.22 (HC=CH), 162.98 and 163.79 [C=O and C=C(CN)₂] ppm.

Table 6.1 Correlating peaks from C-H Correlation spectrum

¹ H NMR peaks (ppm)	¹³ C NMR peaks (ppm)
0.96	13.47
1.36	13.86, 19.22
1.65	29.93
3.49	52.66
4.27	61.50
6.44	131.81
7.16	135.22

Synthesis of Ethyl (Z)-4-Dicyanomethylene-4-*p*-anisidino-2-butenolate (206)

p-Anisidine (0.6 g, 4.8 mmol) in diethyl ether (30 cm³) was added dropwise with stirring to a solution of ethyl (Z)-4-dicyanomethylene-4-chloro-2-butenolate (177)

(0.5 g, 2.4 mmol) in diethyl ether (30 cm³) Stirring was continued at room temperature for 1 hour, after which the precipitated solid was filtered off, washed with diethyl ether (2x20 cm³) and dried to yield *p*-anisidine hydrochloride (0.103 g) The filtrate was placed in a separating funnel, washed with 1% v/v dilute hydrochloric acid (2x25 cm³) and water (2x25 cm³) and dried over anhydrous magnesium sulphate Removal of diethyl ether by rotary evaporation yielded ethyl (Z)-4-dicyanomethylene-4-*p*-anisidino-2-butenate (206) (0.6 g, 85%) as a brown oil An analytically pure sample was obtained following column chromatography on silica gel using diethyl ether/light petroleum (3:1) as eluent The yellow fraction was collected and removal of diethyl ether and light petroleum by rotary evaporation yielded a yellow oil which on standing solidified to give ethyl (Z)-4-dicyanomethylene-4-*p*-anisidino-2-butenate (206) Recrystallisation from light petroleum (60-80 °C) gave yellow crystals, m.p. 97-98 °C, Microanalysis Found C, 64.61, H, 5.10, N, 14.16% C₁₆H₁₅N₃O₃ requires C, 64.64, H, 5.08, N, 14.13%, UV λ_{max} 234 (ε 15,447), 286 (ε 7,055) and 364 (ε 5,874) nm, IR ν_{max} 3237, 2996, 2839 (aromatic and aliphatic C-H), 2219, 2200 (s, CN), 1732, 1724, 1708 (C=O), 1655, 1642 (C=C), 1616, 1596, 1577, 1561, 1514, 1452, 1362, 1319, 1279, 1263, 1247, 1199, 1173, 1029, 825, 754 and 738 cm⁻¹, ¹H-NMR δ 1.29 (3H, t, J 7.4, CH₃), 3.82 (3H, s, OCH₃), 4.22 (2H, q, J 7.4, CH₂), 6.74 (1H, d, J 16.2, vinylic-H), 6.90 (2H, m, aromatic protons), 7.00 [3H, m, vinylic-H (J 16.2) and aromatic protons] and 8.25 (1H, s, NH, exchanges with D₂O) ppm, ¹³C-NMR δ 13.98 (CH₃), 54.95 [C(CN)₂], 55.53 (OCH₃), 61.73 (CH₂), 114.29, 114.64 (CN), 114.94, 126.47, 128.61, 132.33, 132.40, 159.35 (vinylic and aromatic carbons), 163.14 and 164.08 [C=O and C=C(CN)₂] ppm

Synthesis of Ethyl (Z)-4-Dicyanomethylene-4-anilino-2-butenate (207)

Aniline (0.44 cm³, 4.8 mmol) in diethyl ether (30 cm³) was added dropwise with stirring to a solution of ethyl (Z)-4-dicyanomethylene-4-chloro-2-butenate (177) (0.5 g, 2.4 mmol) in diethyl ether (30 cm³) Stirring was continued at room temperature for 1 hour, after which the precipitated solid was filtered off, washed with diethyl ether (2x20 cm³) and dried to yield ethyl (Z)-4-dicyanomethylene-2,4-dianilinobutanoate (178) (0.45 g) Recrystallisation from ethanol gave white crystals, m.p. 161-162 °C, Microanalysis Found C, 70.13, H, 5.61, N, 15.49% C₂₁H₂₀N₄O₂ requires C, 70.17, H, 5.32, N, 15.49%, IR ν_{max} 3377 (s), 3290 (s, NH), 3064, 3000, 2927, 2214 (s), 2198 (s, CN), 1725 (s, C=O), 1605, 1570, 1519, 1494, 1474, 1452, 1421, 1370, 1343, 1326, 1308, 1276, 1257, 1226, 1185, 1226, 1185, 1151, 1143, 1019, 940, 898, 749 and

699 cm^{-1} , $^1\text{H-NMR}$ (DMSO-d_6) δ 1.20 (3H, t, J 7.4, CH_3), 3.07 (2H, d, J 8.37, CH_2), 4.14 (2H, m, J 7.4, 8.37, CH_2), 4.41 (1H, br s, NH, exchanges with D_2O), 6.15 (1H, d, J 8.37, CH), 6.60 (3H, m, J 7.4, aromatic protons), 7.09 (2H, t, J 7.4, 7.9, aromatic protons), 7.21 (2H, d, J 7.9, aromatic protons), 7.34 (1H, t, J 7.4, 6.9, aromatic proton), 7.43 (2H, t, J 7.9, 6.9, aromatic protons) and 10.64 (1H, s, NH, exchanges with D_2O) ppm, $^{13}\text{C-NMR}$ (DMSO-d_6) δ 14.09 (CH_3), 50.98 (CH), 52.11 (CH_2), 54.59 [$\text{C}(\text{CN})_2$], 61.16 (OCH_2), 112.74, 113.88, 117.19, 117.35, 126.10, 128.02, 129.06, 129.09, 136.70, 146.91 (CN and aromatic carbons), 166.68 and 171.56 [$\text{C}=\text{O}$ and $\text{C}=\text{C}(\text{CN})_2$] ppm, DEPT-135 (DMSO-d_6) δ 14.09 (positive), 50.98 (positive), 52.11 (negative), 61.16 (negative), 117.19, 117.35, 126.10, 128.02, 129.06 and 129.09 (all positive) ppm

Table 6.2 Correlating peaks from C-H Correlation spectrum

^1H NMR peaks (ppm)	^{13}C NMR peaks (ppm)
1.20	14.09
3.07	52.11
4.14	61.16
6.15	50.98
6.60	117.19
7.09	117.35
7.21	129.06
7.34	126.10
7.43	128.02, 129.09

The filtrate was placed in a separating funnel, washed with 1% v/v dilute hydrochloric acid ($2 \times 25 \text{ cm}^3$) and water ($2 \times 25 \text{ cm}^3$) and dried over anhydrous magnesium sulphate. Removal of diethyl ether by rotary evaporation yielded ethyl (Z)-4-dicyanomethylene-4-anilino-2-butenate (207) (0.6 g, 85%) as a brown oil. An analytically pure sample was obtained following column chromatography on silica gel using diethyl ether/light petroleum (3:1) as eluent. The yellow fraction was collected and removal of diethyl ether and light petroleum by rotary evaporation yielded a yellow oil which on standing solidified to give ethyl (Z)-4-dicyanomethylene-4-anilino-2-butenate (207) (0.07 g, 11%). Recrystallisation from cyclohexane gave yellow crystals, m.p. 130–131 $^\circ\text{C}$. Microanalysis: Found C, 67.37, H, 4.83, N, 15.61%. $\text{C}_{15}\text{H}_{13}\text{N}_3\text{O}_2$ requires C,

67 40, H, 4 90, N, 15 72%, UV λ_{\max} 248 (ϵ 20,842), 276sh (ϵ 15,342) and 354 (ϵ 9,747) nm, IR ν_{\max} 3215, 3104, 2973 (aromatic and aliphatic C-H), 2224, 2200 (s, CN), 1712 (s, C=O), 1655, 1595, 1577 (s, C=C), 1561 (s), 1509, 1368, 1319 (s), 1273 (s), 1198 (s), 1035, 979, 763 and 692 (aromatic-H) cm^{-1} , $^1\text{H-NMR}$ δ 1 29 (3H, t, J 7 4, CH_3), 4 23 (2H, q, J 7 4, CH_2), 6 76 (1H, d, J 16 2, vinylic-H), 7 06 [3H, m, vinylic-H (J 16 2) and aromatic protons], 7 33 (1H, m, aromatic proton), 7 41 (2H, m, aromatic protons) and 8 21 (1H, s, NH, exchanges with D_2O) ppm, $^{13}\text{C-NMR}$ δ 14 00 (CH_3), 56 47 [$\text{C}(\text{CN})_2$], 61 79 (CH_2), 114 02, 114 30 (CN), 124 59, 128 12, 129 85, 132 24, 132 73, 136 01 (vinylic and aromatic carbons), 162 82 and 163 99 [$\text{C}=\text{O}$ and $\text{C}=\text{C}(\text{CN})_2$] ppm

Addition of Malononitrile to 7-Oxabicyclo[2 2 1]hept-5-ene-2,3-dicarboxylic anhydride (211)

Sodium hydride (0 5 g, 20 mmol) and anhydrous tetrahydrofuran (20 cm^3) were placed in a round-bottom flask fitted with a magnetic stirrer and a dropping funnel. Malononitrile (3 0 g, 45 mmol) in anhydrous tetrahydrofuran (20 cm^3) was added dropwise with stirring at room temperature. The sodiomalononitrile solution was added to a stirred mixture of 7-oxabicyclo[2 2 1]hept-5-ene-2,3-dicarboxylic anhydride (211)¹⁶⁶ (3 4 g, 20 mmol) in anhydrous tetrahydrofuran (30 cm^3) at room temperature. The mixture was heated with stirring under reflux for 1 hour during which time a yellow solid precipitated. The reaction mixture was allowed to cool and the solid was filtered off, washed with tetrahydrofuran (2x20 cm^3) and dried under vacuum to yield sodium (Z)-4-dicyanomethylene-4-hydroxy-2-butenolate (173a) (1 6 g, 46%), m p 90 °C (decomp), IR ν_{\max} 3460 (broad OH), 2216, 2191 (s, CN), 1550 (s, C=O), 1500, 1440, 1386, 1314, 1210, 970 and 805 cm^{-1} , $^1\text{H-NMR}$ (DMSO-d_6) δ 6 11 (1H, d, J 12 8, vinylic-H), 6 74 (1H, d, J 12 8, vinylic-H) and 17 46 (1H, br s, OH, exchanges with D_2O) ppm, $^{13}\text{C-NMR}$ (DMSO-d_6) δ 57 47 [$\text{C}(\text{CN})_2$], 116 97, 117 81 (CN), 133 02, 133 59 ($\text{HC}=\text{CH}$), 165 54 and 182 30 [$\text{C}=\text{O}$ and $\text{C}=\text{C}(\text{CN})_2$] ppm. The melting point, IR and NMR spectral data were identical with an authentic sample of (173a).

Attempted Cyclisation of Ethyl (Z)-4-Dicyanomethylene-4-*p*-anisidino-2-butenolate (206) and Ethyl (Z)-4-Dicyanomethylene-2,4-dianilinobutanoate (178)

(i) Ethyl (Z)-4-dicyanomethylene-4-*p*-anisidino-2-butenolate (206) (0 05 g, 0 17 mmol) was placed in a boiling tube connected to a nitrogen supply and a bubbler. A continuous stream of nitrogen gas was passed through the apparatus for 10 minutes after which the nitrogen supply was turned off. The

yellow solid was heated at 160 °C for 30 minutes using an oil bath, then allowed to cool and the resulting black solid was collected (0.03 g). ¹H NMR and IR analysis of the crude product gave complex spectra suggestive of a complex mixture of products. Similarly, pyrolysis of ethyl (Z)-4-dicyanomethylene-2,4-dianilinobutanoate (178) under the same reaction conditions gave complex decomposition products.

(ii) Ethyl (Z)-4-dicyanomethylene-4-*p*-anisidino-2-butenolate (206) (0.05 g, 0.17 mmol) and *N,N*-dimethylformamide (15 cm³) were placed in a round-bottom flask. The solution was heated under reflux for 2 hours, allowed to cool, then poured into a separating funnel and the product extracted with dichloromethane (3x25 cm³). The extracts were combined, washed with water (3x30 cm³) and dried over anhydrous magnesium sulphate. The dichloromethane was removed by rotary evaporation to yield a brown solid. ¹H NMR and IR gave complex spectra suggestive of a complex mixture of products.

Synthesis of 5,6-Diphenyl-2,3-dicyanopyrazine (235)¹⁷²

Benzil (38.8 g, 185 mmol), diaminomaleonitrile (20.0 g, 185 mmol) and acetic acid (300 cm³) were placed in a round-bottom flask fitted with a reflux condenser. The reaction mixture was stirred under reflux for 1 hour. On cooling, 5,6-diphenyl-2,3-dicyanopyrazine (235) deposited as a yellow crystalline solid. The crystals were filtered off and washed with ethyl acetate (3x25 cm³) to yield 5,6-diphenyl-2,3-dicyanopyrazine (235) (49.7 g, 95%). Recrystallisation from ethyl acetate gave yellow crystals, m.p. 248-250 °C, (lit.¹⁷² 245 °C), IR ν_{max} 3067 (m, aromatic C-H), 2225 (m, CN), 1513 (s), 1447 (s), 1377 (s), 1231 (s), 1225, 1090, 1012, 875, 771 (s), 701 (s) and 689 (s, aromatic-H) cm⁻¹, ¹H-NMR δ 7.37 (4H, m, aromatic protons), 7.47 (2H, m, aromatic protons) and 7.53 (4H, m, aromatic protons) ppm, ¹³C-NMR δ 113.14 (CN), 128.83, 129.78, 129.80, 131.15, 135.17 and 155.35 (aromatic carbons) ppm.

Synthesis of 2,3-Diphenyl-5,7-dimino-6*H*-5,7-dihydropyrrolo[3,4-*b*]-pyrazine (234)

5,6-Diphenyl-2,3-dicyanopyrazine (235) (20.0 g, 71 mmol), preformed sodium methoxide (0.8 g, 15 mmol) and methanol (250 cm³) were stirred together under reflux with the continuous passage of ammonia for 3 hours. The dark solution was filtered hot to remove an insoluble black solid. Removal of methanol from the filtrate by rotary evaporation yielded a dark tacky solid.

Addition of light petroleum to a solution of this solid in tetrahydrofuran (75 cm³) precipitated 2,3-diphenyl-5,7-diimino-6*H*-5,7-dihydropyrrolo[3,4-*b*]pyrazine (234) (19.3 g, 91%) as a very sparingly soluble grey solid (19.3 g, 91%), m.p. >350 °C, IR ν_{\max} 3416, 3259 (NH), 3068 (aromatic C-H), 1680, 1644 (C=N), 1452, 1410, 1388, 1360 (s), 1225, 1161, 1139, 1075, 933, 890, 776 and 698 (aromatic-H) cm⁻¹, ¹H-NMR (Acetone-d₆) δ 3.07 (3H, br s, NH) and 7.32 (10H, m, aromatic protons) ppm, ¹³C-NMR (Acetone-d₆) δ 125.63, 128.51, 128.55, 129.26, 129.32, 130.43 (aromatic carbons) and 139.04 (C=N) ppm

Synthesis of 2,3-Diphenyl-5-imino-7-phenylimino-6*H*-5,7-dihydropyrrolo[3,4-*b*]pyrazine (236)

Aniline (0.3 cm³, 3.34 mmol) was added to a solution of 2,3-diphenyl-5,7-diimino-6*H*-5,7-dihydropyrrolo[3,4-*b*]pyrazine (234) (1.0 g, 3.34 mmol) in ethanol (20 cm³). The solution was heated under reflux for 2 hours. When cooled, the dark solid was filtered off, washed with ethanol (2x10 cm³) and dried to yield 2,3-diphenyl-5-imino-7-phenylimino-6*H*-5,7-dihydropyrrolo[3,4-*b*]pyrazine (236) (0.8 g, 64%). Recrystallisation from ethyl acetate gave yellow crystals, m.p. 232-234 °C (darkens 230 °C), Microanalysis Found C, 76.39, H, 4.64, N, 18.57% C₂₄H₁₇N₅ requires C, 76.78, H, 4.56, N, 18.65%, UV λ_{\max} 224sh (ϵ 30,729), 236sh (ϵ 28,174), 302 (ϵ 23,041) and 400 (ϵ 6,922) nm, IR ν_{\max} 3434 (NH), 3050, 2924 (aromatic C-H), 1689, 1640 (C=N), 1536, 1354, 1177, 1157, 772 and 699 (aromatic-H) cm⁻¹, ¹H-NMR (DMSO-d₆) δ 7.09 (1H, m, aromatic proton), 7.36 (10H, m, aromatic protons), 7.45 (4H, m, aromatic protons), 8.81 (1H, br s, NH, exchanges with D₂O) and 8.99 (1H, br s, NH, exchanges with D₂O) ppm, ¹³C-NMR (DMSO-d₆) δ 123.90, 124.05, 128.11, 128.13, 128.20, 128.23, 128.86, 128.89, 129.89, 138.29, 138.51, 146.63, 149.39, 151.01, 152.52, 153.67 (aromatic carbons), 160.46 and 168.05 (C=N) ppm

Synthesis of the Ammonium salt of 2,3-Diphenyl-5,7-bis(dicyanomethylene)-6*H*-5,7-dihydropyrrolo[3,4-*b*]pyrazine (238)

Malononitrile (13.2 g, 200 mmol) in tetrahydrofuran (100 cm³) was added dropwise with stirring to a solution of 2,3-diphenyl-5,7-diimino-6*H*-5,7-dihydropyrrolo[3,4-*b*]pyrazine (234) (30.0 g, 100 mmol) in tetrahydrofuran (200 cm³). The reaction mixture was stirred at room temperature for 1 hour, after which the tetrahydrofuran was removed by rotary evaporation to yield a dark orange oil. Addition of light petroleum to a solution of this oil in tetrahydrofuran (75 cm³) precipitated the ammonium salt (238) (41.3 g, 99%) as a red solid, m.p. 200 °C

(decomp), UV λ_{\max} 220sh (ϵ 25,750), 330 (ϵ 20,100), 481 (ϵ 23,000) and 511 (ϵ 22,650) nm, IR ν_{\max} 3174, 2214 (s, CN), 1509 (s), 1409, 1345, 1267, 1217, 1153, 1025, 976, 776 and 719 (aromatic-H) cm^{-1} , $^1\text{H-NMR}$ (Acetone- d_6) δ 7.35 (6H, m, aromatic protons) and 7.60 (4H, m, aromatic protons) ppm, $^{13}\text{C-NMR}$ (Acetone- d_6) δ 55.86 [$\text{C}(\text{CN})_2$], 114.35, 115.34 (CN), 127.56, 128.55, 129.58, 137.81, 141.81, 152.03 and 166.91 [aromatic and $\text{C}=\text{C}(\text{CN})_2$ carbons] ppm

Synthesis of 2,3-Diphenyl-5,7-bis(dicyanomethylene)-6H-5,7-dihydropyrrolo[3,4-b]pyrazine (237)

p-Toluenesulphonic acid (2.3 g, 12 mmol) in tetrahydrofuran (50 cm^3) was added dropwise with stirring to the ammonium salt (238) (5.0 g, 12 mmol). The solution was stirred at room temperature for 1 hour after which the white solid that precipitated [ammonium *p*-toluenesulphonate as verified by IR and ^1H and ^{13}C NMR (1.14 g)] was filtered off, washed with tetrahydrofuran (2x30 cm^3) and dried. Removal of tetrahydrofuran from the filtrate by rotary evaporation yielded 2,3-diphenyl-5,7-bis(dicyanomethylene)-6H-5,7-dihydropyrrolo[3,4-b]pyrazine (237) (4.2 g, 89%). Recrystallisation from acetonitrile gave yellow crystals, m.p. 336-338 $^\circ\text{C}$ (darkens 264 $^\circ\text{C}$), Microanalysis Found C, 72.44, H, 2.70, N, 24.59%. $\text{C}_{24}\text{H}_{11}\text{N}_7$ requires C, 72.53, H, 2.79, N, 24.67%, UV λ_{\max} 223 (ϵ 32,250), 327 (ϵ 21,200), 387 (ϵ 34,500), 410 (ϵ 32,000), 481 (ϵ 6,650) and 511 (ϵ 6,660) nm, IR ν_{\max} 3141, 3018, 2825 (aromatic and aliphatic C-H), 2240, 2224, 2214 (s, CN), 1634 (s), 1598, 1547, 1535, 1491, 1458, 1421, 1345, 1220, 1194, 1155, 1024, 770, 730, 700 and 692 (aromatic-H) cm^{-1} , $^1\text{H-NMR}$ (Acetone- d_6) δ 3.53 (1H, br s, NH, exchanges with D_2O), 7.40 (4H, m, aromatic protons), 7.48 (2H, m, aromatic protons) and 7.66 (4H, m, aromatic protons) ppm, $^{13}\text{C-NMR}$ (Acetone- d_6) δ 63.03 [$\text{C}(\text{CN})_2$], 111.54, 112.08 (CN), 128.88, 130.56, 130.74, 137.70, 143.22, 155.43 and 157.22 [aromatic and $\text{C}=\text{C}(\text{CN})_2$ carbons] ppm

Synthesis of Tetraalkylammonium salts of 2,3-Diphenyl-5,7-bis(dicyanomethylene)-6H-5,7-dihydropyrrolo[3,4-b]pyrazine (242)

General procedure

The desired tetraalkylammonium halide in methanol was added dropwise to a solution of the ammonium salt of 2,3-diphenyl-5,7-bis(dicyanomethylene)-6H-5,7-dihydropyrrolo[3,4-b]pyrazine (238) (1 equivalent) in methanol. On addition an orange solid precipitated. Stirring was continued at room temperature for 1 hour. The solid was filtered off, washed with methanol and dried to yield the tetraalkylammonium salt as an orange solid.

Synthesis of the Tetramethylammonium salt of 2,3-Diphenyl-5,7-bis(dicyanomethylene)-6H-5,7-dihydropyrrolo[3,4-b]pyrazine (242a)

Tetramethylammonium chloride (2.12 g, 19.2 mmol) in methanol (30 cm³) and the ammonium salt (238) (8.0 g, 19.2 mmol) in methanol (60 cm³) gave the tetramethylammonium salt (242a) (4.0 g, 44%), isolated as the monohydrate. It was assumed that the water came from the methanol used in the reaction. Recrystallisation from methanol gave red crystals, m.p. 308-310 °C, Microanalysis Found C, 68.62, H, 4.83, N, 22.81% C₂₈H₂₂N₈·H₂O requires C, 68.83, H, 4.95, N, 22.93%, UV λ_{max} 221 (ε 22,674), 270 (ε 17,914), 318 (ε 17,540), 331 (ε 18,396), 370sh (ε 12,834), 481 (ε 21,765) and 511 (ε 21,551) nm, IR ν_{max} 3427 (OH), 2209 (s, CN), 1510 (s), 1485, 1451, 1416 (s), 1355 (s), 1279, 1223, 1155, 1075, 1027, 950, 813, 776, 738 and 701 cm⁻¹, ¹H-NMR (DMSO-d₆) δ 3.07 (12H, s, CH₃), 7.36 (6H, m, aromatic protons) and 7.48 (4H, m, aromatic protons) ppm, ¹³C-NMR (DMSO-d₆) δ 54.38 (1 t, J 4.06, CH₃), 55.65 [C(CN)₂], 115.28, 116.00 (CN), 128.27, 129.21, 129.88, 138.08, 148.34, 152.13 and 167.71 [aromatic and C=C(CN)₂ carbons] ppm

Synthesis of the Tetraethylammonium salt of 2,3-Diphenyl-5,7-bis(dicyanomethylene)-6H-5,7-dihydropyrrolo[3,4-b]pyrazine (242b)

Tetraethylammonium bromide (15.2 g, 72.4 mmol) in methanol (100 cm³) and the ammonium salt (238) (30.0 g, 72.4 mmol) in methanol (300 cm³) gave the tetraethylammonium salt (242b) (18.2 g, 48%). Recrystallisation from ethanol gave red crystals, m.p. 301-302 °C (decomp 298 °C), Microanalysis Found C, 73.22, H, 5.75, N, 21.31% C₃₂H₃₀N₈ requires C, 72.98, H, 5.74, N, 21.27%, UV λ_{max} 222 (ε 29,500), 271 (ε 16,100), 318 (ε 23,100), 332 (ε 24,050), 374sh (ε 18,100), 482 (ε 28,000) and 512 (ε 27,500) nm, IR ν_{max} 3447, 2205 (s, CN), 1714, 1508 (s), 1451, 1410, 1353, 1278, 1228, 1173, 1145, 998, 773 and 704 cm⁻¹, ¹H-NMR (DMSO-d₆) δ 1.14 (12H, t of t, J 2.0, 7.4, CH₃), 3.18 (8H, q, J 7.4, CH₂), 7.36 (6H, m, aromatic protons) and 7.47 (4H, m, aromatic protons) ppm, ¹³C-NMR (DMSO-d₆) δ 7.06 (CH₃), 51.34 (1 t, J 3.05, CH₂), 55.62 [C(CN)₂], 115.26, 115.97 (CN), 128.25, 129.20, 129.87, 138.07, 148.32, 152.12 and 167.69 [aromatic and C=C(CN)₂ carbons] ppm

Synthesis of the *N*-Benzylpyridinium salt of 2,3-Diphenyl-5,7-bis(dicyanomethylene)-6*H*-5,7-dihydropyrrolo[3,4-*b*]pyrazine (242c)

Benzylpyridinium chloride was prepared¹⁸⁰ by heating pyridine (0.78 cm³, 9.6 mmol) with benzylchloride (1.12 cm³, 9.6 mmol) for 30 minutes. The resulting pink solution which solidified on cooling, was dissolved in methanol (30 cm³) and added to the ammonium salt (238) (4.0 g, 9.6 mmol) in methanol (80 cm³) to give the *N*-benzylpyridinium salt (242c) (2.7 g, 49%). Recrystallisation from methanol gave red crystals, m.p. 258-259 °C, Microanalysis Found C, 76.02, H, 3.94, N, 19.96% C₃₆H₂₂N₈ requires C, 76.31, H, 3.91, N, 19.77%, UV λ_{max} 222sh (ε 31,466) 262 (ε 23,314), 318 (ε 21,956), 330 (ε 22,429), 372sh (ε 15,121), 482 (ε 26,054) and 510 (ε 25,655) nm, IR ν_{max} 3139, 3061 (aromatic C-H), 2209 (s, CN), 1515 (s), 1448, 1412, 1355 (s), 1285, 1221, 1156, 1025, 743, 700 and 684 cm⁻¹, ¹H-NMR (DMSO-*d*₆) δ 5.83 (2H, s, CH₂), 7.42 (15H, m, phenyl protons), 8.16 (2H, t, J 7.4, pyridyl protons), 8.60 (1H, t, J 7.4, pyridyl proton) and 9.17 (2H, d, J 5.9, pyridyl protons) ppm, ¹³C-NMR (DMSO-*d*₆) δ 55.66 [C(CN)₂], 63.32 (CH₂), 115.26, 115.97 (CN), 128.22, 128.47, 128.74, 129.17, 129.22, 129.36, 129.85, 134.20, 138.04, 144.78, 145.95, 148.32, 152.09 and 167.67 [phenyl, pyridyl and C=C(CN)₂ carbons] ppm

Attempted Synthesis of 2,3-Diphenyl-5,7-bis(dicyanomethylene)-6-ethyl-5,7-dihydropyrrolo[3,4-*b*]pyrazine (243b)

(i) Tetraethylammonium salt of 2,3-diphenyl-5,7-bis(dicyanomethylene)-6*H*-5,7-dihydropyrrolo[3,4-*b*]pyrazine (242b) (1.0 g, 1.9 mmol) was placed in a boiling tube connected to a nitrogen supply and a bubbler. A continuous stream of nitrogen gas was passed through the apparatus for 10 minutes after which the nitrogen supply was turned off. The red solid was heated at 300 °C for 30 minutes, then allowed to cool and the resulting black solid was collected (0.95 g). IR and NMR spectral data of the crude product were identical to those reported for an authentic sample of (242b).

(ii) Tetraethylammonium salt of 2,3-diphenyl-5,7-bis(dicyanomethylene)-6*H*-5,7-dihydropyrrolo[3,4-*b*]pyrazine (242b) (0.5 g, 0.95 mmol) was added to 1,2-dichlorobenzene (25 cm³) in a 50 cm³ round-bottom flask. The reaction mixture was heated under reflux (177-181 °C) for 30 hours and allowed to cool. The orange crystals which deposited were filtered off, washed with diethyl ether (2x30 cm³), dried and weighed (0.45 g). IR and NMR spectral data of the product were identical to those reported for an authentic sample of (242b).

Synthesis of 2,3-Diphenyl-5,7-bis(dicyanomethylene)-6-alkyl-5,7-dihydropyrrolo[3,4-b]pyrazine derivatives (243)

General Procedure

The desired quaternary ammonium salt of 2,3-diphenyl-5,7-bis(dicyanomethylene)-6*H*-5,7-dihydropyrrolo[3,4-b]pyrazine (~10 g) was added to 1,2,4-trichlorobenzene (25 cm³) in a 50 cm³ round-bottom flask. The reaction mixture was heated under reflux (213-214 °C) for 20 hours and allowed to cool. The dark solid which deposited was filtered off, washed with diethyl ether (2x30 cm³) and dried. For the tetraethyl- and tetramethyl-ammonium salts, melting point, IR and NMR spectra showed this to be unreacted quaternary ammonium salt. In the case of the *N*-benzylpyridinium salt, no precipitate deposited. Removal of diethyl ether and 1,2,4-trichlorobenzene by reduced pressure distillation gave the crude product as a dark brown solid which was purified by column chromatography on silica gel using dichloromethane as eluent. Removal of dichloromethane by rotary evaporation yielded the 2,3-diphenyl-5,7-bis(dicyanomethylene)-6-alkyl-5,7-dihydropyrrolo[3,4-b]pyrazine derivative which was further purified by recrystallisation.

Synthesis of 2,3-Diphenyl-5,7-bis(dicyanomethylene)-6-methyl-5,7-dihydropyrrolo[3,4-b]pyrazine (243a)

Tetramethylammonium salt of 2,3-diphenyl-5,7-bis(dicyanomethylene)-6*H*-5,7-dihydropyrrolo[3,4-b]pyrazine (242a) (0.8 g, 1.67 mmol) in 1,2,4-trichlorobenzene (20 cm³) gave unreacted tetramethylammonium salt (242a) (0.27 g) and 2,3-diphenyl-5,7-bis(dicyanomethylene)-6-methyl-5,7-dihydropyrrolo[3,4-b]pyrazine (243a) (0.33 g, 48%). Recrystallisation of (243a) from methanol gave yellow crystals, m.p. 330-332 °C (darkens 310 °C), Microanalysis Found C, 72.74, H, 3.17, N, 23.83%. C₂₅H₁₃N₇ requires C, 72.98, H, 3.18, N, 23.83%, UV λ_{max} 218sh (ε 26,492), 248sh (ε 10,801), 330 (ε 16,480), 394 (ε 29,183) and 414 (ε 28,365) nm, IR ν_{max} 3103, 3061 (aromatic C-H), 2222 (s, CN), 1580 (s), 1561, 1545, 1426, 1355 (s), 1282, 1212, 1169, 1073, 774, 707 and 691 (aromatic-H) cm⁻¹, ¹H-NMR δ 4.29 (3H, s, CH₃), 7.37 (4H, m, aromatic protons), 7.46 (2H, m, aromatic protons) and 7.68 (4H, m, aromatic protons) ppm, ¹³C-NMR δ 35.56 (CH₃), 64.18 [C(CN)₂], 110.60, 112.01 (CN), 128.86, 130.22, 132.16, 136.25, 140.67, 154.01 and 157.50 [aromatic and C=C(CN)₂ carbons] ppm.

Synthesis of 2,3-Diphenyl-5,7-bis(dicyanomethylene)-6-ethyl-5,7-dihydropyrrolo[3,4-b]pyrazine (243b)

Tetraethylammonium salt of 2,3-diphenyl-5,7-bis(dicyanomethylene)-5,7-dihydropyrrolo[3,4-b]pyrazine (242b) (1.0 g, 1.9 mmol) in 1,2,4-trichlorobenzene (25 cm³) gave tetraethylammonium salt (242b) (0.63 g) and 2,3-diphenyl-5,7-bis(dicyanomethylene)-6-ethyl-5,7-dihydropyrrolo[3,4-b]pyrazine (243b) (0.3 g, 37%). Recrystallisation of (243b) from chloroform/light petroleum (60-80 °C) gave yellow crystals, m.p. 325-326 °C (darkens 318 °C), Microanalysis Found C, 73.03, H, 3.70, N, 22.48% C₂₆H₁₅N₇ requires C, 73.40, H, 3.55, N, 23.04%, UV λ_{max} 222 (ϵ 28,100), 250sh (ϵ 16,500), 332 (ϵ 19,100), 392 (ϵ 29,700) and 414 (ϵ 28,400) nm, IR ν_{max} 3070, 2934 (aromatic and aliphatic C-H), 2220 (s, CN), 1579 (s), 1541, 1423, 1346 (s), 1213, 1167, 1095, 778, 708 and 699 (aromatic-H) cm⁻¹, ¹H-NMR δ 1.69 (3H, t, J 7.4, CH₃), 4.79 (2H, q, J 7.4, CH₂), 7.37 (4H, m, aromatic protons), 7.45 (2H, m, aromatic protons) and 7.69 (4H, m, aromatic protons) ppm, ¹³C-NMR δ 16.11 (CH₃), 41.85 (CH₂), 63.51 [C(CN)₂], 110.80, 111.95 (CN), 128.84, 130.20, 131.11, 136.26, 140.74, 152.19 and 157.39 [aromatic and C=C(CN)₂ carbons] ppm, HRMS Found M⁺ 425.138 C₂₆H₁₅N₇ requires M, 425.138

Synthesis of 2,3-Diphenyl-5,7-bis(dicyanomethylene)-6-benzyl-5,7-dihydropyrrolo[3,4-b]pyrazine (243c)

N-Benzylpyridinium salt of 2,3-diphenyl-5,7-bis(dicyanomethylene)dihydropyrrolo[3,4-b]pyrazine (242c) (1.0 g, 1.76 mmol) in 1,2,4-trichlorobenzene (25 cm³) gave 2,3-diphenyl-5,7-bis(dicyanomethylene)-6-benzyl-5,7-dihydropyrrolo[3,4-b]pyrazine (243c) (0.49 g, 57%). Recrystallisation of (243c) from ethanol gave purple crystals, m.p. 259-260 °C (darkens 256 °C), Microanalysis Found C, 76.53, H, 3.58, N, 19.75% C₃₁H₁₇N₇ requires C, 76.37, H, 3.51, N, 20.11%, UV λ_{max} 224sh (ϵ 21,127), 250sh (ϵ 11,737), 331 (ϵ 13,146), 389 (ϵ 22,066) and 412 (ϵ 21,268) nm, IR ν_{max} 3075, 2933 (aromatic and aliphatic C-H), 2221 (s, CN), 1587, 1538, 1466, 1430, 1360, 1324, 1210, 1168, 1082, 783, 741 and 698 (aromatic-H) cm⁻¹, ¹H-NMR δ 6.05 (2H, s, CH₂), 7.15 (2H, m, aromatic protons), 7.42 (9H, m, aromatic protons) and 7.72 (4H, m, aromatic protons) ppm, ¹³C-NMR δ 49.19 (CH₂), 64.56 [C(CN)₂], 110.74, 111.66 (CN), 125.26, 128.88, 129.09, 129.71, 130.23, 131.23, 132.55, 136.24, 140.67, 152.88 and 157.61 [aromatic and C=C(CN)₂ carbons] ppm

Crystal Structure Determination

Structure Analysis and Refinement

All collections of crystallographic data were carried out at Trinity College Dublin. X-ray diffraction data were collected using Mo-K α radiation ($\lambda=0.71609$ Å) monochromatised with a graphite plate giving N independent reflections, N_0 of these being used in the structure analysis. The index range is given for each crystal. All structures were solved using Patterson heavy atom method with partial structure expansion to find all non-hydrogens using SHELXS-86¹⁸¹. The atomic co-ordinates were refined with full matrix least squares refinement using SHELXL-93¹⁸². Hydrogen atoms were located in their calculated positions and refined with respect to the carbon and nitrogen atoms to which they are attached.

Crystal Data for Ethyl (Z)-4-Dicyanomethylene-2,4-diaminobutanoate (178)

Crystallised from ethanol to give white cubic crystals. Crystal dimensions 0.6 x 0.5 x 0.2 mm. $M=360.41$, monoclinic, space group $P2_1/n$, $a=9.170(3)$, $b=14.012(2)$ and $c=14.928(4)$ Å, $V=1871.2(7)$ Å³, $Z=4$, $D_x=1.279$ g/cm³, $N=3398$, $N_0=3195$, index range = $0 \leq h \leq 10$, $0 \leq k \leq 15$, $-15 \leq l \leq 15$, $R=0.0867$, $wR=0.1276$.

Crystal Data for *N,N,N',N'*-Tetramethyl-*p*-phenylenediaminium salt of 2,3-Diphenyl-5,7-bis(dicyanomethylene)-6*H*-5,7-dihydropyrrolo[3,4-*b*]pyrazine (255)

Crystallised from acetonitrile to give red cubic crystals. Crystal dimensions 0.7 x 0.4 x 0.3 mm. $M=561.65$, triclinic, space group $P-1$ (No. 2), $a=9.9359(11)$, $b=10.2668(13)$ and $c=15.1862(13)$ Å, $V=1451.5(3)$ Å³, $Z=2$, $D_x=1.285$ g/cm³, $N=3821$, $N_0=3567$, index range $0 \leq h \leq 10$, $-10 \leq k \leq 10$, $-15 \leq l \leq 15$, $R=0.0539$, $wR=0.1092$.

Synthesis of Charge-Transfer Complexes

General procedure

The donor in acetonitrile was added to a boiling solution of the desired acceptor (1 equivalent) in acetonitrile. The solution was allowed to cool and the crystals that deposited were filtered off, washed with acetonitrile and dried.

Attempted C-T Complex formation between 2,3-Diphenyl-5,7-bis(dicyanomethylene)-6*H*-5,7-dihydropyrrolo[3,4-*b*]pyrazine (237) and TMPD

TMPD (0.04 g, 0.25 mmol) in acetonitrile (5 cm³) and 2,3-diphenyl-5,7-bis(dicyanomethylene)-6*H*-5,7-dihydropyrrolo[3,4-*b*]pyrazine (237) (0.1 g, 0.25 mmol) in acetonitrile (10 cm³) gave the *N,N,N',N'*-tetramethyl-*p*-phenylenediaminium salt of 2,3-diphenyl-5,7-bis(dicyanomethylene)-6*H*-5,7-dihydropyrrolo[3,4-*b*]pyrazine (255) (0.09 g, 64%). Recrystallisation from acetonitrile gave red crystals, m.p. 215-217 °C (darkens 213 °C), Microanalysis Found C, 72.63, H, 4.75, N, 22.26% C₃₄H₂₇N₉ requires C, 72.71, H, 4.84, N, 22.44%, UV λ_{max} 222sh (ϵ 47,904), 266 (ϵ 57,570), 318 (ϵ 38,796), 370sh (ϵ 25,484), 482 (ϵ 43,834) and 512 (ϵ 43,218) nm, IR ν_{max} 3117, 3061, 2219, 2204 (CN), 1611, 1504, 1452, 1412, 1354, 1279, 1268, 1220, 1178, 813, 779, 740, 717 and 703 cm⁻¹.

Synthesis of (237)-TTF C-T Complex

TTF (0.025 g, 0.12 mmol) in acetonitrile (5 cm³) and 2,3-diphenyl-5,7-bis(dicyanomethylene)-6*H*-5,7-dihydropyrrolo[3,4-*b*]pyrazine (237) (0.048 g, 0.12 mmol) in acetonitrile (10 cm³) gave yellow crystals of unreacted (237) (0.04 g) (melting point, IR, ¹H and ¹³C NMR spectra). Removal of acetonitrile by rotary evaporation and recrystallisation of the remaining yellow solid from acetonitrile gave dark purple crystals of the 2:1 (237):TTF C-T complex (0.07 g), m.p. 270 °C (decomp.), Microanalysis Found C, 64.77, H, 2.53, N, 19.46, S, 12.72% C₅₄H₂₆N₁₄S₄ requires C, 64.92, H, 2.62, N, 19.62, S, 12.82%, UV λ_{max} 222sh (ϵ 46,422), 268 (ϵ 22,157), 330 (ϵ 28,333), 386 (ϵ 32,010), 410 (ϵ 27,892), 481 (ϵ 19,265) and 511 (ϵ 18,529) nm, IR ν_{max} 3267, 3180, 3080, 3025, 2925, 2225 (CN), 1631, 1622, 1542, 1509, 1458, 1424, 1347, 1220, 1195, 797, 775, 703, 696 and 626 cm⁻¹.

Synthesis of 2,3-Diphenyl-5,7-bis(dicyanomethylene)-6-ethyl-5,7-dihydro-pyrrolo[3,4-b]pyrazine (243b)-TMPD C-T Complex

TMPD (0.013 g, 0.08 mmol) in acetonitrile (5 cm³) and 2,3-diphenyl-5,7-bis(dicyanomethylene)-6-ethyl-5,7-dihydro-pyrrolo[3,4-b]pyrazine (243b) (0.034 g, 0.08 mmol) in acetonitrile (10 cm³) gave dark purple crystals of the 2:1 (243b)-TMPD C-T complex (0.02 g, 43%), isolated as the monohydrate. It was assumed that the water came from the acetonitrile used in the reaction. Recrystallisation from acetonitrile gave dark purple crystals, m.p. 252-254 °C (darkens 238 °C), Microanalysis Found C, 71.80 (72.17), H, 4.68 (4.82), N, 21.66 (22.07)% C₆₂H₄₆N₁₆·H₂O requires C, 72.07, H, 4.68, N, 21.69, UV λ_{max} 223 (ϵ 34,475), 253 (ϵ 20,197), 330 (ϵ 23,361), 393 (ϵ 39,590) and 414 (ϵ 39,082) nm, IR ν_{max} 3069, 2933, 2219 (CN), 1579, 1541, 1424, 1348, 1213, 1168, 1095, 819, 776, 708 and 697 cm⁻¹.

Attempted C-T Complex formation between 2,3-Diphenyl-5,7-bis(dicyanomethylene)-6-ethyl-5,7-dihydro-pyrrolo[3,4-b]pyrazine (243b) and TTF

TTF (0.025 g, 0.12 mmol) in acetonitrile (5 cm³) and 2,3-diphenyl-5,7-bis(dicyanomethylene)-6-ethyl-5,7-dihydro-pyrrolo[3,4-b]pyrazine (243b) (0.048 g, 0.12 mmol) in acetonitrile (10 cm³) gave purple crystals of unreacted (243b) (0.01 g) (melting point, IR, ¹H and ¹³C NMR spectra). Removal of acetonitrile from the filtrate by rotary evaporation and recrystallisation of the remaining yellow solid from acetonitrile gave additional quantities of (243b).

Cyclic Voltammetry

HPLC grade acetonitrile was used in the electrochemical measurements. Lithium perchlorate was used as supporting electrolyte. Electrochemical cells were of conventional design and were thermostated within ± 0.2 °C using a Julabo F10-HC refrigerated circulating bath. All potentials were quoted with respect to a BAS Ag/AgCl gel-filled reference electrode, the potential of which was 35 mV more positive than that of the saturated calomel electrode (SCE). Cyclic voltammetry was performed using an EG&G model 273 mercury electrode as part of a conventional three electrode system. All solutions were degassed by bubbling under nitrogen and a blanket of nitrogen was maintained over the solution during the experiment.

Chapter 7

References

- 1 (a) H N McCoy and W C Moore, *J Am Chem Soc* , 1911, **33**, 273,
(b) H Kraus, *J Am Chem Soc* , 1913, **34**, 1732
- 2 J B Torrance, *Acc Chem Res* , 1979, **12**, 79
- 3 (a) P N Prasad and D J Williams, *Introduction to Nonlinear Optical Effects in Molecules and Polymers*, Wiley, New York, 1991, (b) R Dagani, *Chem Eng News*, 1996, **74** (10), 22
- 4 P M Chaikin and R L Greene, *Physics Today*, 1986, 24
- 5 W A Little, *Sci Am* , 1965, **212**, 21
- 6 H Akamatu, H Inokuchi and Y Matsunaga, *Nature (London)*, 1954, **173**, 168
- 7 (a) D S Acker, R J Harder, W R Hertler, W Mahler, L R Melby, R E Benson and W E Mochel, *J Am Chem Soc* , 1960, **82**, 6408, (b) D S Acker and W R Hertler, *J Am Chem Soc* , 1962, **84**, 3370
- 8 F Wudl, G M Smith and E J Hufnagel, *J Chem Soc , Chem Commun* , 1970, 1453
- 9 (a) J Ferraris, D O Cowan, V V Walatka, Jr and J H Perlstein, *J Am Chem Soc* , 1973, **95**, 948, (b) L B Coleman, M J Cohen, D J Sandman, F G Yamagishi, A F Garito and A J Heeger, *Solid State Commun* , 1973, **12**, 1125
- 10 K Bechgaard, C S Jacobsen, K Mortensen, H J Pedersen and N Thorup, *Solid State Commun* , 1980, **33**, 1119
- 11 S S P Parkin, E M Engler, R R Schumaker, R Lagier, V Y Lee, J C Scott and R L Greene, *Phys Rev Lett* , 1983, **50**, 270
- 12 J M Williams, A M Kini, H H Wang, K D Carlson, U Geiser, L K Montgomery, G J Pyrka, D M Watkins, J M Kommers, S J Boryschuk, A V S Crouch, W K Kwok, J E Schirber, D L Overmyer, D Jung and M H Whangbo, *Inorg Chem* , 1990, **29**, 3272
- 13 T T M Palstra, O Zhou, Y Iwasa, P E Sulewski, R M Fleming and B R Zegarski, *Solid State Commun* , 1995, **93**, 327
- 14 R S Mulliken, *J Am Chem Soc* , 1952, **74**, 811
- 15 M R Bryce and L C Murphy, *Nature (London)*, 1984, **309**, 119 and references therein
- 16 J S Chappell, A N Bloch, W A Bryden, M Maxfield, T O Poehler and D O Cowan, *J Am Chem Soc* , 1981, **103**, 2442
- 17 T E Phillips, T J Kistenmacher, J P Ferraris and D O Cowan, *J Chem Soc , Chem Commun* , 1973, 471
- 18 R C Wheland and J L Gillson, *J Am Chem Soc* , 1976, **98**, 3916
- 19 A W Hanson, *Acta Crystallogr* , 1965, **19**, 610

- 20 L R Melby, R J Harder, W R Hertler, W Mahler, R E Benson and W E Mochel, *J Am Chem Soc* , 1962, **84**, 3374
- 21 M R Bryce, A J Moore, M Hasan, G J Ashwell, A T Frazer, W Clegg, M B Hursthouse and A I Karaulov, *Angew Chem , Int Ed Engl* , 1990, **29**, 1450
- 22 J K Burdett, *Chem Soc Rev* , 1994, 299
- 23 K Bechgaard, K Carneiro, F B Rasmussen, M Olsen, G Rindolf, C S Jacobsen, H J Pedersen and J C Scott, *J Am Chem Soc* , 1981, **103**, 2440
- 24 J Bardeen, L N Cooper and J R Schrieffer, *Phys Rev* , 1957, **108**, 1175
- 25 J P Ferraris, T O Poehler, A N Bloch and D O Cowan, *Tetrahedron Lett* , 1973, **27**, 2553
- 26 H K Spencer, M P Cava, F G Yamagishi and A F Garito, *J Org Chem* , 1976, **41**, 730
- 27 (a) M G Miles, J D Wilson, D J Dahm, and J H Wagenknecht, *J Chem Soc , Chem Commun* , 1974, 751, (b) G le Coustumer and Y Mollier, *J Chem Soc , Chem Commun* , 1980, 38
- 28 C U Pittman, Jr , M Narita and Y F Liang, *J Org Chem* , 1976, **41**, 2855
- 29 D C Green, *J Chem Soc , Chem Commun* , 1977, 161
- 30 D C Green, *J Org Chem* , 1979, **44**, 1476
- 31 (a) A J Moore and M R Bryce, *J Chem Soc , Chem Commun* , 1991, 1638, (b) A J Moore, M R Bryce, G Cooke, G J Marshallsay, P J Skabara, A S Batsanov, J A K Howard and S T A K Daley, *J Chem Soc , Perkin Trans 1*, 1993, 1403
- 32 M R Bryce, G J Marshallsay and A J Moore, *J Org Chem* , 1992, **57**, 4859
- 33 M Mizuno, A F Garito and M P Cava, *J Chem Soc , Chem Commun* , 1978, 18
- 34 (a) E Aharon-Shalom, J Y Becker, J Bernstein, S Bittner and S Shaik, *Tetrahedron Lett* , 1985, **26**, 2783, (b) S Y Hsu and L Y Chiang, *J Org Chem* , 1987, **52**, 3444, (c) A M Kini, B D Gates, M A Beno and J M Williams, *J Chem Soc , Chem Commun* , 1989, 169
- 35 R R Schumaker and E M Engler, *J Am Chem Soc* , 1977, **99**, 5521
- 36 T K Hansen, I Hawkins, K S Varma, S Edge, S Larsen, J Becher and A E Underhill, *J Chem Soc , Perkin Trans 2*, 1991, 1963

- 37 R D McCullough, J A Belot, A L Reingold and G P A Yap, *J Am Chem Soc* , 1995, **117**, 9913
- 38 (a) K S Varma, A Bury, N J Harris and A E Underhill, *Synthesis*, 1987, 837, (b) J Larsen and C Lenoir, *Synthesis*, 1989, 134
- 39 (a) G Saito, T Enoki, K Toriumi and H Inokuchi, *Solid State Commun* , 1982, **42**, 557, (b) J M Williams, M A Beno, H H Wang, P E Reed, L J Azevedo and J E Schirber, *Inorg Chem* , 1984, **23**, 1790
- 40 H Kobayashi, A Kobayashi, Y Sasaki, G Saito, T Enoki and H Inokuchi, *J Am Chem Soc* , 1983, **105**, 297
- 41 E Amberger, H Fuchs and K Polborn, *Angew Chem , Int Ed Engl* , 1985, **24**, 968
- 42 H H Wang, M A Beno, U Geiser, M A Firestone, K S Webb, L Nuñez, G W Crabtree, K D Carlson, J M Williams, L J Azevedo, J F Kwak and J E Schirber, *Inorg Chem* , 1985, **24**, 2465
- 43 E B Yagubskii, I F Shchegolev, V N Laukhin, P A Kononovich, M W Karatsovnik, A V Zvarykina and L I Buravov, *Pis'ma Zh Eksp Fiz* , 1984, **39**, 12, *JEPT Lett (Engl Trans)* , 1984, **39**, 12
- 44 H Urayama, H Yamochi, G Saito, K Nozawa, T Sugano, M Kinoshita, S Sato, K Oshima, A Kawamoto and J Tanaka, *Chem Lett* , 1988, 55
- 45 A M Kini, U Geiser, H H Wang, K D Carlson, J M Williams, W K Kwok, K G Vandervoort, J E Thompson, D L Stupka, D Jung and M H Whangbo, *Inorg Chem* , 1990, **29**, 2555
- 46 K Kikuchi, Y Honda, Y Ishikawa, K Saito, I Ikemoto, K Murata, H Anzai, T Ishiguro and K Kobayashi, *Solid State Commun* , 1988, **66**, 405
- 47 A M Kini, M A Beno, D Son, H H Wang, K D Carlson, L C Porter, U Welp, B A Vogt, J M Williams, D Jung, M Evain, M H Whangbo, D L Overmyer and J E Schirber, *Solid State Commun* , 1989, **69**, 503
- 48 T Suzuki, H Yamochi, G Srdanov, K Hinkelmann and F Wudl, *J Am Chem Soc* , 1989, **111**, 3108
- 49 F Wudl, H Yamochi, T Suzuki, H Isotalo, C Fite, H Kasmai, K Liou, G Srdanov, P Coppens, K Maly and A Frost-Jensen, *J Am Chem Soc* , 1990, **112**, 2461
- 50 (a) M A Beno, H H Wang, A M Kini, K D Carlson, U Geiser, W K Kwok, J E Thompson, J M Williams, J Ren and W H Whangbo, *Inorg Chem* , 1990, **29**, 1599, (b) S Kahlich, D Schweitzer, I Heinen, S E Lan, B Nuber, H J Keller, K Winzer and H W Helberg, *Solid State Commun* , 1991, **80**, 191

- 51 (a) Y Ueno, M Bahry and M Okawara, *Tetrahedron Lett* , 1977, **52**, 4607, (b) Y Ueno, A Nakayama and M Okawara, *J Chem Soc , Chem , Commun* , 1978, 74
- 52 Z Yoshida, T Kawase, H Awaji, I Sugimoto, T Sugimoto and S Yoneda, *Tetrahedron Lett* , 1983, **24**, 3469
- 53 Z Yoshida, T Kawase, H Awaji and S Yoneda, *Tetrahedron Lett* , 1983, **24**, 3473
- 54 Z Yoshida, H Awaji and T Sugimoto, *Tetrahedron Lett* , 1984, **25**, 4227
- 55 (a) V Y Khordorkovskii, L N Veselova and O Y Neiland, *Khim , Geterotsiki , Soedin* , 1990, **1**, 130 (*Chem Abstr* , 1990, **113**, 22868), (b) A J Moore, M R Bryce, D J Ando and M B Hursthouse, *J Chem Soc , Chem Commun* , 1991, 320, (c) T K Hansen, M V Lakshmikantham, M P Cava, B M Metzger and J Becher, *J Org Chem* , 1991, **56**, 2720
- 56 A J Moore and M R Bryce, *Tetrahedron Lett* , 1992, **33**, 1373
- 57 M R Bryce, M A Coffin and W Clegg, *J Org Chem* , 1992, **57**, 1696
- 58 (a) M V Lakshmikantham and M P Cava, *Curr Sci* , 1994, **66**, 28, (b) T K Hansen, M V Lakshmikantham, M P Cava, R E Niziurski-Mann, F Jensen and J Becher, *J Am Chem Soc* , 1992, **114**, 5035
- 59 (a) M Salle, A Belyasmine, A Gorgues, M Jubault and N Soyer, *Tetrahedron Lett* , 1991, **32**, 2897, (b) E Cerrada, M R Bryce and A J Moore, *J Chem Soc , Perkin Trans 1* , 1993, 537
- 60 E M Engler and V V Patel, *J Am Chem Soc* , 1974, **96**, 7376
- 61 K Bechgaard, D O Cowan and A N Bloch, *J Chem Soc , Chem Commun* , 1974, 937
- 62 (a) F Wudl and D Nalewajek, *J Chem Soc , Chem Commun* , 1980, 866, (b) L Y Chiang, T O Poehler, A N Bloch and D O Cowan, *J Chem Soc , Chem Commun* , 1980, 866
- 63 A Moradpour, V Peyrussan, I Johansen and K Bechgaard, *J Org Chem* , 1983, **48**, 388
- 64 A N Bloch, D O Cowan, K Bechgaard, R E Pyle, R H Banks and T O Poehler, *Phys Rev Lett* , 1975, **34**, 1561
- 65 C S Jacobsen, K Mortensen, J R Andersen and K Bechgaard, *Phys Rev B Condens Matter* , 1978, **18**, 905
- 66 Y Tomkiewicz, J R Andersen and A R Taranko, *Phys Rev B Solid State* , 1978, **17**, 1579

- 67 D Jerome, A Mazaud, M Ribault and K Bechgaard, *J Phys Lett*, 1980, **41**, L95
- 68 K Bechgaard, *Mol Cryst Liq Cryst*, 1982, **79**, 1
- 69 F Wudl, *J Am Chem Soc*, 1981, **103**, 7064
- 70 S S P Parkin, F Creuzet, M Ribault, D Jerome, K Bechgaard and J M Fabre, *Mol Cryst Liq Cryst*, 1982, **79**, 249
- 71 M H Whangbo, J M Williams, M A Beno and J R Dorfman, *J Am Chem Soc*, 1983, **105**, 645
- 72 M A Beno, G S Blackman, P C W Leung and J M Williams, *Solid State Commun*, 1983, **48**, 99
- 73 F Wudl and E Aharon-Shalom, *J Am Chem Soc*, 1982, **104**, 1154
- 74 K Lerstrup, D Talham, A Bloch, T Poehler and D Cowan, *J Chem Soc, Chem Commun*, 1982, 336
- 75 R D McCullough, G B Kok, K A Lerstrup and D O Cowan, *J Am Chem Soc*, 1987, **109**, 4115
- 76 D E Herr, M D Mays, R D McCullough, A B Bailey and D O Cowan, *J Org Chem*, 1996, **61**, 7006
- 77 (a) C Wang, A Ellern, V Khodorkovsky, J Y Becker and J Bernstein, *J Chem Soc, Chem Commun*, 1994, 2115, (b) J Y Becker, J Bernstein, M Dayan and L Shahal, *J Chem Soc, Chem Commun*, 1992, 1048
- 78 D O Cowan, R McCullough, A Bailey, K Lerstrup, D Talham, D Herr and M Mays, *Phosphorus, Sulfur and Silicon*, 1992, **67**, 277
- 79 D O Cowan, M Mays, M Lee, R McCullough, A Bailey, K Lerstrup, F Wiygul, T Kistenmacher, T Poehler and L Y Chiang, *Mol Cryst Liq Cryst*, 1985, **125**, 191
- 80 (a) J B Torrance, J J Mayerle, V Y Lee and K Bechgaard, *J Am Chem Soc*, 1979, **101**, 4747, (b) V P Parini, *Russ Chem Rev (Engl Transl)*, 1962, **31**, 408
- 81 R E Merrifield and W D Phillips, *J Am Chem Soc*, 1958, **80**, 2778
- 82 W R Hertler, H D Hartzler, D S Acker and R E Benson, *J Am Chem Soc*, 1962, **84**, 3387
- 83 W J Simons, P E Bierstedt and R G Kepler, *J Chem Phys*, 1963, **39**, 3523
- 84 A J Epstein, S Etemad, A F Garito and A J Heeger, *Phys Rev B*, 1972, **5**, 952

- 85 (a) R C Wheland and E L Martin, *J Org Chem* , 1975, **40**, 3101,
(b) J R Andersen and O Jorgensen, *J Chem Soc , Perkin Trans 1*,
1979, 3095
- 86 J Diekmann, W R Hertler and R E Benson, *J Org Chem* , 1963, **28**,
2719
- 87 A Kini, M Mays and D Cowan, *J Chem Soc , Chem Commun* ,
1985, 286
- 88 R C Wheland, *J Am Chem Soc* , 1976, **98**, 3926
- 89 B Rosenau, C Krieger and H A Staab, *Tetrahedron Lett* , 1985, **26**,
2081
- 90 W Lehnert, *Tetrahedron Lett* , 1970, **54**, 4723
- 91 N Martin and M Hanack, *J Chem Soc , Chem Commun*, 1988,
1522
- 92 J Y Becker, J Bernstein, S Bittner, E Harlev and J A R P Sarma, *J
Chem Soc , Perkin Trans 2*, 1989, 1157
- 93 M R Bryce, S R Davies, A M Grainger, J Hellberg, M B Hursthouse,
M Mazid, R Bachmann and F Gerson, *J Org Chem* , 1992, **57**, 1690
- 94 (a) A Aumuller and S Hunig, *Liebigs Ann Chem* , 1984, 618, (b) B S
Ong and B Keoshkerian, *J Org Chem* , 1984, **49**, 5002
- 95 T Czekanski, M Hanack, J Y Becker, J Bernstein, S Bittner, L
Kaufman-Orenstein and D Peleg, *J Org Chem* , 1991, **56**, 1569
- 96 (a) M Uno, K Seto, M Masuda, W Ueda and S Takahashi,
Tetrahedron Lett , 1985, **26**, 1553, (b) M Uno, T Takahashi and
S Takahashi, *J Chem Soc , Perkin Trans 1*, 1990, 647
- 97 Y Miura, E Torres, C A Panetta and R M Metzger, *J Org Chem* ,
1988, **53**, 439
- 98 (a) W A Davis and M P Cava, *J Org Chem* , 1983, **48**, 2774,
(b) M R Bryce, M Hasan and G J Ashwell, *J Chem Soc , Chem
Commun* , 1989, 529, (c) M R Bryce, A M Grainger, M Hasan, G J
Ashwell, P A Bates and M B Hursthouse, *J Chem Soc , Perkin
Trans 1*, 1992, 611
- 99 A F Garito and A J Heeger, *Acc Chem Res* , 1974, **7**, 232
- 100 D J Sandman and A F Garito, *J Org Chem* , 1974, **39**, 1165
- 101 A W Addison, N S Dalal, Y Hoyano, S Huizinga and L Weiler, *Can
J Chem* , 1977, **55**, 4191
- 102 (a) K Bechgaard, C S Jacobsen and N H Andersen, *Solid State
Commun* , 1978, **25**, 875, (b) P A Berger, D J Dahm, G R Johnson,
M G Miles and J D Wilson, *Phys Rev B*, 1975, **12**, 4085

- 103 W R Hertler, USP 3 153 658/1965 (*Chem Abstr* , 1964, **62**, 4145)
- 104 E Aharon-Shalom, J Y Becker and I Agranat, *Nouv J Chim* , 1979, **3**, 643
- 105 M Maxfield, D O Cowan, A N Bloch and T O Poehler, *Nouv J Chim* , 1979, **3**, 647
- 106 M Maxfield, S M Willi, D O Cowan, A N Bloch and T O Poehler, *J Chem Soc , Chem Commun* , 1980, 947
- 107 S Chatterjee, *J Chem Soc B*, 1967, 1170
- 108 S Yamaguchi, H Tatemitsu, Y Sakata and S Misumi, *Chem Lett* , 1983, 1229
- 109 (a) S Hotta, T Tosaka, N Sonoda and W Shimotsuma, EP 61 264/1983 (*Chem Abstr* , 1983, **98**, 99701), (b) Matsushita Electric Industrial Co , Ltd , Jap P 10 554/1983 (*Chem Abstr* , 1983, **98**, 197809), (c) S Hotta, T Tosaka, N Sonoda and W Shimotsuma, EP 76 639/1983 (*Chem Abstr* , 1983, **99**, 105013)
- 110 A M Kini, D O Cowan, F Gerson and R Mockel, *J Am Chem Soc* , 1985, **107**, 556
- 111 N Martin, R Behnisch and M Hanack, *J Org Chem* , 1989, **54**, 2563
- 112 N Martin, J L Segura, C Seoane, P de la Cruz, F Langa, E Orti, P M Viruela and R Viruela, *J Org Chem* , 1995, **60**, 4077
- 113 F Iwasaki, *Acta Crystallogr , Sect B*, 1971, **27**, 1360
- 114 U Schubert, S Hunig and A Aumuller, *Liebigs Ann Chem* , 1985, 1216
- 115 J Silverman and N F Yannoni, *J Chem Soc B*, 1967, 194
- 116 (a) P de la Cruz, N Martin, F Miguel, C Seoane, A Albert, F H Cano, A Leverenz and M Hanack, *Synth Metals*, 1992, **48**, 59, (b) P de la Cruz, N Martin, F Miguel, C Seoane, A Albert, F H Cano, A Gonzalez and J M Pingarron, *J Org Chem* , 1992, **57**, 6192
- 117 K Kobayashi and C L Gajurel, *J Chem Soc , Chem Commun* , 1986, 1779
- 118 F Gerson, R Heckendorn, D O Cowan, A M Kini and M Maxfield, *J Am Chem Soc* , 1983, **105**, 7017
- 119 (a) T Mitsuhashi, M Goto, K Honda, Y Maruyama, T Sugawara, T Inabe and T Watanabe, *J Chem Soc , Chem Commun* , 1987, 810, (b) T Mitsuhashi, M Goto, K Honda, Y Maruyama, T Inabe, T Sugawara and T Watanabe, *Bull Chem Soc Jpn* , 1988, **61**, 261
- 120 S Gronowitz and B Uppstrom, *Acta Chem Scand , Ser B*, 1974, **28**, 981

- 121 M Uno, K Seto and S Takahashi, *J Chem Soc , Chem Commun* , 1984, 932
- 122 H Ishida, K Yui, Y Aso, T Otsubo and F Ogura, *Bull Chem Soc Jpn* , 1990, **63**, 2828
- 123 (a) K Yui, Y Aso, T Otsubo and F Ogura, *J Chem Soc , Chem Commun* , 1987, 1816, (b) K Yui, Y Aso, T Otsubo and F Ogura, *Chem Lett* , 1988, 1179
- 124 (a) K Yui, H Ishida, Y Aso, T Otsubo and F Ogura, *Chem Lett* , 1987, 2339, (b) K Yui, H Ishida, Y Aso, T Otsubo, F Ogura, A Kawamoto and J Tanaka, *Bull Chem Soc Jpn* , 1989, **62**, 1547
- 125 (a) S Yoshida, M Fujii, Y Aso, T Otsubo and F Ogura, *J Org Chem* , 1994, **59**, 3077, (b) F Ogura, T Otsubo, Y Aso and S Fujii, *Jap P 80 672/1994 (Chem Abstr, 1994, 121, 108764)*
- 126 M Fujii, Y Aso, T Otsubo and F Ogura, *Synth Metals*, 1993, **55-57**, 2136
- 127 J H Perlstein, *Angew Chem , Int Ed Engl* , 1977, **16**, 519
- 128 Y Aso, K Yui, H Ishida, T Otsubo, F Ogura, A Kawamoto and J Tanaka, *Chem Lett* , 1988, 1069
- 129 (a) T Suzuki, Y Yamashita, C Kabuto and T Miyashi, *J Chem Soc , Chem Commun* , 1989, 1102, (b) T Suzuki, H Fujii, Y Yamashita, C Kabuto, S Tanaka, M Harasawa, T Mukai and T Miyashi, *J Am Chem Soc* , 1992, **114**, 3034
- 130 A Aumuller and S Hunig, *Liebigs Ann Chem* , 1986, 142
- 131 A Aumuller and S Hunig, *Angew Chem , Int Ed Engl* , 1984, **23**, 447
- 132 A Aumuller and S Hunig, *Liebigs Ann Chem* , 1986, 165
- 133 (a) M R Bryce and S R Davies, *J Chem Soc , Chem Commun* , 1989, 328, (b) N Martin, J A Navarro, C Seoane, A Albert, F H Cano, J Y Becker, V Khodorkovsky, E Harlev and M Hanack, *J Org Chem* , 1992, **57**, 5726
- 134 E Barranco, N Martin, J L Segura, C Seoane, P de la Cruz, F Langa, A Gonzalez and J M Pingarron, *Tetrahedron*, 1993, **49**, 4881
- 135 A Aumuller, E Hadicke, S Hunig, A Schatzle and J U von Schutz, *Angew Chem , Int Ed Engl* , 1984, **23**, 449
- 136 A Aumuller, P Erk, S Hunig, J U von Schutz, H P Werner, H C Wolf and G Klebe, *Chem Ber* , 1991, **124**, 1445
- 137 E Gunther, S Hunig, K Peters, H Rieder, H G von Schnering, J U von Schutz, S Soderholm, H P Werner and H C Wolf, *Angew Chem , Int Ed Engl* , 1990, **29**, 204

- 138 A Aumuller, P Erk, G Klebe, S Hunig, J U von Schutz and H P Werner, *Angew Chem , Int Ed Engl* , 1986, **25**, 740
- 139 K Sinzger, S Hunig, M Jopp, D Bauer, W Bietsch, J U von Schutz, H C Wolf, R K Kremer, T Metzenthin, R Bau, S I Khan, A Lindbaum, C L Lengauer and E Tillmanns, *J Am Chem Soc* , 1993, **115**, 7696
- 140 R Kato, H Kobayashi and A Kobayashi, *J Am Chem Soc* , 1989, **111**, 5224
- 141 G Steimecke, H J Sieler, R Kirmse and E Hoyer, *Phosphorus Sulfur*, 1979, **7**, 49
- 142 M Bousseau, L Valade, J P Legros, P Cassoux, M Garbauskas and L V Interrante, *J Am Chem Soc* , 1986, **108**, 1908
- 143 M Bousseau, L Valade, M F Bruniquel, P Cassoux, M Garbauskas, L Interrante and J Kasper, *Nouv J Chim* , 1984, **8**, 3
- 144 L Brossard, M Ribault, L Valade and P Cassoux, *Physica B*, 1986, **143**, 378
- 145 A Kobayashi, H Kim, Y Sasaki, R Kato, H Kobayashi, S Moriyama, Y Nishio, K Kajita and W Sasaki, *Chem Lett* , 1987, 1819
- 146 A Kobayashi, H Kobayashi, A Miyamoto, R Kato, R A Clark and A E Underhill, *Chem Lett* , 1991, 2163
- 147 A Kobayashi, H Kim, Y Sasaki, K Murata, R Kato and H Kobayashi, *J Chem Soc , Faraday Trans* , 1990, **86**, 361
- 148 P M Allemand, A Koch, F Wudl, Y Rubin, F Diederich, M M Alvarez, S J Anz and R L Whetten, *J Am Chem Soc* , 1991, **113**, 1050
- 149 F Zhou, G J van Berkel and B T Donovan, *J Am Chem Soc* , 1994, **116**, 5485
- 150 G Saito, T Teramoto, A Otsuka, Y Sugita, T Ban, M Kusunoki and K Sakaguchi, *Synth Metals*, 1994, **64**, 359
- 151 R C Haddon, *Acc Chem Res* , 1992, **25**, 127
- 152 P M Allemand, K C Khemani, A Koch, F Wudl, K Kolczar, S Donovan, G Gruner and J D Thompson, *Science*, 1991, **253**, 301
- 153 T Ohno, N Martin, B Knight, F Wudl, T Suzuki and H Yu, *J Org Chem* , 1996, **61**, 1306
- 154 Farbenfabriken Bayer A -G , FP 1 537 299/1968 (*Chem Abstr* , 1970, **72**, 33250)
- 155 A Eckell, H Eilingsfeld, A Elzer, F Feichtmayr, G Hoffmann, R J Leyrer and P Neumann, GP 3 110 953/1982 (*Chem Abstr* , 1983, **98**, 98798)

- 156 F Closs, R Gompper, U Nagel and H U Wagner, *Angew Chem , Int Ed Engl* , 1987, **26**, 1037
- 157 S P Conway, Ph D Thesis, DCU, 1996
- 158 (a) P J Babidge and R A Massy-Westropp, *Aust J Chem* , 1977, **30**, 1629, (b) W Flitsch and H Peters, *Tetrahedron Lett* , 1969, 1161
- 159 G B Gill, G D James, K V Oates and G Pattenden, *J Chem Soc , Perkin Trans 1* , 1993, 2567
- 160 J A Moore and J H Kim, *Tetrahedron Lett* , 1991, **32**, 3449
- 161 H G Heller, D S Hughes, M B Hursthouse and K V S Koh, *J Chem Soc , Chem Commun* , 1994, 2713
- 162 J A Moore and D R Robello, *Macromolecules*, 1989, **22**, 1084
- 163 P G Gassmann and D C Heckert, *J Org Chem* , 1965, **30**, 2859
- 164 K Wallenfels, K Friedrich, J Rieser, W Ertel and H K Thieme, *Angew Chem , Int Ed Engl* , 1970, **15**, 261
- 165 J March, *Advanced Organic Chemistry*, Wiley, 4th Edition, p 393
- 166 R B Woodward and H Baer, *J Am Chem Soc* , 1948, **70**, 1161
- 167 (a) S Torii, T Okamoto and H Tanaka, *J Org Chem* , 1974, **39**, 2486, (b) A I Meyers and R F Spohn, *J Org Chem* , 1985, **50**, 4872, (c) B El Ali and H Alper, *J Org Chem* , 1991, **56**, 5357
- 168 (a) J A Elvidge, J S Fitt and R P Linstead, *J Chem Soc* , 1956, 235, (b) J A Elvidge and R P Linstead, *J Chem Soc* , 1952, 5000
- 169 Y Tsubata, T Suzuki, T Miyashi and Y Yamashita, *J Org Chem* , 1992, **57**, 6749
- 170 (a) G Charles, *Bull Soc Chim Fr* , 1963, 1576, (b) G Charles, *Bull Soc Chim Fr* , 1963, 1559
- 171 P J Brach, S J Grammatica, O A Ossanna and L Weinberger, *J Heterocycl Chem* , 1970, 1403
- 172 R P Linstead, E G Noble and J M Wright, *J Chem Soc* , 1937, 911
- 173 W K Musker, *J Am Chem Soc* , 1964, **86**, 960
- 174 (a) A R Katritzky, *Tetrahedron*, 1980, **36**, 679, (b) A R Katritzky, G Liso, E Lunt, R C Patel, S S Thind and A Zia, *J Chem Soc , Perkin Trans 1* , 1980, 849
- 175 Y Okuda, M V Lakshmikantham and M P Cava, *J Org Chem* , 1991, **56**, 6024

- 176 P F Clark, J A Elvidge and J H Golden, *J Chem Soc* , 1956, 4135
- 177 (a) C R Bruce, R E Norberg and S I Weissman, *J Chem Phys* , 1956, **24**, 473, (b) C S Johnson, Jr , *J Chem Phys* , 1963, **39**, 2111, (c) A D Britt, *J Chem Phys* , 1964, **41**, 3069
- 178 A J Bard and L R Faulkner, *Electrochemical Methods-Fundamentals and Applications*, Wiley and Sons, Chicester, 1980
- 179 Y Yamashita, T Suzuki, G Saito and T Mukai, *Chem Lett* , 1986, 715
- 180 B S Furniss, A J Hannaford, P W G Smith and A R Tatchell, *Vogel's Textbook of Practical Organic Chemistry*, Wiley, New York, 1989, 5th ed , p 1274
- 181 G M Sheldrick, *Acta Crystallogr* , 1990, **46**, 467
- 182 G M Sheldrick, SHELX 93, Program for Crystal Structure Determination, 1993